



Durham E-Theses

The reliability of wind turbines

Spinato, Fabio

How to cite:

Spinato, Fabio (2008) *The reliability of wind turbines*, Durham theses, Durham University. Available at Durham E-Theses Online: <http://etheses.dur.ac.uk/1918/>

Use policy

The full-text may be used and/or reproduced, and given to third parties in any format or medium, without prior permission or charge, for personal research or study, educational, or not-for-profit purposes provided that:

- a full bibliographic reference is made to the original source
- a [link](#) is made to the metadata record in Durham E-Theses
- the full-text is not changed in any way

The full-text must not be sold in any format or medium without the formal permission of the copyright holders.

Please consult the [full Durham E-Theses policy](#) for further details.

The Reliability of Wind Turbines

Fabio Spinato

The copyright of this thesis rests with the author or the university to which it was submitted. No quotation from it, or information derived from it may be published without the prior written consent of the author or university, and any information derived from it should be acknowledged.

A Thesis presented for the degree of
Doctor of Philosophy



Energy Group
School of Engineering
Durham University
England

December 2008

26 JAN 2009

Dedicated to

*my unforgotten grandfather Isidoro, miner and lumberjack,
and his profound and contagious passion for sciences*

In memoriam.

The Reliability of Wind Turbines

Fabio Spinato

Submitted for the degree of Doctor of Philosophy

December 2008

Abstract

The residual scepticism surrounding the installation of wind turbines, is mainly due to the perceived lack of reliability and expense of these energy converters. Because of the commercial significance of reliability, few sources of such data are publicly available, with the result that knowledge of the true reliability of wind turbines is fragmentary and sometimes anecdotal, even among operators and professionals in the wind energy industry.

In order to “crystallise” the knowledge emerging from these publicly available data sources, and supply solid reliability figures, various analyses have been made using appropriate theory, including the implementation of a reliability growth model, based on the Power Law Process. The results of the analysis of average failure frequency has shed light on the most important reliability features of current wind turbines, their parts, called subassemblies, and on possible alternative wind turbine architectures, called concepts. With the implementation of the PLP model, reliability time trends, characterising the behaviour the various turbine subassemblies, have been revealed. A model sensitivity analysis have been carried out by using simulated failure data. Finally, the model results have been analysed and reported in a systematic way with the help of two statistical test. From these analyses, despite some clear deficiencies of the available data, this thesis offers an important insight into the current reliability of wind turbines, with clear indication about the most problematic subassemblies and the ones for which reliability improvement should more likely be expected.

Declaration

The work in this thesis is based on research carried out in the Energy Group of the School of Engineering, Durham University, England. No part of this thesis has been submitted elsewhere for any other degree or qualification and it all my own work unless referenced to the contrary in the text.

Copyright © 2008 by Fabio Spinato.

“The copyright of this thesis rests with the author. No quotations from it should be published without the author’s prior written consent and information derived from it should be acknowledged”.

Acknowledgements

The work in this thesis was sponsored by an award of a CASE studentship entitled “Toward a Zero Maintenance Wind Turbine” funded by EPSRC and co-funded by Evolving Generation Ltd. The author would like to thank Prof. Ed Spooner of Evolving Generation for supporting the studentship.

This thesis has been made possible also thanks to the invaluable help of many people, that I would like to thank.

Firstly, my supervisor, Prof. Peter J. Tavner, for his guidance, passion and patience. His teachings, wisdom and common sense have always indicated to me the right bearing in a discipline otherwise arduous to navigate.

Thanks to Prof. Frank Coolen of the Mathematical Department for his effort and precious help that allowed me to deepen the interpretation of the mathematical models, and thanks to Dr. Dimple Venkat.

Thanks to Prof. van Bussel of Technical University of Delft. His availability and collaboration has proven crucial for this thesis. May the collaboration with the TU Delft develop even further in the future. From the same TU Delft thanks to Erika Echavarria and Efstathios Koutoulakos.

Thanks to Nick Stannard for his moral and spiritual support in my most “volatile” moments.

Finally, a special thank to Michael Wilkinson and Dr. Anthony Hill, colleagues and friends, for their most amazing help, “logistic” support and kindness. Kindness that I can only aspire to return, one day.

Contents

Abstract	iii
Declaration	iv
Acknowledgements	v
Nomenclature	1
1 Background	4
1.1 Global warming and climate change	4
1.2 The energy question and the peak oil	7
1.2.1 Solutions to the peak oil	9
1.3 Kyoto protocol	10
1.4 Wind Energy and Reliability	13
1.5 Going off-shore	19
1.6 Original contribution of this thesis	19
2 Literature Review	21
2.1 Introduction	21
2.2 An Early Document	22
2.3 DOWEC	24
2.3.1 Introduction to DOWEC	24
2.3.2 DOWEC Results	25
2.3.3 Conclusion of the DOWEC Report	30
2.4 Industrial Failure Surveys	30
2.5 What The Experts Say	32

2.5.1	Current Turbines Reliability and Availability	34
2.5.2	Reliability trends	37
2.5.3	Offshore Turbines Desired Reliability	41
2.6	Availability figures	43
2.7	Conclusion	45
3	Elements of Reliability Theory	47
3.1	Introduction	47
3.2	Non Repairable Systems	48
3.3	Repairable Systems	52
3.4	Point Processes, HPP and NHPP	53
3.4.1	Point Processes	53
3.4.2	Poisson Processes	54
3.4.3	The “Bathtub” curve and the <i>PLP</i>	55
3.4.4	On the meaning of the Bathtub curve	57
4	Wind Turbine Failure Data	61
4.1	Introduction	61
4.2	The Wind Turbine	63
4.2.1	The Rotor	64
4.2.2	The Drive Train	65
4.2.3	The Electrics	67
4.2.4	The Tower	68
4.2.5	Electrical Control	69
4.2.6	Other	70
4.3	WindStats and LWK	71
4.3.1	Number of Turbines	76
4.3.2	Terminology	78
4.4	The Average Failure Frequency	79
4.4.1	Weather Effects	82
4.4.2	Reliability Growth	84
4.4.3	Technology	87

4.5	Analysis of Turbine Concepts	89
4.5.1	Definition of Concepts	89
4.5.2	The Reliability of Subassemblies	91
4.5.3	Downtimes	93
4.5.4	Results	96
4.5.5	Conclusions and Remarks	101
5	Reliability Growth Analysis	104
5.1	Introduction	104
5.2	Reliability Growth Methods	105
5.3	Crow-AMSAA for grouped data	108
5.4	Total Time on Test	110
5.5	Statistical tests	115
5.6	The aggregation process	117
5.7	Model Results	121
5.8	Values of the Intensity Function	122
5.9	Goodness of Fit	122
5.10	An alternative Model	124
5.10.1	Using Calendar Time	124
5.10.2	Results comparison	126
5.10.3	Discussion	129
6	Commentary on the Power Law Process Results	130
6.1	Introduction	130
6.2	Results for Whole Turbine	131
6.3	Results for Gearboxes	132
6.4	Results for Generators	138
6.5	Results for Electrical Control and Electrics	142
6.6	Results for Hydraulics	148
6.7	Conclusions	151

7	Simulation of Failure Events	153
7.1	Introduction	153
7.2	Generation of PLP random numbers	156
7.3	Simulation Results	159
7.4	PLP Model's Sensitivity Analysis	163
7.4.1	Introduction	163
7.4.2	Case 1	165
7.4.3	Case 2	170
7.4.4	Case 3	172
7.5	Conclusions	172
8	Conclusions	176
8.1	Introduction	176
8.2	WT Reliability Data	177
8.3	WT Subassemblies	179
8.4	WT Concepts	181
8.5	Future Work	183
A	Weibull Analysis of Converters Failure Data	185
A.1	Introduction	185
A.2	Data Set	186
A.3	Weibull Analysis	189
A.4	Actuarial Correction	192
A.5	Results: First Data Set, Type A	194
A.6	Results: Second Data Set: Types B-H	196
A.7	Conclusions	203
B	Reliability Growth Results Tables	205
C	A Survey Among WT Experts	218
C.1	Preface	219
C.2	Questionnaire	219
C.3	References	223

List of Figures

1.1	Reconstructed carbon dioxide concentration of the last 400000 years [23]	6
1.2	Recorded atmospheric carbon dioxide concentration compared with the last 1000 years [23]	7
1.3	The wind turbine designed by Ulrich Hutter, in the 1950s [26]	14
1.4	A milestone of the wind industry; the MOD-2, rated at 2.5 MW, 1981 [25]	14
1.5	The MOD-5, the last product of the U.S. FWEF, rated at 3.2 MW, 1987 [24]	15
1.6	The progenitor of the Danish concept the “Gedser mill”, rated at 200 kW, early 1960’s [64]	17
1.7	A development of the Danish concept WEGA 1; the Tjaereborg rated at 2MW, 1985 [70]	17
1.8	A modern Indirect Drive WT, Vestas V90, rated at 3 MW, 2007 [68]	18
1.9	A modern Direct Drive WT, Enercon E82, rated at 2 MW, 2007 [69]	18
2.1	Wind turbine subassembly failure frequencies compared with industrial data of Table 2.6	31
2.2	The three proposed failure trends. The figure are generic and give a visual impression of the failure trends.	39
2.3	Availability, Capacity Factor and Wind Speed of four wind farms [5, 37, 38, 47, 57, 58]	44
3.1	The bathtub curve for the intensity function (repairable)	56
3.2	The power law function, parametrised in terms of β	56
3.3	The bathtub curve for the hazard function (unrepairable)	59

4.1	The subassemblies of an indirect wind turbine: 1. Nacelle, 2. Heat exchanger, 3. Generator, 4. Control panel, 5. Main frame, 6. Noise isolation, 7. Parking brake, 8. Noise isolation, 9. Gearbox, 10. Yaw drive, 11. Yaw drive, 12. Main shaft, 13. Oil cooler, 14. Pitch control, 15. Hub, 16. Nose cone	63
4.2	A rotor of a direct drive machine, being mounted on the nacelle [66] .	65
4.3	The high speed shaft and the gearbox of an indirect drive wind turbine [27]	67
4.4	Wind turbine yaw system; drive and gear wheel [65]	69
4.5	The scheme of a indirect drive variable speed WT with a doubly fed induction generator [67]	70
4.6	Number of wind reporting turbines	77
4.7	Average rating of the wind reporting turbines	77
4.8	The failure reporting form taken from WMEP, Windenergie Report Deustschland	80
4.9	The average frequency of failures from the two WindStats populations	81
4.10	Spectrum for 2 WEI data sets: 96-03 and 87-03. The longer set displays a sharper peak at angular frequencies equivalent to 12 months. The angular frequency is expressed in rad/month.	84
4.11	Spectrum of failure rate data before and after linear trend has been removed. 54 month peak has decreased significantly, other 3 main angular frequencies have changed little. Angular frequency is expressed in rad/months. For some of the points the equivalent self correlation period is reported	85
4.12	Cross-Correlogram of Turbine Failure Rate to WEI, 1994-2004	85
4.13	The average age of the LWK turbines	86
4.14	The failure intensity in historical context	88
4.15	The average failure frequency for each subassembly, failures per year .	92
4.16	The failure distribution among the subassemblies	94
4.17	The failure distribution compared with another survey	94

4.18	LWK Survey hours lost per failure comparison : period 1993-2004, 158-643 turbines	95
4.19	LWK Survey hours lost per failure comparison, segregated by WT group: period 1993-2004, 158-643 turbines	96
4.20	The average failure frequency of Group I, small turbines	97
4.21	The average failure frequency of Group II, medium turbines	97
4.22	The average failure frequency of Group III, large turbines	98
4.23	The average failure frequency of the three turbines groups	98
4.24	The average failure frequency of the small turbines Group I	100
4.25	The average failure frequency of the medium turbines Group II	100
4.26	The average failure frequency of the large turbines Group III	101
5.1	The model implemented for a particular case of a Vestas V27 turbine.	109
5.2	Demonstrated reliability for an early failure case	113
5.3	Demonstrated reliability for a constant failure case	114
5.4	An example of deterioration phase; gearbox subassembly of Vestas V39 wind turbine	114
6.1	Whole WT, example 1, M530	133
6.2	Whole WT, example 2, TW600	133
6.3	Whole WT, example 3, N52/54	134
6.4	Gearbox, example 1, TW600	135
6.5	Gearbox, example 2, V39	136
6.6	Gearbox, example 3, N52/54	136
6.7	Gearbox, example 4, V27	137
6.8	Generator, example 1, V27	139
6.9	Generator, example 2, V27	139
6.10	Generator, example 3, M530	140
6.11	Generator, example 4, TW600	140
6.12	Generator, example 5, N52/54	141
6.13	Generator, example 6, E66	141
6.14	Electrical control, example 1, E40	143

6.15	Electrical control, example 2, E66	144
6.16	Electrical control, example 3, TW1.5s	144
6.17	Electrics, example 1, TW600	146
6.18	Electrics, example 2, E40	147
6.19	Electrics, example 3, E66	147
6.20	Hydraulics, example 1, TW600	149
6.21	Hydraulics, example 2, V39	149
6.22	Hydraulics, example 3, All WTs	150
7.1	The representation of the simulation cycle	155
7.2	From left to right and from top to bottom: simulate failure intensity time curve for monthly grouped data for populations of 10, 50, 100, 200, 500 or 2000 WTs. The original intensity function for the population is shown in red.	160
7.3	From left to right and from top to bottom: resulting failure intensity time curve of yearly grouped data for populations of 10, 50, 100, 200, 500 or 2000 WTs. The original intensity function for the population is shown in red	161
7.4	An example of the data reported on the figures below. The failure rate refers to a single WT, [failure / year] = [failure / WT / year] . .	164
7.5	Simulation case 1.1	166
7.6	Simulation case 1.2	166
7.7	Simulation case 1.3	167
7.8	Simulation case 1.4	167
7.9	Simulation case 1.5	168
7.10	Simulation case 1.6	168
7.11	Simulation case 2.1	170
7.12	Simulation case 2.2	171
7.13	Simulation case 2.3	171
7.14	Simulation case 3.1	173
7.15	Simulation case 3.1	173
7.16	Simulation case 3.1	174

7.17 Simulation case 3.1	174
A.1 The graphical calculation of shape and scale parameters	191
A.2 Weibull Analysis result for Type A converter	194
A.3 Weibull Analysis result for Type A converter after removal of deliver delay period of 70 days	195
A.4 The graphical calculation of shape and scale parameters	196
A.5 The graphical calculation of shape and scale parameters	197
A.6 The graphical calculation of shape and scale parameters	197
A.7 The graphical calculation of shape and scale parameters	198
A.8 The graphical calculation of shape and scale parameters	198
A.9 The graphical calculation of shape and scale parameters	199
A.10 Example of Bi-Weibull: two interpolating lines fit better the Weibull chart of type G converter	200

List of Tables

2.1	Reliability figures in [44]	23
2.2	The failure frequencies adopted for the DOWEC project [59] from one year of real data	25
2.3	The wind turbine concepts featured in [60]. The DOWEC project has been the progenitor of the systematic study of the WT concepts.	27
2.4	A further set of reliability data used for the DOWEC project [60]. Onshore data, from which offshore data are derived from, are the results of expert brainstorming	28
2.5	The failure frequencies adopted in [60] in failure per years as modified to reflect electrical and mechanical concepts and maintenance category	29
2.6	Industrial failure frequencies of some subassemblies extracted from [31]	31
2.7	Comparison of electrical machine failure frequencies as reported in [54]	33
2.8	Q1 - Current Onshore WTs Availability	35
2.9	Q2 - Current Onshore WTs Failure Frequency	35
2.10	Q3 - Useful Life	36
2.11	Q4 - Least Reliable subassembly	36
2.12	Q5 - Failure modes considered to be important	37
2.13	Q6 - Gearbox failure trend	38
2.14	Q7 - Reasons for gearbox failure trend	39
2.15	Q8a - Generator failure trend	39
2.16	Q8b - Reasons for generator failure trend	40
2.17	Q9a - Blades failure trend	40
2.18	Q9b - Reasons for blades failure trend	40
2.19	Q10 - Most reliable concept	41

2.20	Q11 - Main obstacle to offshore installation	42
2.21	Q12 - Desired offshore reliability	42
2.22	Q13 - Economically acceptable offshore failure frequency	42
2.23	The four wind farms considered in figure 2.3	43
4.1	An example of failure data for WSDK turbines for January 2001 [17]	72
4.2	An example of the causes of stoppage and failure data for WSD for January-March 2001 [17]	72
4.3	An example of causes of stoppage shown for WSDK turbines for Jan- uary to March 2001 [17]	73
4.4	An example of wind turbine data for the two WindStats populations for January to March 2001 [17]	74
4.5	An example of the turbine failure data from the LWK record for a TW600 wind turbine [15]	75
4.6	The terminology used for the wind turbine subassemblies	79
4.7	Overall average failure intensity and age	87
4.8	The features of the selected wind turbine models from LWK data . . .	90
4.9	Number of turbines and extension of the recording period of the LWK survey	90
4.10	The average failure frequency for each subassembly for all three pop- ulations	92
5.1	The calculation of the <i>TTT</i> for Vestas V27 turbine electrics subassem- bly, see Fig. 5.1	112
5.2	The check table for the determination of the final result	117
5.3	An example of the effect of the aggregation process for Case 1 (sparse data)	119
5.4	An example of the effect of the aggregation process for Case 2 (noisy data)	120
5.5	The three data record considered; failures for whole WT, gearbox and electrics of V39/500 wind turbine	127

5.6	The results for the three cases considered, two parameter model and <i>TTT</i>	127
5.7	The results for the three cases considered, four parameter model and <i>CT</i>	127
6.1	Synthetic results for the whole wind turbine, all subassemblies	132
6.2	The synthetic results for the gearbox	135
6.3	Synthetic results for the generator	138
6.4	The synthetic results for the electrical control	143
6.5	The synthetic results for the electrics	146
6.6	The synthetic results for the hydraulics	148
7.1	Matrix of the TTF of the simulated occurrences	157
7.2	Simulated number of failures: 200 WT, grouped by semester	158
7.3	Simulated number of failures: 200 WT, grouped by quarter	158
7.4	Results for the first cycle of simulations, $\beta = 0.7$	165
7.5	Results for the second cycle of simulations, $\beta = 1.8$	170
7.6	Results for the third cycle of simulations, $\beta = 1.0$	172
A.1	An example of the original data failure data; converter A	187
A.2	The failure data of converter A converted into the “Nevada” format .	188
A.3	Calculation of the unreliability using the Kaplan-Meier ranking method [62]	193
A.4	The results of the Weibull Analysis for the second set of converter data	196
A.5	The intersection point for each converter type	200
A.6	The results of the first interpolating line	201
A.7	The results of the second interpolating line	202
B.1	The PLP model results for the whole turbine	206
B.2	The PLP model results for the hydraulics	207
B.3	The PLP model results for the gearbox	208
B.4	The PLP model results for the generator	209
B.5	The PLP model results for the rotor	210

B.6	The PLP model results for the electrical system	211
B.7	The PLP model results for the electronics	212
B.8	The PLP model results for the yaw system	213
B.9	The PLP model results for the pitch control	214
B.10	The PLP model results for the air brake	215
B.11	The PLP model results for mechanical brake	216
B.12	The PLP model results for mechanical brake	217

Nomenclature

α	Confidence level in a goodness of fit test
β	Shape parameter for the Weibull function
\exists	Exists
\forall	For all
$\hat{\beta}$	Estimate of the shape parameter
$\hat{\rho}$	Estimate of the scale parameter
λ	Constant value of the intensity function
$\Lambda(t)$	Point process mean function
$\lambda(t)$	Intensity function
Λ_i	Average intensity of failures in the interval i
$\mu(t)$	Rate of Occurrence of Failure, ROCOF
ρ	Scale parameter for the Weibull function
θ	A function of the scale parameter λ
$A(t)$	Availability
CT	Calendar Time
E	Expected value of a random variable
e_i	expected number of failures in the period

Nomenclature

$F(t)$	Cumulative Distribution Function
$f(t)$	Probability density function
GoF	Goodness of Fit Test
$h(t)$	Hazard function
h_i	Number of hours in the interval i
I	Maximum number of periods
i	Counting variable indicating the period
k	Counting variable for the subassemblies
L_i	Hours lost in the interval i
N	Counting random variable
n	Number of failures
N_i	Number of wind turbines in the interval i
n_i	Number of failures in the interval i
P	Probability
P	Produced Power
P_{avg}	Long term expected power with average weather
$R(t)$	Survival function or reliability
t	Value assumed by X
TBF	Time Between Failures
TTF	Time To Failure
TTT	Total Time on Test
X	Random variable for the lifetime

December 6, 2008

Nomenclature

<i>cdf</i>	Cumulative distribution function
<i>iid</i>	Independent and identically distributed (random variable)
<i>pdf</i>	Probability density function
CCGT	Combine Cycle Gas Turbine
GoF	Goodness of Fit (Test)
HPP	Homogeneous Poisson Process
LWK	Landwirtschaftskammer Schleswig-Holstein
MLE	Maximum Likelihood Estimate
MTBF	Mean Time Between Failure
MTTF	Mean Time To Failure
NHPP	Non Homogeneous Poisson Process
PLP	Power Law Process (Weibull Process)
ROCOF	Rate of Occurrence of Failures
SCR	Squared Correlation Coefficient
TBF	Time Between Failure
WEI	Wind Energy Index
WSD	WindStats Germany
WSDK	WindStats Denmark
WT	abbreviation of wind turbine

Chapter 1

Background

*Penso che un sogno così non ritorni mai più
mi dipingevo le mani e la faccia di blu
poi d'improvviso venivo dal vento rapito
e incominciavo a volare nel cielo infinito*¹

Domenico Modugno, "Nel Blu Dipinto Di Blu"

1.1 Global warming and climate change

Contemplating the sky, nowadays, Domenico Modugno would not, likely, find in it the same beauty that inspired his masterpiece *Nel Blu Dipinto Di Blu*, the song that made him popular worldwide. Contrary to the poetical blue of the famous Italian singer-writer, the sky is often shaded by a grey veil, especially above the overcrowded cities of the world and, to the more sensitive, it is more a source of concern rather than of ecstatic serenity and infinite freedom.

Furthermore the atmosphere, like many other natural resources, that have hitherto been considered infinite is, as a matter of fact, astonishingly limited.

The most external part of the atmosphere, the thermosphere, reaches 560 km from

¹I think a dream like that will never return

I painted my hands and face blue
then suddenly I was taken by the wind
and I started to fly in the infinite sky

the surface of the planet, but 99% of the air mass is located in the denser troposphere and stratosphere, the first two layers, that extend for 50 kilometers. If the earth were represented with a sphere with a diameter of 50 centimeters, as for a common educational globe, then the thickness of these two atmospheric layers would be less than 2 millimeters.

It is a fact that the growing activities of a constantly and rapidly increasing human population has had a deep impact on the delicate atmospheric blanket that surrounds the earth, allowing the existence of life.

In the last decades, various emergencies regarding the effects of human produced pollutants on the atmosphere have been identified. Initially, warnings were issued on the quality of the air in the proximity of industrial centres or large urban aggregations, but more recently the problems have reached a global scale. Concerns that were raised in the eighties about the reduction of the ozone layer, and the consequent reduction of its ability to filter the highly ionizing UV-rays have been overwhelmed, more recently, by a new planetary emergency commonly known as *global warming*. Excluding some marginal controversy, often driven by biased social and economical interests, scientists all over the world agree on some scientific evidence [7, 23, 63].² about the chemical and physical changes that are happening in the atmosphere and their consequence on climate and other geophysical features:

- There is an evident correlation between the global average temperature and the density of carbon dioxide (CO₂) in the atmosphere. CO₂ tends to increase the global temperature allowing solar rays to penetrate the atmosphere and at the same time reducing the re-emission of infra-red rays from the Earth surface to the space, a process referred as the *greenhouse effect*. Other pollutants, like methane and water vapour, are also greenhouse gases and will have to be more carefully controlled in the future, but the vast usage of fossil fuels and the consequent production of CO₂ has the predominant impact.
- The concentration of CO₂ has reached unprecedented levels in the last 400000

²The bibliography is listed in alphabetically by author's name. The entry number refers to this listing order

years. The CO_2 atmospheric density has been worked out from proxy indicators, that is an indirect measurement, analysing, for example, cores from the Vostok ice shell [40], as illustrated in Figures 1.1 and 1.2. The role of human activities within the framework of the current industrial or post-industrial civilization, that is based on the availability and the exploitation of fossil fuels, as an explanation of the surge in CO_2 density during the last 50 years, is now generally agreed.

- As a consequence, there are clear and rapid climate variations now occurring, like increases in extreme weather conditions, and harsher drought and flood cycles, even in regions normally characterised by a mild climate.
- Some biological and geophysical indicators also confirm the increase in temperature. More tropical species are found in temperate areas and species composition changes are being observed, while the total world ice sheet surface is rapidly reducing in both the ice caps and mountain glaciers. Even discount-

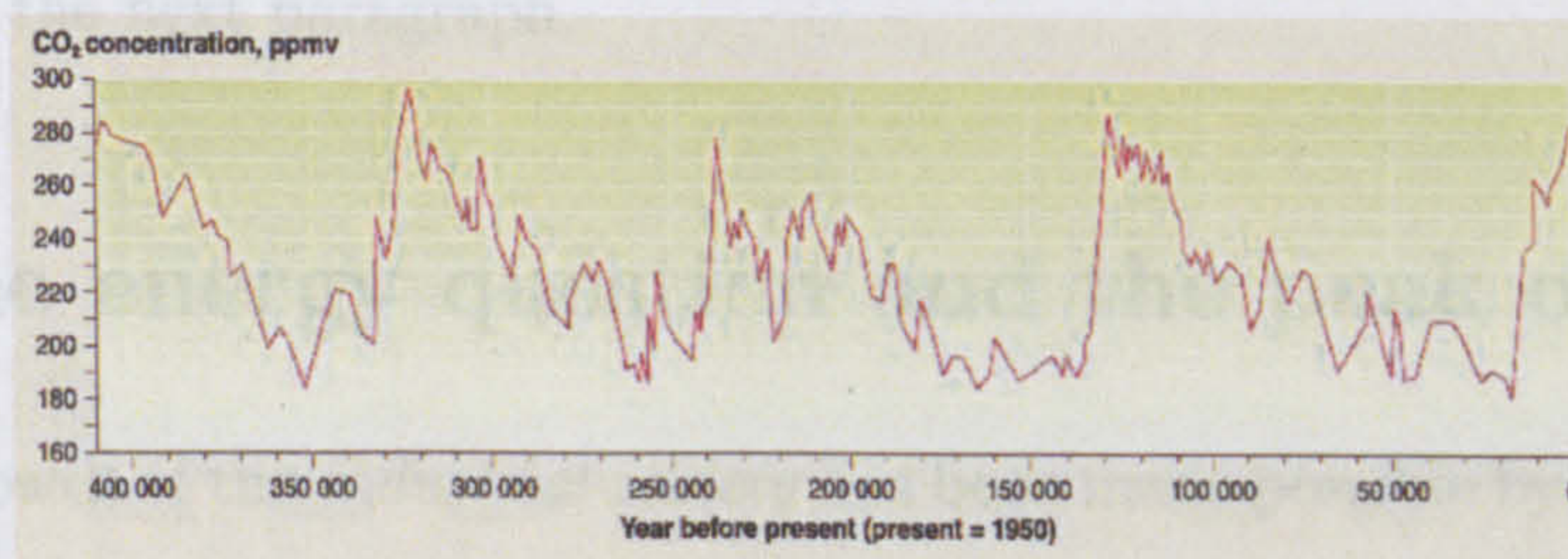


Figure 1.1: Reconstructed carbon dioxide concentration of the last 400000 years [23]

ing the more catastrophic scenarios, described in the press, involving positive feedback phenomena, like the release of CO_2 or methane from oceans or the biomass lying underneath the permafrost, as a consequence of the temperature rise, the picture is alarming enough to encourage a rapid global action. Global Warming is being considered the most severe threat to the human race in the coming years, quoting Sir David King, the former Chief Scientific Adviser to the UK Government [30].

Beside the ecological emergency there are further considerations that urge a change in our energy usage and supply, and if accepted, should convince the ones who

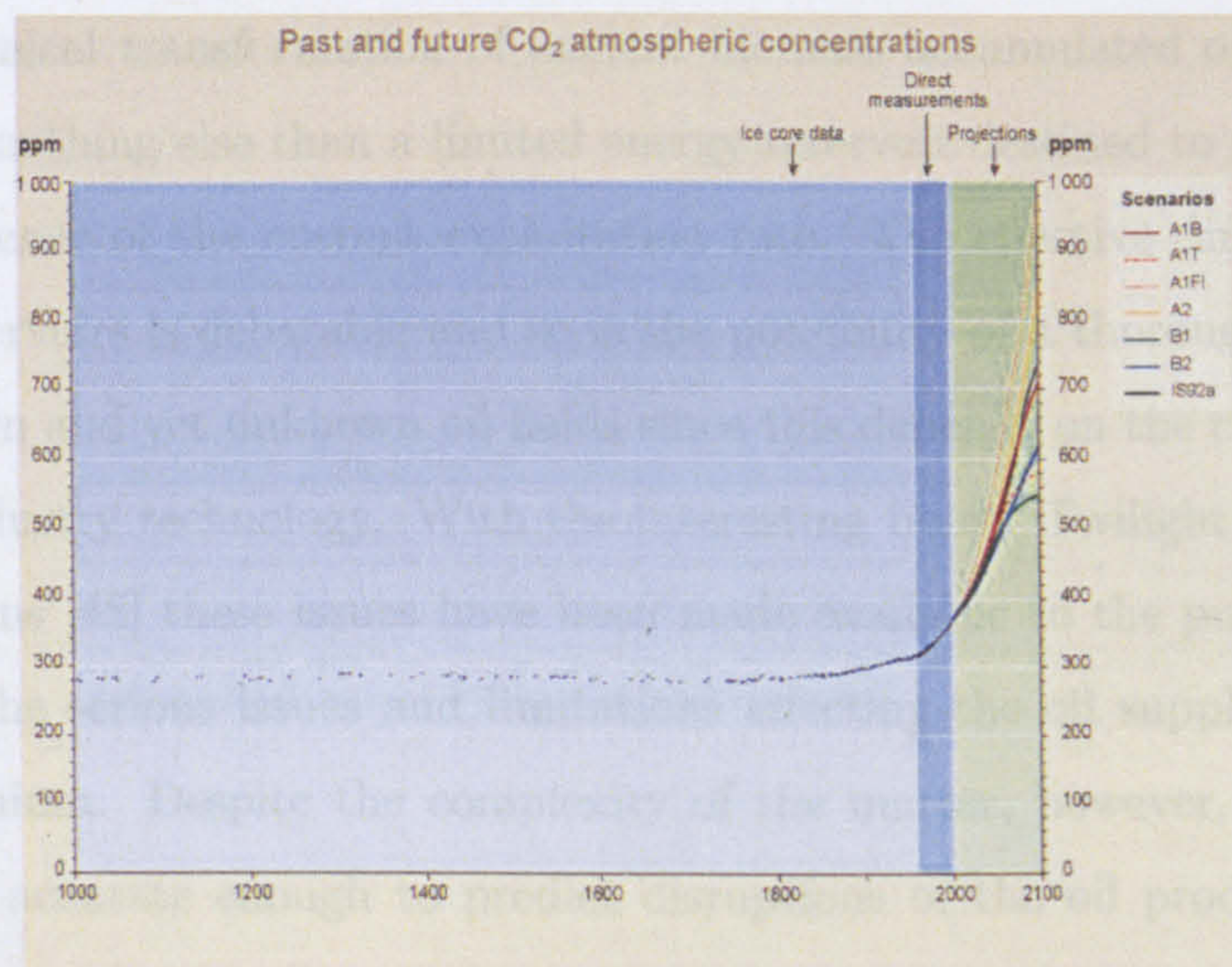


Figure 1.2: Recorded atmospheric carbon dioxide concentration compared with the last 1000 years [23]

are more sensitive to economic reasons rather than environmental ones. These are illustrated in the next paragraph.

1.2 The energy question and the peak oil

The rapid growth of the *industrial society* has been made possible by the large availability of fossil fuels. Coal at first and later fluid fossil fuels, like oil and gas, have powered spectacular economic growth in many countries in the last century. Oil in particular, with its high energy density and flexibility in extraction and transportation, has played a major role in the economic boom, fulfilling about 40% of the total energy consumption to the extent that the global economy can now be referred to as an oil economy.

The economic cost of oil dependency is now a major concern for western governments. The cost per barrel, after recent events in the Middle East exceeded 135\$, a level which is, in terms of “constant currency”, comparable if not higher than the cost in 1971, when the first large scale oil crisis occurred. However, political instability of the larger oil producers is not the only threat to the oil economy.

As is well known oil is a non renewable resources since it is the result of extremely

complex chemical transformation of ancient biomass accumulated over millions of years. Oil is nothing else than a limited energy reservoir destined to rapidly dry up as a consequence of the current exploitation rate. The effective dimension of the world oil reservoirs is debatable and so is the possibility of a thorough exploitation of both known and yet unknown oil fields since this depends on the current and the future oil industry technology. With the interesting book “Twilight in the desert” by M. Simmons [45] these issues have been made available to the public dominion, illustrating the serious issues and limitations affecting the oil supply chain in the third millennium. Despite the complexity of the matter, however, some theories have proved accurate enough to predict disruptions of the oil production rate in some noteworthy historical cases.

In 1956 the geophysicist Marion King Hubbert predicted a coming oil production crisis in the United States with a theory known as the *Hubbert Peak* [29], that was firstly officially published in 1949 [28]. The production crisis occurred punctually in the early 70s and culminated with the events of 1973, the embargo from OPEC (the association of oil producers), whose effects reverberated internationally. According to the Hubbert theory the production in time of any non-renewable resource follows a specific bell-shaped curve characterized by a net peak after which the production inevitably decreases at a rate that depends on the extraction technology. Apart from the quoted case in the USA, the theory had been confirmed by a number of historical cases and the peak observed in several situations. These include the production of whale oil in the 19th century, coal in Pennsylvania in 1925 and, more recently, the production of oil in USSR and in the North Sea in 1990s. The peak is mainly due to the rapid depletion of the cheapest resources and the consequent growth of the investments necessary to discover and exploit the remaining resources. When these are no longer sustainable production, after a brief stationary period, inevitably decreases with a rate that depends on the technology used for the extraction.

The theory has been implemented to predict the global oil peak and it is striking how different studies have led to a similar result. Restricting the study to “conventional oil” supplies, which are those that can be extracted from wells in a non viscous form, the peak of production has been predicted for 2005 while the peak

for the non conventional oil, which is extracted from tar sands, oil shale and bitumen is predicted to be in 2070. The overall peak for the “liquids production”, that is including both conventional and non-conventional is in 2010. There are many publications about global peak oil for example [3, 18].

1.2.1 Solutions to the peak oil

The solutions available to tackle a peak of production of a primary source are various. The first is the geographical transition, that is; the production must be moved to a different location. This is what happened in 1971 when the production was shifted to the Middle East, with dramatic political consequences, like the OPEC oil embargo in 1973 and the consequent production crisis. This option is obviously impracticable for the solution of a production crisis on a global scale.

The second solution is a resource transition, that is the exploitation of non-renewable resource other than oil, like uranium, thorium or other fissile elements. Apart from the risk of catastrophic incidents, nuclear energy has other disadvantages; the first are the problems about treatment and storage of the nuclear waste, resulting in increased costs and outstanding implication on health and environment. The second is the risk of nuclear weapons proliferation, which is particularly worrying in the light of the world political fragmentation of the post cold war era. Furthermore nuclear energy does not have the flexibility of fluid fossil fuels, and does not appear to solve the problem of transport, where fluid fuels are needed, even with the adoption of hydrogen. The utilization of hydrogen as a energy carrier presents problems about cost and efficiency that, at the current status of the technology for both production and utilization of hydrogen from nuclear sources, are unacceptable. Finally, Uranium and other fissile fuels as a non non-renewable resource are subjected to the Hubbert theory and the adoption of this energy resource would simply shift the problems in time.

The third solution is a technological transition, that is the development of technologies allowing the exploitation of renewable energies like direct solar, biomass, wave, tidal currents and, finally, wind. Renewable resources, with the exception of the tides, originate directly or indirectly from the solar radiation, have a com-

pletely different availability curve. This does not decay with time (hence their name) but follows an increasing S-shaped curve, that stabilizes at the saturation of the available surface. Physical or sociological phenomena, presenting natural or intrinsic limiting factors as always happens in nature, are governed or described by Volterra's equations whose solution is a logistic curve, which is precisely an S-shaped curve. Among renewable resources wind energy is, for different reasons, the most immediately available and attractive.

The last mention must be dedicated to nuclear fusion, that for its energy yield and abundance of prime matter, like deuterium or helium, can be considered a renewable energy even though it is technically non renewable. No doubts can be raised about its relative cleanness or its intrinsic safety but the technological challenges involved for the exploitation of this "holy grail" of the energy sources appear to be beyond the current knowledge and technology, to the point that even the most optimistic predictions do not consider a possible successful application, on an industrial scale, before 2060.

1.3 Kyoto protocol

Aware of possible catastrophic consequences of the greenhouse effect, most of the world countries agreed in 1997 to sign a convention of 28 articles for the adoption of measures for the mitigation of carbon emissions [35]. Despite some exceptions like the United States of America, by far the largest polluter *pro capite*, the protocol has been successfully ratified by most of the original signatory countries making the measures mandatory. The protocol specifies various actions to be taken in particular about renewable energies, as stated in article 2:

Each party . . . shall: Research on, and promotion, development and increased use of, new and renewable forms of energy, of carbon dioxide sequestration technologies and of advanced and innovative environmentally sound technologies.

On the basis of the Kyoto protocol, Great Britain released in 2003 the *The Energy White Paper* [13] a document that set explicit emission objectives like a 60 % reduc-

tion in carbon dioxide emissions by 2050 with “real progress in 2020”, that is cutting carbon emissions by 25 million tonnes. The same paper specified “an aspirational target of 20% of the electricity market to be produced from renewable sources by 2020”³.

The emphasis put on the adoption of renewable energy technologies is remarkable and boosts the interest for renewables in general. The document also stresses the role of wind power, with Great Britain having “over one third of Europe’s entire potential for offshore wind energy” (see chapter 4, low carbon generation). The carbon emission targets have ever since become binding at European level (20% for EU, 15% for UK by 2020) and with the *The Energy White Paper 2007* [14] further measures for the achievement of such targets have been outlined. It is stated that the measures to be taken could lead to almost a ten-fold increase in use of renewables from the 2006 level. It is also stated that the 2007 wind generation capacity, on and off shore, will have to increase 10 times to meet the targets, implying that a certain urgency is required since, with no policy change, the renewable energy share in 2020 will be 6%. The measures proposed in [14] include a number of activities as the extension of the Renewable Obligation (see below), the introduction of new financial incentive mechanisms and the provision of long term policy and legislative framework.

For what wind energy is concerned some scenarios considered in [14] depict an even more drastic rise of this electricity generation. Given the inability of other energy sector to deliver the renewable target (transport and home heating in particular) the energy production from wind power could be required to reach 32% of the electricity demand, that is 19% offshore and 12% onshore. The fact that, in the Energy White Paper, the focus has been put on off shore wind generation has a primary

³By an electricity market it is meant the energy supplied electrically in 2020 with no reference to the installed power, which depends on the chosen technology. In this regard, in order to discourage misled (and misleading) arguments against the wind power, it is particularly important to note that wind energy has a capacity factor (see definition on the next footnote) naturally lower than other sources, due to the intermittency of the wind. Consequently, to achieve a certain energy market share, wind power needs to constitute a relatively larger portion of the “installed power”

importance for the research presented in this thesis, as will be explained in the next paragraphs.

With the *Renewable Obligation Order* (RO) Great Britain introduced, in 2002, a practical legislative tool for supporting renewable energy. The scheme places an annual obligation on all licensed electric energy suppliers to buy a certain percentage of their supply from renewable sources. The percentage initially set at 3% in 2002-3 will be raised at 10.4 % in the period 2010-11. The compliance to the RO is monitored by the UK gas and electricity markets regulator (OFGEM), that issues the renewable obligation certificates (ROC), in the measure of 1 ROC for every MWh produced from renewable source. The certificates, banked in each year, can be sold to operators which need to fulfil their obligation, creating for “green” producers a further revenue stream, balancing the intrinsically higher cost of the electricity from renewable source and making investment in renewable energy production more competitive.

The *White Paper 2007* sets out proposals to reform the RO. The necessity of reforming the RO originates from the high cost of some renewables, i.e. offshore wind energy, which can not be supported effectively by the current RO schemes. The RO reform proposals include:

- Raise of the RO to 20% for those technologies whose growth justify the rise.
- Breaking the link to the retail price index to keep the overall costs to consumers broadly similar to those within the existing projections.
- proposals to band the Obligation to differentiate levels of support to renewable technologies to maximise the contributions from established and emerging technologies.

The emphasis put by the UK government and EU institution to wind power is a clear indicator of the opportunity represented by this energy source. Challenges are also outlined, as offshore wind cost, and these need to be thoroughly addressed for a rapid development.

1.4 Wind Energy and Reliability

Among renewable resources wind energy is, because of the relative maturity of the technology, the most immediately available, constituting in some countries like Germany, Denmark and Spain a tangible reality. Apart from some early pioneering experiments, the first development of large wind turbines on vast scale took place in United States and Denmark, following the “Arab Oil Crisis” in 1973, supported by government subsidies like the U.S. Federal Wind Energy Program (FWEP), that produced, in the United States, favourable economic conditions for the wind energy conversion, such as the Public Utility Regulatory Policies Act (PURPA) of 1978. PURPA integrated research programs aimed at the development of large wind turbines like the U.S. Federal Wind Energy Program launched in the 1974. The development program eventually resulted in the development of 13 small wind turbine designs [21], 4 large and a number of vertical axis wind turbines in a period of seven years, until 1981.

Most of the funding was concentrated on the development of multimegawatt wind turbines, like the MOD-0, MOD-1, MOD-2, MOD-5 and MOD-6 (Figures 1.4 and 1.5), that were inspired by a two bladed German design by Ulrich Hutter, illustrated in figure 1.3. The Hutter design was considered more likely to work reliably from the start, because the previous experience accumulated on this configuration. However the teetering hub, featured in the original project, was implemented only in the MOD-2 prototype, showing that in reality the two bladed concept was not well understood at that initial stage. The teetering hub is an apparatus that was vital for two bladed machines of older aerodynamic technology and allowed the original Hutter machines to withstand the huge cyclic dynamic loads, induced by the passage of the lower blade on the tower “shadow” [22]. In the light of modern reliability engineering it can be noted that the application of reliability techniques as FMECA, this macroscopic design deficiency could have been avoided.

As a consequence, the reliability of the entire MOD series (from the word *modification*) has never proven to be satisfactory to the point that none of the prototypes have been able to reach a commercial application. Smaller designs, like the Enertech 44/15, a 40-60 kW, a three bladed machine, showed a much higher reliability,

December 6, 2008



Figure 1.5: The MOD-5, the last model of the WEP, rated at 3.2 MW, 1987 [24]

but despite that they did not have the same success as the MOD series turbines.

Figure 1.3: The wind turbine designed by Ulrich Hutter, in the 1950s [26]

In the early 1980s, as a consequence of a change of the political panorama with the advent of the Reagan administration, the US Federal Program was abandoned for more financially attractive energy tax credits. Overestimating the maturity of the technology, the new financial tools had the effect of stopping the development of new wind turbines favoring the direct acquisition of existing designs, aiming at the immediate production. Only four new turbine were developed in the period. The MOD-5 and MOD-6 were already decided, were far more reliable technology.

Interestingly the tax credits were aimed at the energy produced rather than the energy produced as the importance of the quality factor was not well understood for gen-



Figure 1.4: A milestone of the wind industry; the MOD-2, rated at 2.5 MW, 1981 [25]

The capacity factor of a energy producer is the ratio between the energy effectively produced in a period and the energy that it would be produced if the converter worked at its nominal power



Figure 1.5: The MOD-5, the last product of the U.S. FWEP, rated at 3.2 MW, 1987 [24]

but despite that they did not achieve a energy production success comparable to the MOD series machines. As a result the program could be defined as a success, not so much for the number of designs effectively marketed, but for the engineering experience gained.

In the early 1980s, as a consequence of a change of the political panorama with the advent of the Reagan administration, the US Federal Program was abandoned for more financially attractive energy tax credits. Overestimating the maturity of the technology, the new financial tools had the effect of stopping the development of new wind turbines favouring the direct application of existing designs, aiming at the immediate production of energy, to the point that only four new turbine were developed in the period between 1981 and 1988. So wind turbines like MOD-2, MOD-5 and MOD-6 were developed and put in service but their design, as has been already elucidated, were undermined by a lack of maturity or early failures as in the reliability terminology.

Interestingly the tax credits were based on installed power rather than the energy produced as the importance of the capacity factor was not well understood for generation from renewable sources ⁴. The absence of governmental control in the US

⁴The capacity factor of a energy converter is the ratio between the energy effectively produced in a period and the energy that it would be produced if the converter worked at its nominal power

on the quality of the designs together with shortened development phase, due to financial pressure, had the effect of utilising market-ready turbines designs with no attention to their reliability or availability. As a result, the Danish wind turbine concept took over the market because, in spite of its lower efficiency, it had a well understood and more reliable design. The concept was the three bladed upwind configuration, with an electrically or hydraulically driven yaw mechanism and an asynchronous generator, directly connected to the grid. This concept was derived from the Gedser mill design illustrated in Figure 1.6. The Danish concept, although improved with further important modifications, such as a variable speed drive asynchronous generator, is the concept that is dominating the scene nowadays.

Interestingly the Danish concept has been developed by another government funded project, the program WEGA I of the European community, of which the Tjiaereborg 2MW , shown in Figure 1.7, is the most important example.

The Danish concept has proven to be the winning technology and modern large WTs are all directly derived from it. Differences between modern WTs concern the control system, that can be active or passive, pitch or stall according to the measures taken to adjust the blades position and the internal electromechanical configuration. There are three main electromechanical configuration that are currently competing; fixed speed with induction generator, variable speed with either induction machine or Doubly Fed Induction Generator (DFIG) and a partially rated converter, finally direct drive with synchronous generator and fully rated converter.

Such a combination of control technology and electromechanical architecture is called the “concept”. One of the objectives of this thesis is, within the limits of the available failure data, to compare the reliability of the various concepts and the

for the same period. In the case of renewable energy converters this ratio depends also from the availability of the source of energy, the wind in the case of the wind turbines. On the other hand the case of generation from fossil fuel, which can rely on a guaranteed source of energy, is different because the capacity factor is mainly determined by its availability, that is the probability of being in service at a certain time. Thus, while for a traditional generation units a typical value for the capacity factor is about 60%, for wind turbines a capacity factor of about 35% can be considered good.



Figure 1.6: The progenitor of the Danish concept the “Gedser mill”, rated at 200 kW, early 1960’s [64]



Figure 1.7: A development of the Danish concept WEGA 1; the Tjaereborg rated at 2MW, 1985 [70]

following chapters some consideration about the reliability of the various concepts will be outlined.

1.5 Going off

In more recent years wind energy has seen a rapid growth in some countries of northern Europe. Generally the wind turbines designs have reached a level of maturity. However other problems like the noise produced by the blades or the visual impact of the turbines are still an issue. However other issues have arisen, such as the impact of the turbines on the environment. This is often not accepted by the local population. In some cases the turbines represent a great opportunity of further development and, as a matter of



Figure 1.8: A modern Indirect Drive WT, Vestas V90, rated at 3 MW, 2007 [68]

these sites and its consequent impact on maintenance and repair costs constitutes the most important barrier to the achievement of this objective. It can be estimated that the cost for off-shore operation is two times the cost of the same operation for on-shore wind turbines [59,60]. This makes the role played by the reliability of the future turbines crucial.

1.6 Original contr

Having in mind the crucial role of wind turbines for a further development of wind energy the reliability of these machines is a key factor. Due to the high level of confidence required in the design and construction of these machines, the information available is often limited. This is particularly true for the entire wind energy industry. In the academic environment tends to produce highly specific and detailed analysis tools that cannot be implemented outside specific cases.



Figure 1.9: A modern Direct Drive WT, Enercon E82, rated at 2 MW, 2007 [69]

cluding the failure of thousands of units represents a positive step forward in knowledge, in comparison with the current status of the publicly available informa-

following chapters some consideration about the reliability of the various concepts will be outlined.

1.5 Going off-shore

In more recent years wind energy has experienced an impressive growth in some countries of northern Europe, as well as Spain and Asia. Generally the wind turbines designs have reached a discrete reliability level and some problems like the noise produced by the blades or the power control have been overcome. However other issues have arisen, such as the visual impact of large multi-megawatt machines which is often not accepted by the local communities. For this and other reasons marine locations represent a great opportunity of further development and, as a matter of fact, the future of the wind energy. It is known that costs and difficult access to these sites and its consequent impact on maintenance and repair costs constitutes the most important barrier to the achievement of this objective. It can be estimated that the cost for off-shore operation is ten times the cost of the same operation for on-shore wind turbines [59,60]. This makes the role played by the reliability of the future turbines crucial.

1.6 Original contribution of this thesis

Having in mind the crucial role of reliability analysis of wind turbines for a further development of wind energy this thesis aims at supplying solid reliability figures. Due to the high level of confidentiality, to which failure data are subjected the information available is often fragmentary and anecdotal with a damaging effect for the entire wind energy industry. On the other hand, the academic environment tends to produce highly specific data manipulation and analysis tools that cannot be implemented outside specific cases.

The systematic analysis of large failure data bases of actual wind turbines, including the failures of thousands of units represents a palpable step forward in knowledge, in comparison with the current status of the publicly available informa-

tion. The extension of the databases analysed is novel so that some deficiencies of the data are overcome by adjusting the width of the population of WTs of interest, using analysis.

The thesis provides a powerful mathematical tool, for the definition of solid reliability figures from the, sometimes incomplete, WT databases, and the detection of possible reliability time trends affecting the data. The application of reliability growth methods outside the reality of reliability growth programs has proven challenging and interesting. Thus, the thesis is able to supply a mathematical model which is relatively simple and that has been tested on both real and simulated data.

Chapter 2

Literature Review

2.1 Introduction

One of the aims of this thesis is to “crystallise” the knowledge about the reliability of wind turbines by presenting and comparing failure rate figures from different sources. Accessing the information on the reliability of wind turbines, as well as of other large machinery, is a difficult task that has been illustrated above. This chapter reports an overview of the current knowledge about this topic to the best of the author’s knowledge.

In most studies, for example the work carried out in the Netherlands within the DOWEC project, it turns out that a deeper understanding of the reliability of the wind turbines is necessary. Section 2.3 is dedicated to a review of the vast output from the DOWEC project. The comparison of the reliability of wind turbines subassemblies with the reliability of similar pieces of equipment in traditional installations can also be illuminating and, for that reason, some industrial failure data are also presented. The industrial data are extracted from the IEEE “Gold Book” [61], which refers to traditional applications of electromechanical machinery, and have been reviewed in section 2.4. Finally section 2.5 provides a qualitative view from wind industry experts of wind turbine reliability.

2.2 An Early Document

The Netherlands Energy Research Foundation (ECN) has produced an interesting early document about the reliability of wind turbines [44]. The paper, illustrates results of the effort made by ECN to introduce non-deterministic design procedures, as the Probabilistic Safety Assessment, a method which includes analysis methods such as FMECA, Event Sequence Analysis and Fault Tree Analysis. In this document the probabilistic analysis, is based on reliability figures derived from the collection of data concerning 11 Lagerwey 15/75 turbine model, over about 26 years. The turbines are rated at 75 kW and interestingly are defined as “medium size” wind turbines, a definition that collides with the classification of the modern wind turbines. The reliability figures are summarised in Table 2.1

The classification of failure is made on the basis of failure modes, identified by their initiating event, rather than turbine parts, and the figures are interesting. According to Table 2.2, failures of both inverter and grid dominate the reliability of the WTs considered, with failure rate figures that are not dissimilar from the figures of current turbines, as will be shown in Chapter 4. The attention inevitably falls onto the reliability figure supplied for the inverter of the machine. Although the converter size and technology is inevitably much different from the technology of modern inverters (power electronic converters), being made of line commutated thyristors rather than pulsed modulated IGBTs, the observation of the failure rate is interesting. The failure rate figure for the Lagerwey 15/75 is in fact comparable to the failure rate of modern WTs and one can conclude that the reliability improvement of modern WTs is striking giving the higher rating complexity and operational advantages achieved.

Wind turbines reliability studies have been carried out in two other research institutes, namely the Risø National Laboratory of the Technical University of Denmark and the Sandia National Laboratories in the USA. Both institutions have extensively studied WTs reliability issues and published a great number of documents. However, since for both the institutes most of the research has been focused on the rotor, blades in particular, the review of the produced material will not proceed further.

Initiating Event	Failure Frequency [failure/WT/year]		
	Total	Shutdown	Partial Damage
Overspeed	0.650	0.650	0.0032000
Excessive vibration	0.950	0.930	0.0230000
Inverter temperature	0.038	0.038	0.0000042
Inverter Control	0.230	0.220	0.0096000
Grid failures	3.120	2.980	0.0001200
Generator overload	0.420	0.400	0.0002100
Total	5.410	5.210	0.0280000

Table 2.1: Reliability figures in [44]

2.3 DOWEC

2.3.1 Introduction to DOWEC

The necessity of improving the reliability of the wind turbine, in view of their offshore installation, is demonstrated by a series of publications [55, 59, 60] produced from the Dutch Wind Energy Converter program (DOWEC).

The project, that involved various Dutch institutions and firms, aimed at developing and delivering a tested large off-shore wind turbine. The driver for the project was the economic optimization of various aspects of the offshore wind technology, like the selection of the most suitable wind turbine architectures, the selection of large wind farm layouts and the definition of the best operation and maintenance (O&M) strategies. Some key concepts that emerge from the papers produced by the program [20, 59] and can be summarised as follows:

- The reliability of offshore wind turbines is crucial to the final cost of energy.
- The reliability of the current onshore wind turbines is inadequate for an economic offshore installation.
- Reliability data for wind turbine subassemblies was difficult to determine at the time of the DOWEC work.

According to the results of the availability models developed from DOWEC, the reliability of wind turbines needs to be improved because of the difficult accessibility of marine locations which raises the cost of delivered energy to unacceptable levels. This is a consequence of the loss of generation during the periods needed to reach and repair each offshore wind installation. The cost of O&M actions is also higher for offshore installations, due to the high cost of the crane vessel, necessary for both installation and some corrective maintenance operations. In these DOWEC papers, particularly, the models for the optimization of the O&M actions were based on reliability figures reproduced from onshore experience which this thesis wishes to analyse critically.

2.3.2 DOWEC Results

In an early paper [59], produced by one of the major contributors to the project, the cost of O&M activities were estimated to be the 30% of the final cost of the energy, assuming an availability ¹ of 98%. Interestingly, these figures appear unchanged also in most recent publications. The O&M cost mode, in the DOWEC project, has been implemented through Monte Carlo simulations, and based on reliability figures extracted from [16], a publication that uses failure data of wind turbines operating along the coast the German region of Schleswig-Holstein, for the year 1996. The original figures were then improved by 25%, assuming the possibility of achieving such an improvement “without major modification of the design”, and the values that were ultimately used are summarised in Table 2.2.

Subassembly	failure/WT/year
Blades	0.44
Gearbox, Generator and Yaw	0.14
Electronics and Control system	0.29
Hydraulics	0.22
Electrics	0.37
Other	0.33
Total	1.79

Table 2.2: The failure frequencies adopted for the DOWEC project [59] from one year of real data

Thus the indications of one single annual data record, for the failures in an arbitrary year, have been generalised and adopted for the DOWEC model. Since the wind turbines are subjected to highly variable conditions, the failure figures above need a verification suggesting that further research on this subject can be made.

In [60], a paper produced in 2002, the same principal author produced a RAMS ²

¹The availability $A(t)$ of a system is the probability of being able of performing the required function at a certain time

²RAMS, Reliability Availability Maintainability Safety

analysis on six wind turbines concepts of different electrical and mechanical architecture, as summarised in Table 2.3.

The reliability of the concepts was assessed using failure frequencies reported in Table 2.4. The values, shown in the offshore column of Table 2.4, were determined by expert brainstorming, in the absence of real data. Expert brainstorming is valuable as a first approach to define reliability figures, but for a thorough investigation like RAMS analysis, it would be valuable to deepen the information with measured reliability figures, especially for offshore wind turbines for which high reliability is important. The data of Table 2.4 have been subjected to two further corrections. Firstly the failure frequency of some of the subassemblies have been reduced, assuming an improvement of reliability can be achieved by:

- selection of the most reliable implementation
- adding redundancy
- using military standard (MIL-STD) components

Table 2.4 shows the original reliability data for subassemblies in the left column and the reduced data on the right.

Secondly for the determination of failure frequency of the concepts, a further modification has been introduced, introducing a correction for each subassembly failure frequency.

The resultant figures are summarised in Table 2.5, where they have been grouped by electrical and electrical and mechanical architecture and maintenance category. The categories refer to the ease of repair of the sub-assemblies, a feature that is quantified by the so called *repairability* related to qualitative aspects like personnel, equipment, time and logistic that are needed for repair action. From the value of the total concept failure frequency in Table 2.5 the figures appear to be rather optimistic.

The conclusions are that, in spite of such low failure frequencies, the resultant reliability is considered insufficient in the more remote and harsh marine locations. Two other conclusions are worthy of mention, and reported here:

	Turbine Concept					
	Base Line	Advanced	Robust	Stall	Smart	Direct
				teeter	stall	drive
Power control	active stall	pitch	passive stall	passive stall	smart stall	pitch
No. of blades	3	3	2	2	3	3
Rotor speed	constant/ double	partially variable	constant variable	double variable	variable	variable
Inverter	none	30%	none	full	full	full
Tower	tubular	tubular	tubular	truss	tubular	tubular
Foundation	poles	poles	monopile	gravity based	poles	poles
Rotor	upwind	upwind	upwind	downwind	upwind	upwind
Hub	fixed	fixed	fixed	fixed	fixed	fixed

Table 2.3: The wind turbine concepts featured in [60]. The DOWEC project has been the progenitor of the systematic study of the WT concepts.

Subassembly	Onshore failure frequency [failure/WT/year]	Offshore failure frequency [failure/WT/year]
Shaft & Bearings	0.02	0.02
Brake	0.05	0.05
Generator	0.05	0.05
Brake	0.05	0.05
Electrics	0.14	0.10
Blade	0.16	0.11
Yaw System	0.23	0.15
Blade tips	0.28	0.14
Pitch Mechanism	0.28	0.14
Gearbox	0.30	0.15
Inverter	0.32	0.16
Control	0.34	0.17
Total	2.20	1.28

Table 2.4: A further set of reliability data used for the DOWEC project [60]. Onshore data, from which offshore data are derived from, are the results of expert brainstorming

Maintenance categories	Base Line	Advanced	Robust	Stall	Smart	Direct
Heavy, external crane	0.17	0.17	0.14	teeter 0.18	stall 0.17	drive 0.18
Large, internal crane	0.45	0.46	0.33	0.47	0.46	0.47
Small, 48 hrs repair time	0.15	0.31	0.20	0.34	0.34	0.31
Heavy, 24 hrs repair time	0.22	0.24	0.22	0.22	0.24	0.24
Total concept	0.99	1.18	0.89	1.21	1.21	1.20

Table 2.5: The failure frequencies adopted in [60] in failure per years as modified to reflect electrical and mechanical concepts and maintenance category

- “An increase by a factor of two of the reliability of wind turbines can be achieved through reasonable effort and cost . . .”
- “A yearly failure frequency of around one for each turbine will prevent the application of such designs to more demanding less accessible sites”

In [55] the DOWEC project participants attempted to establish more reliable failure figures by investigating a number different surveys, some of which are publicly available, namely: Windstats, LWK, WEMP and EPRI. The first two data set will be described in full in the next chapter, since they constitute the main source of data that has been analysed in this thesis.

2.3.3 Conclusion of the DOWEC Report

Research carried out at high level, by different research institutions, has proven valuable to produce WTs reliability or availability studies and models. One can conclude from the above that it is questionable to base availability estimates on reliability figures extracted from a single year of generation or a single survey.

One may also conclude that there are risks in manipulating reliability data by subjective judgements, such as brainstorming, if such a figures are to be relied upon.

The basis of this thesis will be to try and build upon this earlier work and place the analysis of wind turbine reliability data on a firm analytical data.

2.4 Industrial Failure Surveys

In work carried out at Durham University, Knowles [31] compared the failure rate of some of the wind turbine subassemblies, extracted from the work illustrated in this thesis, with the failure rate of similar subassemblies coming from the industry as reported in various surveys.

Figure 2.1 reports the average failure frequency of four subassemblies, namely Generator, Hydraulics, Gearbox and Mechanical Brake comparing industrial failure data with the failure frequencies of two wind turbines survey, WindStats and LWK. The first three columns of each subassembly (red, blue and yellow column) refer

Subassembly	Failure Frequency [failures/WT/year]
Generator	see Table 2.7
Hydraulics	0.090
Gearbox	0.155
Mechanical Brake	0.037

Table 2.6: Industrial failure frequencies of some subassemblies extracted from [31]

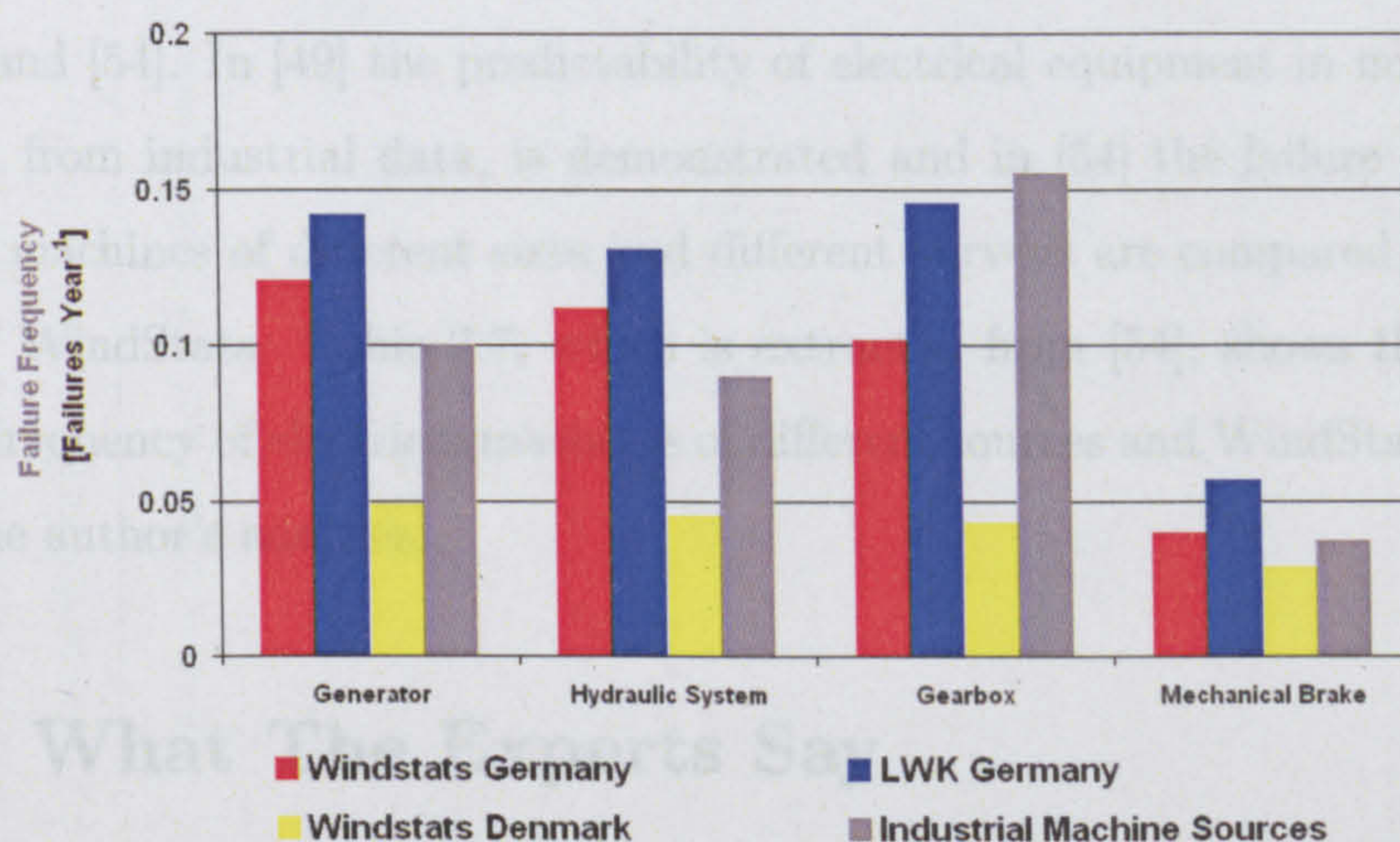


Figure 2.1: Wind turbine subassembly failure frequencies compared with industrial data of Table 2.6

to WindStats Germany, LWK and WindStats Denmark respectively. These are the three data bases that constitute the basis of this thesis and will become familiar in following chapters. The failure frequencies here reported are the fruit of the work of the author. The fourth column of Fig. 2.1 (grey column), as well as data of Table 2.6, reports an average failure frequency of industrial data, that is in traditional applications other than the wind industry including data from [61], the IEEE “Gold Book”. The industrial data are extracted from [31]. One observation that emerges from Knowles work is the limited number of statistics considered in other industrial surveys. For example the IEEE Gold Book, which is widely established and used as a standard, averages the failure data of merely 31 generators. A situation that is rather different from WindStats Germany data, where up to 4000 wind turbines are considered. Nevertheless the traditional application of electrical machines, as reported in the Gold Book, benefit from a more carefully controlled environment and consequently the data would be less volatile. In this report failure data of system installed in the field, as wind turbines are, can be considered potentially subjected to random events, as weather, and consequently more volatile.

The reliability of electrical equipment has been extensively considered by Tavner, in [49] and [54]. In [49] the predictability of electrical equipment in military applications, from industrial data, is demonstrated and in [54] the failure frequency of electric machines of different sizes and different surveys are compared with the results of WindStats. Table 2.7, which is extracted from [54], shows the compared failure frequency of electrical machines of different sources and WindStats, as results from the author’s analysis.

2.5 What The Experts Say

When reliable failure data of a certain system are not available, expert brainstorming is an effective alternative method for the estimation of reliability figures. After all an experienced engineer should be able to design a reliable system without rigorous reliability analysis. For the purpose of this thesis, it would be valuable to illustrate the perception of experts, who are professionally involved in the field of the wind

Typical measured failure rates and for electrical machines obtained from the literature

Machine Type	No. of machines	Machine-years	No. failures	Failure Frequency [failures·years ⁻¹]	MTBF [h]	Source of Data
Large Steam Turbines Generators	Not Known	762	24	0.0315	273,750	Dickinson 1974 [61]
Induction Motors 0.6 - 15 kV	Not Known	4229	171	0.0404	216,831	Dickinson 1974 [61]
Induction Motors > 200 hp	1141	5085	360	0.0707	123,765	O'Donnell 1985 [61]
Induction Motors > 100 hp	6312	41614	1474	0.0354	247,312	Albrecht 1986 [2]
Induction Motors > 11kW	2596	25622	1637	0.0639	137,109	Thorsen 1995 [56]
Wind Turbines Generators	643	5173	710	0.0400	219,000	Tavner, Van Bussel, Spinato 2006 [53]

Table 2.7: Comparison of electrical machine failure frequencies as reported in [54]

power generation, have about the reliability of wind turbines.

The author has interviewed nine high level professionals of different background, academic and industrial, by submitting a questionnaire that has been prepared *ad hoc*, with the intention of “take the pulse” about the perceived and desired reliability of wind turbines. The questionnaire, which is shown in appendix C, consisted of 13 questions concerning three general issues; current status of WT reliability and availability, reliability trend and failure modes and expected reliability for future offshore application of WT. This section shows the outcome of such an investigation.

2.5.1 Current Turbines Reliability and Availability

The first part of the questionnaire focused on the perceived reliability and availability of current onshore wind turbines. Presenting availability and reliability on the same section has had the scope of clarifying the difference between the two quantities. Reliability is related exclusively to the frequency of failures, and not to their severity, however it is often influenced by qualitative considerations, when quoted outside rigorous investigation. On the other hand availability is partially affected by the severity of failures, which influences downtime and hence the probability of the system to be operative at a certain moment t . In the absence of more specific information about the failures occurring, downtime is certainly a good indicator of the severity of the failure. In the first section of the questionnaire, availability and reliability concepts are referred together, in order to make the interviewees aware about the formal difference between the two concepts.

The interviewees were asked to answer to the following questions:

1. What in your experience is the overall average availability of large (> 1 MW) onshore wind turbines?
2. What in your experience is the overall failure rate, in failures per turbine per year, of large (> 1 MW) onshore wind turbines?
3. What is the “useful life” in years of onshore wind turbines?

4. Among the following wind turbine subassemblies (see Table 2.11 for options), which in your opinion is the least reliable?
5. Indicate what is the most common failure mode or root cause for the subassembly chosen as the least reliable above.

Tables 2.8 to 2.12 summarise the answers to the above questions. The response n.a. signifies no answer. Some numbers of answers, including the category “n.a.”, do not sum to 9, the number of experts interviewed, because of the possibility of multiple choice for that specific question.

Availability [%]	number of answers
<90	1
90 - 95	1
95 - 97	4
>97	1
n.a.	2

Table 2.8: Q1 - Current Onshore WTs Availability

Failure Frequency [failures/WT/year]	number of answers
<0.6	1
0.6 - 1	3
1 - 1.5	1
>1.5	3
n.a.	1

Table 2.9: Q2 - Current Onshore WTs Failure Frequency

Table 2.8 gives a clear indication of current onshore WT availability, consistent with the availability declared by many operators in operational reports. The perceived failure frequency of Table 2.9 is dispersed over a larger range of values. This is an indication that a systematic approach is necessary. From the distribution

Useful Life [years]	number of answers
<10	0
10 - 12	1
12 - 14	2
>14	4
n.a.	2

Table 2.10: Q3 - Useful Life

of answers about the expected “useful time” (Table 2.10), it appears that a life of more than 14 years is expected from current wind turbines.

Subassembly	number of answers
Hydraulic system	0
Generator	1
Transformer	1
Gearbox	4
Pitch control	1
Blades	1
Converter	2
Electrics	1

Table 2.11: Q4 - Least Reliable subassembly

Given the subject of this thesis questions 4 and 5, the answers to which are summarised in Tables 2.11 and 2.12 respectively, constitute an important part of the survey. The answers to question 4, about the least reliable subassembly are dominated by the gearbox subassembly. As it will turn out from the next chapters, the gearbox is in reality not the least reliable subassembly. Issues about the severity of any failure occurring to this subassembly are not in discussion, nor are the costs involved in maintaining and repairing such a vital mechanical part, but, as will be shown below that other subassemblies such as “electrics” show a higher frequency of failures. An interesting answer states that the main transformer is

Observed failure modes

Transformer motion causing insulation failure
 Lightning causing planet bearing failure, blade loss
 Bearing failure
 Gearbox misalignment
 Pitch rate or asymmetry error
 Lack of knowledge
 Bearing design, weight saving in bearing design
 n.a. (2 answers)

Table 2.12: Q5 - Failure modes considered to be important

the least reliable subassembly. Typically transformer failures are included into the electrics subassembly, along with failures of many other electrical parts or components. Data are seldom detailed enough to show the specific failure frequency of the main transformer, which is an expensive part of any electrical power system. The converter is defined the least reliable subassembly in two cases.

Concerning the failure modes bearing dominate the scene and misalignment problems emerge in one case. In [11], it is stated that misalignment and bearing failures are strictly interconnected and, in many cases, the former cause the latter. The failure mode of pitch control subassembly can be due to either asymmetry or pitch error indicating that the control system may be at fault and that could have a software origin.

2.5.2 Reliability trends

For repairable systems, especially larger and more expensive ones, subjected to a continuous development, reliability shows a dynamic behaviour with time. In chapter 3 the bathtub curve for both repairable and non repairable systems, or sets of systems, will be explained. The bathtub curve is a conceptual and mathematical model that represents three different phases of engineering systems dynamic behaviour. Since the investigation of reliability trends of wind turbines constitute an

important part of this thesis, the second part of questionnaire attempted to understand the experts perception of reliability trends, by proposing three reliability trends, representing the bathtub phases, namely; improvement, constant trend and deterioration. It is known that reliability analysis are typically made on the basis of average failure frequencies, therefore the second part of the questionnaire was characterised by the following questions:

6. Representing the failure rate as a function of time, which of the graphs below, in your experience, would best represent the failure pattern of a wind turbine gearbox?
7. Can you briefly justify the reasons that determine the graph chosen above?
8. Repeat points 6 and 7 for the generator.
9. Repeat points 6 and 7 for the blades.

The interviewees were asked to associate the perceived failure rate trend of three key subassemblies as gearbox, generator and blades, with three continuous curves that are characterised by a decreasing, constant and increasing trend respectively, as shown in Fig. 2.2. Answers are reported in Tables 2.13 to 2.18.

Trend	Number of answers
Improving	5
Constant	0
Deteriorating	2
n.a.	2

Table 2.13: Q6 - Gearbox failure trend

It is surprising how in many cases the gearbox subassembly has been considered being in the early failures phase. Wind turbine gearboxes have dominated the attention of designers in the past because of the severity of failures concerning this subassembly, and it should be now be “mature technology”. It will be demonstrated from the two sets of data analysed, WindStats and above all LWK (see chapter 4 for

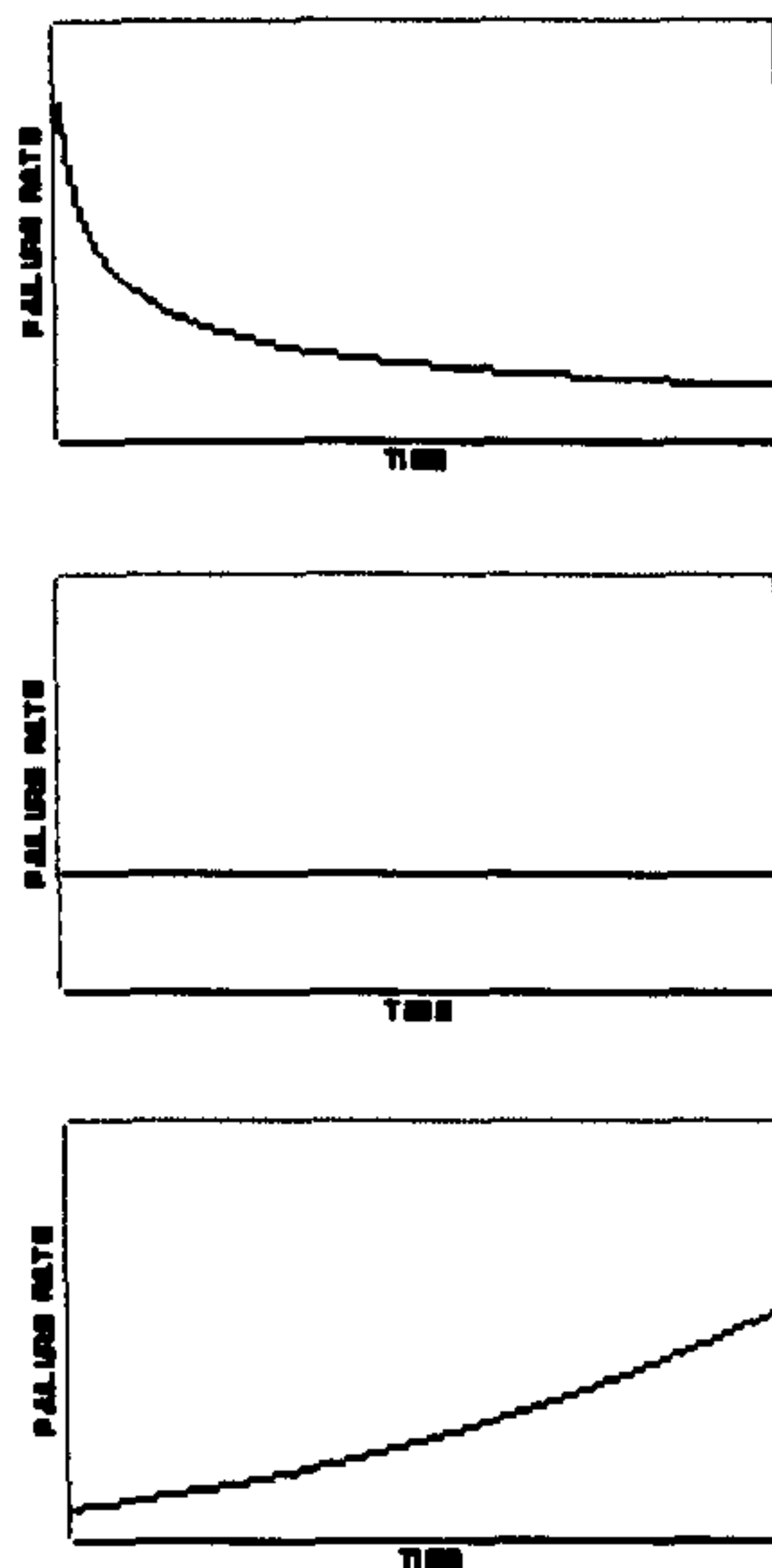


Figure 2.2: The three proposed failure trends. The figure are generic and give a visual impression of the failure trends.

Case	Reason
Improvement	Misalignment and teething problems solved
	Manufacturing errors
	Short test Period
	Not initially robust design
Deterioration	Rapid ageing
	Wear

Table 2.14: Q7 - Reasons for gearbox failure trend

Trend	Number of answers
Improving	3
Constant	1
Deteriorating	4
n.a.	2

Table 2.15: Q8a - Generator failure trend

Case	Reason
Improvement	Misalignment problems solved (2 answers)
	Manual labor induced failures solved
Constant	Material technology improvement
Deterioration	Bad lubrication of bearings
	Bearings
	Wear, stator-rotor contact
	Mechanical failure

Table 2.16: Q8b - Reasons for generator failure trend

Trend	Number of answers
Improving	2
Constant	4
Deteriorating	3
n.a.	0

Table 2.17: Q9a - Blades failure trend

Case	Reason
Improvement	Manufacturing improvement
	Material technology improvement
Constant	Random nature of lightning
	Random overloads
	Random nature of weather (2 answers)
Deterioration	Fatigue (2 answers)
	Wear

Table 2.18: Q9b - Reasons for blades failure trend

further detail). that a substantially different situation is shown. Conversely generators are considered subassemblies subjected to rapid deterioration, while blades, are dominated by failure events with a constant intensity. From the answers in Table 2.18 it is clear that the random nature of atmospheric events is thought to dominate the failures of the blades. The consideration of these results needs to be deepened in subsequent chapters, where the results of a mathematical model analyse of reliability trend have been implemented.

2.5.3 Offshore Turbines Desired Reliability

Finally the experts were asked to give their opinion on the desired reliability and availability for future offshore turbines, by submitting the following questions.

10. Comparing direct and indirect drive turbines, which do you consider the most reliable?
11. From the reliability point of view, what would you consider to be the main obstacle to the installation of the wind turbines in an offshore environment?
12. What availability, in your opinion, should offshore wind turbines be trying to achieve?
13. What, in your opinion is the maximum economically acceptable failure rate, in failures per turbine per year, for offshore installed wind turbines?

Trend	Number of answers
Direct drive	2
Indirect Drive Fixed Speed	4
Indirect Drive Variable Speed	0
n.a.	3

Table 2.19: Q10 - Most reliable concept

Reason
Harsher wind conditions
Increased stress on foundation
Corrosion
Increased dynamic loads on the drive train
Scaling effects

Table 2.20: Q11 - Main obstacle to offshore installation

Availability [%]	number of answers
<80	0
80 - 85	1
85 - 90	1
90 - 95	3
>95	3
n.a.	1

Table 2.21: Q12 - Desired offshore reliability

Failure frequency [failures/WT/year]	number of answers
<0.5	0
0.5 - 0.75	2
0.75 - 1.0	1
1.0 - 1.5	2
>1.5	1
n.a.	3

Table 2.22: Q13 - Economically acceptable offshore failure frequency

2.6 Availability figures

The ultimate objective of improving the reliability of wind turbine is to achieve a high WT availability, which is strictly correlated to the economic performance of the wind power plant and, for this reason, of great interest to WT investors and operators. The survey shown above has illustrated that, different from the reliability of wind turbines, their availability and capacity factor are better understood.

Very little data is currently available for offshore WTs but real data about availability and capacity factors is available from onshore and offshore wind farms. This is illustrated in Fig. 2.3 where data about four wind farms in UK and USA in 2005 are compared. The four wind farms data are described in Table 2.23 and include three UK offshore wind farms and an American onshore wind farm.

Wind Farm	Country	Location	N. WT	WT Power	WT Type
Scroby Sands	UK	offshore	30	2 MW	Vestas V80
North Hoyle	UK	offshore	30	2 MW	Vestas V80
Kentish Flats	UK	offshore	30	3 MW	Vestas V90
Texas	USA	onshore	160	1 MW	Mitsubishi M1000

Table 2.23: The four wind farms considered in figure 2.3

In Fig. 2.3 the results are grouped by availability (grey shaded area), capacity factor (pink shaded area), and average wind speed, shown in the bottom. The figure allows a direct comparison between offshore and onshore installations. The graph for the American onshore wind farm for both availability and capacity factor are highlighted in red.

The availability figures reported here confirm two considerations that have been outlined above: firstly the availability figures of current onshore wind farms is high, higher than 97% and secondly high the capacity factor obtained by the new UK offshore wind farms, which peaks at 50% in the most favorable periods.

Apart from an exceptional month affected by the Tornado "Anna", data for the American wind farm report an average availability which is comfortably above 97%.

Nevertheless, the difference between the two environments is striking; the offshore

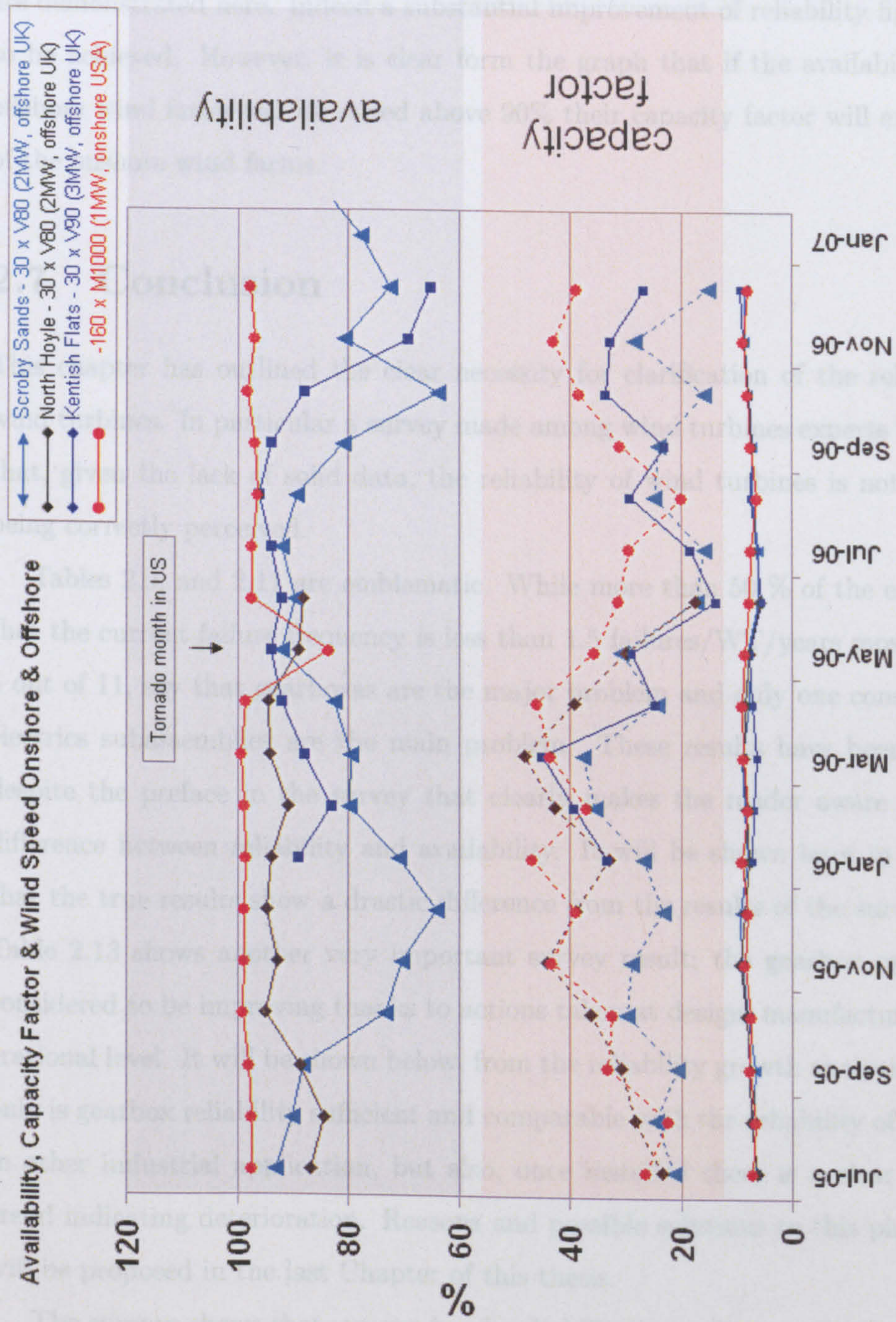


Figure 2.3: Availability, Capacity Factor and Wind Speed of four wind farms [5, 37, 38, 47, 57, 58]

average availability ranges between the about 92% for the North Hoyle wind farm down to the about 80% for the Scroby Sands wind farm. The reasons for the lower availability of offshore wind farms have already been described in section 1.5 and are demonstrated here. Indeed a substantial improvement of reliability figures have to be achieved. However, it is clear from the graph that if the availability of the offshore wind farms can be raised above 90% their capacity factor will exceed that of the onshore wind farms.

2.7 Conclusion

This chapter has outlined the clear necessity for clarification of the reliability of wind turbines. In particular a survey made among wind turbines experts has shown that, given the lack of solid data, the reliability of wind turbines is not currently being correctly perceived.

Tables 2.9, and 2.11 are emblematic. While more than 50 % of the experts say that the current failure frequency is less than 1.5 failures/WT/years most of them, 4 out of 11, say that gearboxes are the major problem and only one considers that electrics subassemblies are the main problem. These results have been obtained despite the preface in the survey that clearly makes the reader aware about the difference between reliability and availability. It will be shown later in the thesis that the true results show a drastic difference from the results of the survey.

Table 2.13 shows another very important survey result; the gearbox reliability is considered to be improving thanks to actions taken at design, manufacturing or operational level. It will be shown below, from the reliability growth analysis, that not only is gearbox reliability sufficient and comparable with the reliability of gearboxes in other industrial application, but also, once installed there is a clear reliability trend indicating deterioration. Reasons and possible solutions to this phenomenon will be proposed in the last Chapter of this thesis.

The surveys shows that, on one hand, reliability issues have to be clarified, with the “crystallization” of reliability data, on the other hand availability is perceived more accurately by experts. Possibly this is due to the fact that availability is strictly

connected to the productivity of wind turbines an issue on which operators are understandably particularly expert and sensitive. Thus current perceived onshore and future offshore WT availabilities (Tables 2.8 and 2.21) are realistic, despite the fact that a high offshore availability will require a large effort from designers and operators.

Chapter 3

Elements of Reliability Theory

3.1 Introduction

The systematic study of failures patterns of devices as well as the formalization in a theory started as a consequence of the “horrendous reliability” [20] of the electronic components whose utilization on a vast scale began during World War II.

Nowadays the concepts and methodologies of reliability science are extended to more complex machines or systems, such as distribution networks, with beneficial effects on different aspects of their design, maintenance, management, life prediction and costs.

The reliability of an item can be defined as follows:

Definition 3.1.1 (Reliability) The probability that an item will perform a required function under stated conditions for a stated period of time.

Such a statement is reminiscent of the familiar definition of the *quality* of an item with the difference that reliability is strongly concerned with characteristics of the item over time.

Reliability theory identifies two main categories of systems; repairable and non repairable. The “repairability” of a system is determined exclusively by economic considerations. Thus, a object is either repaired or discarded if the cost of repairing it is respectively lower or higher than the cost of a complete replacement. Nowadays a failed domestic iron or TV set are seldom repaired, because of the mass production

systems that have greatly lowered the production cost of these systems. In these cases the cost of the labour involved to repair is not competitive with the industrial production cost and the system must be considered non repairable. Conversely, a wind turbine is a good example of a *repairable system*, that is a system which is not discarded after a failure, since its repair cost is normally smaller than the cost of the replacement of the entire unit. However, reliability theory had been developed to study and improve the functionality of small, non repairable devices, such as electronic components, and for that reason the next section of this chapter will focus on some basic definitions concerning non repairable systems. Some conceptual differences between repairable and non repairable systems will be introduced later in the chapter.

3.2 Non Repairable Systems

In all subsequent chapters the letter X will denote a random variable representing the *lifetime* of certain objects while t will be used to indicate any value in the range of X . For a non repairable system, a failure in one element of a population does not affect the life of all the others. Thus X is said to be *independent*. The theory of probability [43] states that two or more sets are independent when the probability of their intersection is exactly the product of probabilities of the single set, in formula:

$$P(A \cap B \cap C \dots) = P(A) \cdot P(B) \cdot P(C) \dots \quad (3.1)$$

If at the same time it is possible to assume that the lifetimes of a group of objects have the same distribution the random variable is then said to be *independent and identically distributed* or *iid*. Reasonably this is the case for items made by the same manufacturer in controlled conditions, as typically happens in the electronic industry. This constitutes a first difference about a repairable system for which every repair action generally influences the subsequent failures and in only a few exceptional, although important, cases the assumption of independence and identical distribution is valid.

Definition 3.2.1 (Probability Density Function) The probability density func-

tion (*pdf*), written as $f(t)$, is the probability that the object fails in the interval $(t, t + dt]$ that is the probability for the random variable X to acquire values between t and $t + dt$.

Since the lifetime must be positive the probability that a unit fails for $t < 0$ is identically zero.

Definition 3.2.2 (Cumulative Distribution Function) The cumulative distribution function (*cdf*), which is denoted $F(t)$, expresses the probability that the random variable is less than or equal to the time t .

In formula form ¹ :

$$F(t) = P(X \leq t) \quad (3.2)$$

The *cdf* can be obtained by integrating the *pdf* as follows:

$$F(t) = \int_{-\infty}^t f(u) du = \int_0^t f(u) du \quad (3.3)$$

Its complementary function

$$R(t) = P(X > t) = 1 - P(X \leq t) = 1 - F(t) \quad (3.4)$$

is called **Survival Function** or **Reliability**. The relationship shown leads to the following definition for the Reliability.

Definition 3.2.3 (Survival Function or Reliability) The survival function or reliability indicates the probability that the item will carry out its mission through the time t or , in other words, the probability that the random variable X will assume values greater than t .

¹For practical reasons only continuous functions will be considered in this brief *excursus* on reliability theory. For the case of discrete distributions the correct terms must substitute the ones used for continuous functions. Thus, for example, the probability density function and the the cumulative distribution function become respectively the **mass density function** and the **cumulative discrete distribution**. In that case the equivalent sums must take the place of corresponding integrals.

A widely used function in reliability science is the **hazard function** which is defined as follows:

Definition 3.2.4 (Hazard function)

$$h(t) = \lim_{\Delta t \rightarrow 0} \frac{P(X \in (t, t + \Delta t] | X > t)}{\Delta t} \quad (3.5a)$$

$$= \lim_{\Delta t \rightarrow 0} \frac{P(X \in (t, t + \Delta t], X > t)}{\Delta t P(X > t)} \quad (3.5b)$$

$$= \lim_{\Delta t \rightarrow 0} \frac{1}{R(t)} \frac{P(X \in (t, t + \Delta t])}{\Delta t} \quad (3.5c)$$

$$= \frac{f(t)}{R(t)} = \frac{f(t)}{1 - F(t)} \quad (3.5d)$$

The same definition illustrates that the *hazard function* is a limit of the **conditional** probability that a unit will fail in “the next moment” divided by the length of the interval, given the condition that the same item has survived since time zero, that is since the beginning.

The probability of an event A given the occurrence of an event B , which constitutes the condition, is the ratio between the intersection of the two sets and the probability of occurrence of the condition. as expressed in the following symbolic formula:

$$P(A|B) = \frac{P(A \cap B)}{P(B)} \quad (3.6)$$

The conditional probability is higher than the plain probability. In its application to reliability, the conditional probability represents the risk of failure of the **remaining** or survivor population, which is higher than the normal probability of failure exactly because the population is older. The only exception is represented by populations with an exponential *pdf* whose hazard function is identically constant (memoryless property).

The importance of an exhaustive understanding of this definition will appear later when the failure intensity function, a **non conditional** probability limit for repairable systems, is introduced, noting that the two functions are often confused. Two important observation must be made about the hazard function.

Firstly, it must be noted that the hazard function is not a distribution and does not generally integrate to 1. Secondly, as the last equivalence (3.5) states, the hazard function completely defines the *pdf*.

Depending on the tendency of the hazard function to decrease, increase or show a constant trend, three different phases are recognized and are respectively called as follows:

- **Burn-in** or, more dramatically, **infant mortality**; when the hazard function is decreasing.
- **Useful life**; when the hazard function is constant.
- **Wear-out**; when the hazard function is increasing.

For a population of non repairable systems the hazard function is also called the failure rate function. Another relevant quantity reliability science is the mean time to failure (MTTF), which is simply the expected value for X . It must be remarked that the most widely used term Mean Time Between Failure (MTBF) has meaning effectively only in the case of a repairable object even though, there is a formal analogy between the two definitions, if the intensity function replaces the hazard function.

Definition 3.2.5 (Mean Time To Failure)

$$MTTF = E[X] = \int_0^{\infty} t f(t) dt \quad (3.7)$$

Since, by definition, a non repairable system is discarded after a failure, all the above quantities have validity only if referred to a large, ideally infinite, population of similar items. Hence, referring to the original population, the $f(t) dt$ is the fraction of items failed in the interval dt at time t , as well as the reliability is the fraction of items surviving at time t and so on.

The concepts illustrated above are widely applied in reliability engineering and various distributions are used in different cases, environments or for different scopes. An example that deserves particular mention is the Weibull analysis, which is based on the homonym distribution.

$$f(t) = \rho \beta t^{\beta-1} e^{-\rho t^{\beta}} \quad (3.8)$$

If the lifetime of a population is Weibull distributed the relative hazard function assumes the following form:

$$\lambda(t) = \rho \beta t^{\beta-1} \quad (3.9)$$

The Weibull analysis consists in plotting the so called Weibull Plotting Function, based on the cumulative hazard function, on a specific chart. If the population lifetime is Weibull distributed then the diagram lies on a straight line. The properties of the distribution can then be obtained directly from the chart.

Details of this technique are illustrated in Appendix A, where the method is implemented for failure data of industrial power converters.

In the case of a repairable system, since the failures constitute a series of events in time, the analysis can be made even on a single system. The next paragraph illustrates the most common mathematical tools available to perform this analysis.

3.3 Repairable Systems

According to [42] a repairable system can be restored after a failure to an operating condition by some repair process other than complete replacement. In the introduction of this chapter it has been illustrated how “repairability” is merely determined by economic considerations. As stated before a repairing action on a repairable system influences its future behaviour and in general the random variables representing the Time Between Failures (*TBF*) are not *iid*. As clarified in [42], repairing models can be classified as:

- **Minimal Repair** when the failed unit is brought back to the same condition it was just before the failure.
- **Perfect Repair** when the failed unit is brought back to the same condition it was as new and *TBF* are identically distributed.
- **Renewal Model** a perfect repair for which the independence of *TBF* can be assumed (*TBF* are *iid*).

The assumption of minimal repair leads to the Non Homogeneous Poisson Process, a statistical model which is widely used for non repairable systems whose “reliability” tends to improve or deteriorate, and the renewal model leads to the Renewal Process [42]. Among renewal processes a number of different processes can be identified, whose characteristics are a compromise between the minimum repair and the renewal model. Different repair models lead to different mathematical models, or stochastic processes, some of which are described in the next paragraph.

3.4 Point Processes, HPP and NHPP

3.4.1 Point Processes

A point process is a stochastic process describing the occurrence of events in time, that is a family of random variables parametrized by some index. In reliability engineering the events are failures and the index is normally related to a set of either times or other variables expressing the life of the objects, such as the mileage in a car, number of copies produced by a photocopier, and so on. Times between events are not in general independent nor identically distributed so are not *iid*.

The following functions characterize a point process:

Definition 3.4.1 (Counting Random Variable) $N(t)$ is the number of failures in $(a, b]$

$$N(a, b] = N(b) - N(a) \quad (3.10)$$

Definition 3.4.2 (Point Process Mean Function) $\Lambda(t)$ is the expected number of failures in the interval through the time t

$$\Lambda(t) = E[N(t)] \quad (3.11)$$

Definition 3.4.3 (Rate of Occurrences of Failure) $\mu(t)$ is the rate of change of expected number of failures with time

$$\mu(t) = \frac{d}{dt} \Lambda(t) \quad (3.12)$$

Definition 3.4.4 (Intensity Function) $\lambda(t)$ is the limit of the probability of having one or more failures in a small interval divided by the length of the interval.

$$\lambda(t) = \lim_{\Delta t \rightarrow 0} \frac{P[N(t, t + \Delta t) \geq 1]}{\Delta t} \quad (3.13)$$

The intensity function, which is often misleadingly referred to as the *failure rate* and, unlike the hazard function, is not obtained from a conditional probability. In fact it concerns the **unconditional** probability of a failure in a small interval, which is not necessarily the first failure. With the usual aim of differentiating between repairable and non repairable case the intensity function will also be called **intensity of failures**.

It can be demonstrated that if the probability of simultaneous failures is zero, which occur only where the mean function $\Lambda(t)$ is discontinuous, then:

$$\lambda(t) = \mu(t) \quad (3.14)$$

It is possible to define the Poisson Process, a noteworthy case of Point Process, which is important an tool for the analysis of failure data.

3.4.2 Poisson Processes

A point process, as defined above, is said to be a *Poisson Process* if the following conditions are satisfied.

$$a) \quad N(0) = 0 \quad (3.15a)$$

$$b) \quad \forall a < b \leq c < d \Rightarrow N(a, b] \text{ and } N(c, d] \text{ are independent} \quad (3.15b)$$

$$c) \quad \exists \lambda(t) : \quad \lambda(t) = \lim_{\Delta t \rightarrow 0} \frac{P[N(t, t + \Delta t) = 1]}{\Delta t} \quad (3.15c)$$

$$d) \quad \forall t : \quad \lim_{\Delta t \rightarrow 0} \frac{P[N(t, t + \Delta t) \geq 2]}{\Delta t} = 0 \quad (3.15d)$$

In words, the first condition fixes the beginning of the period of observation at $t = 0$, while the second states the independence of the number of failures, the third states the existence of the intensity function and finally the fourth guarantees the impossibility of simultaneous failures. The importance of a Poisson Process lies in the fact that by making these reasonable assumptions it can be demonstrated that

the number of failures in an interval (a, b) is a random variable having a Poisson distribution with mean

$$\Lambda(a, b) = E[N(a, b)] = \int_b^a \lambda(u) du \quad (3.16)$$

That is:

$$P(N(t) = n) = \frac{1}{n!} \left(\int_0^t \lambda(u) du \right)^n \exp \left(- \int_0^t \lambda(u) du \right) \quad (3.17)$$

A **Homogeneous Poisson Process (HPP)** is a Poisson process with constant intensity function $\lambda(t) = \lambda$. A point process is an HPP with intensity λ if and only if the TBF are *iid* exponential random variables with mean λ . Where the exponential distribution has a *pdf* defined by:

$$f(t) = \lambda \exp(-\lambda t) \quad (3.18)$$

If the intensity function is not constant the Poisson Process is defined as a **Non Homogeneous Poisson Process (NHPP)** and in the next sections the most widely used among the family of NHPP, the Power Law Process (*PLP*), will be introduced.

3.4.3 The “Bathtub” curve and the *PLP*

The reliability of a repairable system can be described with a model commonly known as the “bathtub” curve. This model incorporates three phases of the failure intensity of the observed system, that are named as:

- **Early failure phase**; when the failure intensity is decreasing.
- **Intrinsic failure phase**; when the failure intensity is constant
- **Deteriorating phase**; when the intensity function is increasing.

Although, as it will be explained in the following section, the three phases are due to substantially different causes, it is common to represent the “entire life” of a repairable system with the bathtub curve, whose name is due to the similarity with the cross section of a bathtub, as shown in figure 3.1. The observation of the entire bathtub curve is, however, a rare event since it is not common to have a range of data extensive enough. The Power Law Process (*PLP*), also called the Weibull Process,

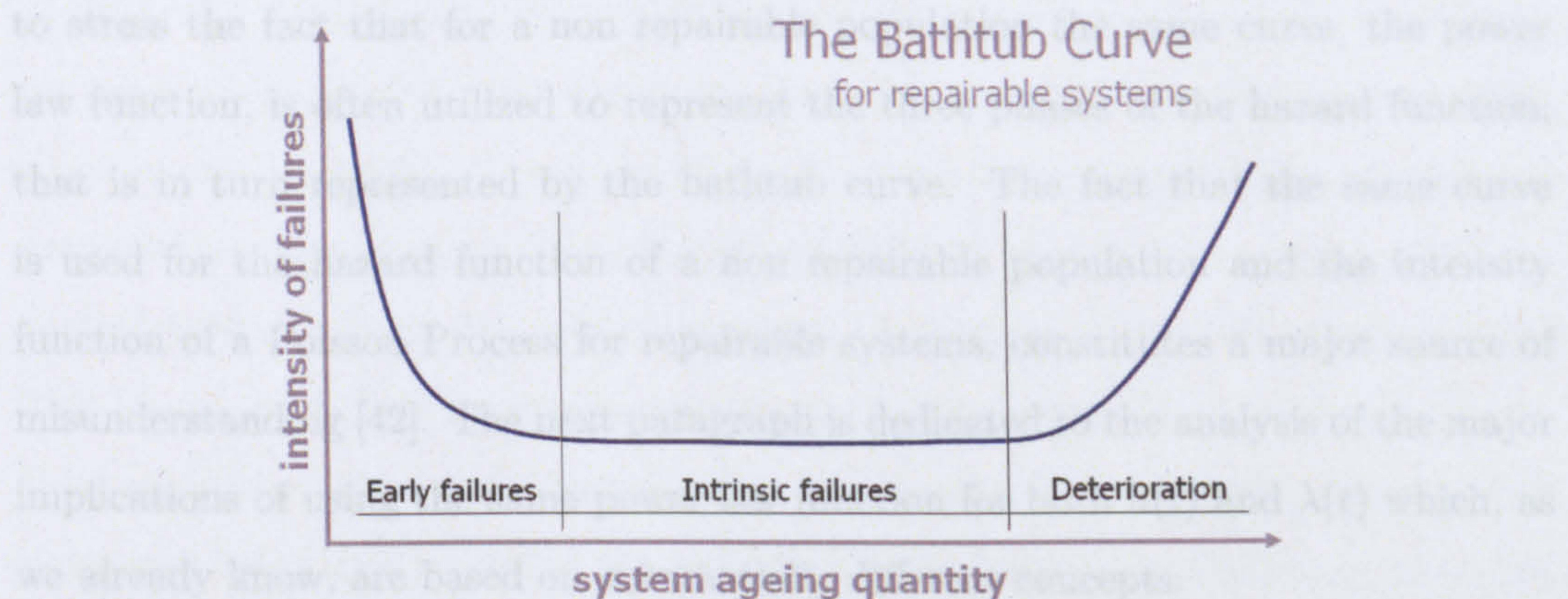


Figure 3.1: The bathtub curve for the intensity function (repairable)

whose intensity function is flexible enough to represent the three different phases, is particularly suitable to model the reliability of repairable systems, constituting also the basis of the Crow-AMSAA model [12]. The PLP, is a NHPP with intensity:

$$\lambda(t) = \rho \beta t^{\beta-1} \quad (3.19)$$

The parameter β determines the trend of the curve and is called *shape parameter*. For $\beta > 0$ or $\beta < 0$ the curve shows respectively a downward or an upward trend. When $\beta = 1$ the intensity function of the PLP is identically constant $\lambda = \rho$, and by definition the process becomes a HPP. Figure 3.2 illustrate the ability of equation 3.19 to model the three phases. The parameter ρ is a scale factor which has units

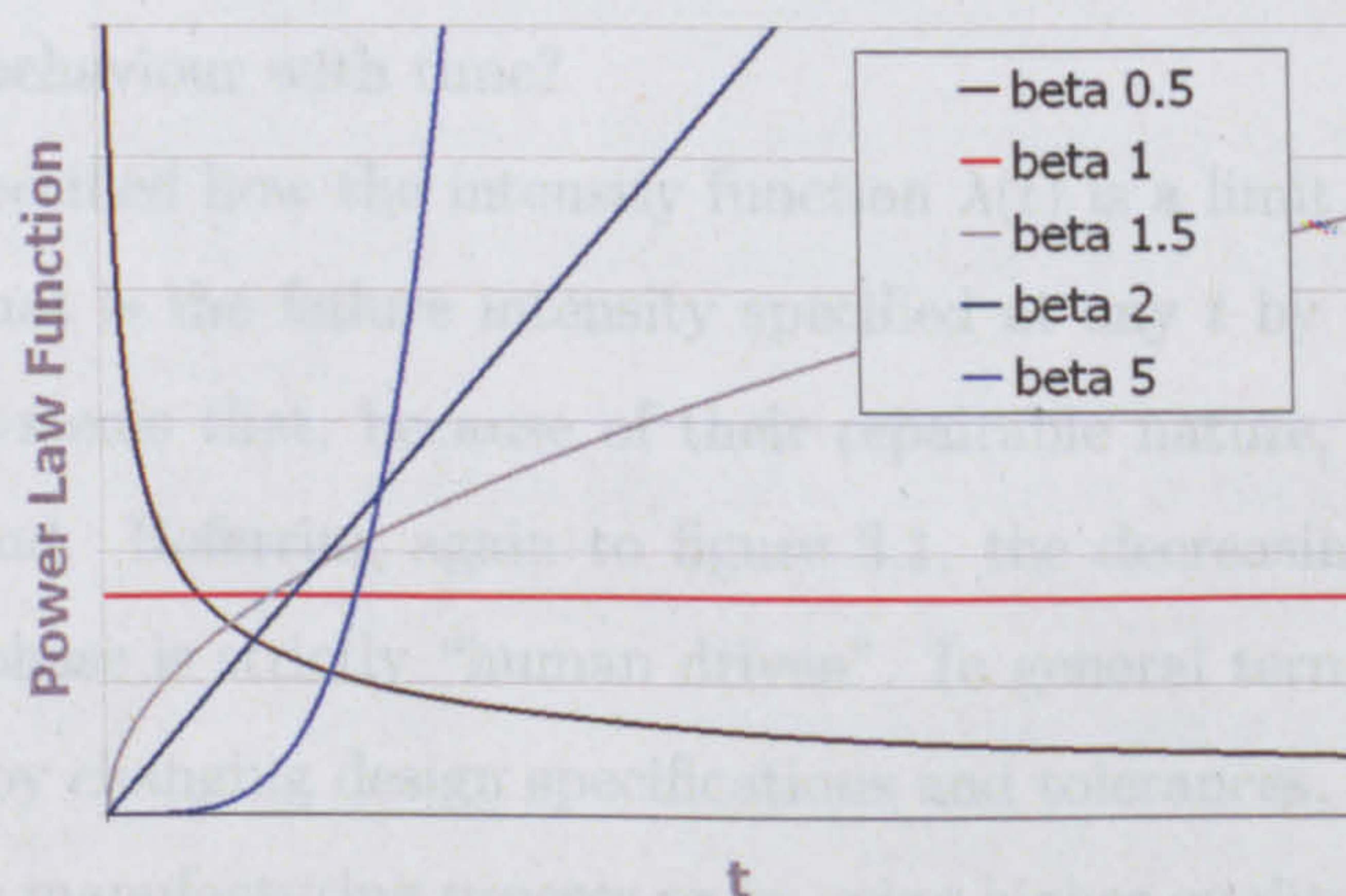


Figure 3.2: The power law function, parametrised in terms of β

that depend from the ageing quantity chosen, typically time. It is fundamental

to stress the fact that for a non repairable population the same curve, the power law function, is often utilized to represent the three phases of the hazard function, that is in turn represented by the bathtub curve. The fact that the same curve is used for the hazard function of a non repairable population and the intensity function of a Poisson Process for repairable systems, constitutes a major source of misunderstanding [42]. The next paragraph is dedicated to the analysis of the major implications of using the same power law function for both $h(t)$ and $\lambda(t)$ which, as we already know, are based on substantially different concepts.

3.4.4 On the meaning of the Bathtub curve

The three phases of both the intensity function and the the hazard function, as well as their representation with function 3.19 have already been illustrated. The analogy between the two is, however, exclusively formal since, as previously stated, there is a conceptual difference between the two functions [42] and the different terminology adopted reflects this distinction . It is fundamental, at this point, to analyze the meaning of terms like improving or deteriorating, comparing the causes of either the intensity or hazard functions reducing, increasing or remaining constant. In particular it is necessary to clarify the meaning of the use of the power law function to model the two functions.

Let's now focus on the following question: why do systems, either repairable or not, change their behaviour with time?

It has been specified how the intensity function $\lambda(t)$ is a limit of a non conditional probability, that is the failure intensity specified at any t by $\lambda(t)$ refers to an entire fleet of systems that, because of their repairable nature, survive through the observed period. Referring again to figure 3.1, the decreasing failure rate of the early failure phase is strictly "human driven". In general terms, the reliability can be improved by changing design specifications and tolerances, derating, more strict control on the manufacturing process or by using higher quality materials. Learning about usage and preventive maintenance techniques also plays an important role in achieving an improved reliability. The parameter β indicates the effort put into an improvement program and in the case of a fleet of systems, also reflects the speed

at which the technological innovation spreads throughout the fleet [46].

On this basis the PLP is applied to track the reliability growth during the developing stage, in order to verify the validity of the changes adopted in the design. This is for example the spirit of the Military Handbook 189 [12], that defines a protocol for the management of a reliability growth program. According to [12], when applying the PLP for the reliability growth management, *it is assumed* that if no further modifications to the design are adopted, after time t_0 , the failures would continue with constant a rate (HPP) equal to $\lambda(t_0)$ which is defined as the *demonstrated reliability*. The intrinsic failure phase shows no reliability trend. This phase is commonly associated with a period where wear and tear does not yet manifest itself and no development is done. Analysing wind turbines failure data the author has noticed a constant failure rate is likely to occur in complex systems of relatively mature technology, like the entire electrical system of a wind turbine, where the contemporaneous effect of a number of different failure modes has the effect of flattening the intensity function. That is random failures produce a flat intensity function. The interpretation of the deterioration phase is more intuitive, and can be based on our experience with the behaviour of any piece of machinery, in particular mechanical systems, like cars. The increasing intensity of failures is due to the normal deterioration of materials with time and usage or the phenomenon of fatigue. In general deterioration is the natural tendency of any system to “drift” toward a more disordered state, or a state of higher entropy, using the terminology of the thermodynamics, that eventually prevents the system performing its function.

The interpretation of the bathtub curve, depicted in figure 3.3, changes substantially for non repairable systems.

The hazard function of a large population of items is the risk of failure at time t conditioned to the survival at time t . In practical terms that means that the risk concerns only the surviving population at any t . The burn in phase naturally occurs to a population when items prone to early failure disappear from the population, increasing the reliability of the remaining or surviving set of items. As the population increases its average age the weakest items are “washed out”, therefore this phase is also called infant mortality.

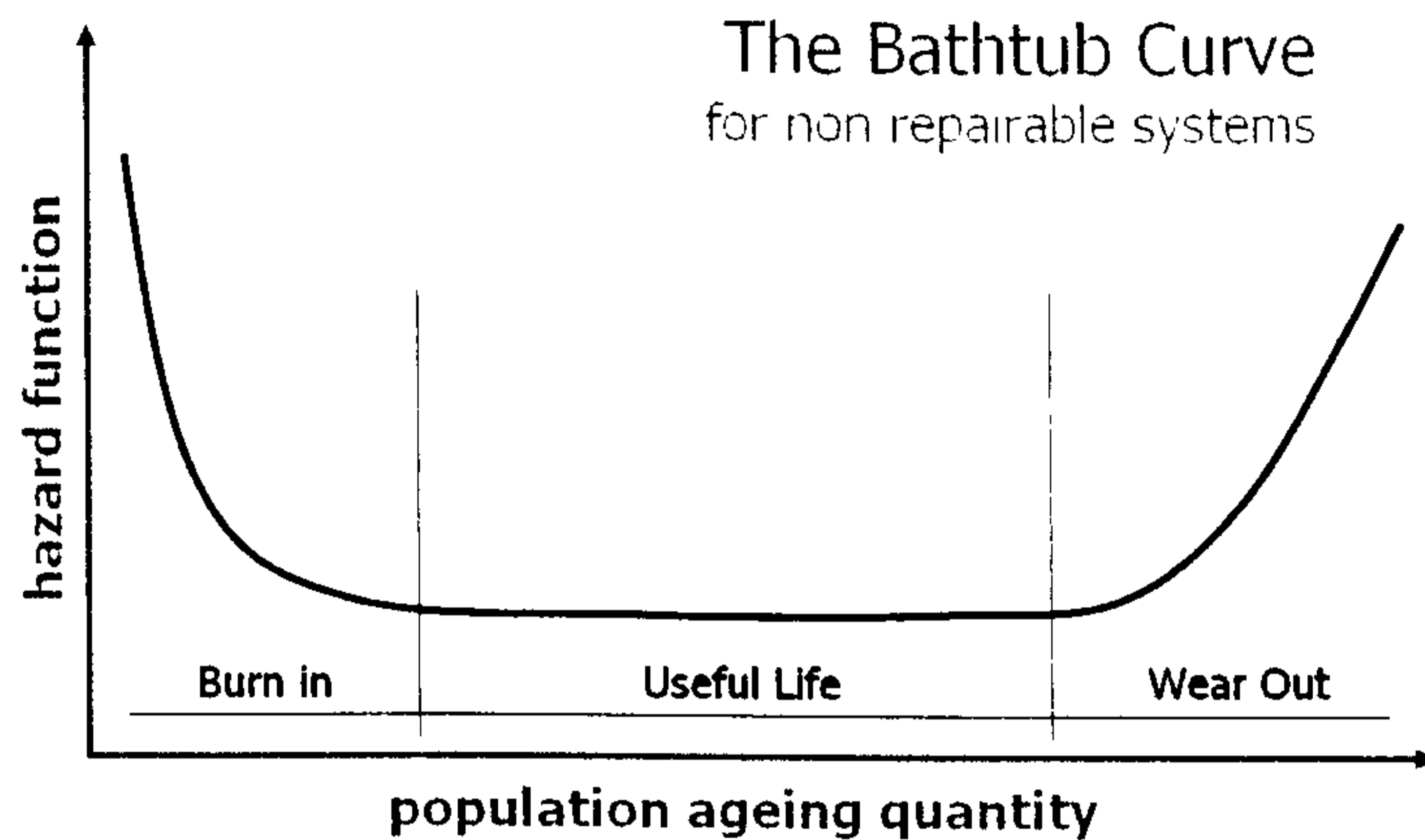


Figure 3.3: The bathtub curve for the hazard function (unrepairable)

If we assume that the distribution of the lifetime of a population follows a Weibull function

$$f(t) = \rho \beta t^{\beta-1} e^{-\rho t^\beta} \quad (3.20)$$

then the relative hazard will be an exact power law function, like 3.19 which is subjected to the considerations illustrated in figure 3.2. Thus, if $\beta \leq 1$ then the failure rate will have a downward trend, naturally occurring without any human intervention. This process suggests the possibility of improving the reliability of a population with the well known method of the burn-in test, to be completed prior to putting the items in service. One of the main objectives of reliability engineering is to establish the optimal length of the test, as a trade off between the cost of the testing and the cost of the unreliability, by applying analysis techniques like the “Weibull Analysis” [1].

This technique is explored in an application to power converters where failure data has been made available from outside the wind industry in Appendix A. The useful life is a period where the population shows an approximately constant failure rate and, for its simplicity, is the most widely adopted model for the reliability of non-repairable devices. Although the model is powerful, the assumption of constant failure rate must be carefully verified, since some wear out failure modes can manifest themselves early in the data. It is interesting that an assumption of constant failure

rate implies that the exponential distribution for the lifetime, as can be worked out from (3.5).

The wear out phase for non repairable systems is induced by the same phenomena described for the repairable case. The hazard function describes however the higher risk of failure to which the remaining population only is subjected. In this case the risk is higher simply because the remaining population is older.

These methods of reliability analysis have been applied to failure data of wind turbine and the results exposed in the details in the next chapter.

Chapter 4

Wind Turbine Failure Data

4.1 Introduction

Obtaining accurate failure data is one of the toughest issues of reliability engineering. Wind turbines constitute a highly specialized technology and because of the commercial relevance of failure data of wind turbines, the installation of which involves important capital investment and therefore risk, operators and manufacturers are reluctant to disclose data about reliability or failure patterns. As a result the sources of information are restricted to a few publicly available databases.

However, considerably more data is available than for other generation sources [54].

Reliability literature deals with data obtained from specific experience on the systems studied under controlled conditions so that the failures are carefully recorded and theoretical models can be directly applied to produce sound reliability profiles. To achieve high quality reliability data the optimal attributes that need to be recorded for a system such as a wind turbine are listed as follows:

- A thorough description of the system and its functions.
- The failure modes that emerge from tests of the system, that is the combination of root causes, patterns and effects constituting the failure.
- The TTF or the TBF of each failure of the system.
- Changes in the environmental conditions during the tests of the system.

- Changes of design and configuration of the system as a consequence of repair actions or a deliberate updating.

But the reality of field data, from the wind energy industry, is not optimal, being made up of practicable recorded reliability data, based on paper forms filled out by O&M operators. The data are often affected by human errors and inaccuracies from manual recording, and are grouped by survey period. That is data is only available as the total number of failures for the entire reported population of systems in each recording interval. The terminology of the reliability statistics refers to this as *grouped data* [12] or *interval censored fleet data*. Dealing with such “practicable” data implies both a higher degree of uncertainty and a necessity to implement mathematical tools that are specifically developed to deal with that type of data.

A recommended approach [4] consists of a progressive analysis from the higher level system to lower level subsystems, or subassemblies, with the aim of becoming familiar with the overall system reliability features before focusing on more specific aspects. This is the approach that is adopted in this thesis. It will be shown, however, that despite the lack of optimal data, it is possible to obtain valuable reliability information, as see for example [49], where the predictability of reliability of defence system electrical apparatus, based on industrial failure data, was demonstrated.

A common problem with field surveys are the differences of the terms used to define the various part of the observed system. For the sake of clarity the following terminology will be used throughout the rest of this thesis:

- **System:** for the entire wind turbine and the connection infrastructures.
- **Subsystem:** to generically indicate part of the wind turbine that deals with the same form of energy, for example the entire drive train.
- **Subassembly:** to indicate devices performing more specific functions for which the failure data are recorded separately, for example the gearbox.
- **Component:** to indicate small devices typically non repairable constituting the subassemblies, for example the gearbox/generator coupling.

The Subsystems of the wind turbine, the system under investigation, will be presented in the next section, each of them constituting a paragraph. The sub-assemblies will be analysed extensively later when the data are introduced. System will also be used as a synonym of "apparatus" or "complex", whenever there is no ambiguity in the definition, as for "electronic system" or "yaw system".

4.2 The Wind Turbine

As an introduction to the failure data, it is necessary to illustrate the structure of a typical wind turbine, which is a complex energy converter system for the production of electric energy from the kinetic energy associated with the motion of the air.

In a wind turbine four major subsystems can be identified, namely: the rotor, which transforms the axial kinetic energy of the wind into rotational mechanical energy, the drive train that delivers the energy to an electrical generator, the electrical system, which interfaces the wind turbine with the distribution or the transmission grid, and the the tower structure, that bears the weight of the nacelle and withstands the dynamic loads developed during operations. Other subassemblies include the control, diagnostic and measurement systems, the cooling system plus other ancillary systems, for example, the internal crane which is adopted in large wind turbines. Figure 4.1 shows the main subassemblies of a geared drive wind turbine.

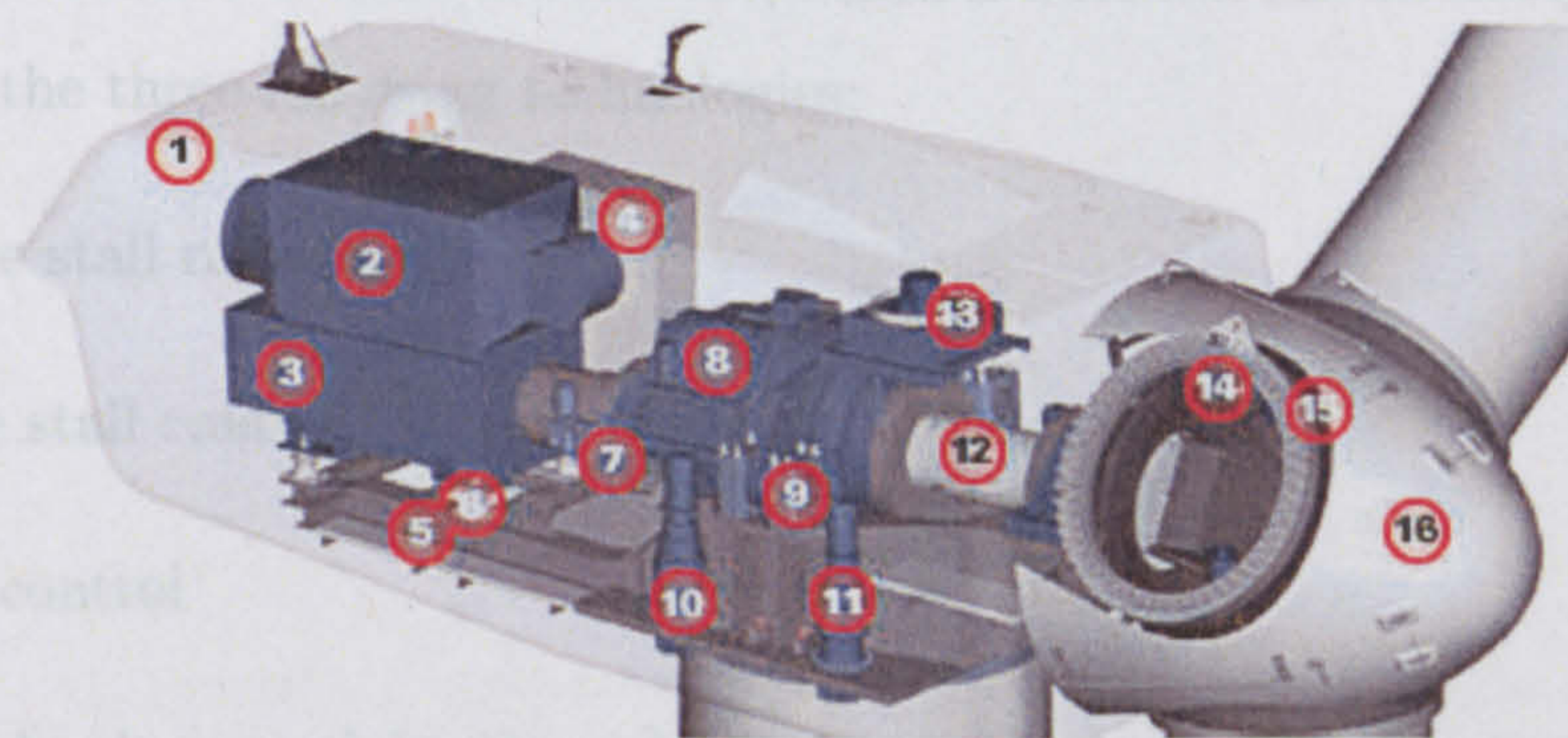


Figure 4.1: The subassemblies of an indirect wind turbine: 1. Nacelle, 2. Heat exchanger, 3. Generator, 4. Control panel, 5. Main frame, 6. Noise isolation, 7. Parking brake, 8. Noise isolation, 9. Gearbox, 10. Yaw drive, 11. Yaw drive, 12. Main shaft, 13. Oil cooler, 14. Pitch control, 15. Hub, 16. Nose cone

4.2.1 The Rotor

Since the first, initial pioneering attempts of wind energy extraction in the 20th century it has become a sophisticated aerodynamic and mechanical complex subsystem. Its dimensions have grown considerably making manufacturing and installation of these elements an extremely complex operation, as illustrated by Figure 4.2. It consists of the blades, the hub, to which the blades are attached, and the pitching mechanism, that has been introduced in chapter 1. The blades are typically three in the number, but two bladed and, more rarely, one bladed machines are also installed. The hub has the dual function of supporting the blades and transmitting the blade torque to the main shaft. The hub can be fixed or tilting. In the second case an additional degree of freedom is provided to allow blades to oscillate out of the vertical plane, perpendicular to the plane of rotation. The tilting system, or teeter, reduces the dynamic loads due to the tower “shadowing” and is essential for two bladed machines.

The position of the rotor, with reference to the tower, determines two different wind turbines concepts; downstream and upstream. The main difference between the two is that, while downstream turbines align automatically with the wind, upstream turbines need an additional active mechanism to yaw the turbine into the wind. The yaw system is described in the section concerning the turbine bearing structure.

The power control of the wind turbine, which is a critical subassembly, is achieved with one of the three following technologies:

- Passive stall regulation
- Active stall control
- Pitch control

The first technology exploits the reduction in power extraction from the wind that occurs at higher wind speed, when the aerodynamic performance of the blade decreases, due to the transition from laminar to turbulent flow and blade stall. The second technology uses a device that rotates the blades on their axis driving the blade “out of the wind” and allowing a controlled stalled situation. Finally the

pitch control, which is similar to the active stall device, finely controls the power of the wind turbine by tuning the angle of attack of the blades, so that the airflow around them remains as close as possible to laminar flow conditions.

Although the power control, either active stall or pitch mechanism is an integral part of the rotor, it will be classified here as a separate subassembly. In all the the wind turbine failure surveys considered in this thesis, failures of the pitch mechanism, or “pitch control”, are reported separately, indicating the important role that this subassembly plays in the reliability of the system.

The pitch mechanism can be driven by either electrical or hydraulic actuators, the latter failures are separately recorded in a subassembly that is usually called “hydraulics”.

The pitch of individual blades can be individually controlled by separate actuators or a single actuator. In the second case the pitch mechanism controls the pitch of all the blades together with the assistance of a yoke.



Figure 4.2: A rotor of a direct drive machine, being mounted on the nacelle [66]

4.2.2 The Drive Train

The drive train is the “heart” of the entire system and as will be shown, is a key subsystem for the reliability of the wind turbine. It consists of the main shaft, the

main bearings, the coupling, the generator and the gearbox if present. The two most important categories of wind turbine design, that are currently competing to dominate the wind energy market, determined by the presence or absence of the gearbox, are the indirect drive, for the geared machines, and the direct drive if the generator shaft is directly coupled the rotor. In the second case the rotational speed of the generator is the same as the rotor.

The gearbox, on an indirect drive WT, is necessary to match the speed of the rotor with the speed of the generator, which depends on the wind speed and number of blades. This speed is a compromise based on the need for the generator to operate at high speed, in order to produce a high voltage, given the magnetic flux density in the generator. This is normally limited by the magnetic property of the generator core material to about 1 T. Gearboxes are major source of concern for wind energy operators, and bearings and the high speed shaft, Fig. 4.3, are the gearbox components that are particular prone to failures. The alternative to the use of a gearbox is to achieve a convenient voltage by increasing the peripheral speed of the electrical machine by increasing its diameter and at the same time increasing the number of pole pairs in the generator. This allows the elimination of the gearbox, that steps up the speed, as occurs for direct drive machines. The price to pay for the elimination of the gearbox is the adoption of a fully rated electronic converter with which it is possible to adjust the frequency of the current, now variable depending on the speed of the shaft/rotor.

The bearings of a wind turbine are critical from a reliability point of view, like most mechanical systems. Bearings are common objects whose design is well known, and have been subjected to extensive study in reliability engineering, but in the case of the wind energy industry the main shaft bearing is large in diameter. The conditions to which the bearings are subjected are also unusual, given the large and varying static and dynamic loads and the inclement environment with a wide range of temperature conditions. Thus, most of the maintenance carried out for the drive train concern either the bearings of the generator and the gearbox or the main bearings of the turbines. All the main bearings in a wind turbine are generally rotating element bearings.

Shaft, gearbox, generator, bearings and coupling are all subassemblies of the drive train for which the failures are normally separately reported.

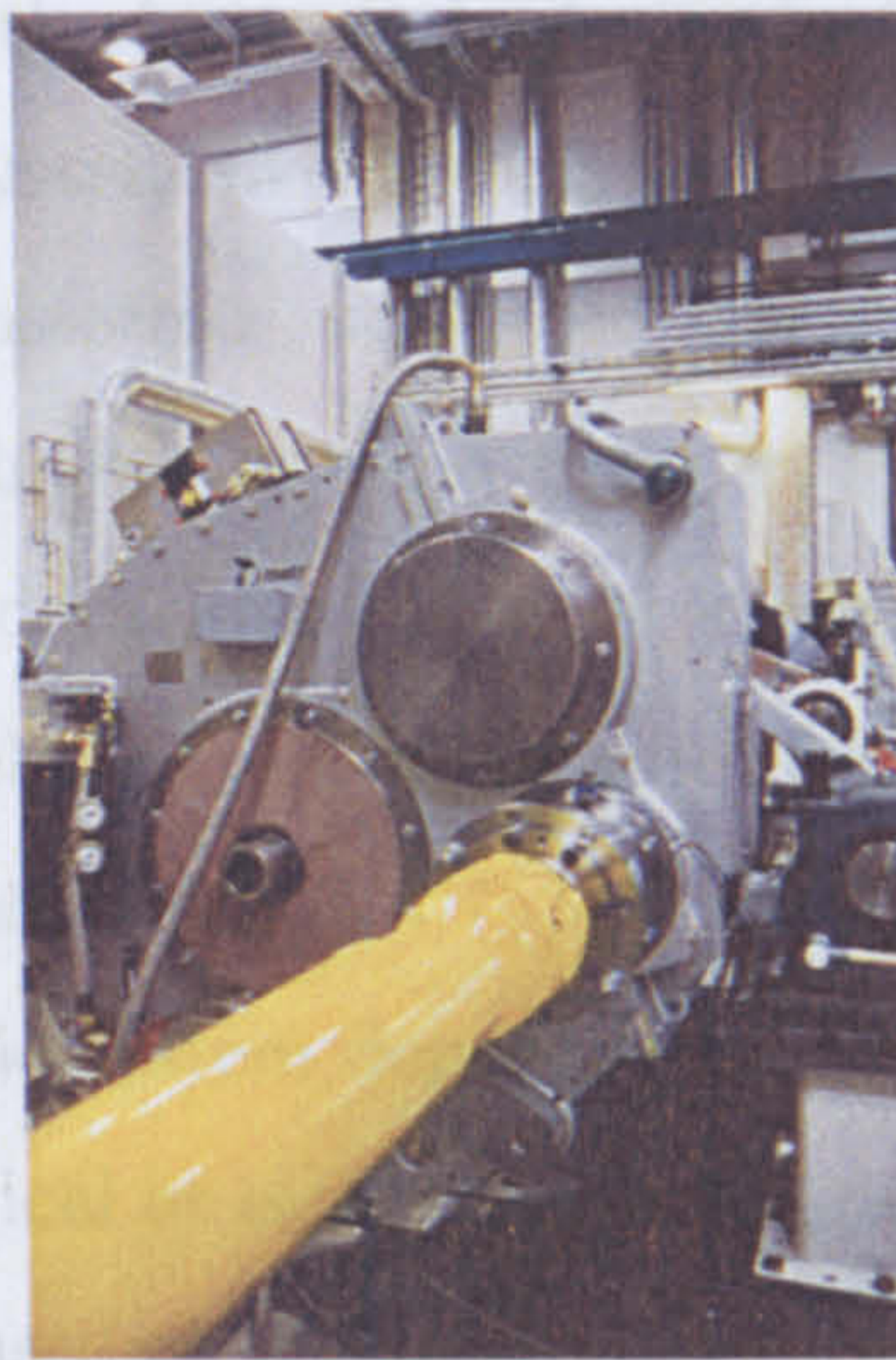


Figure 4.3: The high speed shaft and the gearbox of an indirect drive wind turbine [27]

4.2.4 The Tower

4.2.3 The Electrics

The electric system of a wind turbine is by far the most complex subassembly. Apart from the generator, which constitutes a different subassembly, the electrical system includes all the electro-mechanical devices that allow the connection of the generator to the grid and the exchange of both active and reactive power.

The complexity of the electric system is reflected, as it will be seen, in the frequency of failure of this subassembly, which is generally high, if not the highest in the wind turbine system. The fact that this is not perceived as the major source of concern is probably due to the reparability of electro-mechanical components which is easier, in comparison to the solely mechanical parts.

Often there is no distinction between component failures and grid induced “events” leading to machine shut-down that are recorded as failures. Shut-down events are harmful for the energy production but they may not imply part replacement.

The main components that are included in the electrical system, are; the machine transformer, switchgear, power cables, protection relays (over/under voltage,

over/under current, over/under frequency and loss of mains), power factor correction units (capacitor banks and relative switchgear), circuit breaker and the earthing system (conductors and earth electrodes). A number of other equipments are also included in the electrical system like earthing reactors, for the connection of the star point centre of the transformer, surge divertors, metering system, voltage and current transformers plus the battery and chargers for the protective relays. More modern turbines also include a lightning protection system. The electronic converter, which is present in all variable speed wind turbine architectures, is typically considered a separate subassembly.

The reliability of the electric system depends upon a great deal of different failure modes of mechanical, electrical or electrodynamic origin. That makes the diagnosis of the failures and their classification uncertain and subject to inaccuracy; for example it is not uncommon for a stoppage due to resetting of a relay to be recorded as a failure.

4.2.4 The Tower

The tower structure includes three main parts, namely; the foundation, the tower and the yaw system.

The third is the most interesting from a reliability point of view although failure of either the foundation or the tower has serious consequences. The yaw system allows the nacelle to align with the wind direction, and it is essential to the functioning of a turbine with an upwind rotor. Typically it is realised by a system of electric or hydraulic motors acting on the base of the nacelle, where an appropriate, large gear wheel is mounted. Figure 4.4 illustrates the yaw system.

Unlike the tower and foundation, the yaw system is an active device, directed by a dedicated control unit governed by the anemometer. The foundation and tower have to withstand to the massive static and dynamic loads and can be of various technologies. The foundation in particular is crucial for the offshore application of wind turbines and can involve sophisticated technology that is the subject of intensive current research.

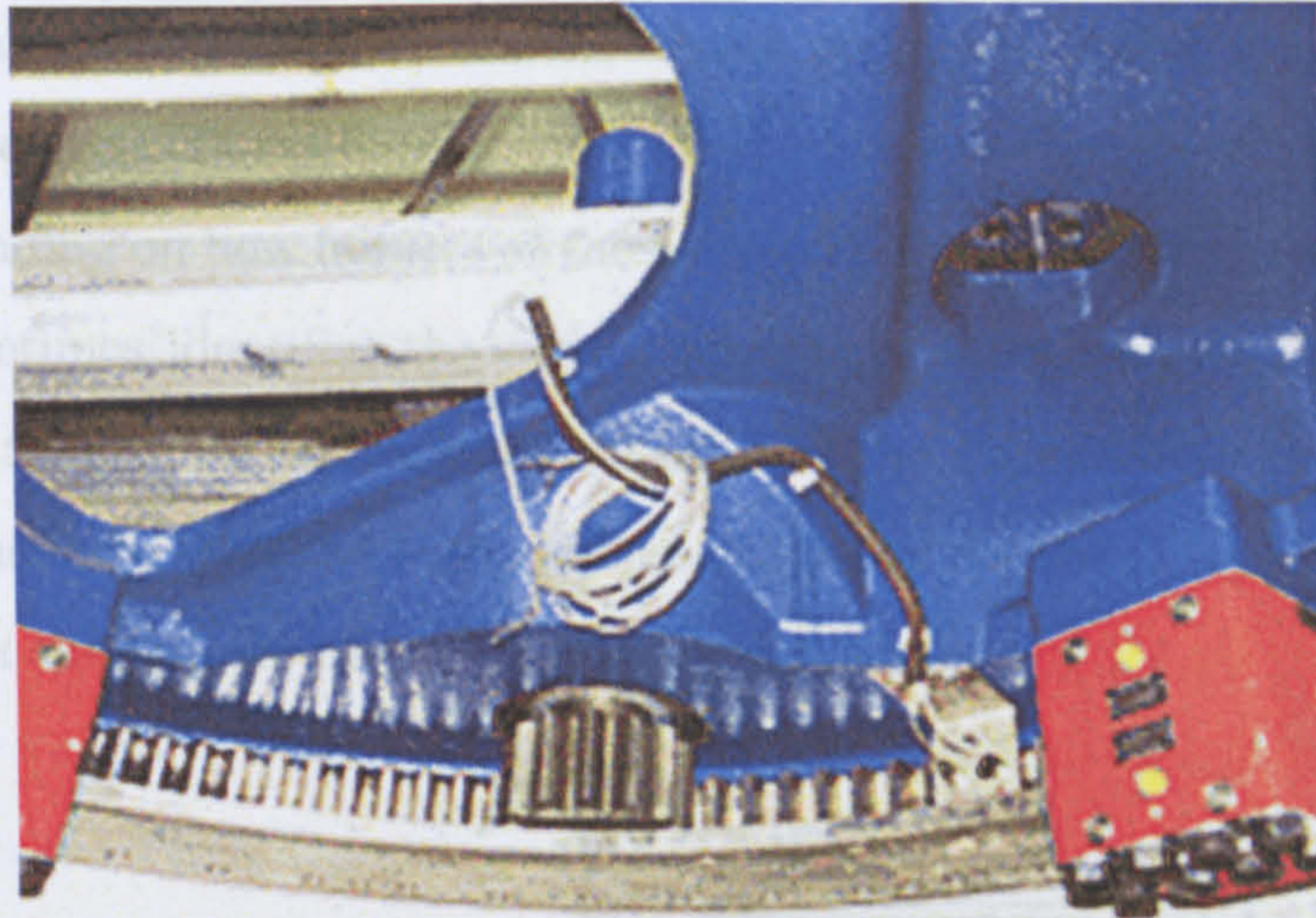


Figure 4.4: Wind turbine yaw system; drive and gear wheel [65]

4.2.5 Electrical Control

The electrical control, which is in this case a synonym for the converter is the interface between the electrical machine and the grid, causing major concern among wind industry operators because of the high cost and the relatively poor reliability. Problems that become particularly virulent for larger size turbines.

The electrical control adjusts the frequency and voltage of the delivered power to values suitable for the grid and it can be fully rated, that is rated for the full WT power, as for direct driven WTs or partially rated as for DFIG generators (Fig. 4.5). The electrical control has for the electrical part of a wind turbine the same importance that the gearbox has for the mechanical side to the point that a competition for the most reliable concept between direct drive and geared machines can be reduced to the competition between the gearbox and the converter. The electrical control is absent in the indirect drive fixed speed machines, partially rated for the indirect drive variable speed machines and fully rated for the direct drive machines. In the second case the converter feeds the rotor of the asynchronous generator, allowing the speed to vary within a larger interval.

There are five major parts of a converter. The gridside inverter (rectifier), the DC link, the machine side inverter, the control electronics and circuit protection system. The DC link, which is typically an electrolytic capacitor that stabilises

the voltage and filters some of the harmonics produced, is the weakest link of the entire subassembly. The different terminology used for the converter parts leads to misunderstanding on how failures of the converter are recorded; in example the term inverter sometimes identifies the entire converter system. As will be shown below the recorded failures for the data record LWK of the subassembly “inverter” are too low to be concerned with the entire subassembly and for the analysis they have been grouped with the failures of “electronics” subassembly.

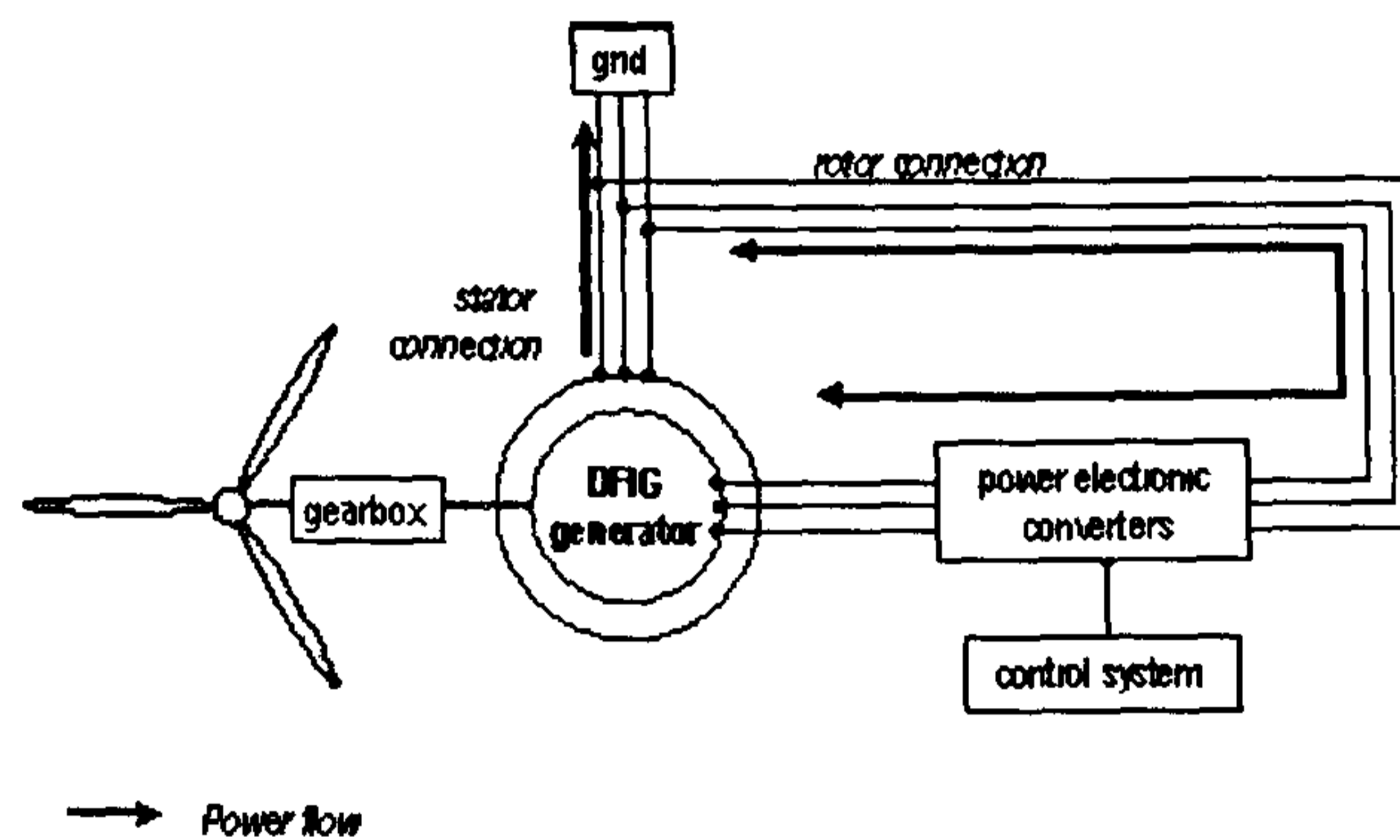


Figure 4.5: The scheme of an indirect drive variable speed WT with a doubly fed induction generator [67]

Failure rates for industrial converters are elusive so the comparison with wind turbine converters is difficult. In [61] the failure rate refers to obsolete systems and it cannot be considered a valid one, while in [34] the failure rate for power converters is not present at all. Given the lack of reliable industrial data the author has established a collaboration with an important manufacturer of power converter, in the attempt to extract useful information. The converters considered are small compared to the WT converters and typically equip small asynchronous motors. Given the nature of the data the analysis has been carried out considering the systems as non repairable and the Weibull analysis has been applied. The results are displayed in Appendix A.

4.2.6 Other

Under the generic name of “other” many different subassemblies are grouped, and is present in all the surveys and can be composed of different components, depending

on the wind turbine concept. The composition of this subassembly is not normally disclosed and the interpretation of its failure figures is problematic. As a subassembly, “other”, can have a high failure rate, often the highest, largely because of the complexity and number of different components involved. Nevertheless, it can be assumed that it is highly repairable, since it does not include any of the major electromechanical subassembly. The possible systems that comprise this subassembly are: the anemometer and other sensors, the condition monitoring system, the cooling system, the air filtering and other ancillary systems, for the larger and more modern turbines, like the already mentioned internal crane.

4.3 WindStats and LWK

WindStats [17] and LWK [15] are two publications collecting failure data of different populations of wind turbines and constitute the main source of information on which this research work has been carried out. Data from both the surveys are not available in digital form. They have been collected, reorganised and analysed extensively and results have been published in several publications [50–52]. WindStats Newsletter is a quarterly international publication, collecting operational data from a great deal of wind turbines installed in various countries over a period spanning about ten years. The newsletter reports the performance of single wind turbines in terms of energy delivered but for two countries in particular, Germany and Denmark, also the number of failures are reported, in different detail.

For practical reasons the abbreviations WSD and WSDK will be used to indicate the surveys WindStats Germany and WindStats Denmark, respectively. The failure data are collectively reported for a population of wind turbines of different age, technology and manufacturer. Data presented in such a form are often referred to as *grouped data* as described above. Despite some data deficiencies, that will be evaluated below, the number of wind turbine involved and the large time span of the survey and make the analysis of the WSD and WSDK failure data valuable, and constitutes an important part of this chapter.

Two examples of the data are reproduced in the Tables 4.1 and 4.2

	Jan 2001				Total
	Destroyed	Replaced	Repaired	Unspecified	
Blades	0	1	3	1	5
Hub	0	0	0	0	0
Axle/Bearing	0	0	1	0	1
Air Brake	0	0	0	0	0
Gearbox	0	2	3	5	10
Coupling	0	0	0	0	0
Brakes	0	1	1	0	2
Generator	0	0	3	2	5
Yaw System	0	0	3	6	9
Tower	0	0	0	0	0
Foundation	0	0	0	0	0
Grid	0	1	0	2	3
Elec control	0	7	5	3	15
Mech control	0	0	0	3	3
Hydraulic	0	0	0	1	1
Entire turbine	0	0	0	1	1
Entire nacelle	0	0	0	5	5
Other	0	0	1	22	23
Total	0	12	20	51	83

Table 4.1: An example of failure data for WSDK turbines for January 2001 [17]

	Jan 01 - Mar 01								Total	%	Average	Rate %
	Cause of stop											
	Maintenance	Weather	Grid break	Wear	Failure	Not Stated	Scheduled stop	Non spec				
Non component	530	132	128	12	0	39	17	19	877	17.3	14.2	0.25
Rotor	2	15	0	41	5	7	0	0	70	2.4	24.8	0.04
Air brake	0	1	0	10	3	0	0	0	14	1.2	61.7	0.02
Mech brake	0	0	0	12	3	0	0	0	15	0.3	12.7	0.00
Pitch adjustment	1	1	0	29	10	0	0	0	41	1.0	18.2	0.02
Shaft/bearing	0	0	0	2	9	1	0	0	12	2.1	127.0	0.03
Gearbox	23	0	0	27	39	9	0	0	98	17.8	130.4	0.26
Generator	0	1	0	32	23	9	0	0	65	10.5	116.0	0.15
Yaw system	0	6	0	20	19	15	0	0	60	1.8	22.1	0.03
Anemometer	0	65	0	17	13	0	0	1	96	1.9	13.9	0.03
Elec. control	0	4	3	77	30	3	0	0	117	3.5	21.5	0.05
Elec system	6	9	4	125	42	11	0	4	202	8.9	31.6	0.13
Hydraulics	0	2	0	42	19	1	0	1	65	2.8	30.9	0.04
Sensor	2	20	0	18	9	1	0	1	51	0.8	11.9	0.01
Other	9	1	0	3	2	21	2	0	38	0.3	5.8	0.00
Non specified	1	1	0	2	1	0	0	1614	1619	27.4	12.2	0.40
Total	580	258	135	469	227	117	19	1640	3454	100	20.8	1.46

Table 4.2: An example of the causes of stoppage and failure data for WSD for January-March 2001 [17]

Some differences are evident. Firstly German data are reported quarterly while Danish are reported on a monthly basis. Secondly, for both the populations, the actual failure modes occurring are not disclosed. Some additional information is available regarding the maintenance actions performed in the Danish case, or generic categories of failures in the German case. The categories concerning the additional information are reproduced in columns of the two tables. German data are integrated with the cumulative number of hours lost for each category of failure, that are reported in each cell of Table 4.2. For a Danish turbine the causes of stoppage, not the failure modes, are reported in a separate table, as shown in Table 4.3, however for two reasons this information has not been considered in the analysis;

1. Not all operators report the cause of failures
2. The information cannot be easily matched with the failure data

Data, for both German and Danish turbines, are finally completed with the number of wind turbines involved in the survey, their average rating , as well as with other information about production, as the total energy delivered in the period and the capacity factor. An example of this data is shown in Table 4.4.

	Jan 01	Feb 01	Mar 01	Total
Inspection	17	22	17	56
Cracks/Breaks	2	3	2	7
Earlier problem	0	0	0	0
Falling component	0	1	1	2
Grid	2	4	4	10
Lightning	0	2	1	3
Other	29	41	39	109
Overproduction	0	15	9	24
Runaway	0	0	0	0
Service	23	37	29	89
Short circuit	3	6	0	9
Storm	1	2	0	3
Wear	8	11	7	26

Table 4.3: An example of causes of stoppage shown for WSDK turbines for January to March 2001 [17]

LandwirtschaftKammer (LWK), concerns wind turbines installed in the region of Schleswig-Holstein in Osterrnfeld, Germany whose failure data are collected and

December 6, 2008

	Jan 01		Feb 01		Mar 01	
	DK	D	DK	D	DK	D
Turbine registered	2878	9329	2895	9397	2910	9483
Registered MW	956.0	6130.9	969.8	6219.3	992.0	6332.5
Turbine reporting	2023	3154	2154	3200	2042	2842
MW reporting	700.5	2045.8	728.9	2094.0	704.1	1840.0
Production [MWh]	90305	277460	130071	343801	115076	291103
Capacity factor [%]	17	18	27	24	22	21
Windex [%]	-	-	-	-	-	-
Month's wind energy [%]	71	84	101	102	84	100
Year's wind energy [%]	71	84	91	93	88	95
New turbines	26	68	18	68	13	86
New capacity	23.8	77.4	13.9	88.4	22.4	113.2

Table 4.4: An example of wind turbine data for the two WindStats populations for January to March 2001 [17]

published by the Chamber of Commerce of that German Lande.

The major difference from WindStats is the length of the data grouping interval, in the LWK case that is one year rather than one quarter for WSD or one month for WSDK, and the segregation of failures for each wind turbine model. The latter is a key feature, since it allows the direct comparison of the reliability performance of alternative wind turbine concepts. In particular the comparison of alternative wind turbine concepts is possible, like direct drive and indirect drive. Table 4.5 shows a record from LWK for a particular wind turbine model.

On LWK table the stoppage events are summarised on the same data table. The stoppages due to subassembly failures are combined in a separate section from the ones that are due to external factors. There are four “non-component” associated categories of plant stoppage (maintenance, grid disturbance/loss, storm and icing). Failures due to non-component associated reasons are not taken into account in the analysis. The category “lightning”, that appears in the component or subassemblies associated failures, has been considered non-component associated and has also been neglected. Accounting for only component associated failures is consistent with the analysis that has been done on the WSD data, where the category “non component” has been excluded from the analysis. In the case of these surveys “component” is synonymous with subassembly by our definition in section 4.1.

	Tacke TW600		
Model			
year	1999		
number of WT	30		
AVG age [months]	54		
	Hours lost	Failures	Hours lost [%]
Maintenance	435	53	0.09
Grid disturbance/loss	418	30	0.09
Storm	535	35	0.12
Icing	0	0	0.00
Total (non comp.)	1388	118	0.30
Lightning	0	0	0.00
Blades	1648	8	0.35
Rotor brake	0	0	0.00
Pitch mechanism	0	0	0.00
Brake	41	4	0.01
Shaft/bearings	32	4	0.01
Gearbox	76	10	0.02
Generator	134	7	0.03
Hydraulics	31	6	0.01
Yaw system	51	4	0.01
Anemometry	9	2	0.00
Electronics	28	5	0.01
Electrics	145	14	0.03
Inverter	0	0	0.00
Sensors	12	3	0.00
Other	226	12	0.05
Total (comp.)	2433	79	0.53

Table 4.5: An example of the turbine failure data from the LWK record for a TW600 wind turbine [15]

4.3.1 Number of Turbines

The graphs of the number of wind turbines and the average rating of the three populations investigated, are reported respectively in Fig. 4.6 and Fig. 4.7, and highlight some interesting features.

It is clear that trends in number and average rating of the investigated population reflect the changes that have been taken place in the wind energy market in the last decade, although the reporting turbines are only a fraction but an important one, of the total number of wind turbines installed. The number of reporting wind turbines follow three completely different patterns which are increasing, decreasing and about constant for WSD, WSDK and LWK respectively. The national policies for wind power are reflected in the surveys: while Germany assisted the installation of a large number of new wind turbines up to a certain level, Denmark in more recent years has been replacing a large number of smaller turbines with fewer turbines of larger size and more modern technology. The number of turbines surveyed in LWK is less variable although showing a decreasing trend in more recent years, possibly for reasons similar to WSDK.

The increasing average rating for all the populations reflects the well known trend of installing larger machines to reduce the specific capital investment cost [21]. Generally newer wind turbines have a higher rating: the implication of this trend on the reliability is of extreme interest. In the following paragraph some results about the investigation of the correlation between rating/size and failure frequency will be shown.

The average rating trend, which is increasing for the three populations (Fig. 4.7), leads to the conclusion that for both WindStats populations new, larger turbines are constantly being added to the survey; for the Danish case many older, smaller wind turbines are excluded at the same time. The average rating of WSDK, which is smaller than both WSD and LWK, indicates also a difference of technology of the WSDK turbines. Therefore, the elements characterising both number and rating of the wind turbines in the investigation, lead to an important conclusion; it is expected that failures of the German turbines are dominated by newer, larger and probably less reliable turbines, whereas smaller turbines involving a more ma-

ture and, possibly more reliable technology determine the reliability of the Danish machines.

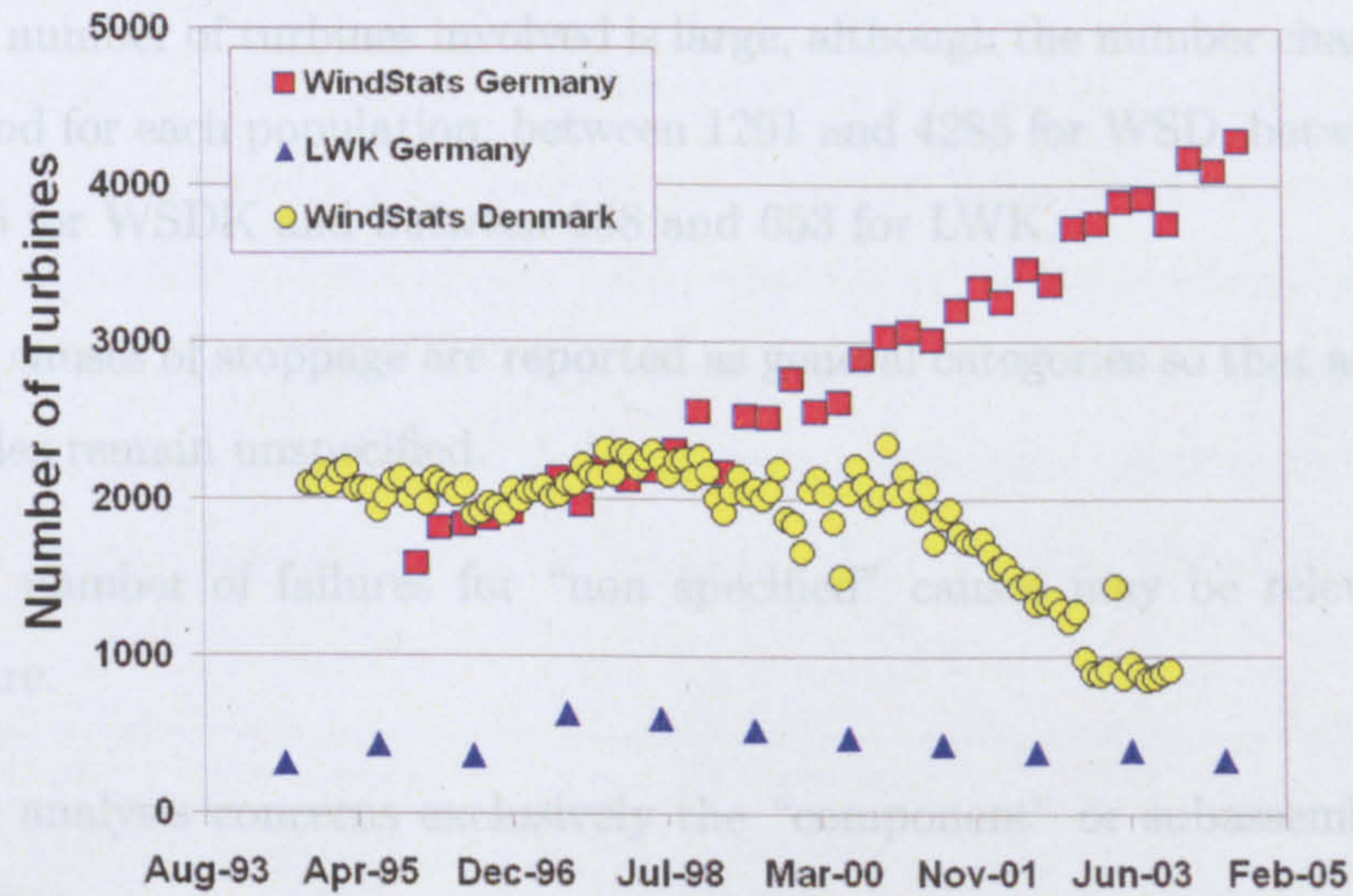


Figure 4.6: Number of wind reporting turbines

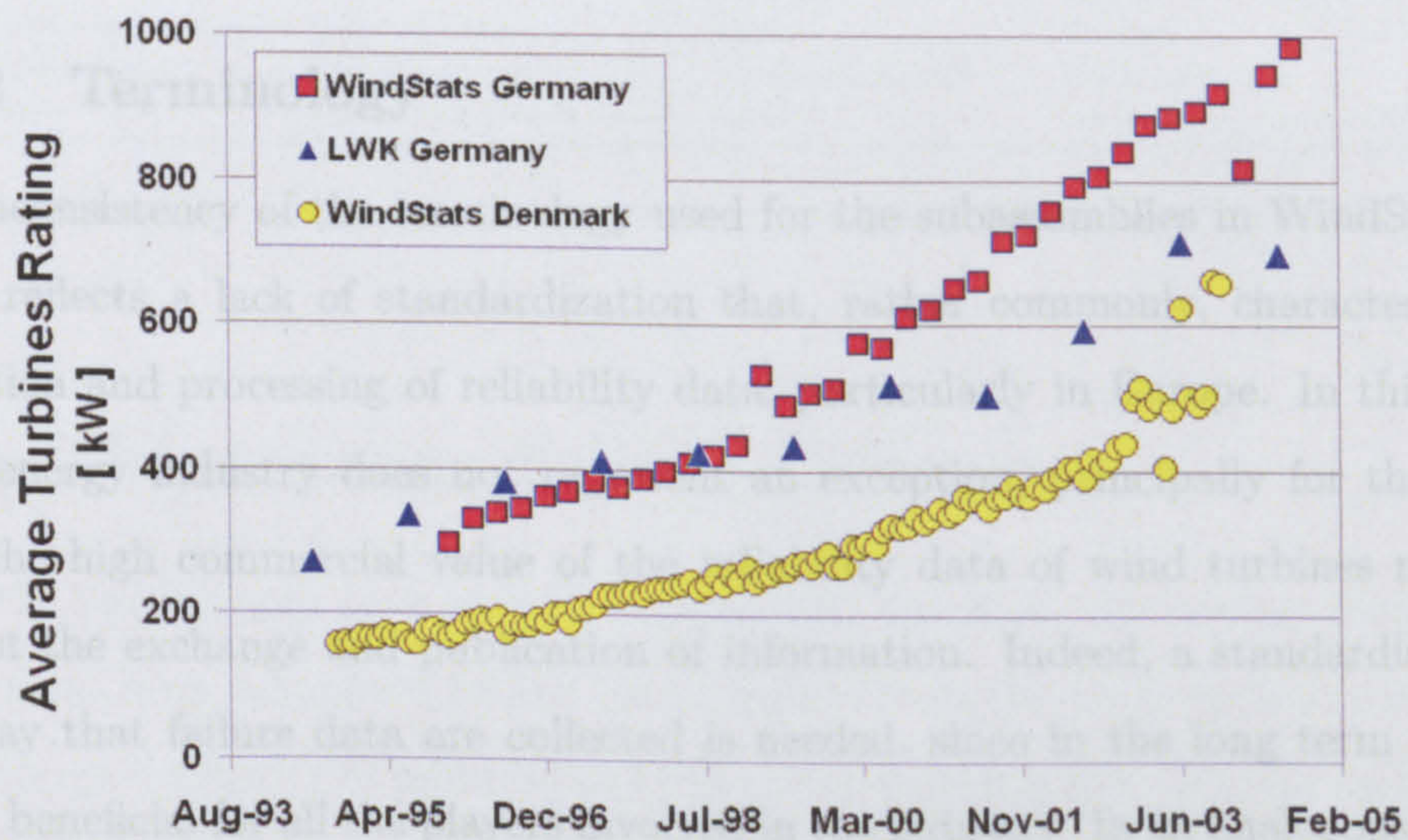


Figure 4.7: Average rating of the wind reporting turbines

The elements characterizing the three surveys can be summarized as follows:

- For WSD, WSDK, and LWK data are collected and grouped respectively quarterly, monthly and yearly.

- The three populations involve various wind turbines models, of different age, technology and manufacturer.
- The number of turbines involved is large, although the number changes in each period for each population; between 1291 and 4285 for WSD, between 851 and 2345 for WSDK and between 158 and 653 for LWK.
- The causes of stoppage are reported as general categories so that actual failure modes remain unspecified.
- The number of failures for “non specified” causes may be relevant for the future.
- The analysis concerns exclusively the “component” or subassemblies related failures.
- The average rating of the three surveys invariably increases over the observed period.

4.3.2 Terminology

The inconsistency of the terminology used for the subassemblies in WindStats and LWK reflects a lack of standardization that, rather commonly, characterises the collection and processing of reliability data, particularly in Europe. In this regard wind energy industry does not represent an exception, principally for the reason that the high commercial value of the reliability data of wind turbines mitigates against the exchange and publication of information. Indeed, a standardisation of the way that failure data are collected is needed, since in the long term it would result beneficial for all the players involved in the industry. In an analogous case the standardisation of the quality control terms in every aspect of manufacturing, has proved to be profoundly useful and has contributed to economic growth. In the case of a wind turbine, which is a complex system embedding sophisticated subassemblies and components, the standardisation of terminology used for the classification of components, subassemblies and failure modes is also crucial.

Failure data are typically collected from operation engineers, who are asked to fill

December 6, 2008

in forms similar to the one shown in picture 4.8, taken from the German survey WMEP [6], after a major failure occurs or during a scheduled maintenance visit, the forms used by WindStats and LWK are not available.

Each survey is based on a particular data form, as has been seen in Tables 4.1, 4.2, and 4.5. The terminology used for each survey subassembly is summarised in Table 4.6. The first column of the table displays the standard term adopted and used throughout this thesis for each subassembly. The standardization has been achieved by aggregating some of the original subassemblies, so it must be borne in mind that each subassembly can be constituted of different elements for different surveys.

This thesis	WindStats D	WindStats DK	LWK
Rotor or blades	Rotor	Blades, Hub	Blades
Air brake	Air brake	Air brake	Rotor brake
Mechanical brake	Mechanical brake	Mechanical brake	Brake
Main shaft	Main shaft/bearing	Axle/bearing, Coupling	Shaft/bearings
Gearbox	Gearbox	Gearbox	Gearbox
Generator	Generator	Generator	Generator
Yaw system	Yaw system	Yaw system	Yaw system
Electrical control	Electrical control	Electrical control	Electronics, Inverter
Hydraulics	Hydraulics	Hydraulic	Hydraulics
Electrical system	Electrical system	Grid	Electrics
Pitch control	Pitch adjustment	Mechanical control	Pitch mechanism
Other	Anemometry, Sensors, Other	Other	Anemometry, Sensors, Other

Table 4.6: The terminology used for the wind turbine subassemblies

4.4 The Average Failure Frequency

With the assumptions that have been previously specified, the average frequency of failures has been calculated for the data supplied from the three surveys considered. The average frequency of failures has been calculated, as a first step, for each recording period and for the entire population of turbines, and the results compared.

In the period i the average failure intensity Λ_i is calculated by dividing the total number of failures by the the total working hours, that is the number of wind turbines in the survey times the number of hours in the period minus the total hour lost. The failure frequency is then scaled on a yearly basis.

In formula:

Maintenance and Repair Report

WMEP 250 MW-Wind

WIND ENERGY

day	month	year	minutes	

cause of malfunction

<input type="checkbox"/> high wind <input type="checkbox"/> grid failure <input type="checkbox"/> lightning <input type="checkbox"/> fire	<input type="checkbox"/> failure of wind speed sensor <input type="checkbox"/> temperature sensor failure <input type="checkbox"/> loosening of parts <input type="checkbox"/> oil leakage <input type="checkbox"/> noise reduction
--	---

effect of malfunction

<input type="checkbox"/> damaged <input type="checkbox"/> repair <input type="checkbox"/> spare <input type="checkbox"/> other	<input type="checkbox"/> reduced power <input type="checkbox"/> bearing failure or damage <input type="checkbox"/> shaft damage <input type="checkbox"/> other consequences
---	--

reason for repair

wind speed sensor failure

wind speed sensor repair or replacement of wind speed sensor or repair of distance

unscheduled repair after malfunction

down time

not stopped

stopped

hour				
day	month	year	reading of meter (hours)	

costs stated on bill

material		EUR
labor		EUR
material		EUR
total cost incl. VAT		EUR

removal of malfunction

perfect for starting of plant after

with delay

emergency or consequential damage

required repair components

<input type="checkbox"/> hub <input type="checkbox"/> sub body <input type="checkbox"/> pitch mechanism <input type="checkbox"/> yaw bearing <input type="checkbox"/> rotor blades <input type="checkbox"/> drive shaft <input type="checkbox"/> disc shaft <input type="checkbox"/> disc end <input type="checkbox"/> planetary gearbox <input type="checkbox"/> generator <input type="checkbox"/> generator cooling <input type="checkbox"/> generator bearing <input type="checkbox"/> bearing <input type="checkbox"/> electric <input type="checkbox"/> control <input type="checkbox"/> fan <input type="checkbox"/> cooling fan <input type="checkbox"/> cable connection <input type="checkbox"/> sensors <input type="checkbox"/> emergency stop <input type="checkbox"/> vibration switch <input type="checkbox"/> temperature <input type="checkbox"/> oil pressure switch <input type="checkbox"/> power switch <input type="checkbox"/> voltage sensor <input type="checkbox"/> control system <input type="checkbox"/> electrical control <input type="checkbox"/> relay <input type="checkbox"/> noise-reducing devices	<input type="checkbox"/> gear box <input type="checkbox"/> bearing <input type="checkbox"/> wheel <input type="checkbox"/> gear shaft <input type="checkbox"/> shaft <input type="checkbox"/> mechanical brake <input type="checkbox"/> disc end <input type="checkbox"/> shaft end <input type="checkbox"/> disc shaft <input type="checkbox"/> drive shaft <input type="checkbox"/> rotor bearing <input type="checkbox"/> bearing <input type="checkbox"/> coupling <input type="checkbox"/> hydraulic system <input type="checkbox"/> hydraulic pump <input type="checkbox"/> control valve <input type="checkbox"/> valves <input type="checkbox"/> hydraulic components <input type="checkbox"/> gear system <input type="checkbox"/> gear bearing <input type="checkbox"/> gear shaft <input type="checkbox"/> shaft end <input type="checkbox"/> structural parts/housing <input type="checkbox"/> foundation <input type="checkbox"/> yaw drive top <input type="checkbox"/> yaw drive <input type="checkbox"/> yaw drive
---	--

operator

name: _____

signature: _____

replaced main components

<input type="checkbox"/> nacelle <input type="checkbox"/> tower <input type="checkbox"/> hub <input type="checkbox"/> gear box <input type="checkbox"/> generator	<input type="checkbox"/> pitch system <input type="checkbox"/> yaw <input type="checkbox"/> control system at nacelle <input type="checkbox"/> transformer
---	---

comments

Figure 4.8: The failure reporting form taken from WMEP, Windenergie Report Deutschland

$$\langle \Lambda_i \rangle = \frac{n_i}{(N_i \cdot h_i) - L_i} \cdot 8760 \quad (4.1)$$

Where n_i and N_i are respectively the cumulative number of failures and turbines in the interval i , h_i is the number of hours of i and L_i is the cumulative hour lost for the same interval.

Since the hours lost are not reported in WSDK the correction over the running time for this thesis is not feasible. However, since the hours lost are usually a small fraction of the total hours, the error is not particularly significant and can be neglected.

The results of the calculation of the average intensity of failure are illustrated in the diagram of Fig. 4.9.

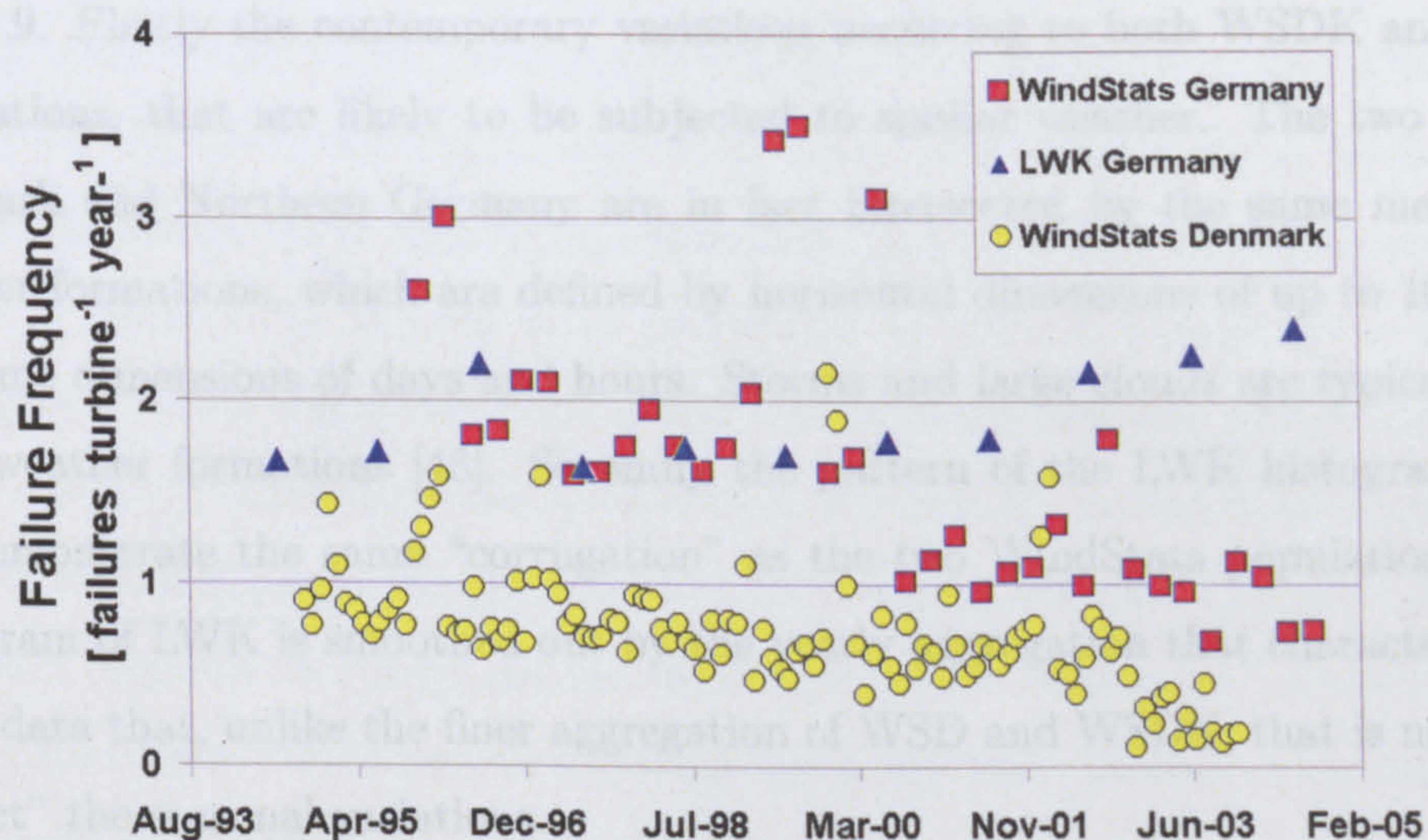


Figure 4.9: The average frequency of failures from the two WindStats populations

The observations made are summarised as follows:

1. The values are rather volatile, in particular for the two WindStat populations.
2. However the failures are characterised by a certain periodicity.
3. Despite the volatility a general trend can be identified for each survey over the entire period.

4. The failure rate is decreasing for both WSD and WSDK and increasing for LWK.
5. The overall average failure rate appear similar for WSD and LWK in Germany and are remarkably lower for WSDK.

4.4.1 Weather Effects

Unlike the traditional generation technologies, whose generation units are enclosed in protected buildings, wind turbine equipment is exposed, in the nacelle, to substantially variable conditions. Weather variations are expected to affect the reliability of the system as confirmed by points 1 and 2 of the previous observations. In particular, the effect of the weather is confirmed by two elements that emerge from Fig. 4.9. Firstly the contemporary variations occurring to both WSDK and WSD populations, that are likely to be subjected to similar weather. The two regions Denmark and Northern Germany are in fact intersected by the same meso-scale weather formations, which are defined by horizontal dimensions of up to 1000 km, and time dimensions of days and hours. Storms and large clouds are typical meso-scale weather formations [48]. Secondly the pattern of the LWK histogram, does not demonstrate the same “corrugation” as the two WindStats populations. The histogram of LWK is smoothed out by the yearly aggregation that characterise the LWK data that, unlike the finer aggregation of WSD and WSDK, that is unable to “detect” the seasonal variations.

The effect of the weather has been thoroughly analysed in [48], to which the author contributed. The publication is based on a final year MSci Physics Project by C. Edwards at Durham University. The project, which aimed to study the correlation between the wind speed and the frequency of failure, has unveiled interesting results. The study is based on three basic elements:

- The wind energy index (WEI)
- The auto-correlation of the data over the entire range
- The cross-correlation between WEI and the average failure frequency

The Wind Energy Index [36] is a tool invented and largely used in the Danish wind energy industry and is defined as the ratio between the actual monthly energy production from a collection of wind turbines and the long term expected monthly energy production from those turbines, in the presence of average weather.

$$WEI = \frac{\int_I P dt}{\int_I P_{avg} dt} \quad (4.2)$$

The WEI is determined by the wind speed, although it can be influenced by other factors, like the unreliability of the wind turbines, that reduces the numerator of the ratio in the most stormy periods. The energy index had been chosen in place of the wind speed because it is averaged over the entirety of Denmark and is more easily available. As expected the autocorrelation analysis for both WEI and the failure rate has resulted in a significant periodicity occurring at 12, 24 and 36 months, that is a periodicity on yearly basis. The cross correlation between the WEI and Λ has been verified on many subassemblies, with correlation coefficients ranging between 0.3 and 0.4. Although the correlation coefficient is not particularly high, it constitutes a point of interest. In fact the cross correlation coefficient is expected to increase substantially, if the the actual wind speed is used in the analysis rather than WEI. This is due to the effect that the failures have, particularly during windy periods, as the energy harvest and consequently the WEI decrease, reduces the cross correlation coefficient. For this and other reasons the subject of the correlation between failures and environmental conditions deserves further study and constitutes an interesting opportunity of research.

The results of [48] are reported here:

1. There is a clear relationship between the Failure Rate of a population of Danish wind turbines and the Wind Energy Index averaged over Denmark
2. That relationship shows that Danish turbine Failure Rates have a 12 monthly periodicity with the peak Failure Rate in the Winter (February) and a secondary peak in the Autumn (October).
3. The cross-correlation analysis has shown that some Danish turbine subassemblies may be less affected by wind-speed characteristics than other subassem-

blies. In particular the blades, hub, main shaft, coupling and gearbox are notable in this respect.

4. The analysis has shown that some other Danish turbine subassemblies are more susceptible to such weather effects, in particular the generator, yaw control, mechanical brake and hydraulic system. It is suggested that this may be because these subassemblies are proprietary engineered products, not designed for the rapidly changing effects of the wind speed variation.

Figures 4.10, 4.11 and 4.12 which illustrate periodograms of WEI and the WS failure rate and the cross-correlogram between the two quantities respectively, confirm the above observations. The two periodograms show the spectral function resulting from the data in function of the angular frequency expressed in rad/months. For some of the points the period expressed in months corresponding to that angular frequency is reported.

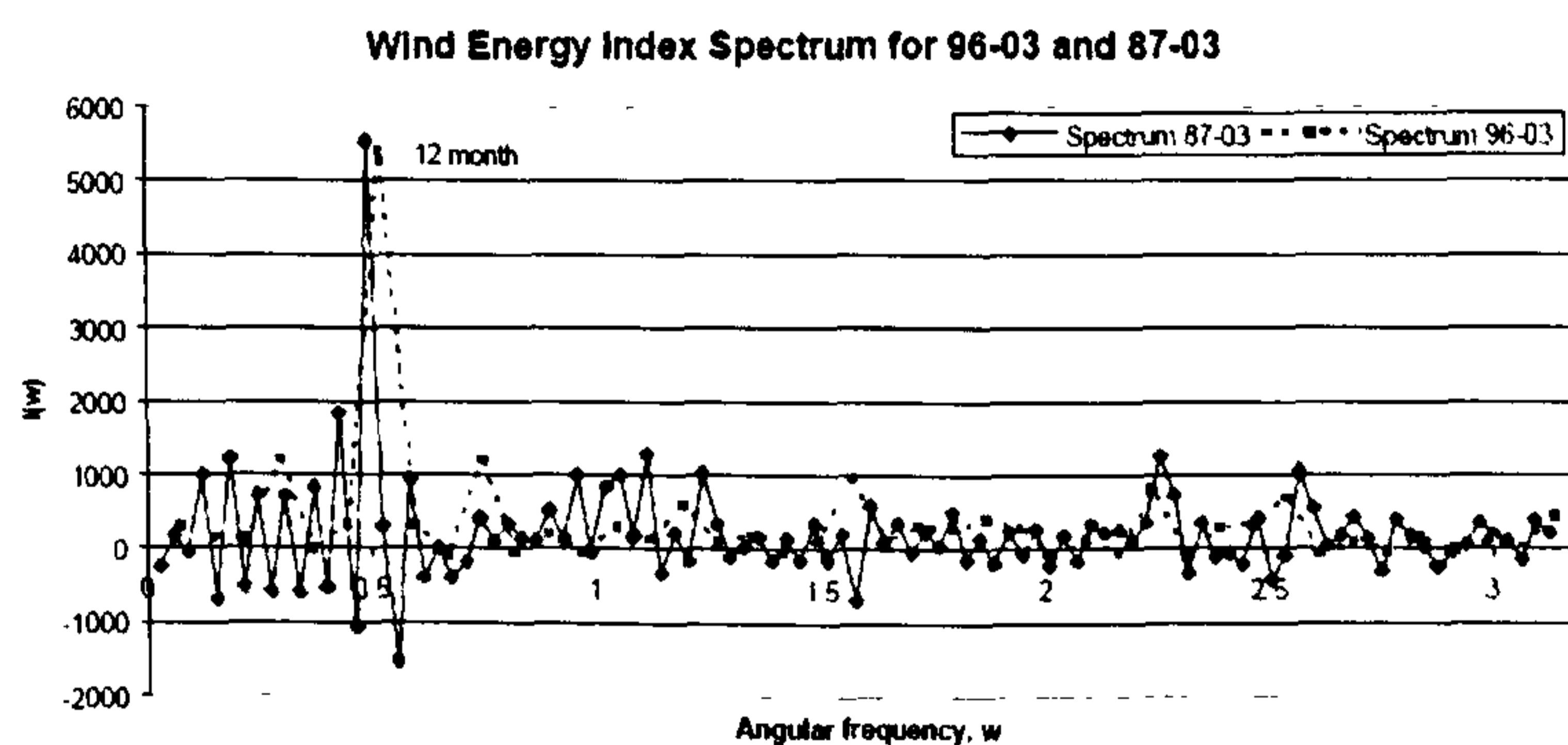


Figure 4.10: Spectrum for 2 WEI data sets: 96-03 and 87-03. The longer set displays a sharper peak at angular frequencies equivalent to 12 months. The angular frequency is expressed in rad/month.

4.4.2 Reliability Growth

The trends of the failure intensity highlighted in point 3 and 4 of the observation in Section 4.4 above deserve particular attention. It is expected that large populations of heterogeneous turbines of different ages, rating, manufacturing techniques and technology show a relatively constant intensity of failure, even over large periods of

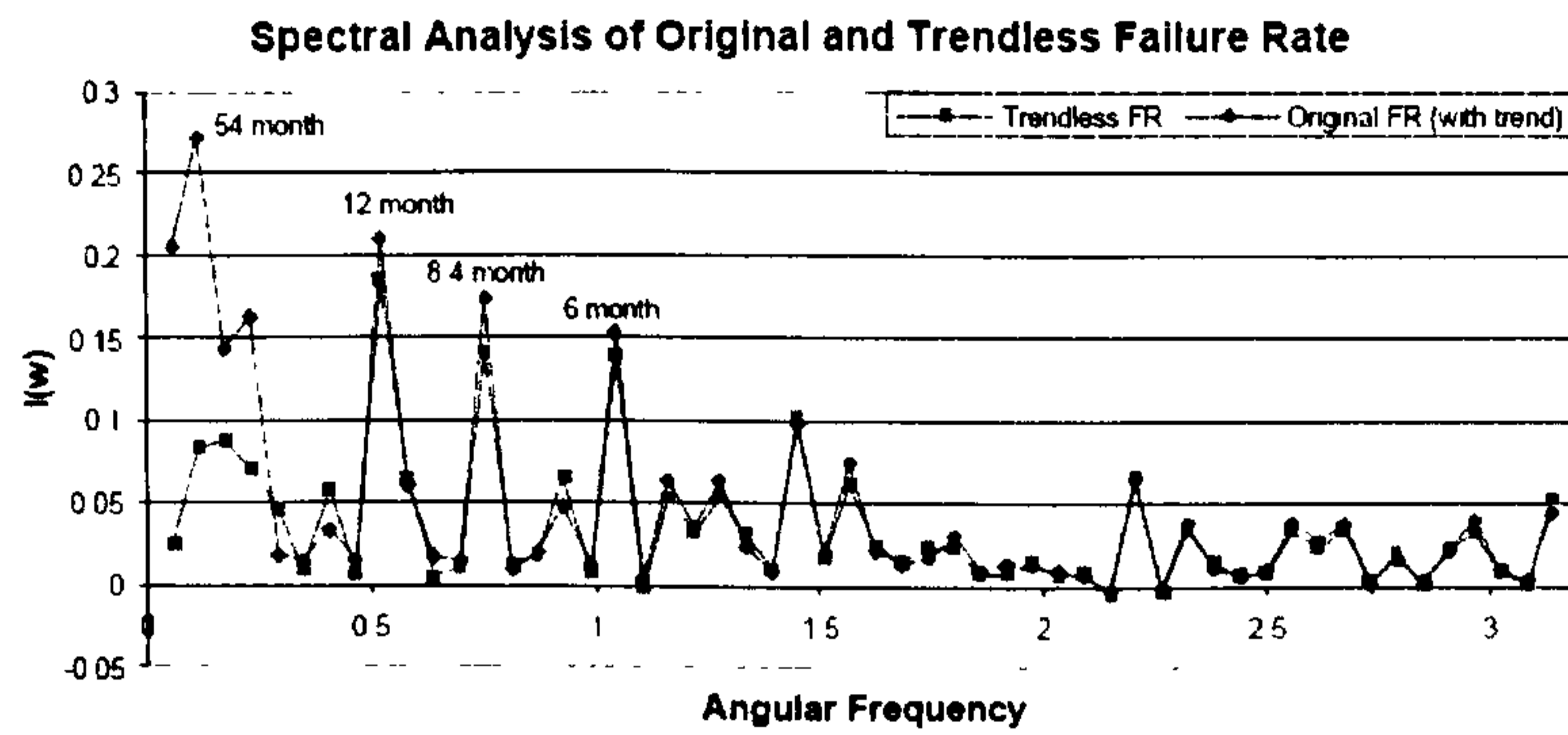


Figure 4.11: Spectrum of failure rate data before and after linear trend has been removed. 54 month peak has decreased significantly, other 3 main angular frequencies have changed little. Angular frequency is expressed in rad/months. For some of the points the equivalent self correlation period is reported

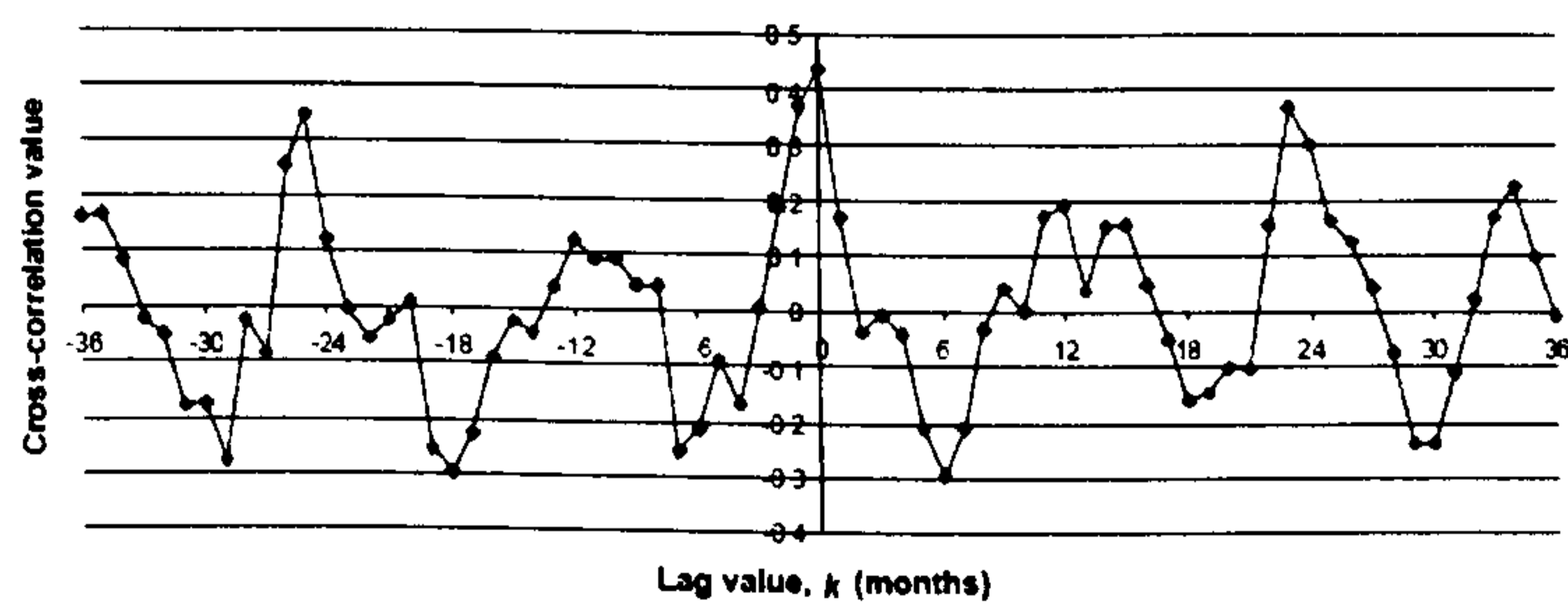


Figure 4.12: Cross-Correlogram of Turbine Failure Rate to WEI, 1994-2004

times. In particular the contemporary presence of turbines of different ages in the population covers reliability trends that can be due to either improvement (positive growth) or deterioration (negative growth). A constant intensity of failure is also the result of many different failure modes having competing and overlapping effects in the definition of the overall reliability of a system. Despite the heterogeneity of the WindStats turbines, the reliability data show a clear downward trend indicating that a better reliability is being achieved and that failures decrease over the period of observation. It is a clear case of reliability growth. The next chapter deals extensively with the reliability growth and resumes the results of the application of dedicated statistical tools. Here it can be stated that the reliability growth can be achieved, in the case of repairable systems, by many means *in primis* by technological improvement concerning materials, design and manufacturing. Nevertheless other "cultural" aspects about usage, preventive maintenance and corrective maintenance, possibly assisted by improved condition monitoring techniques can also produce reliability growth. The interpretation of the increasing failure intensity of LWK presents more difficulty. Possibly, the key lies in the average age of the overall LWK population, whose trend is clearly increasing as identified in Fig. 4.13.

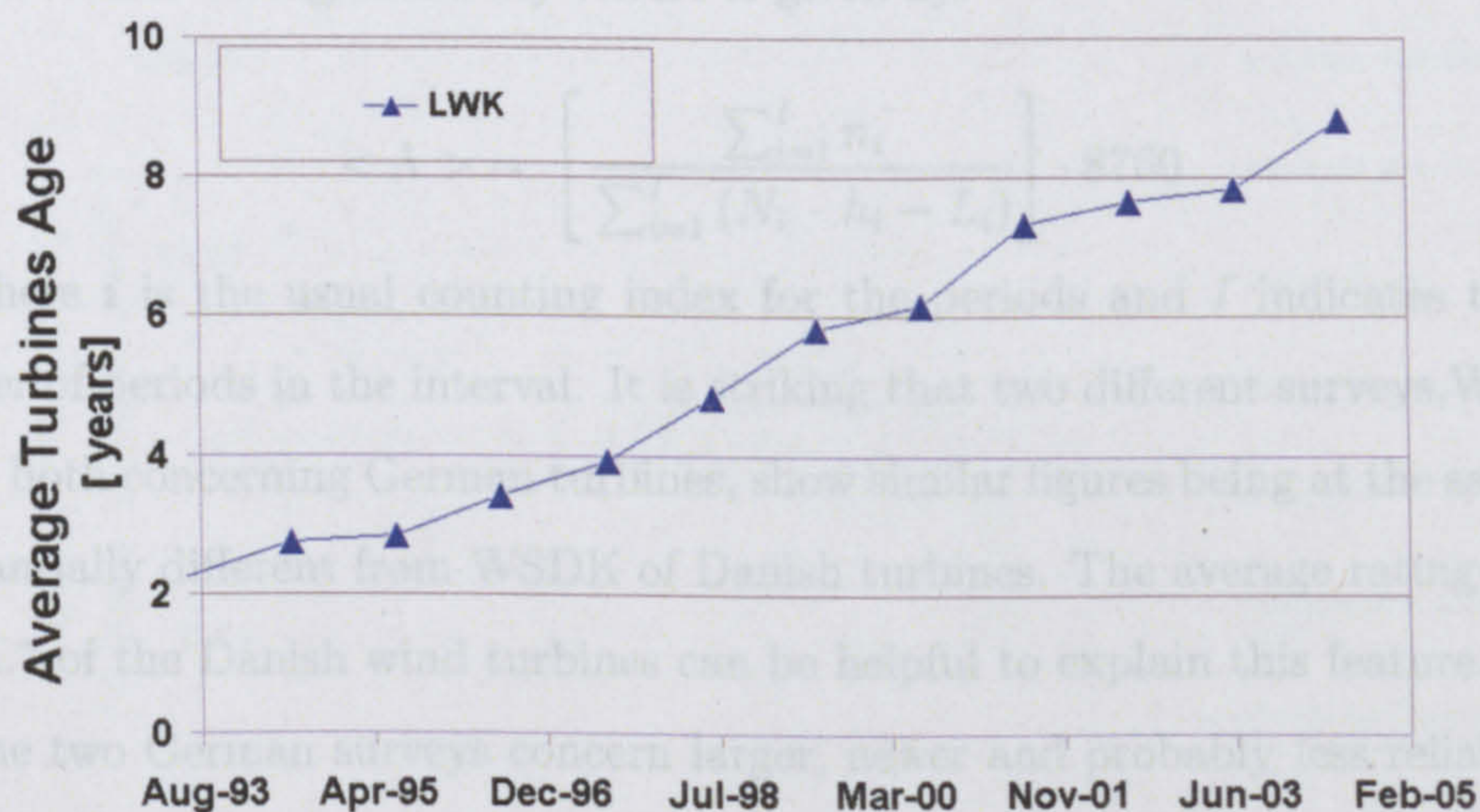


Figure 4.13: The average age of the LWK turbines

Given the increasing average age it is likely that the increment in the failure

intensity is due to the wear out of some dominant subassemblies, most likely the mechanical related subassemblies. The same modest value of the increment might be due to the trade off between the technological improvement achieved and the inevitable wear out of the electro-mechanical systems.

4.4.3 Technology

If the overall average failure rate is analysed neglecting the failure trends that occur during the recording period, some interesting feature are unveiled.

From Fig. 4.9 it appears that the overall failure rate is consistently similar for the two German populations WSD and LWK and higher than WSDK, referring to a Danish population.

Survey	$\langle \Lambda \rangle$ [failures turbine ⁻¹ year ⁻¹]
WSD	1.44
LWK	1.75
WSDK	0.73

Table 4.7: Overall average failure intensity and age

The overall average intensity failure is given by:

$$\langle \Lambda \rangle = \left[\frac{\sum_{i=1}^I n_i}{\sum_{i=1}^I (N_i \cdot h_i - L_i)} \right] \cdot 8760 \quad (4.3)$$

Where i is the usual counting index for the periods and I indicates the total number of periods in the interval. It is striking that two different surveys, WSD and LWK, both concerning German turbines, show similar figures being at the same time substantially different from WSDK of Danish turbines. The average rating given in Fig. 4.7 of the Danish wind turbines can be helpful to explain this feature.

The two German surveys concern larger, newer and probably less reliable wind turbines, while WSDK concerns a population of older, smaller turbines, involving a more mature technology. The maturity of the technology and the size are both important for the reliability of the wind turbines. The first concern the initial design errors or “bugs”, to use the neologism from the world of the information technology.

The role of the second on the reliability is less obvious since larger wind turbines are at the same time tougher and subjected to increased stress. From the data available it appears that larger turbines are intrinsically less reliable as will be demonstrated in the next section.

The reliability of wind turbines can be compared with the reliability of traditional generation technology like steam and gas turbine or diesel engine driven generators too. In the debate about the opportunity of investing in renewable energies, wind energy in particular, this is a hot topic, raising typical concerns and enthusiasms. Reliability is certainly an important economic factor for wind power, at least before the possible occurrence of a peak oil, when the wind power is competing with the cheaper fossil fuels. Figure 4.14 shows a comparison of the failure frequencies of the three surveys with the failure frequencies of steam turbines, combined gas cycle turbines and diesel generation sets, whose data are respectively extracted from different surveys including from the "IEEE Gold Book". The black dots on the left high corner represent the reliability of wind turbines installed in California before 1987, that is during the California Wind Rush, taken from EPRI. The ordinate scale is logarithmic and the improvement since 1987 is striking, being of at least one order of magnitude higher than current failure frequency.

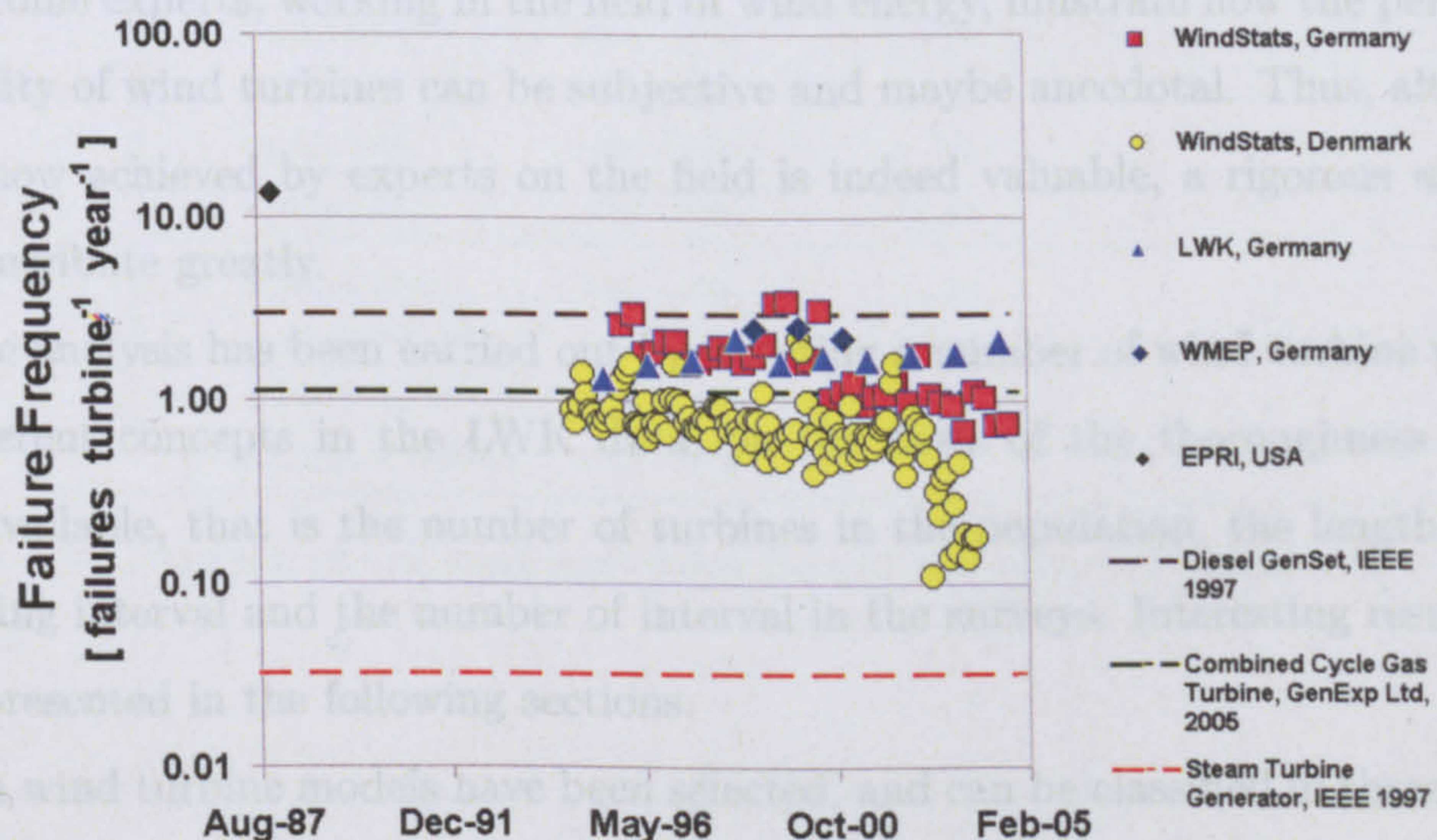


Figure 4.14: The failure intensity in historical context

4.5 Analysis of Turbine Concepts

4.5.1 Definition of Concepts

The possibility of the profitable offshore installation of wind turbines has ignited research intent especially about the definition of the most suitable architecture.

In Chapter 2 work conducted within the DOWEC program has been extensively outlined. In particular, the wind turbine architectures or “concepts”, were described, as defined in [60]. From the results of the DOWEC project it has emerged that reliability is the key factor for the offshore installation and will be decisive for the definition of a winner of the concepts competition.

LWK allows the comparison of single wind turbine models and, within the limits of the available data, ultimately the comparison of different wind turbines concepts. The analysis can be carried out by comparing the reliability of the subassemblies constituting the concepts.

The comparison between the reliability, as it is “perceived” by designers and operators, and the reliability that results from an accurate analysis is also important. In Chapter 2, the results of a questionnaire that has been submitted to a number of high profile experts, working in the field of wind energy, illustrate how the perceived reliability of wind turbines can be subjective and maybe anecdotal. Thus, although know-how achieved by experts on the field is indeed valuable, a rigorous analysis can contribute greatly.

The analysis has been carried out by selecting a number of wind turbine models of different concepts in the LWK data, on the basis of the thoroughness of the data available, that is the number of turbines in the population, the length of the reporting interval and the number of interval in the surveys. Interesting results are then presented in the following sections.

Eleven wind turbine models have been selected, and can be classified in three rating groups; Group I small, for machines rated about 300 kW, Group II medium, for machines of about 500 kW and Group III large, for machines in the megawatt range. Table 4.8 summarises some of the most important features of each of the

selected turbine models while Table 4.9 shows the extension of the recording period and the number of turbines in each model class ¹.

Group	Model	Rating	Drive	Speed	Regulation
I - Small	Vestas V27 *	225	Indirect drive	Fixed speed	Pitch/hydraulic
	Micon M530 *	250	Indirect drive	Fixed speed	Stall
	Nordtank 300	300	Indirect drive	Fixed speed	Stall
II - Medium	Tacke TW600 *	600	Indirect drive	Fixed speed	Stall
	Enercon E40 *	500	Direct drive	Variable speed	Pitch/Electrical
	Vestas V39 *	500	Indirect drive	Variable speed	Pitch/Hydraulic
	Vestas V44	600	Indirect drive	Variable speed	Pitch/Hydraulic
	Vestas V47	660	Indirect drive	Variable speed	Pitch/Hydraulic
III - Large	Enercon E66 *	1500	Direct drive	Variable speed	Pitch/Electrical
	Nordex N52/N54 *	800/1000	Indirect drive	Variable speed	Stall
	Tacke TW1.5s	1500	Indirect drive	Variable speed	Pitch/Electrical
	An Bonus 1MW54	1000	Indirect drive	Variable speed	Pitch/Electrical

Table 4.8: The features of the selected wind turbine models from LWK data

Group	Model	Period	N. of WT (range)	N. of WT (average)
I - Small	Vestas V27 *	1993 - 2004	21 - 55	35
	Micon M530 *	1993 - 2004	19 - 28	20
	Nordtank 300	1993 - 2002	5 - 16	12
II - Medium	Tacke TW600 *	1995 - 2004	25 - 60	38
	Enercon E40 *	1994 - 2004	9 - 75	47
	Vestas V39 *	1993 - 2004	17 - 67	47
	Vestas V44	1998 - 2001	4 - 29	18
	Vestas V47	2000 - 2004	7 - 22	17
III - Large	Enercon E66 *	1998 - 2004	3 - 22	11
	Nordex N52/N54 *	1998 - 2004	8 - 16	14
	Tacke TW1.5s	2000 - 2004	5 - 16	9
	An Bonus 1MW54	2000 - 2004	7 - 9	8

Table 4.9: Number of turbines and extension of the recording period of the LWK survey

¹The asterisk indicates those wind turbine models that have been involved in the reliability growth analysis illustrated in the next chapter. A precondition for the implementation of the reliability growth analysis is a sufficient number of failures, and for this reason turbine models not marked with the asterisk have been excluded.

For wind turbine concepts the alternatives concern the presence or not of the gearbox (indirect and direct drive), the presence or not of the converter (fixed speed and variable speed) and the control philosophy (stall, active stall or pitch regulated). In the case of pitch control the actuator can be either hydraulic or electric with repercussions on the hydraulics and electrics subassemblies. This set of turbine models that have been chosen to represent almost all the possible technology combinations of current turbine concepts.

4.5.2 The Reliability of Subassemblies

As an introduction for the presentation of the results of the concepts analysis it is useful to refine the analysis of the average failure frequency for each turbine subassembly. The calculation of the failure frequency for each subassembly is similar to equation 4.3 with the obvious difference that the number of failures is relative to the single subassembly, thus the previous equation is replaced by equation 4.4:

$$\langle \Lambda_k \rangle = \left[\frac{\sum_{i=1}^I n_{i,k}}{\sum_{i=1}^I (N_{i,k} \cdot h_{i,k} - l_{i,k})} \right] \cdot 8760 \quad (4.4)$$

Where, k is the variable counting the subassemblies. The average failure frequency is reported in Table 4.10 for each defined subassembly, and displayed in Fig. 4.15 where the figures for the three surveys, WSD, WSDK, LWK, are compared. Fig. 4.16 shows how the calculated failure frequency is distributed among the subassemblies, expressed in fraction of the failure frequency of the entire turbine. The failure distribution highlights the consistency that characterise the two German populations. Conversely, the Danish population not only shows an overall failure frequency but also a different distribution of failures among the subassembly. These figures can be compared with those given by ECN and DOWEC in Tables 2.1 and 2.2.

The first consideration concerns the high consistency between the two German populations, WSD and LWK, which show very similar values for all the subassemblies. Conversely WSDK, consisting of much more reliable turbines, is characterised by a different distribution of failures among the subassemblies, see Fig. 4.15 confirm-

	WSD (1291-4285 WTs)	WSDK (851-2345 WTs)	LWK (158-643 WTs)
Electrical system	0.2940	0.0468	0.3200
Rotor or blades	0.1910	0.0486	0.1900
Electrical control	0.1820	0.1500	0.2390
Yaw system	0.1080	0.0645	0.1160
Generator	0.1050	0.0497	0.1390
Hydraulic system	0.0958	0.0451	0.1310
Gearbox	0.0929	0.0425	0.1340
Pitch control	0.0893	0.0141	0.0834
Air brakes	0.0411	0.0164	0.0397
Mechanical brake	0.0330	0.0289	0.0554
Main shaft	0.0212	0.0145	0.0311
Other	0.1880	0.2090	0.3670

Table 4.10: The average failure frequency for each subassembly for all three populations

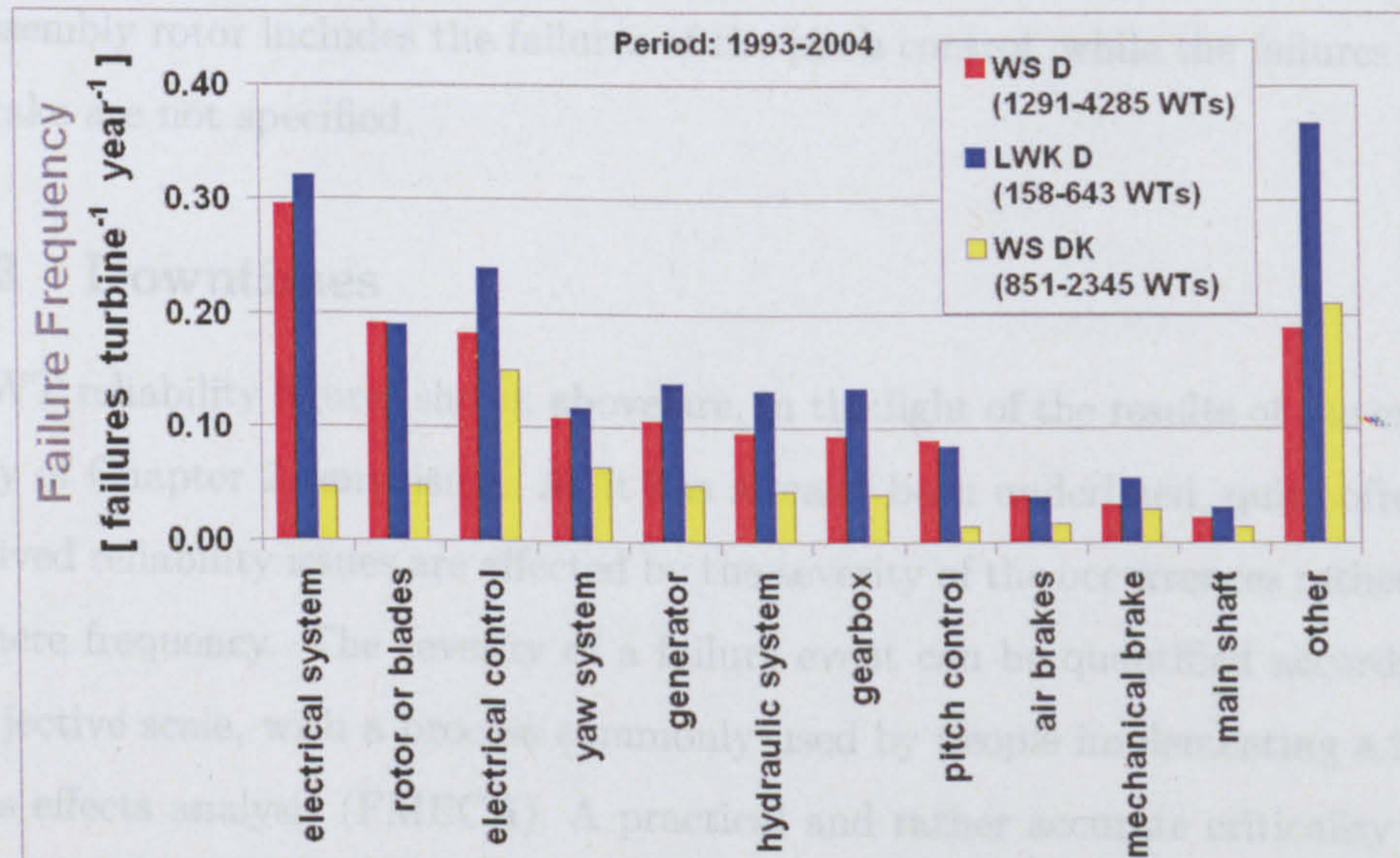


Figure 4.15: The average failure frequency for each subassembly, failures per year

ing the substantial difference of the turbines' technology. As expected the "other" subassembly dominates the failure frequency, suggesting the importance of a improved definition and classification of this area. Further considerations can be summarised as follows:

- Failures in electrical related subassemblies are predominant, the electrical system in particular.
- The reliability of the generator deserves a special mention given its low repairability.
- Failures in the rotor are high in the two German surveys (larger turbines).
- The reliability of the gearbox is relatively good despite anecdotal evidence to the contrary, but again like the generator has a low repairability

In 4.17 the same failure distribution is compared with the Swedish survey "Elforsk annual report" that appears in [41]. The survey, which considers 650 turbines in the period 2000-2004, shows results similar from the two German populations, with the exclusion of the hydraulics and the gearbox. For the Swedish population the subassembly rotor includes the failures of the pitch control, while the failures of the air brake are not specified.

4.5.3 Downtimes

The WT reliability figures shown above are, in the light of the results of the experts survey of Chapter 2, surprising. As it has already been underlined, quite often the perceived reliability issues are affected by the severity of the occurrences rather than the mere frequency. The severity of a failure event can be quantified according to a subjective scale, with a process commonly used by people implementing a failure modes effects analysis (FMECA). A practical and rather accurate criticality index is the total cost of the repair, but unfortunately the failure data do not allow this analysis. Conversely the downtime is available and can be used as a criticality index.

The downtime, resulting from a failure, is subjected to a number of factors of either random or planned nature, as;

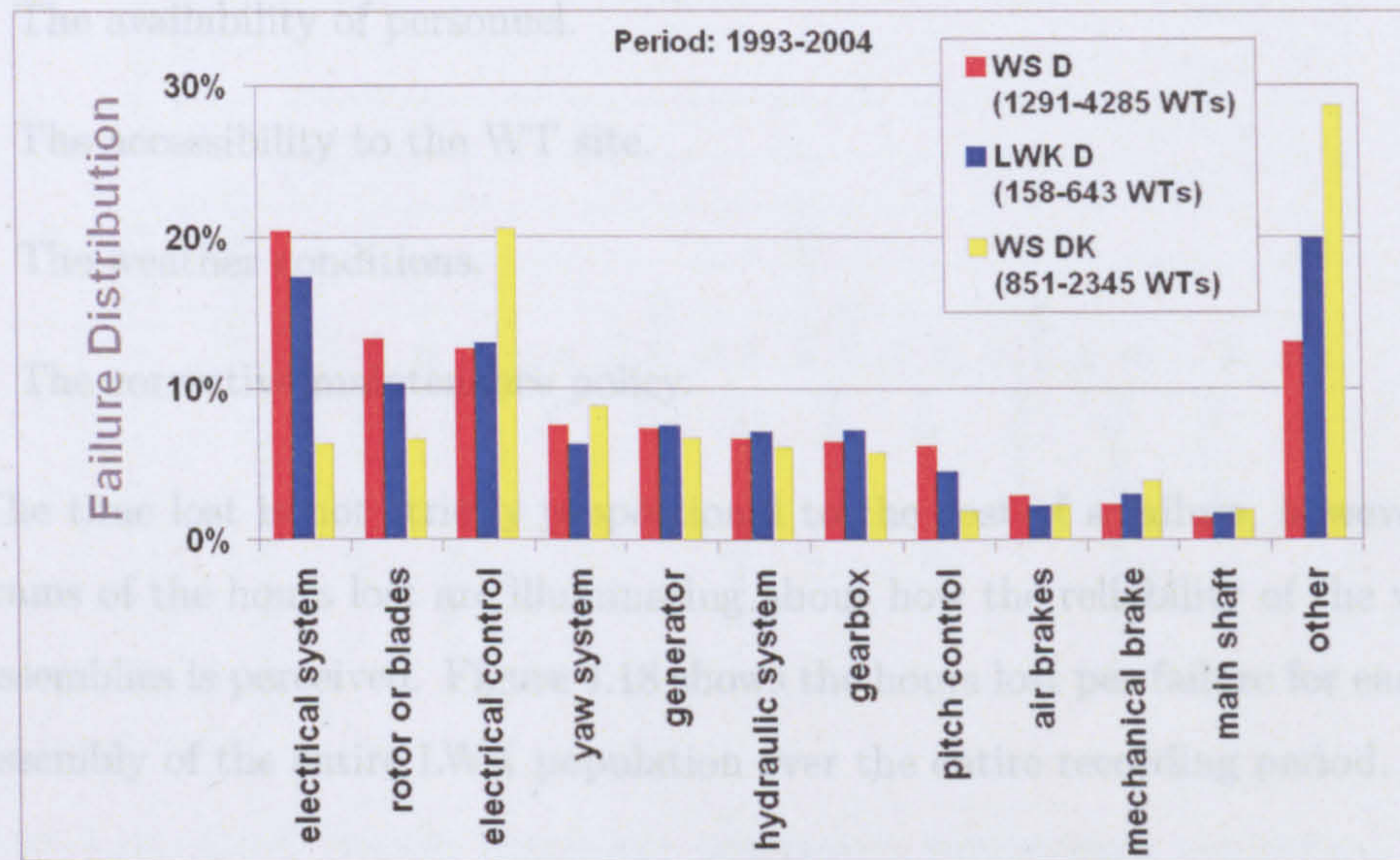


Figure 4.16: The failure distribution among the subassemblies

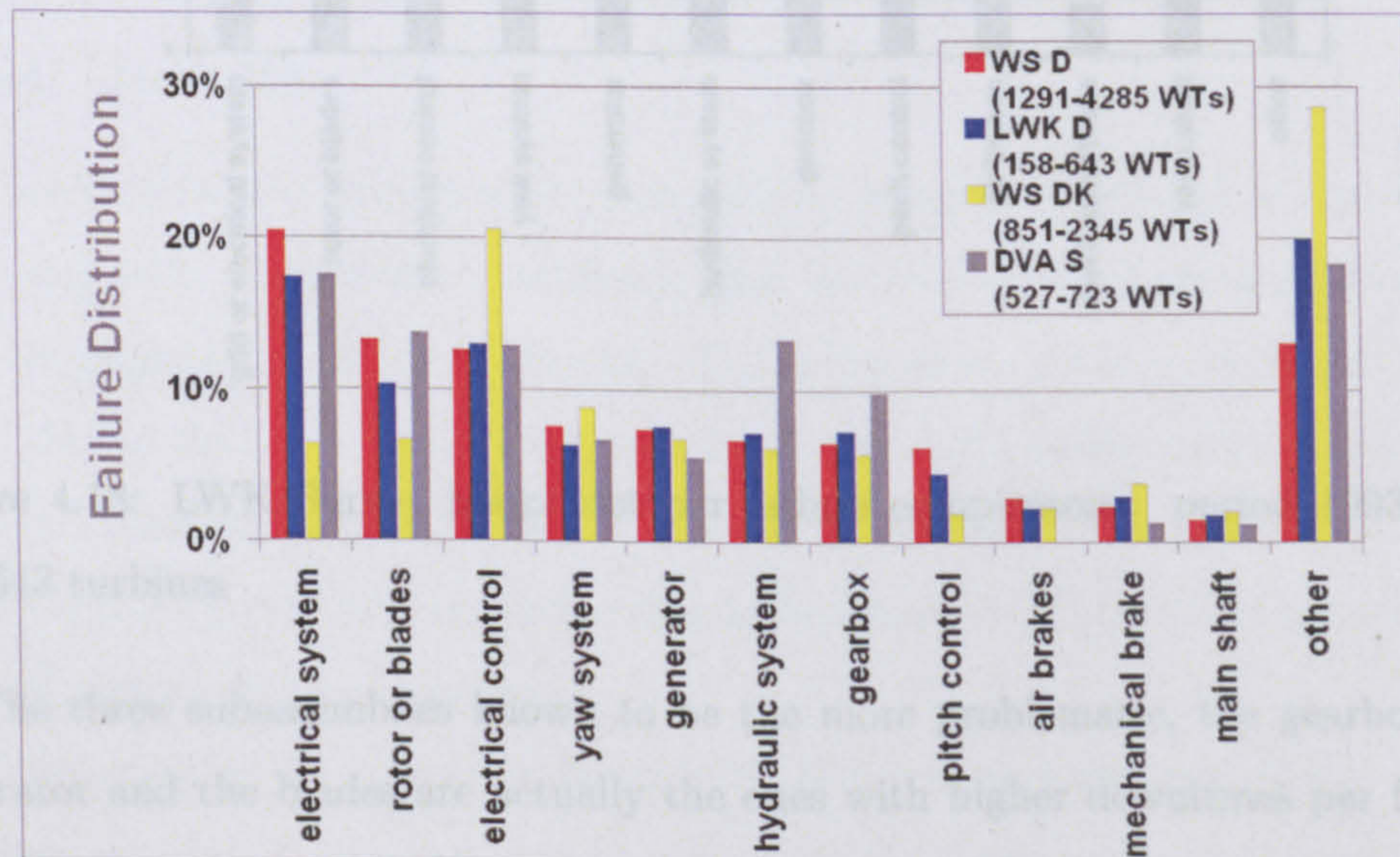


Figure 4.17: The failure distribution compared with another survey

- The availability of spare parts.
- The availability of personnel.
- The accessibility to the WT site.
- The weather conditions.
- The corrective maintenance policy.

The time lost is not strictly proportional to the cost of a failure, however, the diagrams of the hours lost are illuminating about how the reliability of the various subassemblies is perceived. Figure 4.18 shows the hours lost per failure for each WT subassembly of the entire LWK population over the entire recording period.

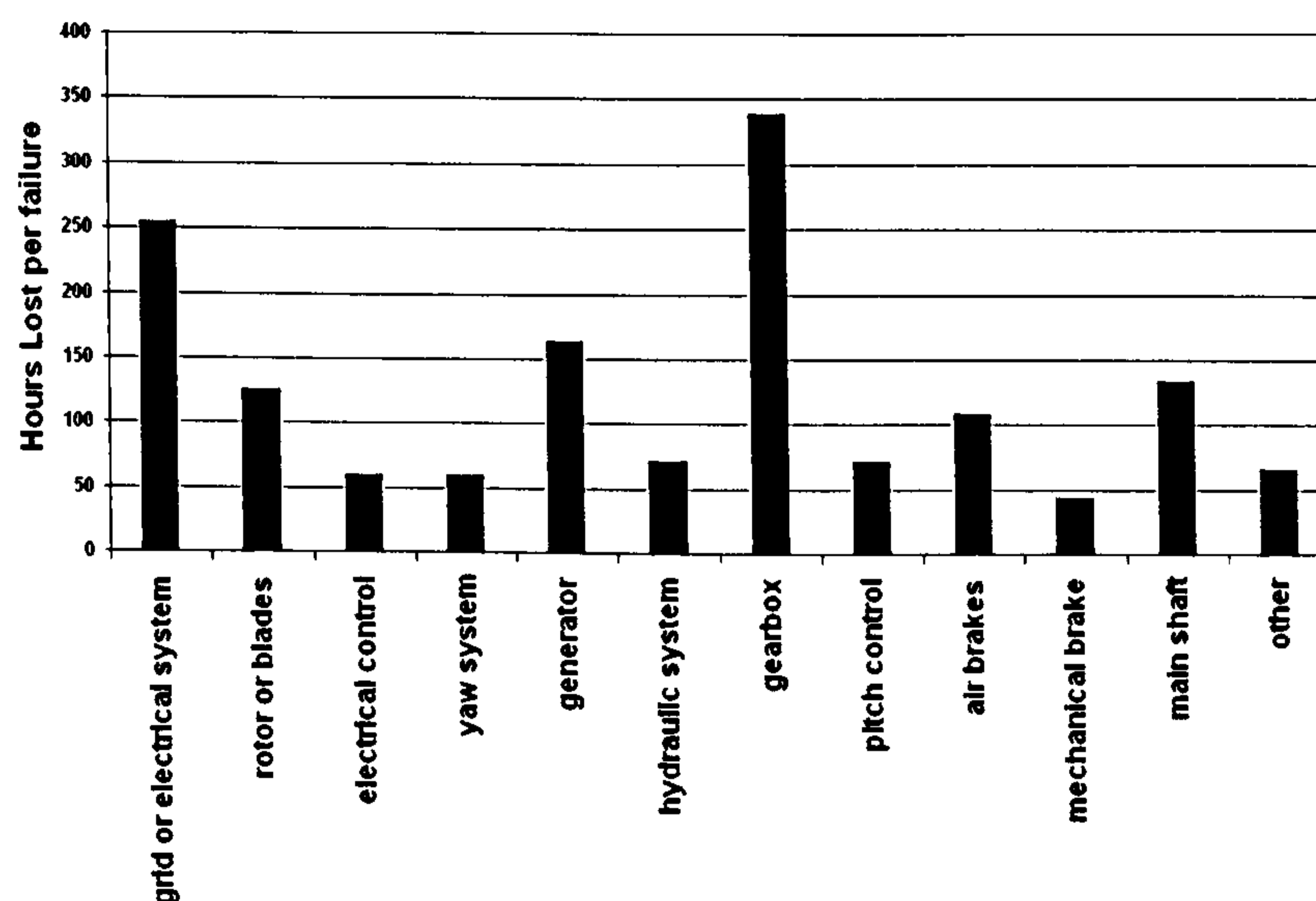


Figure 4.18: LWK Survey hours lost per failure comparison : period 1993-2004, 158-643 turbines

The three subassemblies known to be the more problematic, the gearbox, the generator and the blades are actually the ones with higher downtimes per failure. The electricals subassembly deserves a separate mention. Its downtime is rather high and comparable to the downtime of the gearbox. This outcome, together with the observed high failure rate, makes the electrical subassembly the most critical WT subassembly. Figures 4.18 and 4.19 also show that the problem with the gearboxes

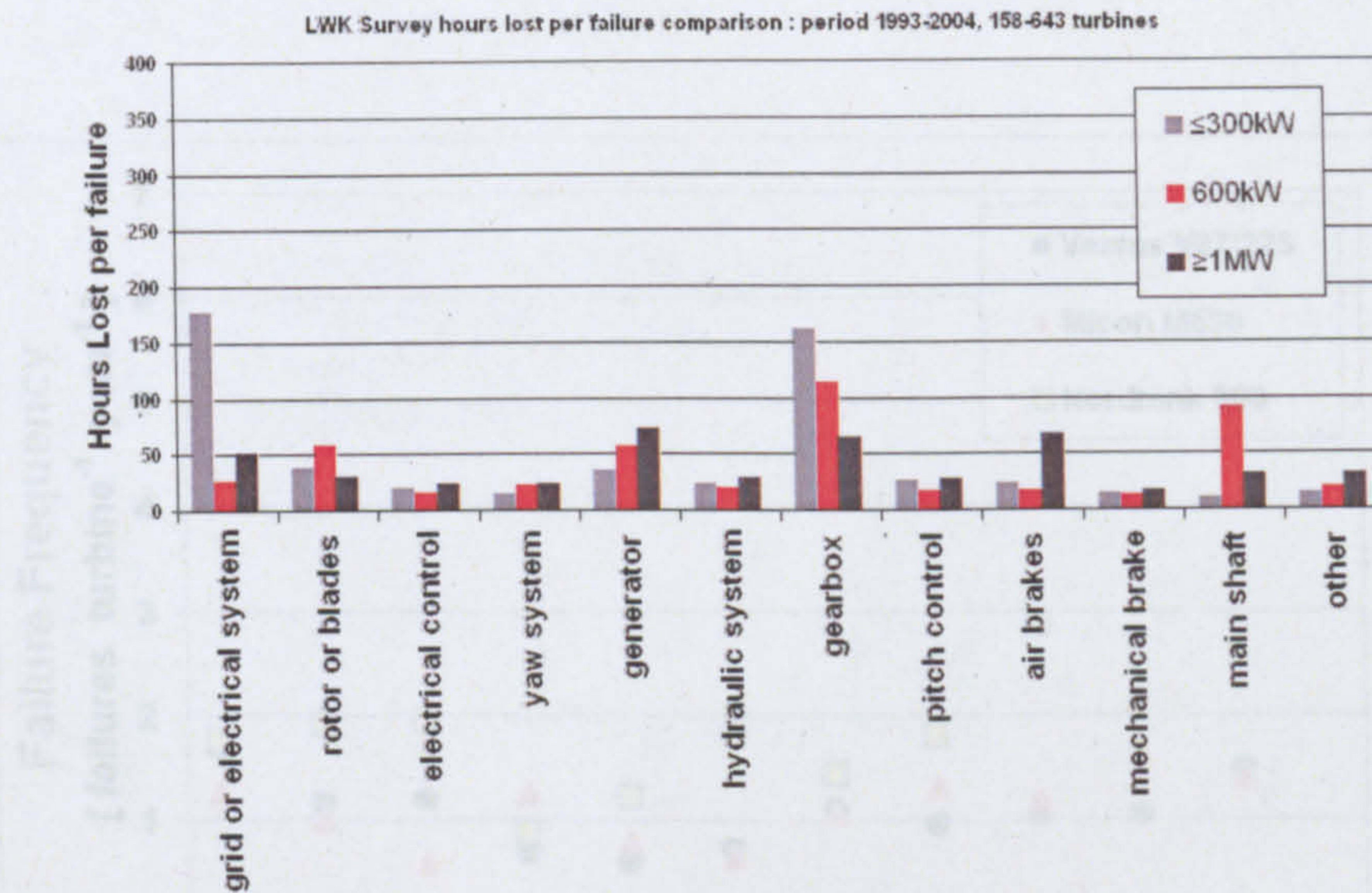


Figure 4.19: LWK Survey hours lost per failure comparison, segregated by WT group: period 1993-2004, 158-643 turbines

is not its failure frequency but above all its downtime. Figure 4.19 illustrates the downtime of the seven only WT models analysed from the LWK survey, aggregated by rating group.

4.5.4 Results

The average failure frequency for each turbine group is illustrated in figures 4.20, 4.21 and 4.22. Trends and periodicity, that are present in all the turbine groups, will be examined in the next chapter. The comparison of the three figures reveals that the reliability of larger wind turbines is generally lower, which supports the same conclusions reached between WSD and WSDK data. The positive correlation between failure rate and turbine rating is confirmed by Fig. 4.23 that shows the overall average failure frequency.

The origin of the increased unreliability of larger turbines can be due to three factors:

1. The newer technology.
2. The higher complexity of the technology.

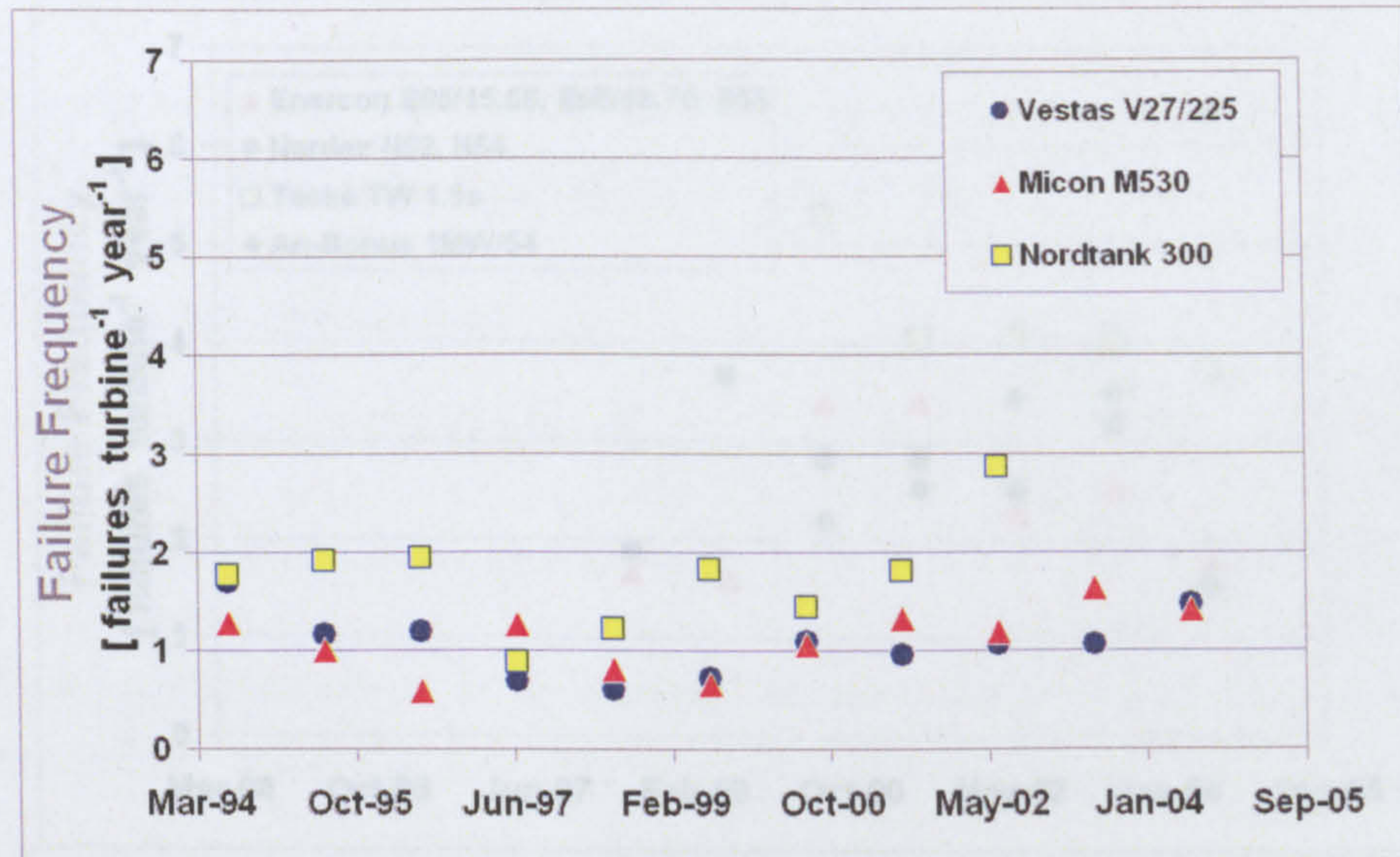


Figure 4.20: The average failure frequency of Group I, small turbines

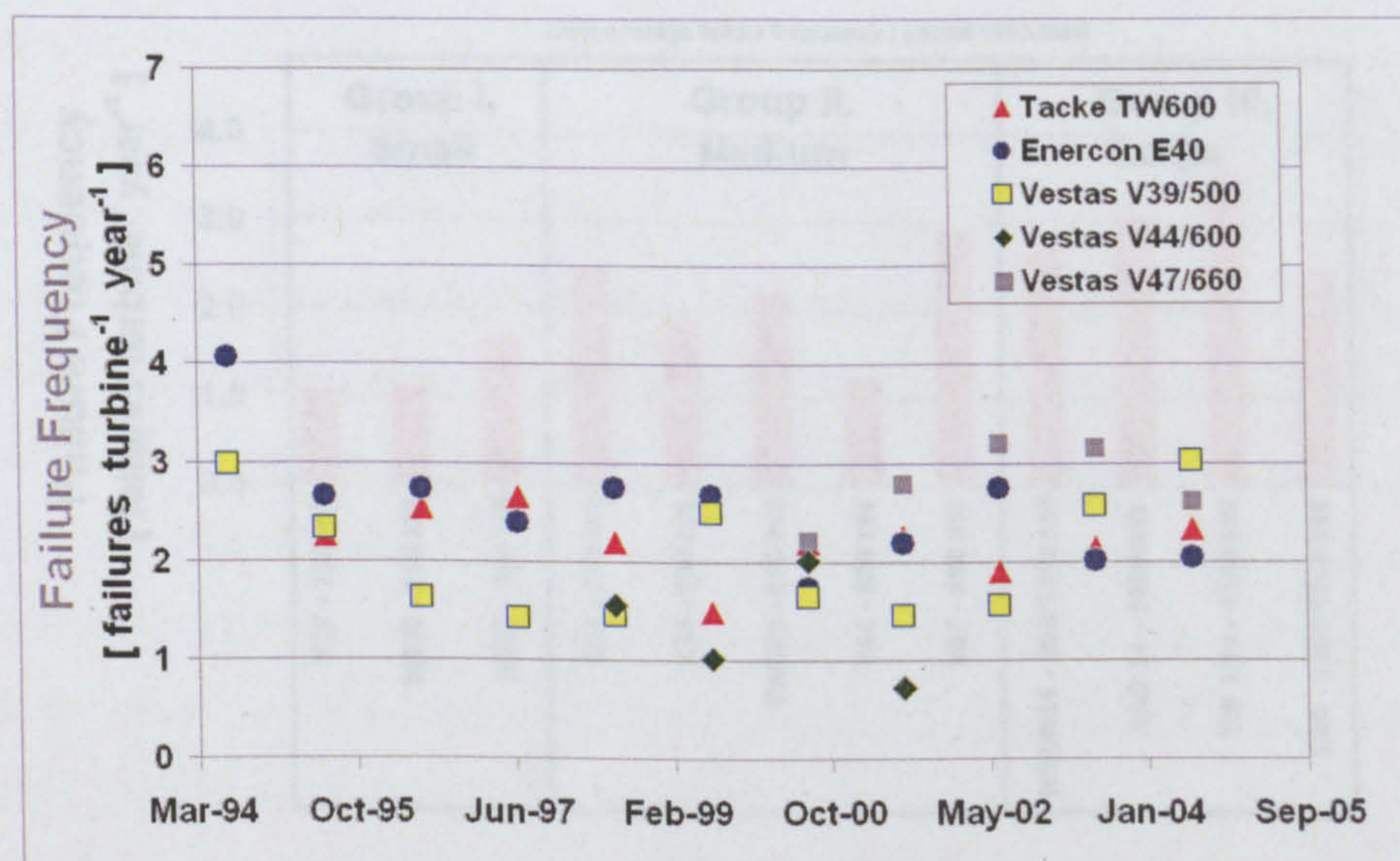


Figure 4.21: The average failure frequency of Group II, medium turbines

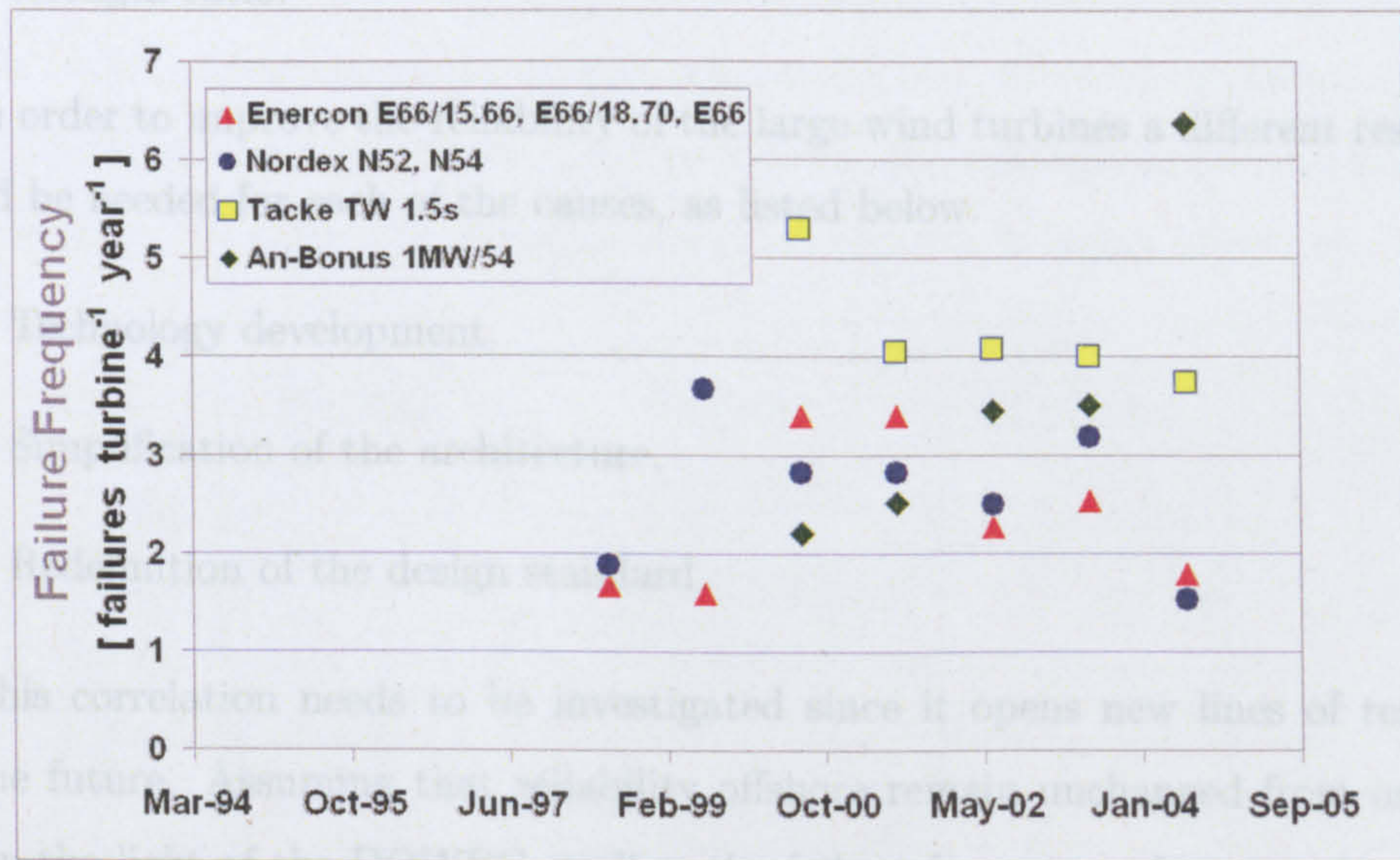


Figure 4.22: The average failure frequency of Group III, large turbines

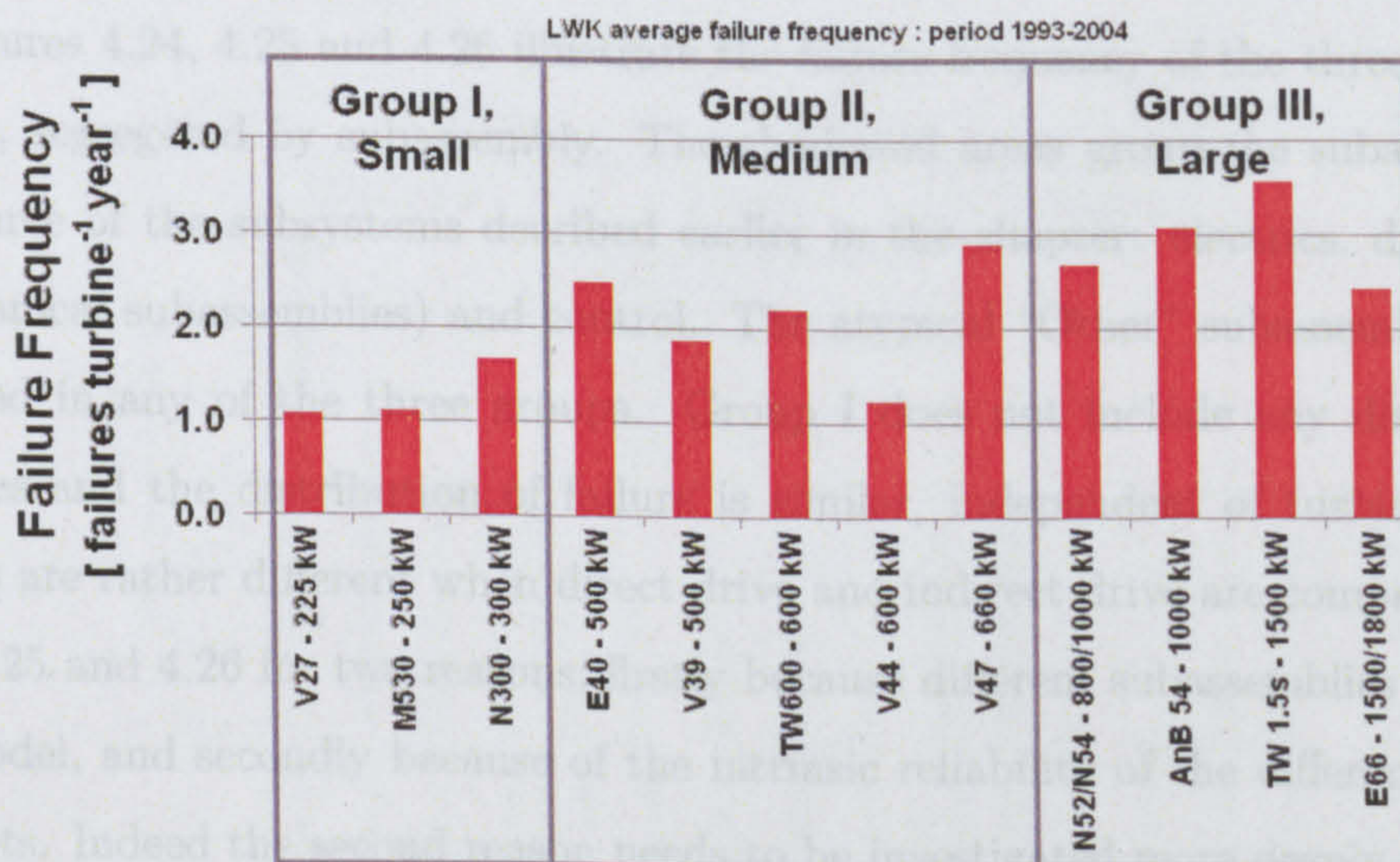


Figure 4.23: The average failure frequency of the three turbines groups

3. The effect of the scaling factor due to turbine size, that is a higher stress-strength ratio.

In order to improve the reliability of the large wind turbines a different response would be needed for each of the causes, as listed below.

1. Technology development.
2. Simplification of the architecture.
3. Redefinition of the design standard.

This correlation needs to be investigated since it opens new lines of research for the future. Assuming that reliability offshore remain unchanged from onshore and in the light of the DOWEC studies, the failure frequency of current large turbines is at least three times the economic limit for application offshore and needs drastic reduction. The available data does not allow further consideration but a thorough reliability analysis on this basis, with the adoption of high quality data and a reliability-oriented design would be beneficial and probably essential for the reduction the the failure frequency.

Figures 4.24, 4.25 and 4.26 illustrate the failure frequency of the three turbines groups, segregated by subassembly. The shadowed areas group the subassemblies into three of the subsystems described earlier in the chapter: electrics, drive train (mechanical subassemblies) and control. The atypical "Other" subassembly is not included in any of the three groups. Group I does not include any direct drive turbines and the distribution of failure is similar, independent of turbine model. Things are rather different when direct drive and indirect drive are compared as in Fig. 4.25 and 4.26 for two reasons; firstly because different subassemblies comprise the model, and secondly because of the intrinsic reliability of the different turbine concepts. Indeed the second reason needs to be investigated more deeply.

For example it appears that an increase of the failure frequency of the electrical related subassemblies of the direct drive concept, particularly of the generator, is a consequence of the elimination of the gearbox. In addition for all wind turbine concepts the absence of the pitch control has a negative effect on the failure rate of

the blades and the gearbox, if one is present.

This is a very important conclusion, demonstrating that not necessarily the most simple turbine architecture is the most reliable. In fact, to avoid the harmful aeroelastic vibrations induced by the stall control and the consequent damage on blade and gearbox, the active regulation of the pitch controls is highly effective.

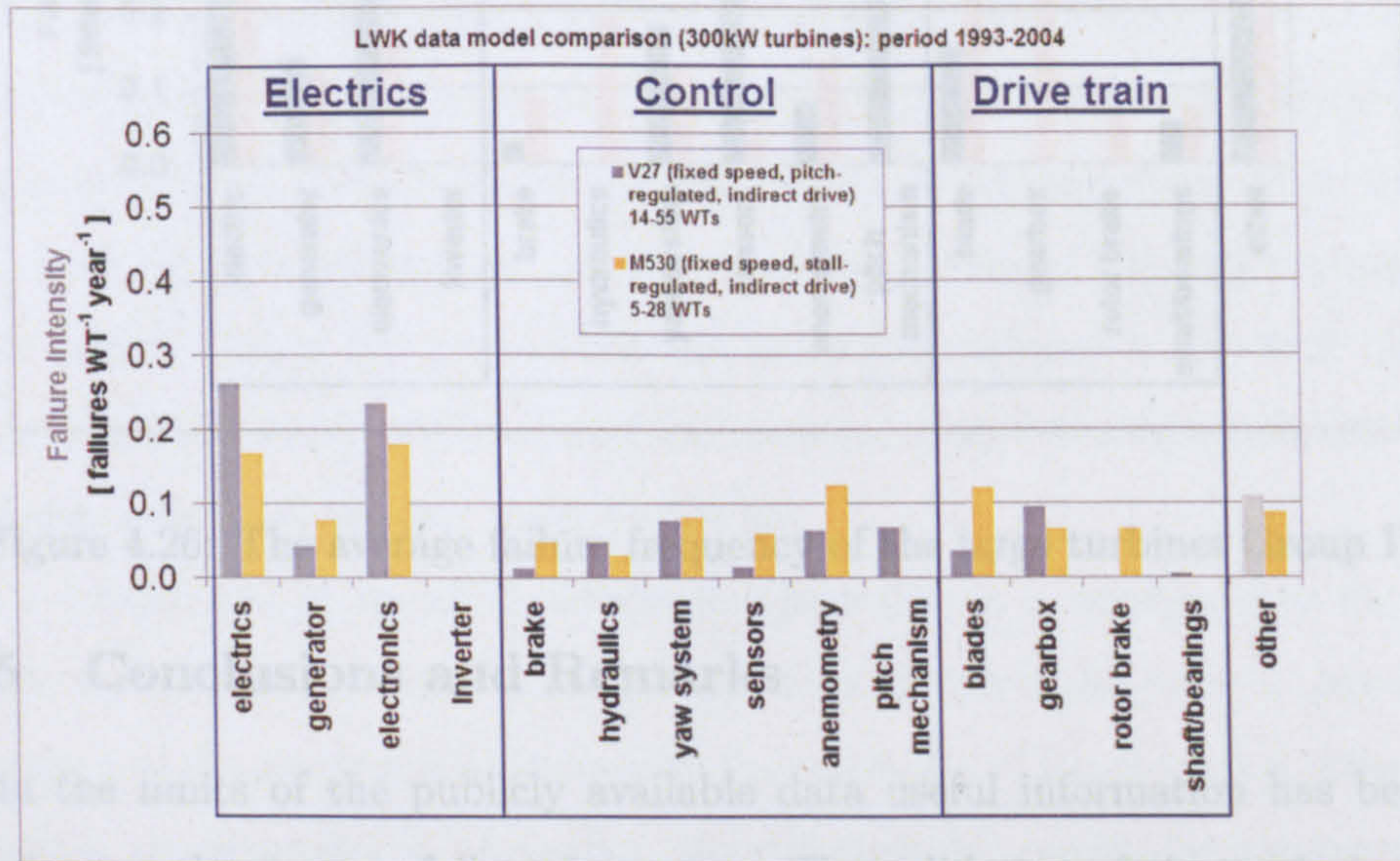


Figure 4.24: The average failure frequency of the small turbines Group I

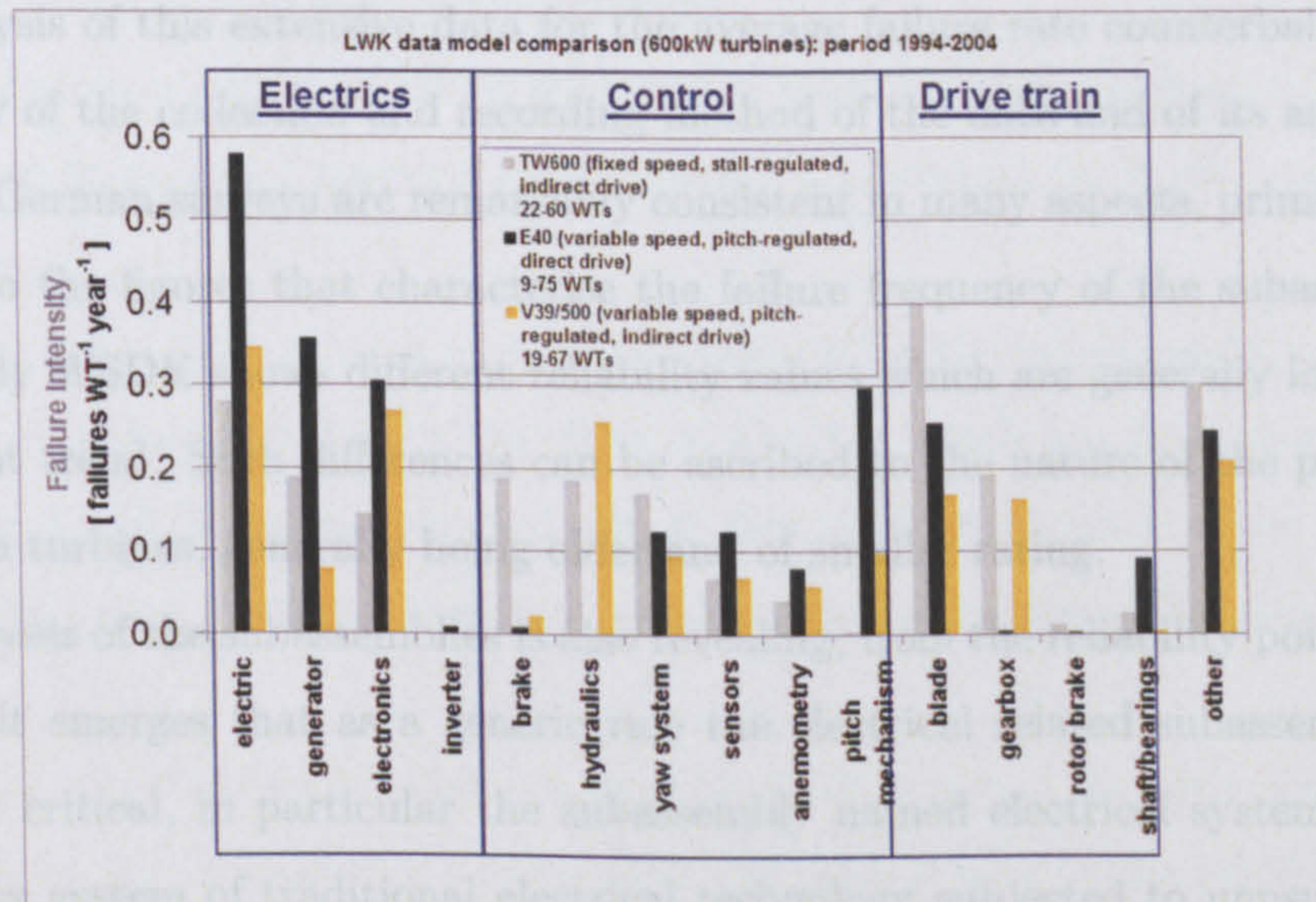


Figure 4.25: The average failure frequency of the medium turbines Group II

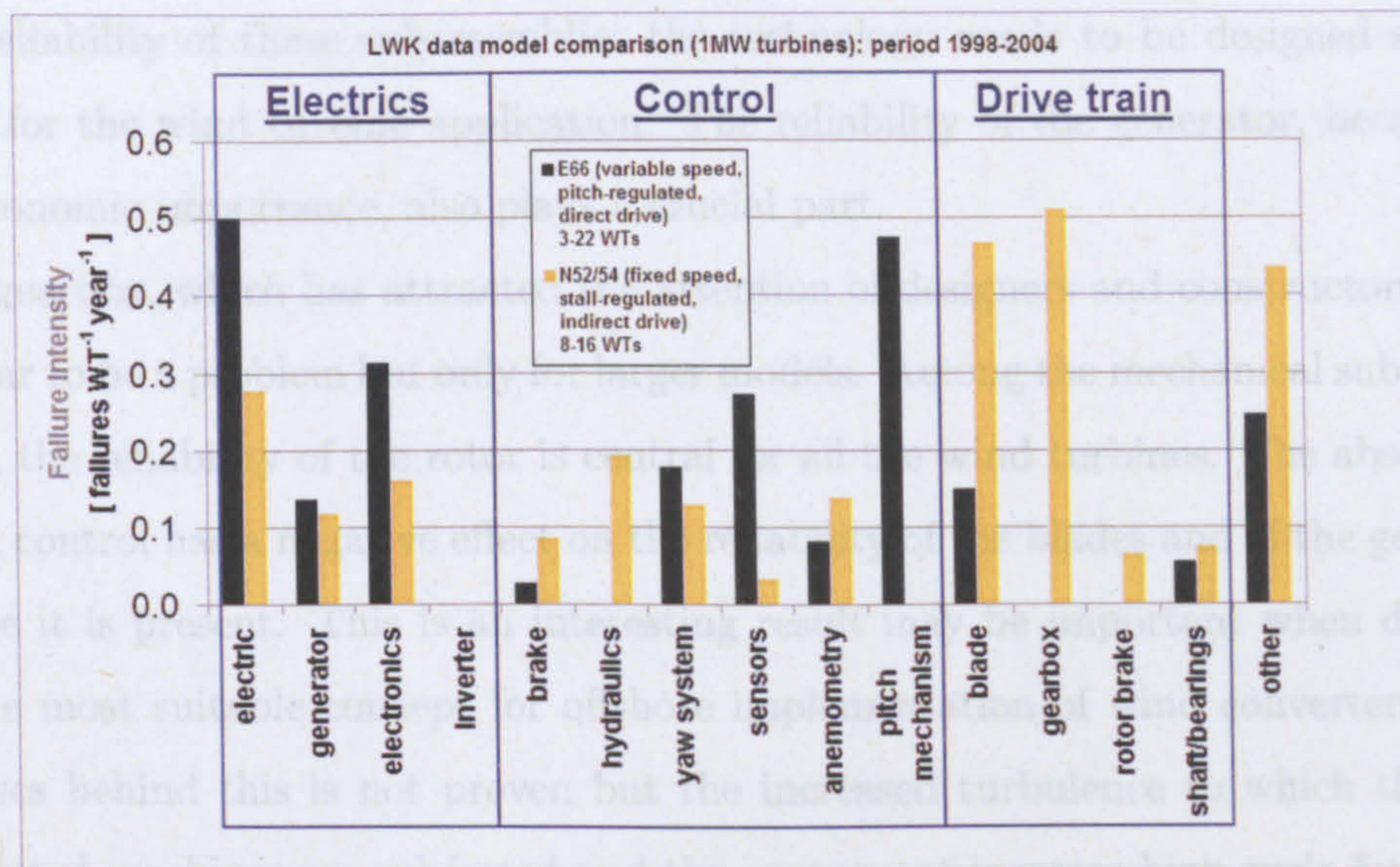


Figure 4.26: The average failure frequency of the large turbines Group III

4.5.5 Conclusions and Remarks

Within the limits of the publicly available data useful information has been extracted using the average failure frequency. The validation of the analysis results comes primarily from the extensive populations of wind turbines including hundreds and thousands of machines and the time reporting period, spanning about ten years. The analysis of this extensive data for the average failure rate counterbalances the simplicity of the collection and recording method of the data and of its analysis.

The two German surveys are remarkably consistent in many aspects, primarily with regards to the figures that characterise the failure frequency of the subassemblies. Conversely WSDK shows different reliability values which are generally lower, with a different trend. Such differences can be ascribed to the nature of the population of Danish turbines, generally being older and of smaller rating.

The analyses of the subassemblies is also revealing; from the reliability point of view because it emerges that as a generic rule the electrical related subassemblies are the most critical, in particular the subassembly named electrical system. This is a complex system of traditional electrical technology subjected to unusual forcing from environmental and network events. The phenomena occurring in the electrical side of the wind energy converter deserve particular attention. For improvement of



the reliability of these subassemblies the technology needs to be designed specifically for the wind turbine application. The reliability of the generator, because of its economic importance, also plays a crucial part.

The gearbox, which has attracted the attention of designers and constructors, does appear to be a problem but only for larger models. Among the mechanical subassemblies, the reliability of the rotor is central for all the wind turbines. The absence of pitch control has a negative effect on the reliability of the blades and of the gearbox, where it is present. This is an interesting result may be important when defining of the most suitable concept for offshore implementation of wind converters. The physics behind this is not proven but the increased turbulence to which the stall regulated machines are subjected and the consequent increase high cycle fatigue to the blades, shaft and gearbox must be the key.

From a comparison of the wind turbine design concepts it emerges that the direct drive is not intrinsically more reliable than indirect drive; the price to pay for the elimination of the gearbox is a decrease of the reliability of the electrical related subassemblies, the generator in particular. Nevertheless the margin for improvement in the reliability of the electric system, electronics and generator are higher, as will be seen in the thesis, and experience shows that it is easier to improve the reliability of electric systems than mechanical systems.

The correlation between failure frequency and machines size also has to be investigated more thoroughly, sparking an interesting opportunity for further research on this subject.

The data are affected by a variability associated with environmental conditions; on the mechanical side due to the effect of weather which has been demonstrated in [48], unreliability on the electrical side, in relation to weaknesses of the grid needs to be investigated. Bayesian statistics could be the tool for the investigation of these matters.

Finally the reliability trend, that has been reported in one of the early observations, Fig. 4.14, has to be treated in a systematic way since it may be the result of genuine reliability improvements or the result of progressively changing weather conditions. The methods of reliability growth analysis can be applied on the available data

in order to determine the phase of the bathtub curve, for repairable systems, that characterises the reporting turbines. The next chapter is entirely dedicated to the applications of this method.

Chapter 5

Reliability Growth Analysis

5.1 Introduction

The results presented in the previous chapter, illuminate some key features characterising the reliability of wind turbines. However, the data presented are influenced by two averaging processes: the first concerning the elements in the surveyed populations, that include turbines of different ages, ratings and technologies and the second concerning time.

Averaging over a large period of time has, on the one hand, the beneficial consequence of producing robust reliability values but on the other the drawback of levelling any reliability trend that characterises the data in the observed period. In the case of field systems, which are subjected to maintenance, improvement or wear and tear, the failure rate cannot be considered constant over the period of observation, and often shows time trends. Such a trend can be relevant, particularly over large periods of time of the order of a decade, to the point that the average value can be significantly different from the expected or “demonstrated reliability” value at the end of the same period of observation. The costs associated with the maintenance of large wind turbines, constitute a significant portion of the final cost of the energy and for that reason the analysis of the reliability trends is particularly interesting.

The fact that the three failure surveys, described in Chapter 4 actually present time trends, as underlined in the previous chapter, suggests the investigation of reliability

trends, in order to compare expected and average failure frequencies. Those methods and results are presented in this chapter. LWK data in particular is suitable for a thorough investigation on the reliability trends since the data are segregated by wind turbine models.

5.2 Reliability Growth Methods

The reliability growth of repairable systems concerns the implementation of the bathtub model with a suitable statistical tool to detect possible reliability trends affecting the system under investigation. In chapter 3 the power law process was introduced as a suitable candidate for the implementation of the model.

According to [10] “reliability growth is the improvement in the reliability of products, components, subsystems or systems, over a period of time due to changes in the product’s design and/or the manufacturing process”.

In general terms “reliability growth occurs from corrective and/or preventive actions based on experience gained from failures and analysis of the equipment, design, production and operation processes”, also reported in [10].

Typically, reliability growth analysis could be part of a an extended reliability growth program, with which a supplier and a purchaser interact to develop a certain system. The results of the analysis could be used by both supplier and purchaser to define and evaluate the progress of the reliability growth program and manage the resources that are available for the development of the system.

Any mechanical or electrical device is initially affected by deficiencies, which normally cause higher unreliability that can be improved with a reliability growth program. As previously introduced the deficiencies are mainly due to bad design or bad maintenance, which are in general a consequence of a lack of information or to manufacturing deficiencies. Thus, differently part from the common practice of trial and error, a reliability growth program is an organic process that can allow a supplier of a system to interact with a purchaser by mutual feedback with the aim of increasing the reliability of the system.

The lack of information concerns the conditions in which the device is asked to oper-

ate or the real effect of the dynamic loads that develop during operations and. often the feedback from the field, is part of the design process, particularly for a complex system. Power electronic converters are a typical example of such a systems.

At the centre of the reliability growth program there is a reliability goal, in terms of the failure rate of the system, that the purchaser wishes to establish or expect. If the reliability of the system is considered inadequate, a reliability growth program can be established, by selecting suitable mathematical tools to verify the reliability of the system at regular intervals during the development phase. It is then the responsibility the of the manager responsible for reliability growth to allocate budget and resources in order to achieve the reliability goal. Reliability growth methods are codified in different standards, of which [12] constitutes the corner stone. The analytical phase of a reliability growth program aims to determine the so called “demonstrated reliability”, that is the reliability achieved at a certain stage of the program, which is then compared to the reliability goal. Any successive decision about the program is made on the basis of the results of this comparison. Such analytical methods are applied in this thesis to the wind turbine failure data from LWK in particular.

The reliability growth method, in its more general meaning, is a systematic learning process. Interestingly the intensity function of the PLP, that identifies the stochastic process, is known as the “Learning Curve”. The term Learning Curve is commonly used to identify the behaviour of any learning process, for which an initial fast improvement, represented by the downward trend of the failure intensity, is followed by a gradually more difficult and less efficient learning process, as the effort required to obtain further improvement increases.

In the case of wind turbines the learning process concerns not only the design, which is typically improved on the basis of the experience gained by the designers, but also also achieved through a better understanding of how the turbine is operated and maintained.

Condition monitoring systems, that are installed in the most modern wind turbines and allow the implementation of the so called proactive maintenance, also contribute to improving the reliability of the wind turbines over a certain period of

time. Proactive maintenance is a maintenance strategy made on the basis of the output of a condition monitoring system that anticipates future breakdown by replacing or adequately maintaining the part that is about to fail and, as with other operational aspects, is subjected to a learning curve.

Whenever the failure trend does not show improvement, that is when it is flat or deteriorating, different considerations must be made, for example with respect to replacement of a subassembly and the holding of spares for it. The interpretation of the results is a vital aspect of the reliability growth method, in its application to wind turbines failure data, and it has been the subject of a study [46]. The next paragraph is dedicated to the illustration of the interpretation of the results.

Reliability growth techniques have been implemented on the wind turbines data to achieve the following goals:

- Validation of the reliability figures. In the case of early failure rate, the value of the instant failure intensity at the end of the period of analysis, $\lambda(t)$ can be assumed to be the “demonstrated reliability” at the end of the development.
- Maturity of the technology. The observation of future failure rates can be assumed from the shape parameter of the failure intensity function, the feasibility of further reliability improvement can then be estimated.
- Random failures hypothesis. In the case of observing a significantly constant failure intensity function, the assumption of HPP as a valid reliability mathematical model.
- Quantification of a deteriorating trend. For increasing trends of the failure intensity function the expected initial failure rate can be estimated.

As outlined before there is an important conceptual difference between the cases of reliability improvement, or positive growth, and deterioration, or negative growth. In the first case the growth is strictly human driven; better design, maintenance or repair activities will spread technological innovation throughout a fleet of repairable systems with a rapidity that is reflected by the value of the shape parameter of the failure intensity function. In the second case physical factors are determining

the negative growth; such as wear and tear, fatigue and the change of the physical-chemical properties of the turbine's materials in particular.

5.3 Crow-AMSAA for grouped data

Data from LWK and WindStats have been interpolated with the Crow-AMSAA model, as described in [12]. The Crow-AMSAA mathematical model is based on the Power Law, or Weibull, Process and the relative failure intensity function $\lambda(t)$ is represented by the exponential expression in 3.19 and repeated here for convenience:

$$\lambda(t) = \rho \beta t^{\beta-1}$$

Given the nature of the reliability data available it has been necessary to use the model in its grouped data version. The two parameters of the intensity function are respectively the shape parameter β that determines the trend of the curve and hence the tend of the intensity of failures and the scale parameter ρ . The estimate of the the shape parameter $\hat{\beta}$ is determined by solving equation 5.1 which is in turn derived applying the Maximum Likelihood Estimate (MLE) method.

$$\sum_{i=1}^I n_i \left[\frac{t_i^{\hat{\beta}} \ln(t_i) - t_{i-1}^{\hat{\beta}} \ln(t_{i-1})}{t_i^{\hat{\beta}} - t_{i-1}^{\hat{\beta}}} - \ln(n_I) \right] = 0 \quad (5.1)$$

Where, by definition:

$$t_0 \ln(t_0) = 0 \quad (5.2)$$

Equation 5.1 is highly non linear and cannot be solved analytically. The equation has been solved with the iterative Bisection Method, exploiting the continuity of the function on the left of the equation. Although the algorithm is not optimised it has proven effective for all the cases investigated and, furthermore, has the advantage of the simplicity.

Once the shape parameter is determined the estimate of the scale parameter $\hat{\rho}$ is determined using equation 5.3, that can be solved without any particular difficulty.

5.4 Total Time on Test

$$\hat{\rho} = \frac{\sum_{i=0}^I n_i}{t_I^{\hat{\beta}}} \quad (5.3)$$

The intensity curve, which is assumed to be the failure intensity, is entirely defined by the two parameters β and ρ . The advantage is that results are clear from Figure 5.1 displaying an example of implementation of the model, in this case on the electric subassembly of the Vestas V27 turbine from the LWK data. In all the reported figures the unit used for the failure intensity is failure/year and shall be intended as failure/WT/year.

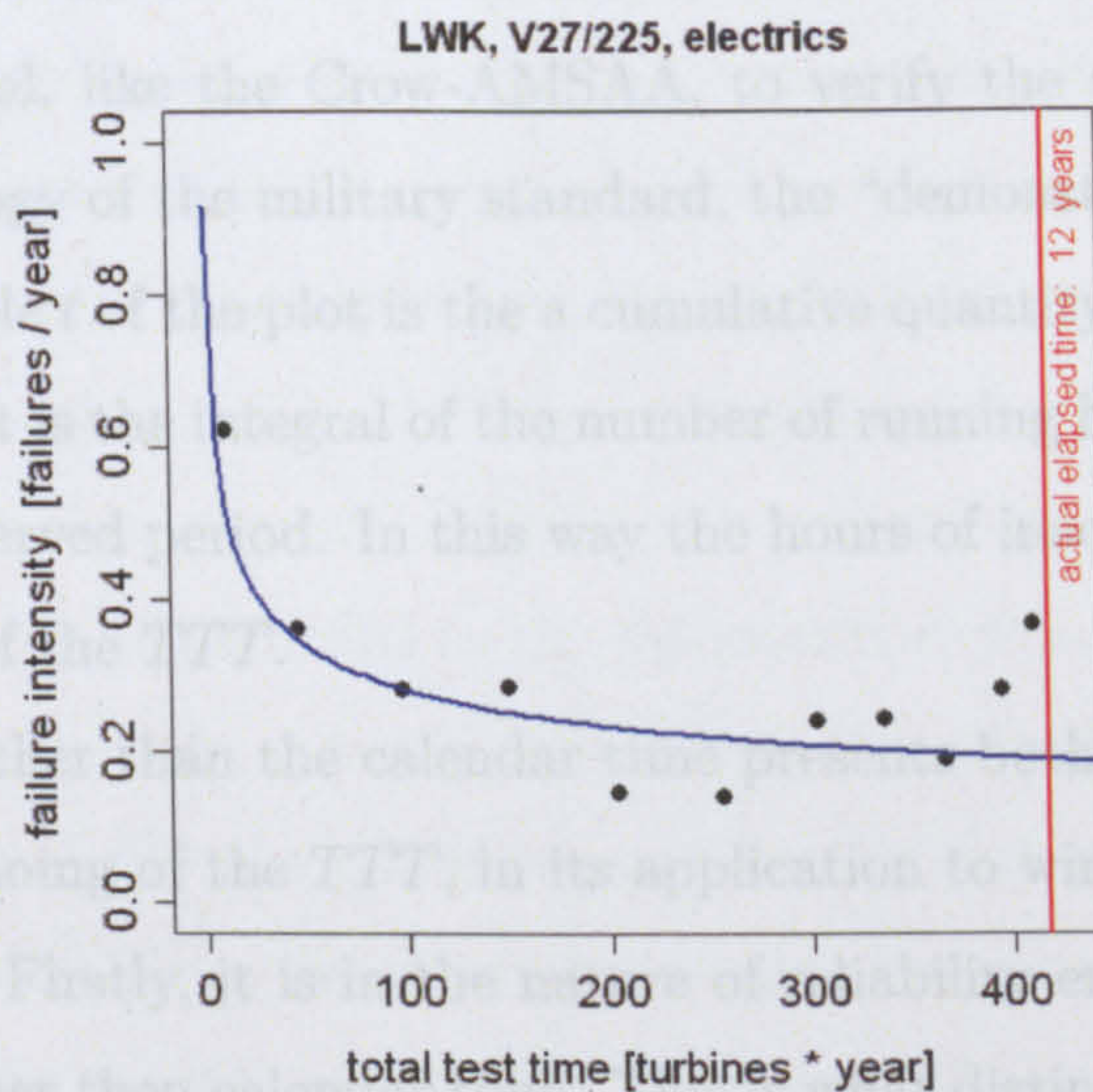


Figure 5.1: The model implemented for a particular case of a Vestas V27 turbine.

In the figure the black dots indicate the average failure frequency data for each recording period, the blue curve is the resulting fitted intensity curve and the red vertical line cursor indicates the right limit of the recording interval in terms of calendar years. It is clear that using the model, a large data set of rather volatile data can be represented with a relatively simple continuous function allowing, for example, the immediate comparison between similar systems.

For data sets like LWK or WindStats the TTT is a certain period TTT_i is calculated adding the first i partial TTT (called ΔTTT_i). For each time cell the ΔTTT is calculated by multiplying the number of wind turbines by the number of

5.4 Total Time on Test

The variable t , that appears in the various equations of the Crow-AMSAA model, represents time but it differs from the “calendar” or “hourly” time, as reported in the failures tables of both WindStats and LWK, see Tables 4.1, 4.2 and 4.5.

Reliability growth, as well as other reliability analysis, should normally be carried out on the basis of specific tests made on systems under investigation. For a repairable system the test is stopped after a failure or a planned inspection and the number of running hours elapsed since the previous failure are recorded. After a number of failures have been accumulated, failure data are interpolated with a mathematical model, like the Crow-AMSAA, to verify the achieved reliability or, using the terminology of the military standard, the “demonstrated reliability”. The independent variable t of the plot is the a cumulative quantity called the Total Time on Test (TTT) that is the integral of the number of running hours of the entire population for the observed period. In this way the hours of inactivity are not included in the evaluation of the TTT .

Using the TTT rather than the calendar time presents both advantages and drawbacks and the meaning of the TTT , in its application to wind turbine failure data, must be clarified. Firstly, it is in the nature of reliability engineering to deal with running hours rather than calendar time. This is what distinguish a reliability analysis from an availability analysis. In this case the age of many electromechanical systems can be measured with the number of cycles completed or the total running hours and often this differs substantially from the calendar age. As an example the “age”, and consequently the reliability, of a car is better illustrated by its mileage rather than by the year of purchase. The calendar time plays an important role in reliability studies where chemical-physical properties deteriorate with time. The insulating property of a dielectric, the grip of a wheel on the road or the sealing property of an O-ring are examples for which the calendar time plays an important role and the degradation occurs even if the system is not actually used.

For data sets like LWK or WindStats the TTT in a certain period TTT_i is calculated adding the first i partial TTT (called ΔTTT_i). For each time cell the ΔTTT is calculated by multiplying the number of wind turbines by the number of

hours in the interval. The recorded total hours lost from wind turbine production, in the interval L_i are then subtracted from this amount, when this information is available. The TTT formula for an arbitrary time cell k is then:

$$t_k = \sum_{i=1}^k \Delta TTT_i = \sum_{i=1}^k [N_i * h_i - l_i] \quad (5.4)$$

To calculate the TTT for LWK data, some considerations are necessary.

Firstly in each time interval, the wind turbines involved in the survey are considered as a representative set of the entire of population. In other words, for each time interval the reliability of the sample is assumed to be the reliability of the entire population. This hypothesis is necessary to overcome one of the major deficiencies of the data that is the variable number of wind turbines in each time interval. In reality any technological innovation does not apply simultaneously to all the wind turbines of the “sample”, nor to the entire population, but will spread throughout the population with a certain rate. The shape parameter β is indicative of this rate. The same concept can be extended to the deterioration phase as long as the sample wind turbines are assumed randomly chosen from the entire population and, in the long run, the usage of the wind turbines is similar for each wind turbine.

Secondly, using the TTT has the effect of stretching the curve on the abscissa. Since TTT depends on the number of turbines considered it has no absolute meaning, as the calendar time would have. The variable t of the plot has significance only concerning the specific population of turbines under examination, however, by showing the cursor in the curve, see Fig. 5.1, the right limit of the population recording interval, in terms of calendar time, is shown.

Thirdly, if the intensity function interpolates data on a scale of TTT scale rather than calendar time, the fit produced is intrinsically weighted. In each period, the failure rate is weighted by the number of turbines in that period. A larger number of wind turbines will result in a larger number of running hours (larger TTT interval) and ultimately in a “stronger” constraint for the fit. The example in Table 5.1 illustrates the calculation of the TTT for the LWK data for the Vestas V27 turbine.

If TTT is used as an independent variable, instead of the calendar time, the fitting curve will stretch to a larger interval, according to the number of WTs sur-

Number of WT N_i	Hours in the interval h_i	Hours lost in the interval L_i	Interval TTT [h] ΔTTT_i	Cumulative TTT [h] TTT_i
21	8760	62	183898	183898
50	8760	289	437711	621609
54	8760	2683	470357	1091966
53	8760	824	463456	1555422
55	8760	391	481409	2036831
50	8760	696	437304	2474135
42	8760	1474	366446	2840581
25	8760	700	218300	3058881
19	8760	249	166191	3225072
18	8760	387	57293	3382365
18	8760	270	157410	3539775
14	8760	53	122487	3662262

Table 5.1: The calculation of the TTT for Vestas V27 turbine electrics subassembly, see Fig. 5.1

veyed and the scale parameter will, consequently, vary. The practical interpretation of the scale parameter and the whole fitting curve is more difficult. It is generally assumed that the fitting process is valid only for the specific case investigated and the results cannot be extended to other cases. However some important information can be extracted from the fitting process in the three cases of early failures, constant failures or deterioration.

In the cases of early and constant failures the most important results concern the demonstrated reliability, that is the failure rate at the end of the development phase which coincides with the entire reporting period. The demonstrated reliability is the value assumed by the intensity function at TTT_I , or $\lambda(TTT_I)$. Figures 5.2, 5.3 and 5.4 illustrate graphically how the demonstrated reliability can be extracted from the intensity function; in both cases the demonstrated reliability is the value at the intersection between the the intensity function (blue line) and the vertical red line indicating the end of the reporting period.

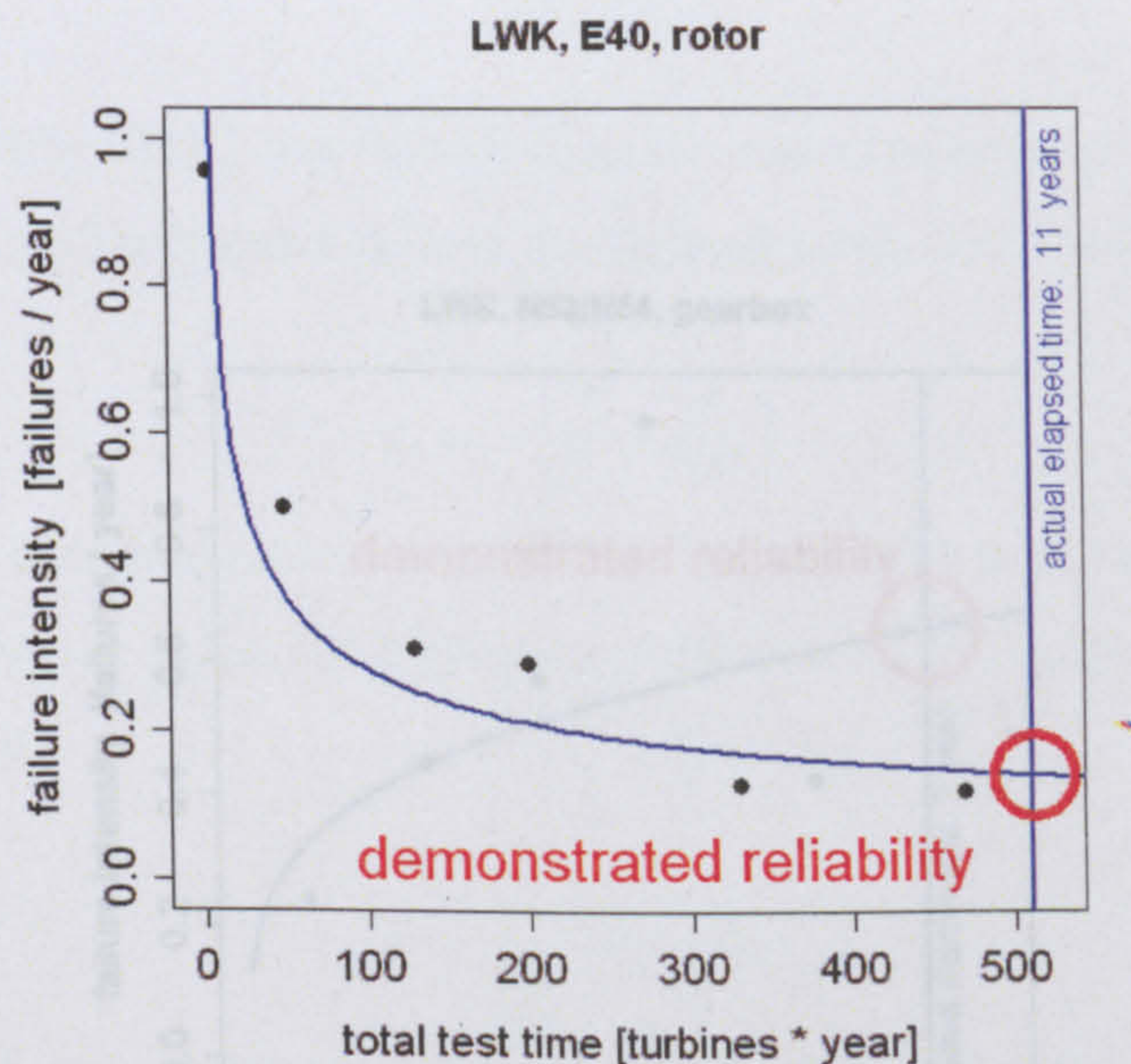


Figure 5.2: Demonstrated reliability for an early failure case

An example of deterioration phase is shown in Fig. 5.4, where the intensity of failures curve is almost a rising straight line because $\beta \cong 2$. The deterioration phase indicates that no improvement is achieved during the observed period or that any

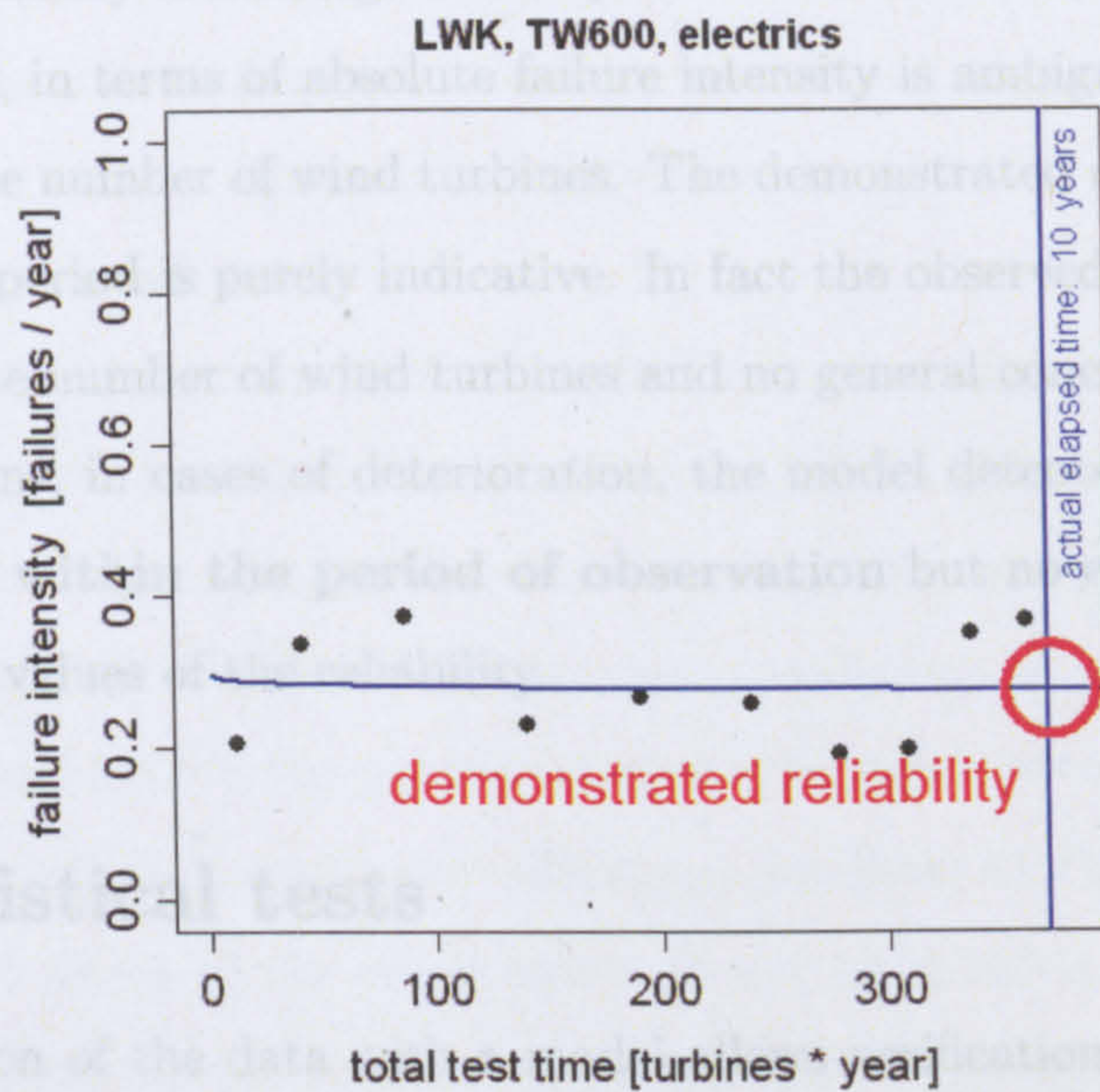


Figure 5.3: Demonstrated reliability for a constant failure case

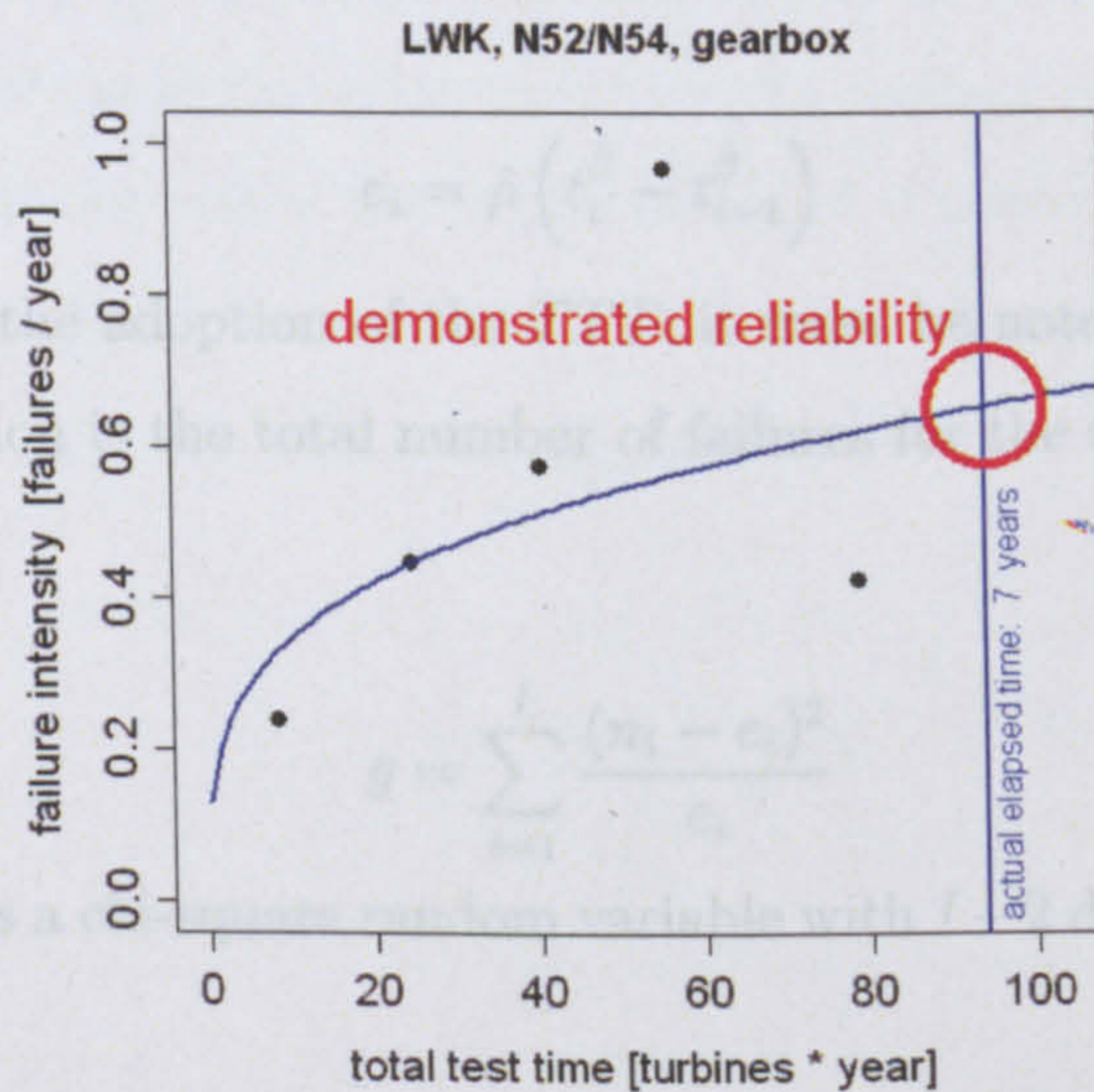


Figure 5.4: An example of deterioration phase; gearbox subassembly of Vestas V39 wind turbine

improvement is effected by the wear and tear. For the deterioration phase, since the curve is monotonically increasing, and despite the known trend, the extrapolation of future reliability, in terms of absolute failure intensity is ambiguous given that this depends from the number of wind turbines. The demonstrated reliability at the end of the observed period is purely indicative. In fact the observed period is arbitrary, depending on the number of wind turbines and no general conclusion can be made. In practical terms, in cases of deterioration, the model detects and “certifies” the reliability trend **within the period of observation** but no extrapolation can be made on future values of the reliability.

5.5 Statistical tests

The interpolation of the data with a model allows verification of the likelihood of that model represents the data by rigorous statistical tests. Two tests have been used simultaneously to verify the the model by both goodness of fit and a particular null hypothesis.

A goodness of fit (GoF) test is built from the expected number of failures in each interval e_i , that can be calculated from the defined integral of the intensity function.

$$e_i = \hat{\rho} \left(t_i^{\hat{\beta}} - t_{i-1}^{\hat{\beta}} \right) \quad (5.5)$$

As an effect of the adoption of the *TTT*, it must be noted, that the integral of the intensity function is the total number of failures for the entire population. The following statistic

$$g = \sum_{i=1}^I \frac{(n_i - e_i)^2}{e_i} \quad (5.6)$$

is distributed as a chi-square random variable with $I - 2$ degrees of freedom, that is:

$$g \sim \chi_{\alpha, I-2}^2 \quad (5.7)$$

for which the critical values can be found in common tables. The hypothesis is accepted if the statistic assumes a value smaller than the critical value, which

is calculated for the level of confidence α chosen. The statistic is distributed as a chi-square random variable, because it is assumed that the difference between expected and the true number of failures is distributed as a normal distribution. Consequently, the sum of squared normal random variables, as 5.6 is, by definition, a chi-square random variable.

The degrees of freedom of the statistic in 5.7 are the number of time cells minus one, due to the known length of the entire interval, minus the number of independent parameters of the curve. Since the estimated shape parameter can be determined from equation 5.3, the number of independent parameters is one and the results of the degrees of freedom are the number of time cells minus two.

It can be argued that a chi-square statistical goodness of fit test does not take into account the shape of the curve and may not be suitable for this case, where testing improvement or deterioration is fundamental. The application of equation 5.6 to the real data has proven rather restrictive, and the acceptance has often been achieved after an aggregating process, illustrated below. The variability of the data is an important factor determining the rejection of the goodness of fit hypothesis, and the aggregating process helps to overcome the variability which, as has been explained in section 4.4.1, is likely to be due mainly to the effects of the weather.

The likelihood of the shape of the curve can be verified by the second statistical test, the null hypothesis which is the possibility of describing the data set with a HPP rather than a NHPP, an additional information about the shape of the curve can be added.

The statistic c :

$$c = \sum_{i=1}^I \frac{(n_i - N \cdot P_i)^2}{N \cdot P_i} \quad (5.8)$$

where

$$P_i = \frac{t_i - t_{i-1}}{t_I} \quad (5.9)$$

is distributed as a chi-square statistic with $I - 1$ degrees of freedom, in formula:

$$c \sim \chi_{\alpha, I-1}^2 \quad (5.10)$$

The degrees of freedom of this statistic are higher than the previous GoF statistic because the number of independent parameters of the curve is zero. In this case, the number of failures and the length of the interval completely define the curve, which is a constant.

Equation 5.8 and 5.9 can then be easily interpreted. If the hypothesis is that the process is a HPP, then in each time cell the expected number of failures has to be proportional to the length of the same time cell. The constant of proportionality is the total number of failures divided by the length of the entire interval, or in other words the constant intensity of failures of the HPP.

Shape Parameter	$H_0 = HPP$	Result
$\beta < 1$	Rejected	Early Failures
$\beta > 1$	Rejected	Deterioration
$0.79 < \beta < 1.2$	Accepted	Constant Failure
$\beta < 0.88$ or $\beta > 1.2$	Accepted	Unknown

Table 5.2: The check table for the determination of the final result

Given acceptance of the goodness of fit test, the final result, that is early failure, constant failure or deterioration, can deduced from the evaluation of the combined results for β and the trend hypothesis test according to Table 5.2:

5.6 The aggregation process

The statistic upon which the tests, for both Goodness of Fit and HPP null hypothesis, are based is a chi-square random variable. The squared difference between the expected and real number of failures makes the statistics particularly sensitive to variable data. The field data of the various surveys that have been considered are subjected to many random events, like weather or grid problems, and are particularly “noisy”.

The variability of the data is accentuated by the squared relationship of the statistics and this often leads to a rejection. The application of the statistic to the original

data has proven difficult but it has been noticed that a reasonable aggregation of the data is beneficial to a successful outcome of the test.

The aggregation may be the process of joining two or more time cells, so that the number of failures of the new aggregated cell is the sum of the original ones.

The aggregation is necessary in two cases

1. To achieve the minimum requirement of 5 events in each time cell, as specifically required in case of sparse data for the application of the Crow-AMSAA model.
2. In attempting to change the result of a Goodness of Fit test from rejection to acceptance, by the rationalization of noisy data.

Table 5.3 illustrates an example of case 1 and shows how an initially sparse data record is aggregated to fulfil the requirement of 5 failures each time cell while Table 5.4 shows an aggregation process for case 2.

With the simple manipulation illustrated in Table 5.4 the GoF result changes from rejection to acceptance. Normally, the aggregation of a few time cells is sufficient to achieve the result. The manipulation of the data, in the second case above, is acceptable whenever the estimate of the curve parameter does not change radically, compared to the original values, that is when the shape parameter remains reasonably similar. It has been noticed that the shape parameter changes substantially as a consequence of the aggregation process, only when data record has a limited number of failures. Larger data records are “stiffer” and the aggregation can be carried out more easily.

The limit of the aggregation is the combination of all the time cells to a single one, and in this case the only interpolating curve possible is a constant intensity function, whose scale parameter is the overall average for the data record. In other words the limit of the aggregation is always the HPP and for this reason the number of remaining time cells, after the aggregation process should be 3 or more.

Given the contemporary minimum number of failures, 5, acceptable in each time cell then the smallest data record acceptable is 15 failures distributed in 3 time cells. In all the cases for the surveys considered where the data do not fulfil this minimum

original			aggregated		
i	n_i	TTT [h]	i	n_i	TTT [h]
1	0	20.9	1	14	124.3
2	4	70.8			
3	10	124.3			
4	3	177.1	2	7	232.0
5	4	232.0			
6	5	281.8	3	5	281.8
7	3	323.4	4	4	416.7.0
8	0	348.3			
9	0	367.2			
10	0	385.1			
11	2	403.0			
12	1	416.7			

Table 5.3: An example of the effect of the aggregation process for Case 1 (sparse data)

original			aggregated		
i	n_i	TTT [h]	i	n_i	TTT [h]
1	8	156.6	1	35	901.1
2	13	470.9			
3	14	901.1			
4	22	1266.0	2	22	1266.0
5	28	1903.9	3	28	1903.9
6	22	2510.3	4	22	2510.3
7	20	3037.3	5	66	3523.6
8	46	3523.6			
9	26	3972.2	6	26	3972.2
10	32	4367.7	7	32	4367.7
11	24	4769.8	8	24	4769.8
12	28	5110.8	9	28	5110.8

Table 5.4: An example of the effect of the aggregation process for Case 2 (noisy data)

requirement the model has not been implemented.

Clearly the aggregation process reduces the information available. For example, the difference of failure frequency of two contiguous time cells could be due to a change of the maintenance strategy rather than a substantial difference in weather conditions, and this information would be lost by aggregating the two time cells. However the information about the maintenance policy is not available to us and the analysis of maintenance strategies is beyond the aims of this thesis, but it can offer a good opportunity of future research.

On the other hand the aim of the reliability growth model model is to “crystallise” information about the reliability of the subassemblies of the turbines given a large data record and to define the demonstrated reliability at the end of the period. The aggregation process represent a practical method to obtain those results.

5.7 Model Results

The results of the implementation of the model to all the valid LWK and WS wind turbine and subassembly data are reported in the Tables B.1 to B.12 in Appendix B. Detailed considerations are given in the following chapter but these sections 5.7, 5.8 and 5.9 describe the general principles and the reader is asked to refer to Tables B.1 to B.12.

The Tables report results for each LWK turbine model analysed and for the two WS populations. There results are the two parameters of the intensity function (β and ρ), three values of the intensity function, the results for the two likelihood tests, and a final comment called “conclusion” that synthesises the results for each data record.

The category “All” includes all the LWK wind turbine set, that is the seven wind turbine models that have been analysed in detail, as tabulated in Table 4.8, plus all the other turbine models of different rating in the LWK survey. For this reason this category is completely independent and must not to be confused with the average of the seven turbine models presented in section 4.5.

5.8 Values of the Intensity Function

While the meaning of the results for the two parameters of intensity function and likelihood test have been described thoroughly above, the values need some clarification.

Specific values have been presented in the tables in Appendix B to supply a numerical impression of the intensity curve and then of the failure intensity for each subassembly under investigation, in terms of failures per year per wind turbine. The selected numerical values of the intensity function are the initial, final and overall average. The intensity curve of the PLP is always steep in the region close to the axis origin, for the both early failures and deterioration phase, and the reliability of the subassembly is not clearly defined. The function of the initial value is to provide a numerical “impression” of the failure intensity in this zone of the diagram. Therefore the initial intensity of failure is the value assumed by the intensity function at $t = 5 \text{ turbine} \cdot \text{years}$. This value of t is purely arbitrary and, is the reliability of that subassembly for a population of 5 WT operating for 1 year or a population of 1 WT operating for 5 years.

The final failure intensity of the table refers to the demonstrated reliability as defined in the Figures 5.2, 5.3 and 5.4 whilst the overall average is simply the total number of failures divided by the TTT of the entire period considered, equation 4.4.

5.9 Goodness of Fit

When for a particular data record the GoF is rejected for any possible aggregation, the model simply cannot be applied and the conventional result is “NOT PLP”. As can be seen from Tables B.1 to B.12 there are many cases of “NOT PLP”. There are two main reasons for a rejection of the GoF test. The first is due to the monotonicity of the intensity function of the PLP, which makes it unsuitable to fit U-shaped data, that is data that presents a U-shaped graph for the failure frequency over the entire period. The U-shaped data, can be either concave or convex, the convex case is noteworthy and by far the most frequent and represent the bathtub curve of Fig. 3.1. As an example in both Figures 5.1 and 5.3 this trend is shown.

From the reliability theory it is known that electro-mechanical devices, over a period of sufficient length, show the entire bathtub curve. In this light the large prevalence of data showing a convex failure intensity is not surprising. The inadequacy of the PLP to represent this kind of data set has led to the necessity of developing an alternative model, called the combined PLP, whose results are illustrated in a section 5.10.

The GoF can also be rejected in case of excessively variable data. The influence of weather and other factors has already been illustrated in Chapter 4. From the definition of the chi-square statistic, based on the squared value of the difference between expected and real number of failures in a period, it is clear that in case of particularly “noisy” data the statistic assumes a high value. Variability of the data affects particular cases where the number of failures is large, such as in the “whole turbine” subassembly or the two WS populations, which involve large numbers of wind turbines.

In all those cases where the GoF test has led to an acceptance of the interpolation the results have been classified according to Table 5.2. The conclusion “unknown” is drawn in two particular cases. Firstly if the number of failures are insufficient to fulfil the requirement of having at least 5 failures for each time cell than the model cannot be implemented and no conclusion can be drawn; the comment “not enough failures” specify this situation. Secondly in the rare cases where there is an evident contradiction between the shape parameter and the the HPP test. As illustrated in Table 5.2 this is the case where beta is very small or very large and the $H_0 : \beta = 1$ hypothesis is accepted. This conclusion has been arisen in the following cases:

- Yaw system of V27, M530 and V39 WTs
- Pitch control of V27 WT
- Air Brake E66
- Mechanical brake of M530 WT

All the above cases involve a small number of failures, but just sufficient to fulfil the condition of the 5 failures for each time cell required by the model. Because of

the small number involved, in all the above cases, the shape parameter statistic leads to an acceptance even though the shape parameter is much greater or smaller than 1, the value that characterises the HPP. The same β changes over a wide range for different aggregation of the data, which is a sign of a problematic implementation of the model on that particular data record. For these reason the conclusion is “unknown”.

5.10 An alternative Model

5.10.1 Using Calendar Time

The use of the Total Time on Test as a time variable has been the subject of a research made in collaboration with the Department of Mathematical Sciences of Durham University. The collaboration, led by Prof. F.P.A. Coolen, to which Dr D. Venkat and the Author have participated, has produced a document published in the special edition of the Journal of Management Mathematics, about the mathematical modelling on reliability [9].

This paper is based on of a mathematical model, which has been developed by Dr. Venkat, representing a development of the reliability growth model illustrated above. Dr Venkat has produced a a four parameter PLP model to represent the entire bathtub curve whose results have been compared for some of the LWK failure data records. The four parameter model results by overlapping two PLP; the first decreasing or constant and the second one increasing or constant. The resulting is described by Equation 5.11.

$$\lambda(t) = \rho_1 \beta_1 t^{\beta_1-1} + \rho_2 \beta_2 t^{\beta_2-1} \quad (5.11)$$

Where

$$\beta_1 \leq 1 \quad (5.12)$$

and

$$\beta_2 \geq 1 \quad (5.13)$$

A description and the results of the application of this model to the WT failure data are illustrated in Section 5.10.2.

Differently from the the reliability growth model, the four parameter model is based on the calendar time (CT). The use of CT for the four parameter model, as opposed to the TTT used for the reliability growth model presented in this thesis, has ignited a deep discussion about the difference between these two time variables. Some basic engineering interpretations implied in the use of TTT have been outlined in Chapter 3, and in the previous paragraph the interpretation of the results are, in the light of the adoption of TTT as a time variable are reported. Conversely, in [9] the discussion regards some mathematical implications underlying the use of one variable or the other.

The meaning of TTT in its application to LWK failure data has been clarified in the previous paragraph while CT is intuitive and does not need further clarification. There are different arguments in favour of the use of TTT or CT , which may occur simultaneously, making the choice between them less obvious, and TTT based inference can differ substantially from CT based inference. Such a difference can, for example, happen with grouped data, such as we are considering here, when the number of items in the population under observation changes per time interval. Using TTT , the number of items in the population modulate the time-axis with effects that reverberate on the estimated parameters of an assumed reliability growth model. This is because when TTT is the length of time interval depends from the number of items in the population, as explained in Chapter 3. Thus, the more the population change in number per time interval the higher the effects are on the parameters of the inferred intensity function.

When processes over time are considered, it is often assumed that the use of CT is most natural. For considerations on reliability growth, one could also argue that several underlying reasons for changes in failure patterns for technical systems are naturally linked to CT . For example, wear-out for single systems is sometimes naturally expressed with the use of CT , in particular if no detailed information on

periods of actual use is available, and also changes that might affect larger populations of systems with repairs and replacements taking place, for example novel designs or changing maintenance strategies, could provide arguments in favour of the use of *CT*. In reality, for fleets of WTs a technological innovation is seldom instantaneous for all the WTs and occurs with a certain rate. This problem has been already faced in Paragraph 5.4 for the *TTT* case.

5.10.2 Results comparison

The four parameter model has not shown the expected results. The idea at the basis of this effort was to model the data records where the simple PLP could not be implemented, allegedly because the the data showed the entire bathtub curve. These records are the ones defined “not PLP” in the results tables of Appendix B. The interpolation has proven unsuccessful for these cases and the convergence never achieved in a satisfactory way.

However, for the majority of data records that have been successfully interpolated with the single PLP model the results have show good agreement, confirming the validity of the two independent interpolations. The fact that the four parameter model was based on calendar time allows comparisons between *TTT* and *CT*.

The implementation of the PLP with calendar time has shown in many cases similar results for the shape parameter β , indicating the same levels of increase or decrease of $\lambda(t)$, and the two statistical tests.

The implementation of the two models for the same set of data has allowed a direct comparison. The chosen data set are reported in Table 5.5

The results for the two models are not dissimilar for each of the three data set, as it can be seen comparing Table 5.6 with Table 5.7. The estimated shape parameters indicate approximately the same levels of increase or decrease of the intensity function over time, for all the subassemblies considered. Thus, accordingly to the results shown, this application, which involves about 10 years of real-world reliability data, might suggest that it does not really matter whether one uses *TTT* or *CT* as time variable in such models. However, care is needed with grouped failure data and, as stated above, substantially differing numbers of wind turbines per year.

year	N. WT	whole WT	gearbox	electrics	TTT [h]
1994	19	58	4	15	166440
1995	59	136	2	18	683280
1996	60	97	4	20	1208880
1997	67	96	7	16	1795800
1998	61	89	6	18	2330160
1999	52	129	15	15	2785680
2000	45	73	5	17	3179880
2001	47	68	7	19	3591600
2002	38	59	12	10	3924480
2003	18	46	9	8	4082160
2004	17	33	7	9	4231080

Table 5.5: The three data record considered; failures for whole WT, gearbox and electrics of V39/500 wind turbine

WT Model	β	ρ
V39 whole WT	0.8731	4.0960
V39 gearbox	1.8440	0.0009
V39 electrics	0.8769	0.7360

Table 5.6: The results for the three cases considered, two parameter model and TTT

WT Model	β_1	ρ_1	β_1	ρ_1
V39 whole WT	0.8546	2.5963	n.a.	0
V39 gearbox	n.a.	0	1.7741	0.0275
V39 electrics	0.8769	0.4794	n.a.	0

Table 5.7: The results for the three cases considered, four parameter model and CT

To understand why attention should be paid a small, extreme and artificial example is useful: suppose that failures of units were recorded for 4 consecutive years, with only 1 unit was in use for each of years 1, 3 and 4, but 100 units were in use for year 2, and suppose that the number of recorded failures in these years were 2, 100, 2, 3, respectively.

The *TTT* method would consider a total of 103 *TTT*-years, with empirical failure intensity of 2 in the first year, 1 (on average) in each of *TTT*-years 2 to 101, 2 in year 102 and 3 in *TTT*-year 103.

The *CT* method would just consider the four years as they occurred, with the obvious respective empirical failure intensities of 2, 1, 2, 3. The evidence for year 2 is very strong compared to the other years due to the number of units in use in that year. Applying the same basic models (PLP) leads to MLEs for the of $\beta = 0.9444$ and $\beta = 01.4975$ for the *TTT* model and the *CT* model respectively.

This is a very substantial resulting difference, with these estimates providing at least some indication of different long-term trends for the intensity function. It should be noted that, for for both these models, a hypothesis of the shape parameter being equal to one (so HPP) would not be rejected.

So any such indications could not be strongly justified for this case.

The main reason for the difference between the models is the effect of “stretching” the 2nd *CT* model year into 100 *TTT* model years. This affects the shape parameter MLEs as these are more influenced by earlier than later years, due to the range of functional shapes of the PLP intensity functions. Stretching the 2nd *CT*-year to 100 *TTT*-years has diminished the influence on the estimate of the final two years, in which the observed failure intensity increased, while the effect of these two years is still strong when *CT* is used.

Nevertheless, there are two special cases in which statistical inference with grouped failure data is identical no matter if *CT* or *TTT* is used, namely if one uses an HPP, or if the number of units in use, that is wind turbines in this context, is the same in every time interval considered. However, the difference between use of *TTT* and *CT* can be quite subtle, and choice requires careful consideration.

5.10.3 Discussion

If one attempts to learn changing failure intensities over time, for populations of repairable systems that also undergo replacements, design changes, and planned or *ad hoc* changes to monitoring and maintenance activities, then it is important to determine whether one wishes to study such changes over *CT* or *TTT*.

Some possible reasons for change may logically be expected to be related to *CT*, whereas other reasons are more logically expected to be related to *TTT*. For example, if changes of maintenance activities are most likely to result directly from observed failures, then *TTT* is the more appropriate choice of time variable, as the number of units in use will affect the likely number of failure occurrences. If changes of maintenance activities are more likely to occur as a result of changes to safety legislation, or to feedback from particular component manufacturers, then the use of *CT* would be more appropriate.

In the reliability literature, many methods for, and applications of, reliability growth modelling are presented, with very little focus on the actually used time variable. The use of *TTT* is common for reliability growth management methods [12], although reliability growth methods are not commonly adopted outside some specific environment, as for defense systems commissioning.

The use of *CT* is most intuitive, and is particularly logical if one considers reliability behaviour over time of a single unit or where time has a strong ageing effect, as for power cables or insulation materials in general.

With an engineering approach to the problem one would find *TTT* model more intuitive, especially for mechanical and electromechanical machinery, for which the actual running hours offer a better indication of their age. Since this is the case of this thesis, it is now clear why the interpretation of the *TTT*, as illustrated in Chapter 3 and above, has been a crucial part of the model presented.

Chapter 6

Commentary on the Power Law Process Results

6.1 Introduction

The results of the application of the PLP model to both LWK and WS data are reported in full detail in the Tables B.1 to B.12 of Appendix B.

Given the large amount of data, a synthetic summary of the results is reported in this Chapter. The summary includes, for each subassembly and turbine model, the shape parameter β as resulting from the implementation of the model to each of the data set and the “conclusion”, as defined in Chapter 5. For each specific case the “conclusion” is determined by the combination of results for the two statistical test and the shape parameter. The combination of results are summarised by Table 5.2, which has the function of a lookup table.

For the sake of brevity the graphs, illustrating the interpolating curves, are shown for some examples, which are selected to show the most significant result for that particular subassembly. The reader is invited to read the title on the top of each diagram to be acquainted with the turbines and subassemblies considered and to refer to the Tables in Appendix B for more detail.

Although generalisations must be carefully scrutinized, given that the model results depend from the specific case analysed, some interesting general conclusions can be drawn. The method, intended as the combination of the aggregation process,

implementation of the statistical model and codification of results according with Table 5.2, has proven to be valid for data records with sufficient failure number. At the same time, for very large data record, like the undifferentiated populations of wind turbines of WSD and WSDK, the implementation of the method has proven rather difficult and is often characterised by rejections of the GoF and, consequently, of the validity of the fit.

This suggests that the development of a dedicated mathematical model, able to “filter” the combined effects of forcing quantities, like weather or grid failures, could be a useful further development. Future models will have to consider the correlation between failure frequency and environmental factors. Bearing in mind that a wind turbine is subjected to both a “mechanical” environment, due to static and dynamic loads on the mechanical parts, and an “electrical” one affecting the electrical subsystems, the notion of “environmental” is being used here in its the widest meaning. It is suggested [8] that the Bayesian statistics could be a useful instrument to study this correlation whenever the failure data would allow such an investigation.

The following sections 6.2 to 6.5 concentrate successively on the whole turbine, the gearbox, the generator, the electrics, the electronics and the hydraulics. These subassemblies largely dominate the reliability of the wind turbine, see Figure 4.15.

6.2 Results for Whole Turbine

Results for the whole wind turbine show some common features.

In Table B.1 it can be noted that the shape parameter, β , of the turbine models are consistently smaller than but close to one, and in many cases the HPP hypothesis is accepted, as it would be expected for complex subassemblies where the effect many different failure modes overlap. At the same time there are no cases of deterioration confirming that the reliability of all these turbines have actually been improving over the observed period. For those cases where the reliability has been improving, the shape parameter β reflects a general improvement that has occurred over the recording period. Given the acceptance of the HPP hypothesis the average intensity of failures as the expected failure intensity is, in the case of the whole turbine,

reasonable.

Model	β	Conclusion
V27/225	0.7467	PLP (early failures)
M530	0.9553	HPP
TW600	0.9585	HPP
E40	0.8926	PLP (early failures)
V39/500	0.8731	PLP (early failures)
E66	0.9447	HPP
N52/54	0.9896	HPP
All		NOT PLP
WSD		NOT PLP
WSDK		NOT PLP

Table 6.1: Synthetic results for the whole wind turbine, all subassemblies

If the final values of the failure intensity are considered as the expected ones, see Table B.1, then a correlation between the turbine rating and failure intensity is revealed. Smaller turbines have a lower demonstrated failure intensity of about 1 failure / year, while medium and larger turbines have higher demonstrated failure intensity of about 2 and 3 failure / year respectively. On the three examples shown in Figures 6.1, 6.2 and 6.3, reporting the fit for one wind turbine model for each size group, this observation can be seen.

The V27/225 wind turbine has the lowest β indicating the most aggressive reliability improvement. This turbine is the smallest and the oldest and subsequent turbines have benefited from this design. The lowest β of the individual subassemblies also belongs to the V27/225 turbine also suggesting that this turbine has been a pioneer of wind turbines technologies.

6.3 Results for Gearboxes

The results for gearboxes are particularly interesting since this subassembly has come in for considerable criticism, not all of it well-founded and, sometimes, anecdotal.

December 6, 2008

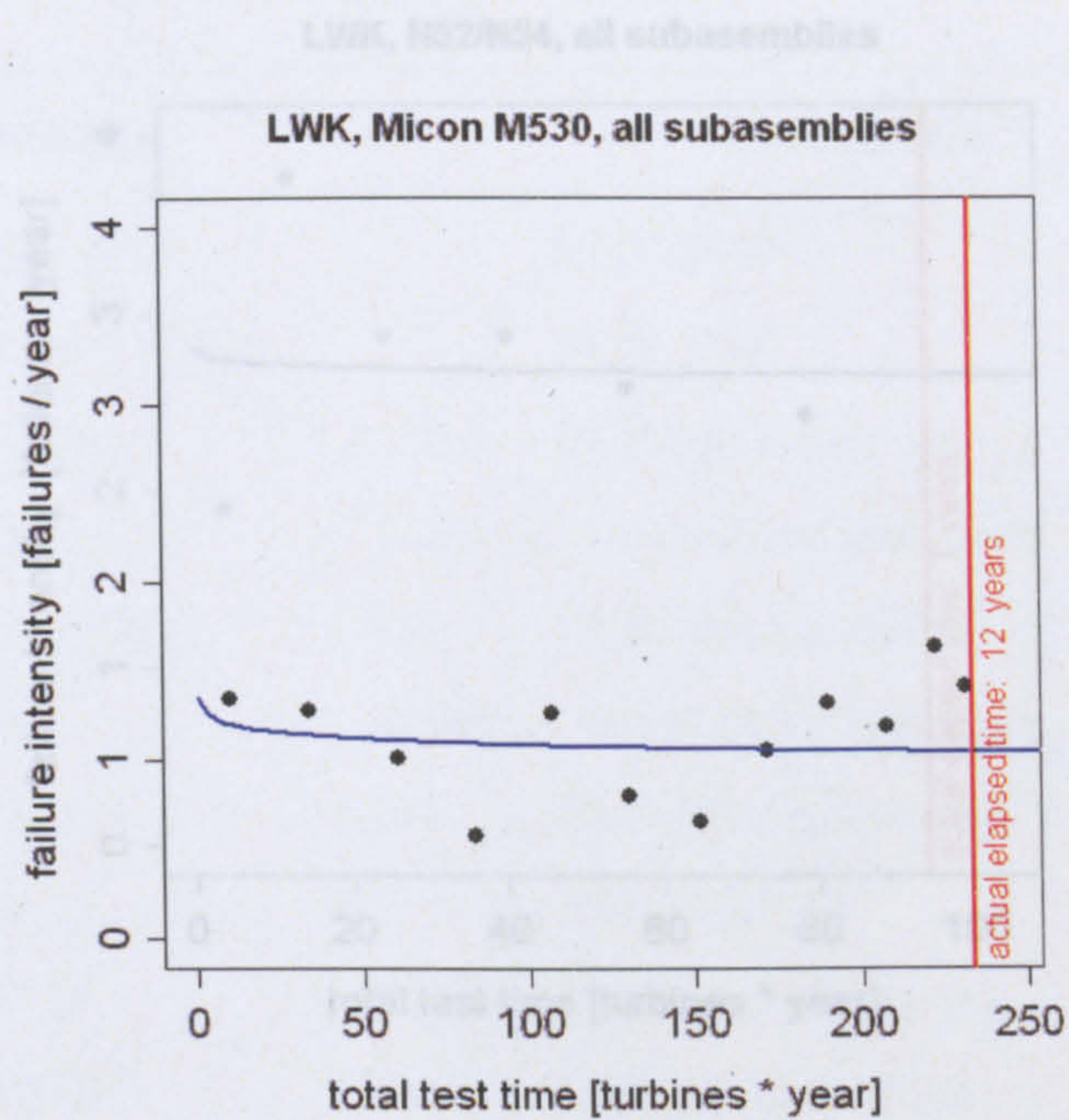


Figure 6.1: Whole WT, example 1, M530

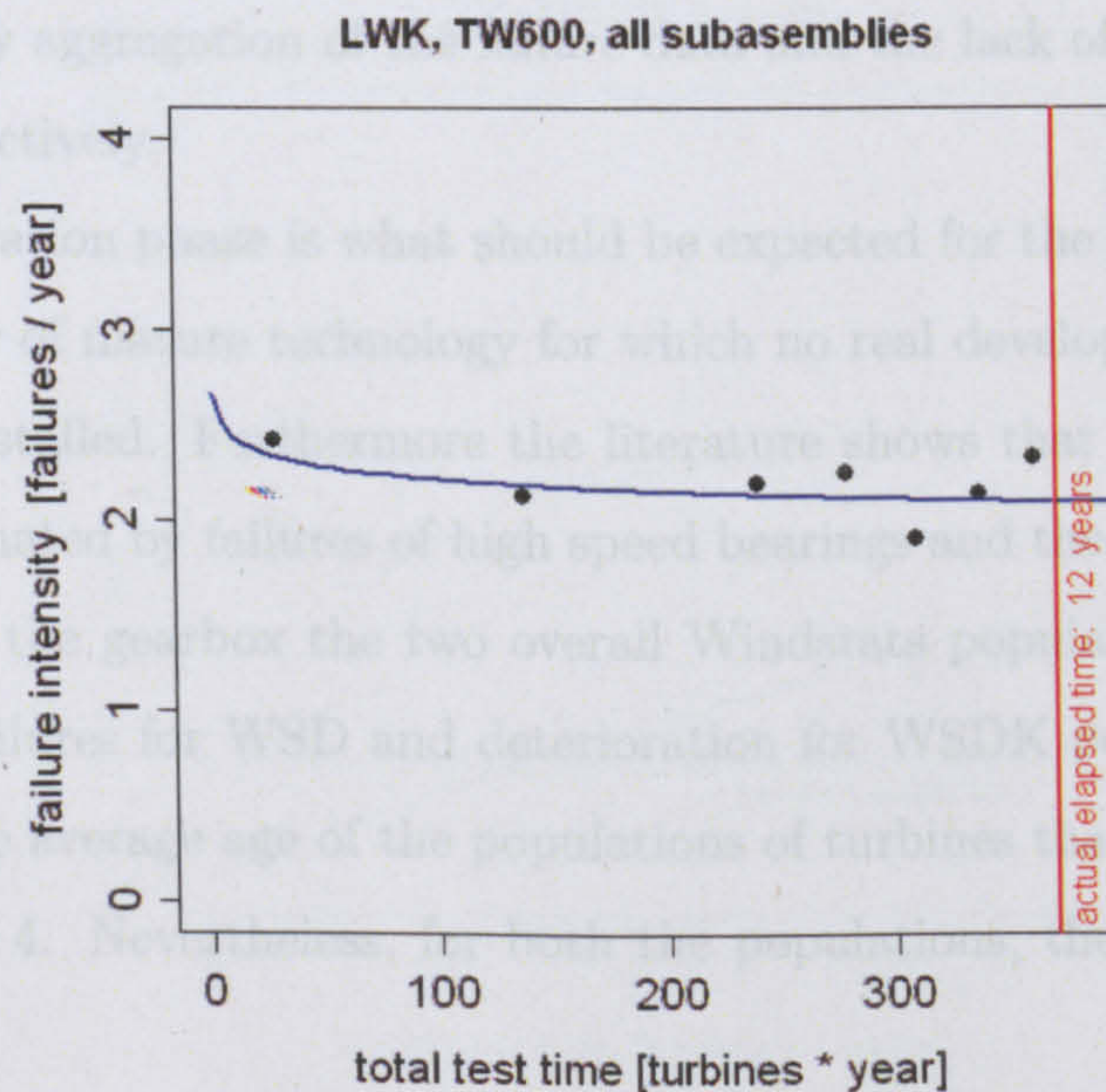


Figure 6.2: Whole WT, example 2, TW600

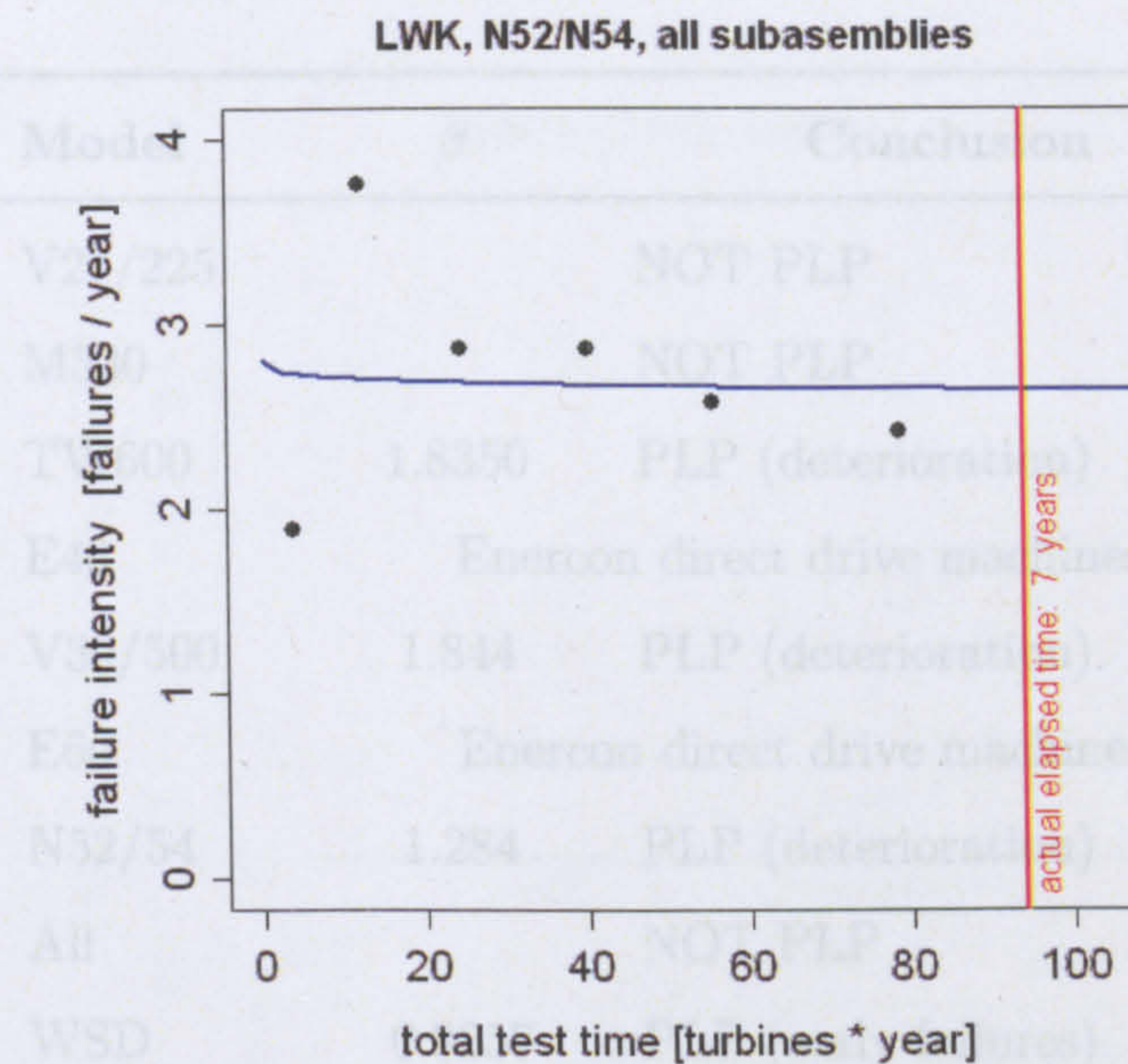


Figure 6.3: Whole WT, example 3, N52/54

The deterioration phase dominates the results for the gearbox as it can be seen on Table 6.2 that summarises the results of Table B.3. For the V27/225 and M530 wind turbines, the PLP model could not be implemented due to the rejection of the GoF test for any aggregation of the failure data and the lack of a sufficient number of failures respectively.

The deterioration phase is what should be expected for the gearbox, a mechanical subassembly of mature technology for which no real development can be implemented once installed. Furthermore the literature shows that the failures of gearboxes are dominated by failures of high speed bearings and the abrasion of the gear teeth [11]. For the gearbox the two overall Windstats populations show opposing trends; early failures for WSD and deterioration for WSDK possibly reflecting the difference in the average age of the populations of turbines that has been described in the Chapter 4. Nevertheless, for both the populations, the shape parameter is close to one.

Figures 6.4, 6.5 and 6.6 illustrate the interpolating curves for the gearboxes of TW600, V39 and N52-54 wind turbines. In these figures a black horizontal line indicates the failure intensity found from outside the wind industry as reported in Table

Model	β	Conclusion
V27/225		NOT PLP
M530		NOT PLP
TW600	1.8350	PLP (deterioration)
E40		Enercon direct drive machines
V39/500	1.844	PLP (deterioration)
E66		Enercon direct drive machines
N52/54	1.284	PLP (deterioration)
All		NOT PLP
WSD	0.9257	PLP (early failures)
WSDK	1.117	PLP (deterioration)

Table 6.2: The synthetic results for the gearbox

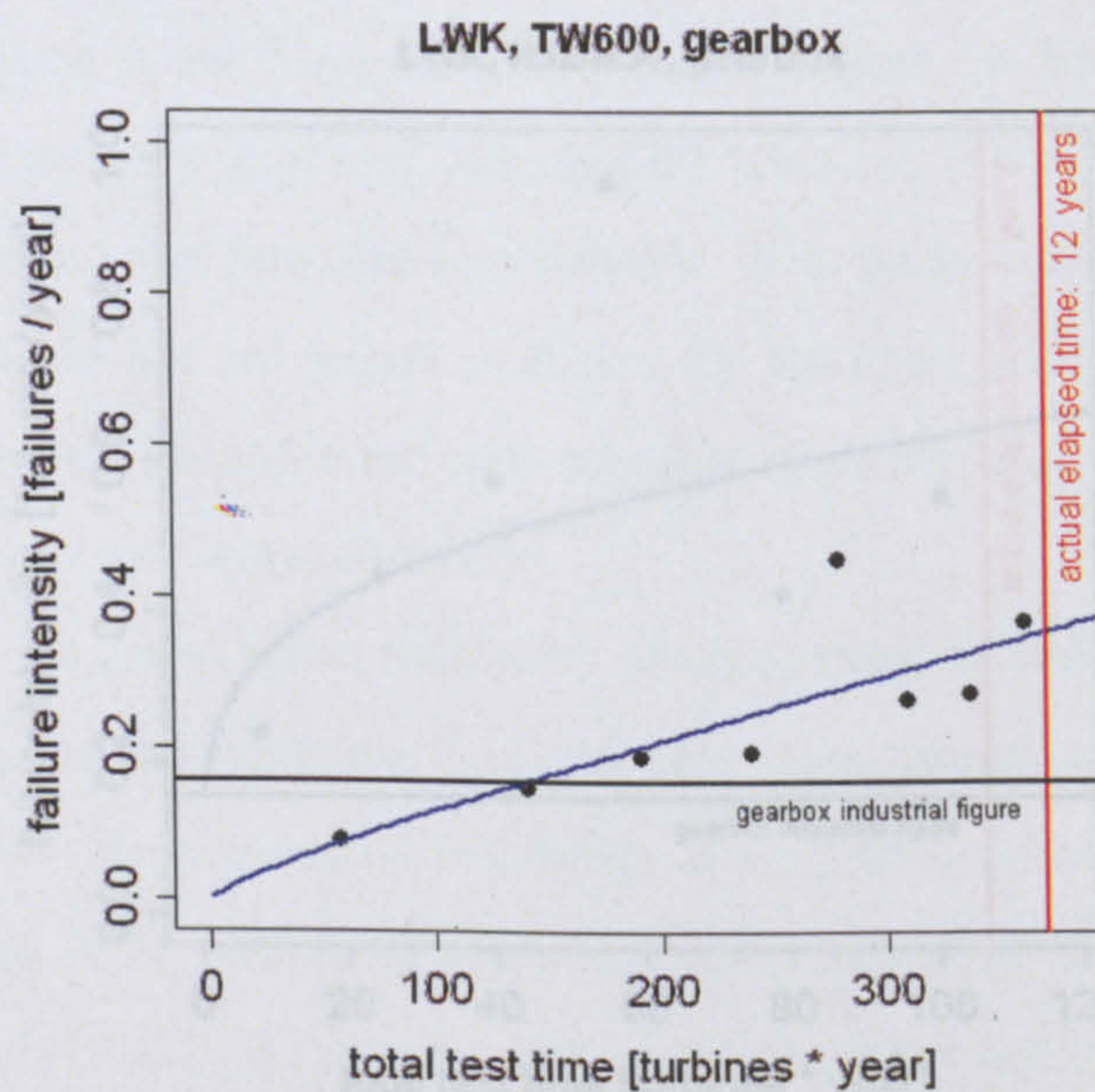


Figure 6.4: Gearbox, example 1, TW600

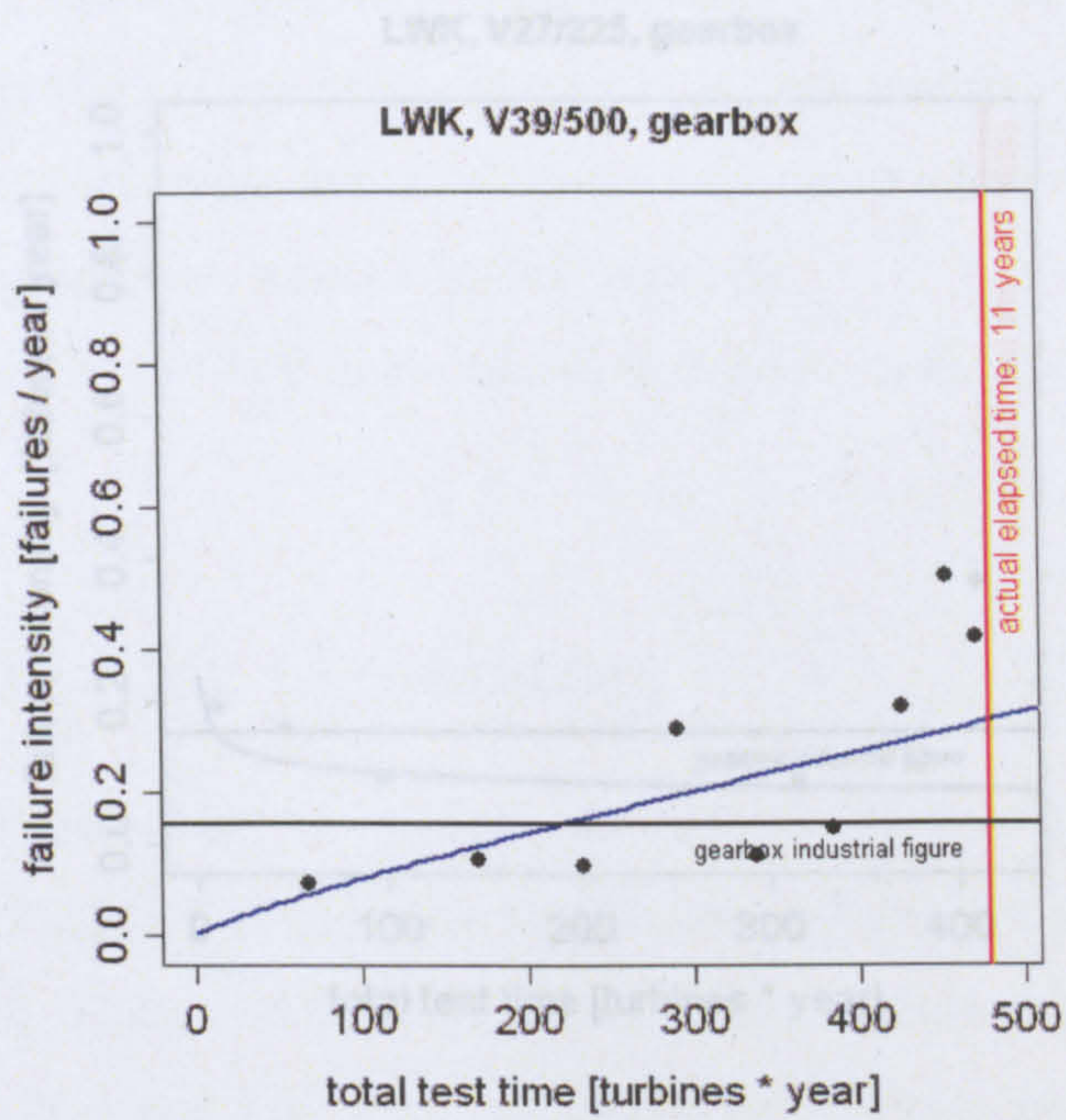


Figure 6.5: Gearbox, example 2, V39

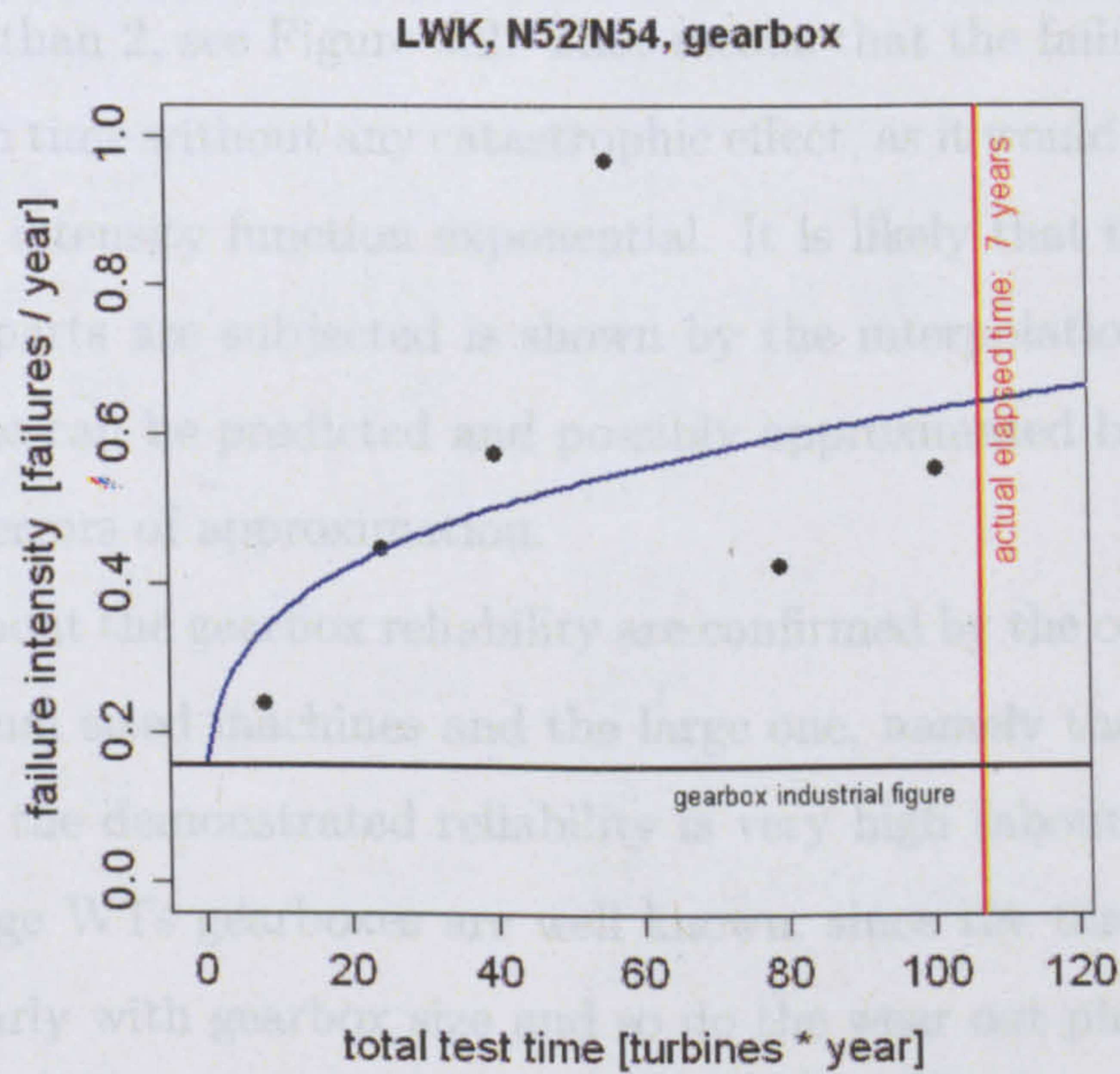


Figure 6.6: Gearbox, example 3, N52/54

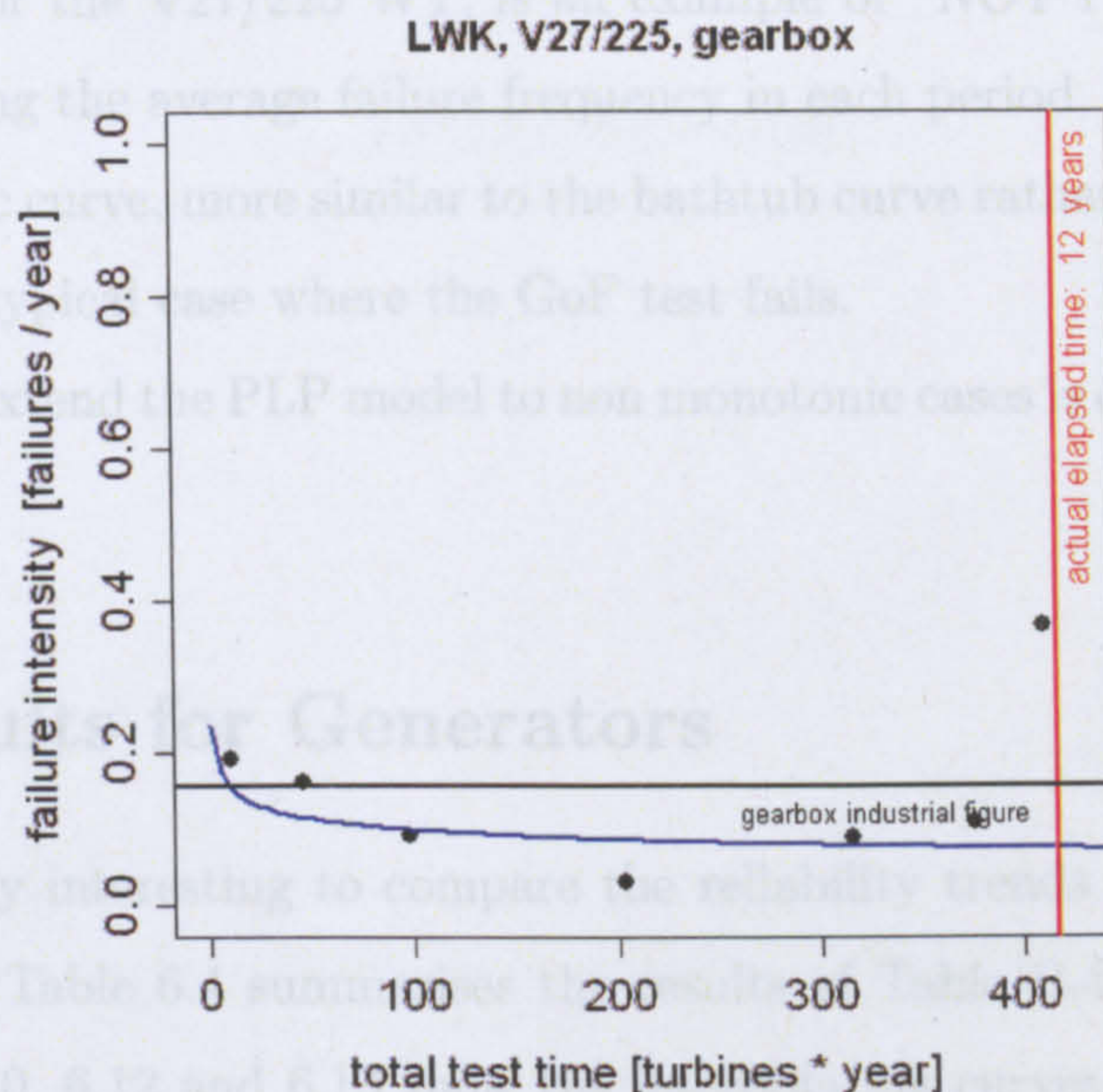


Figure 6.7: Gearbox, example 4, V27

2.6 of chapter 2. As reported in [31] this failure frequency is an average of various industrial surveys.

For those turbine models showing deterioration, the shape parameter β is similar and always less than 2, see Figure 3.2. That means that the failure intensity grows nearly linearly in time without any catastrophic effect, as it would do if β was greater than 2, and the intensity function exponential. It is likely that the maintenance to which gearbox parts are subjected is shown by the interpolation curves. The deterioration phase can be predicted and possibly approximated by a linear function without major errors of approximation.

The concerns about the gearbox reliability are confirmed by the comparison between the small/medium sized machines and the large one, namely the N52-54 wind turbine, for which the demonstrated reliability is very high (about 0.8 years^{-1}). The problems of large WTs gearboxes are well known, since the torque involved grows more than linearly with gearbox size and so do the wear out phenomena described above. The gearbox overrating, commonly adopted in the past for small WTs, cannot be proposed for multi-megawatt machines because of the consequent higher costs and weights that cannot be accepted.

Figure 6.7 for the V27/225 WT, is an example of “NOT PLP” fit. The black dots, representing the average failure frequency in each period, can be described by a non monotonic curve, more similar to the bathtub curve rather than a single phase of it. This is a typical case where the GoF test fails.

An attempt to extend the PLP model to non monotonic cases is described in Chapter 7.

6.4 Results for Generators

It is particularly interesting to compare the reliability trends of the gearbox with the generator. Table 6.4 summarises the results of Table B.4 in a synthetic way. Figures 6.9, 6.10, 6.12 and 6.13 show the interpolating curves for the generator of the E40, M530, N54 and E66 wind turbines in comparison with industrial failure data for the generator. The industrial data are taken from Section 2.7 and are the outcome of the work made by Tavner [54].

The difference from the results of gearbox is substantial; in the case of the generator the intensity of failures is either improving or constant.

Model	β	Conclusion
V27/225	0.4295	PLP (early failures)
M530	0.6242	PLP (early failures)
TW600	1.0860	HPP
E40	1.0110	HPP
V39/500		NOT PLP
E66	0.4666	HPP
N52/54		NOT PLP
All	1.2020	PLP (deterioration)
WSD		NOT PLP
WSDK	0.8422	PLP (early failures)

Table 6.3: Synthetic results for the generator

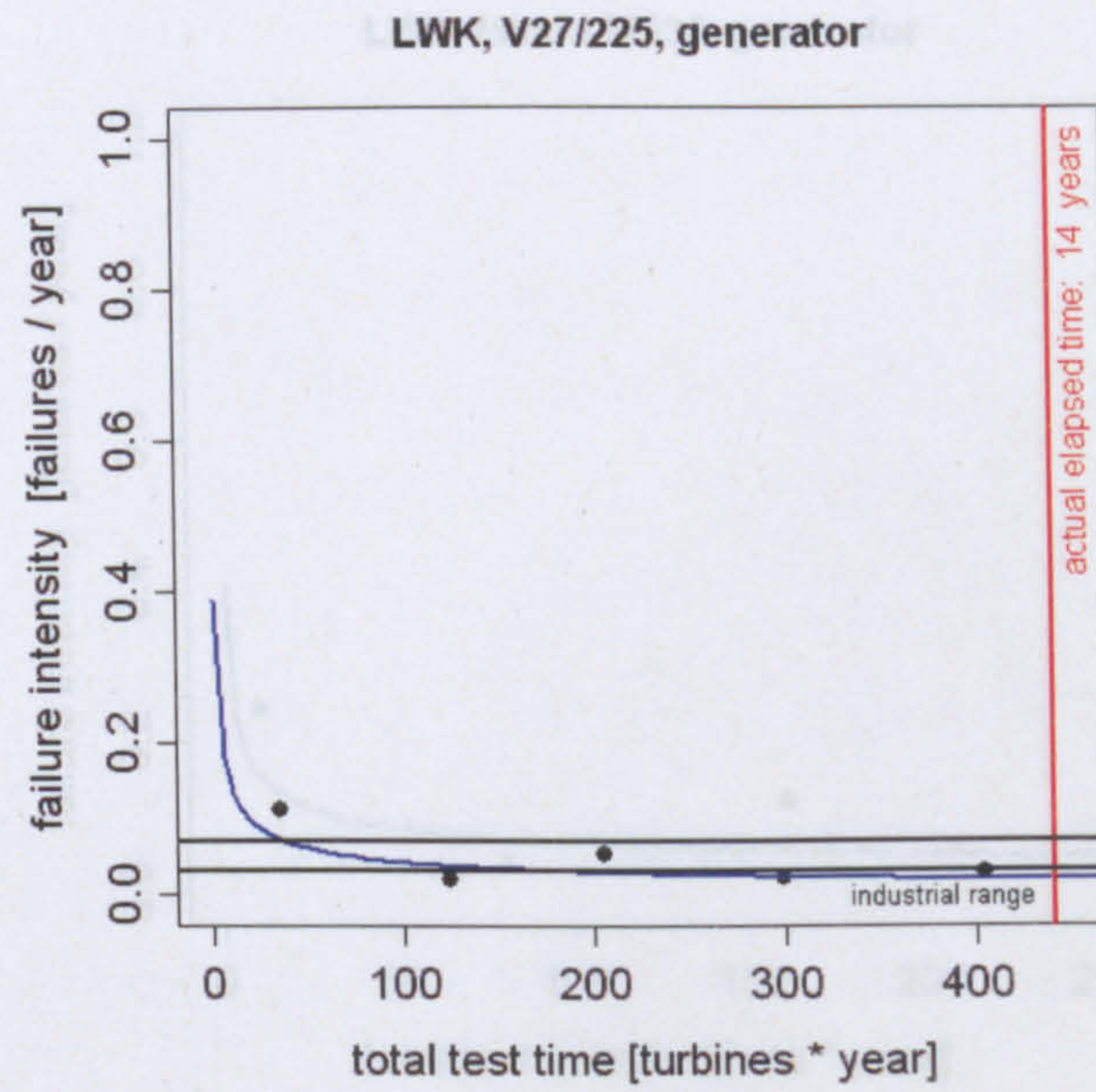


Figure 6.8: Generator, example 1, V27

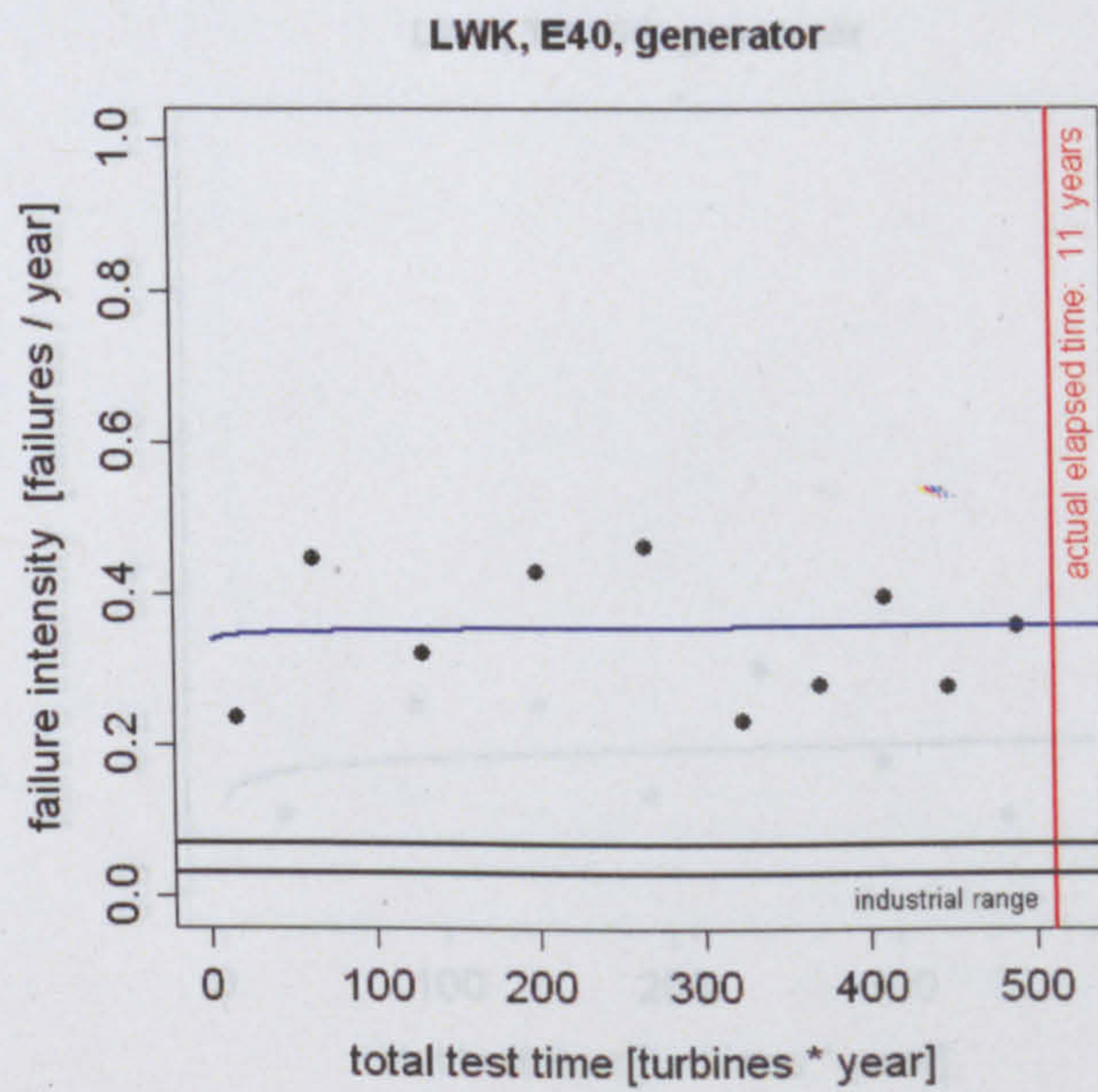


Figure 6.9: Generator, example 2, V27

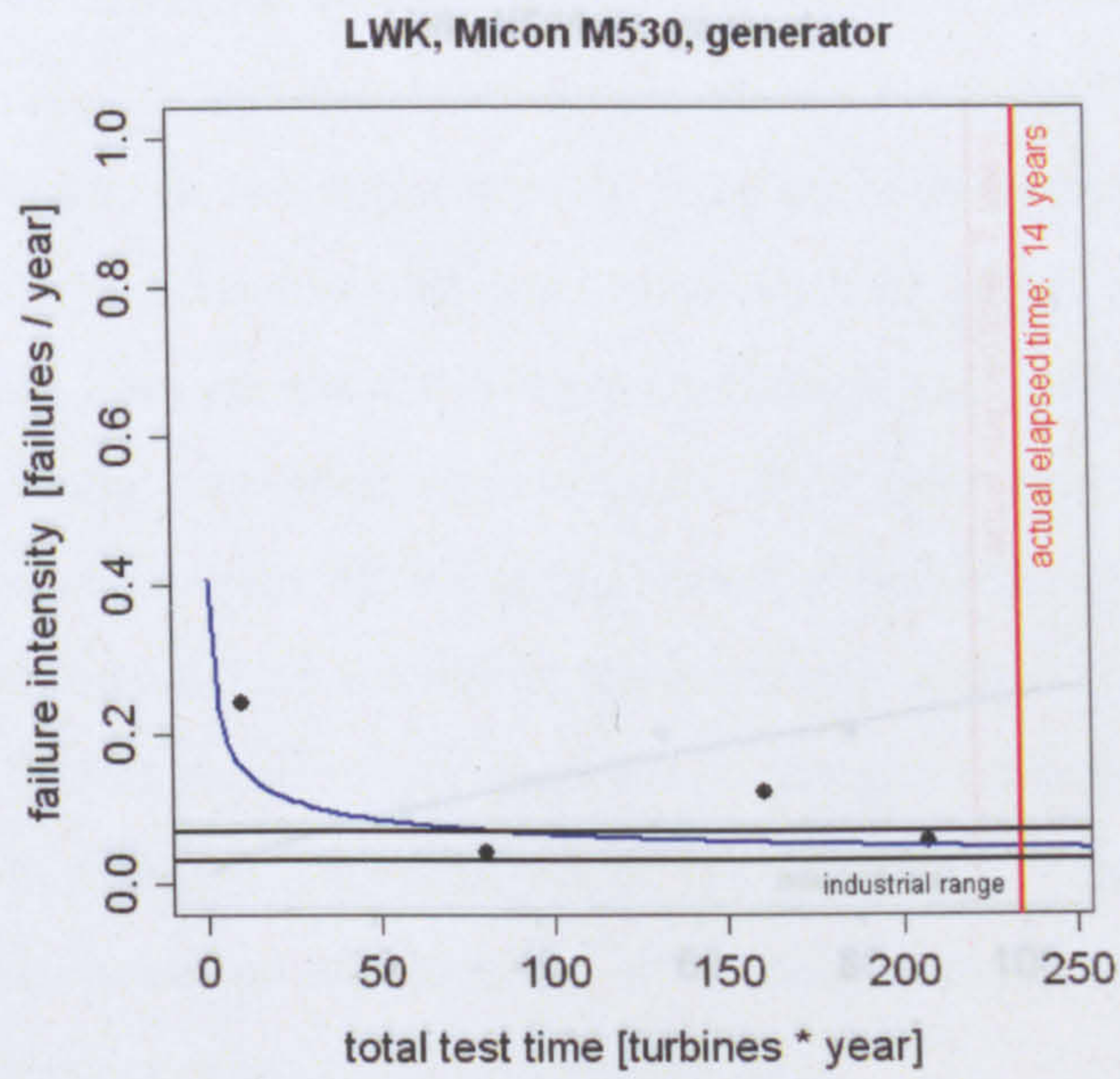


Figure 6.10: Generator, example 3, M530

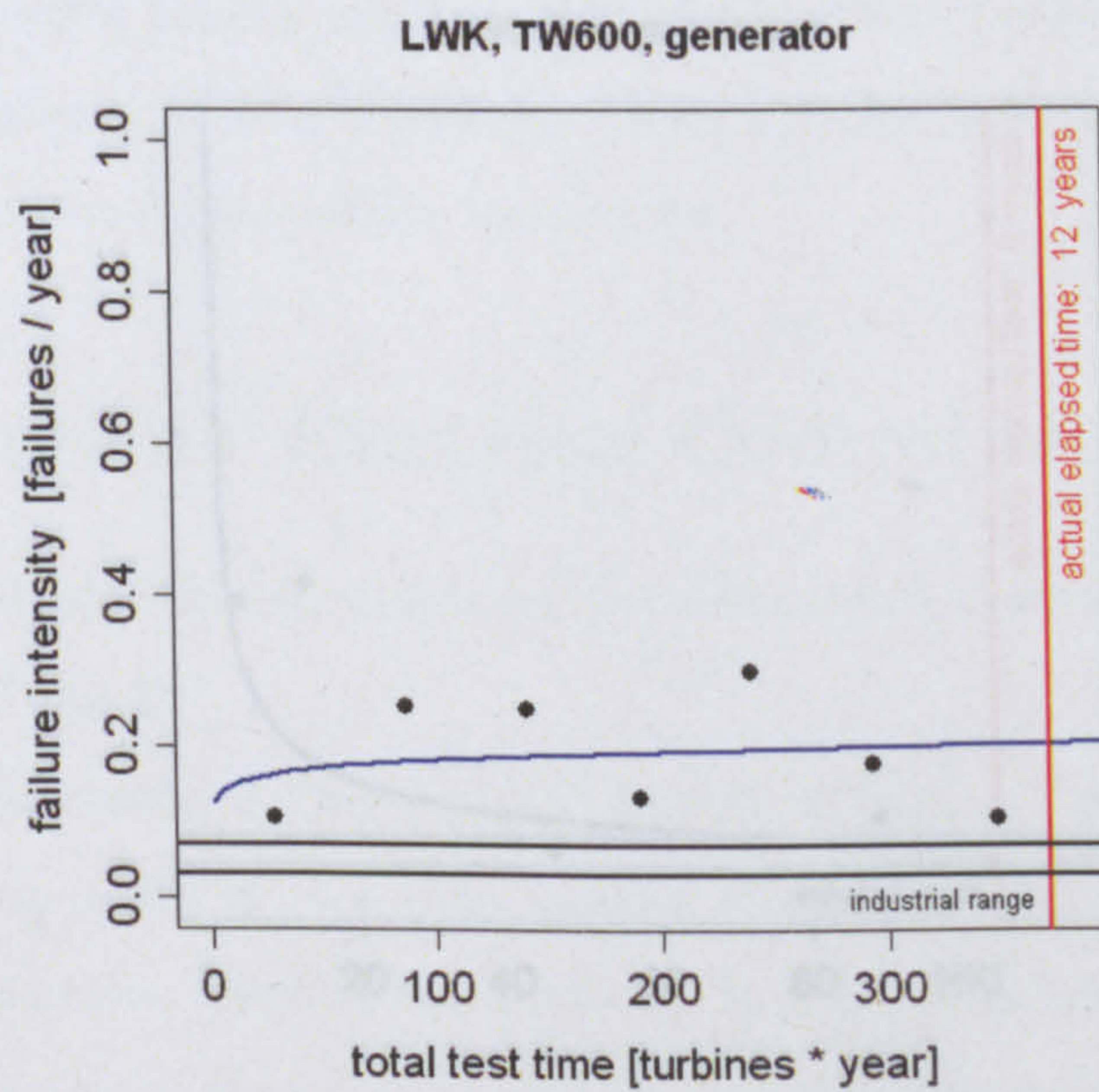


Figure 6.11: Generator, example 4, TW600

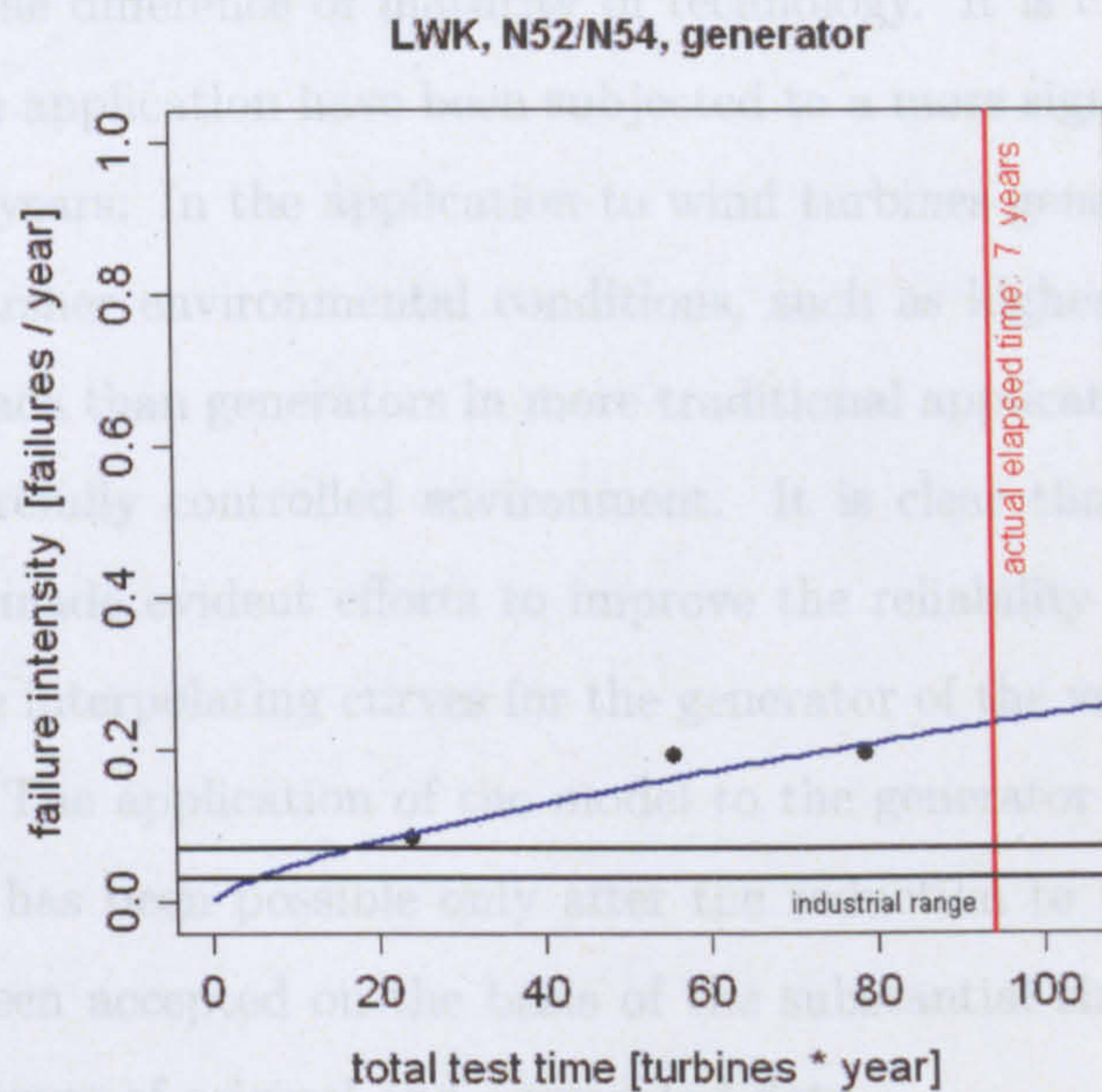


Figure 6.12: Generator, example 5, N52/54

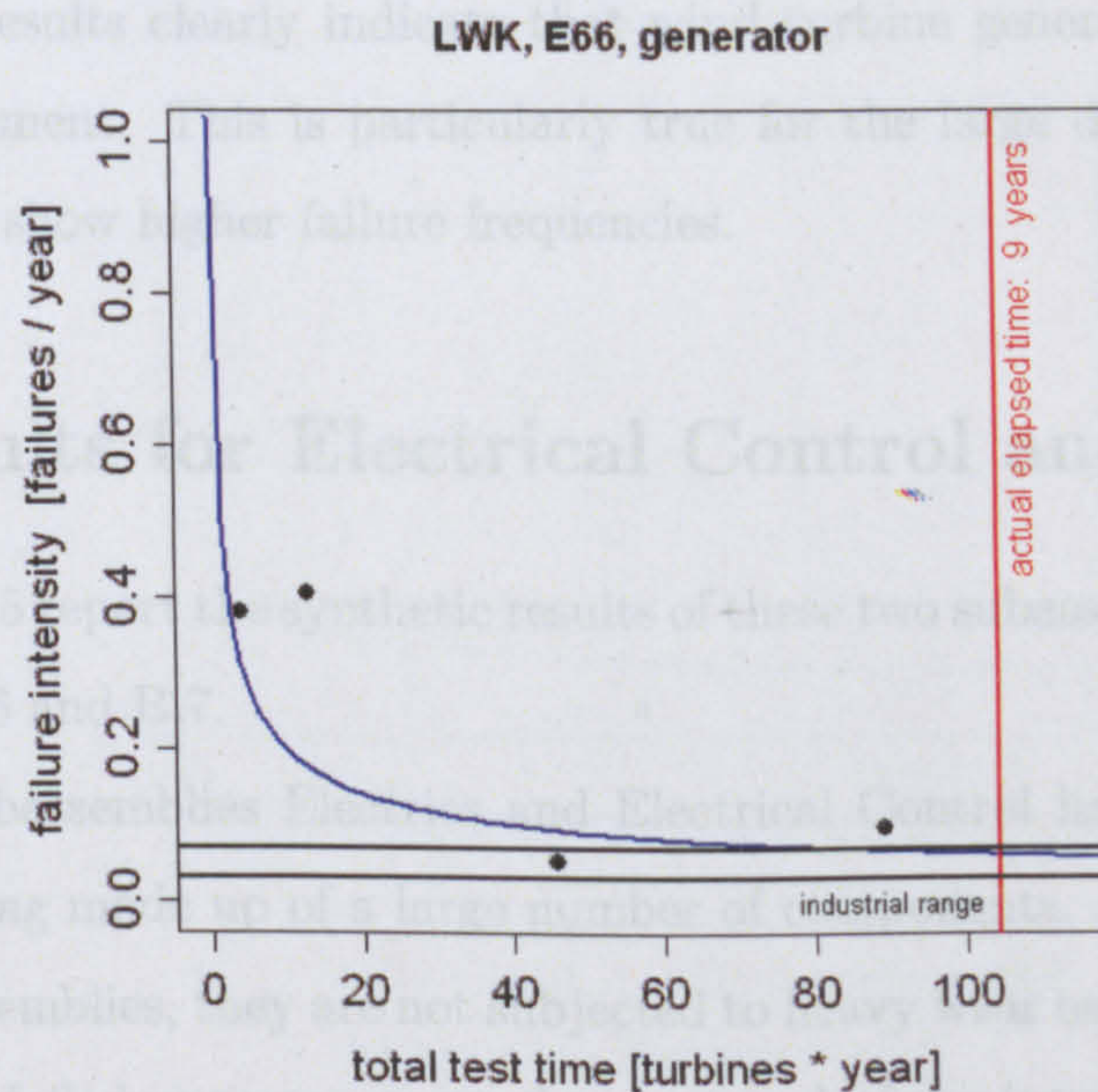


Figure 6.13: Generator, example 6, E66

The difference in trend between gearbox and generator can be explained only in the light of the difference of maturity of technology. It is clear that generators for wind turbine application have been subjected to a more significant development during the last years. In the application to wind turbines generators are generally subjected to harsher environmental conditions, such as higher ambient variations and dynamic loads than generators in more traditional applications, where they are usually in a carefully controlled environment. It is clear that the designers and operators have made evident efforts to improve the reliability of the wind turbine generators. The interpolating curves for the generator of the various turbine reflect this condition. The application of the model to the generator has proven difficult, and often a fit has been possible only after the reduction to three or four points. Results have been accepted on the basis of the substantial similarity between the interpolating curves of original and aggregated data.

The generator is subjected to a high variability of failure data possibly because the generator is an interface between mechanical and electrical “environment” of the turbine and both “environment” affect the reliability of this subassembly. For the generator the segregation of failure data by component or failure mode appears necessary and results clearly indicate that wind turbine generators are capable of further improvement. This is particularly true for the large diameter direct drive generators that show higher failure frequencies.

6.5 Results for Electrical Control and Electrics

Table 6.5 and 6.5 report the synthetic results of these two subassemblies, summarised from Tables B.6 and B.7.

The two subassemblies Electrics and Electrical Control have in common their complexity, being made up of a large number of components. In contrast with mechanical subassemblies, they are not subjected to heavy wear out and the continuous replacement of failed components masks any trend of the intensity of failure of the entire subassembly. Thus, it would be expected that they will not show a substantial failure frequency trend. For the Electrical Control subassembly, it is common prac-

Model	β	Conclusion
V27/225	0.6699	PLP (early failures)
M530	0.6884	PLP (early failures)
TW600	0.8673	HPP
E40	0.9119	HPP
V39/500	0.8975	HPP
E66	1.0020	HPP
N52/54	0.8978	HPP
All	0.8710	PLP (early failures)
WSD		NOT PLP
WSDK		NOT PLP

Table 6.4: The synthetic results for the electrical control

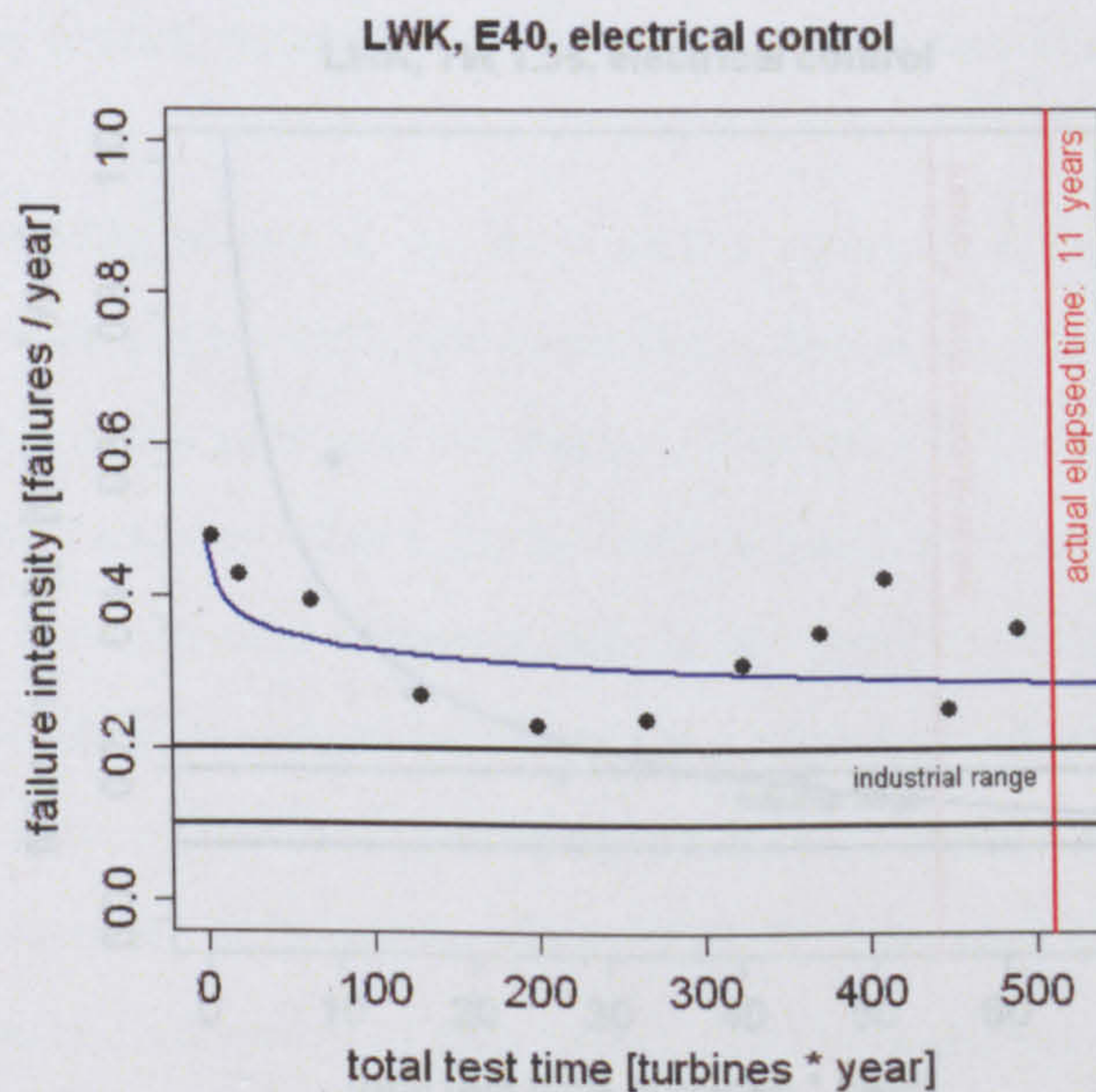


Figure 6.14: Electrical control, example 1, E40

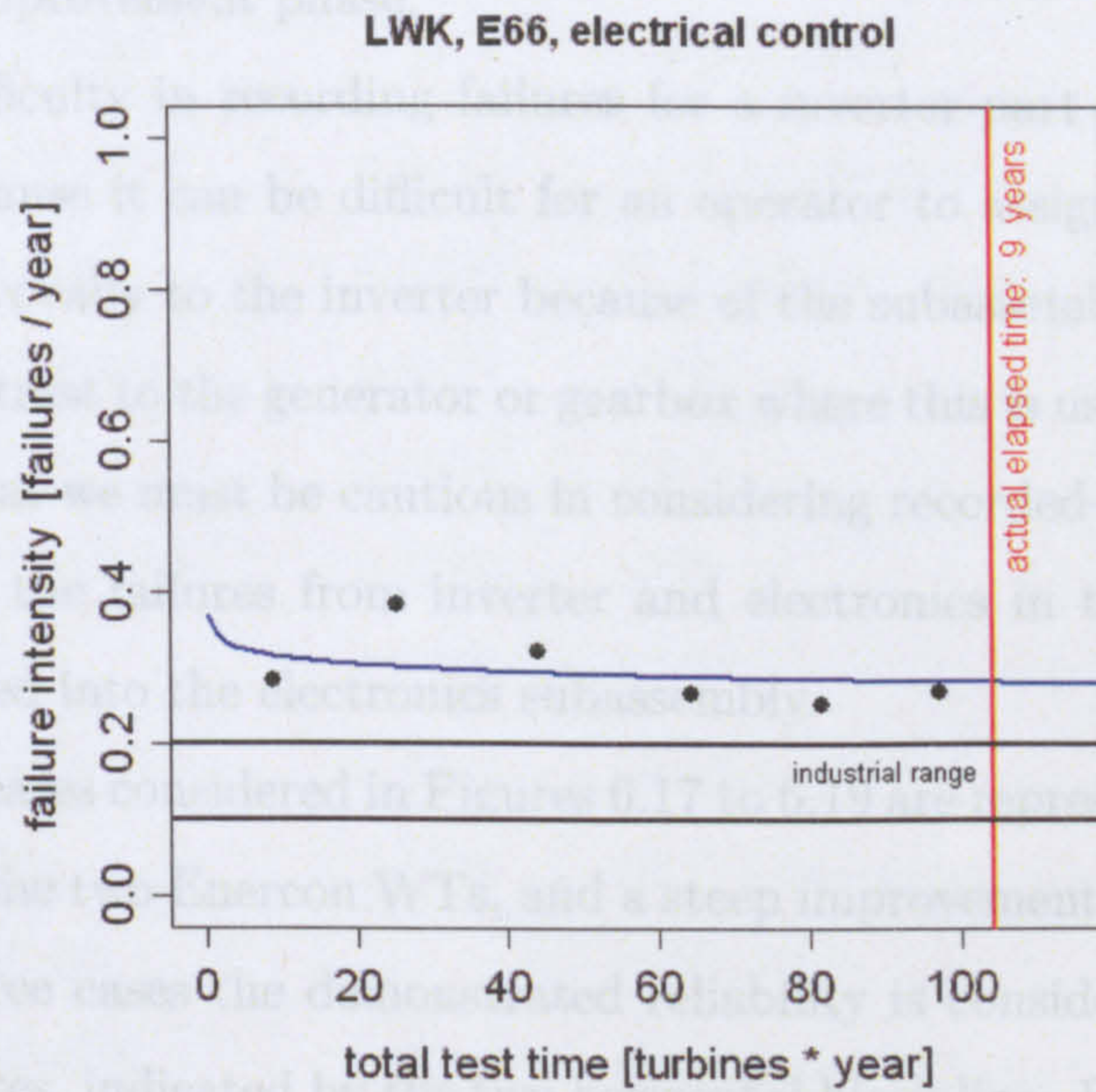


Figure 6.15: Electrical control, example 2, E66

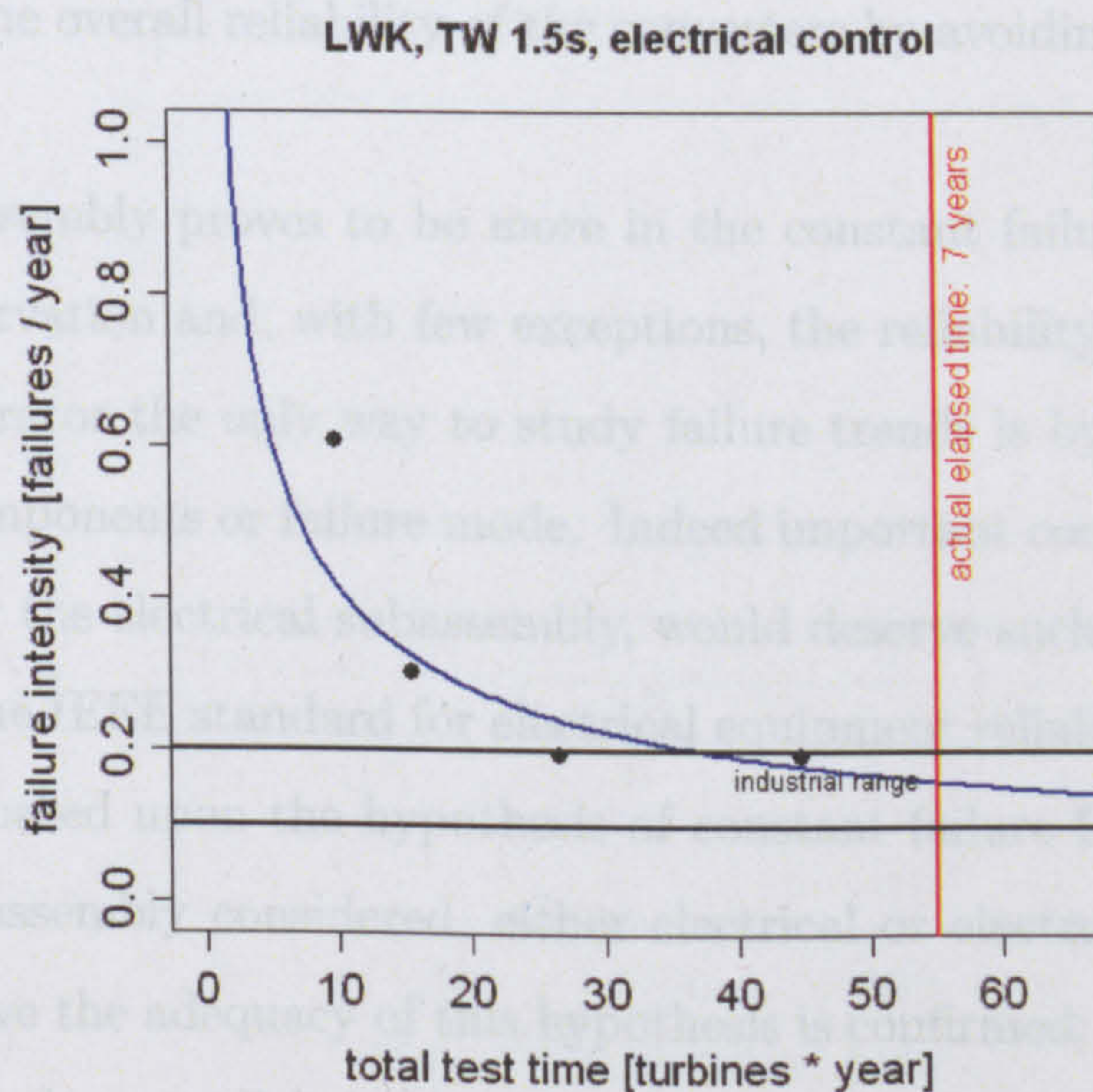


Figure 6.16: Electrical control, example 3, TW1.5s

tice to use feedback about performance to improve the design. This should result in an initial improvement phase.

There is a difficulty in recording failures for a inverter part of the electronic sub-assembly. because it can be difficult for an operator to assign a particular turbine failure unequivocally to the inverter because of the subassembly's complexity. This is in sharp contrast to the generator or gearbox where this is usually straightforward. This means that we must be cautious in considering recorded converter failures. To overcome this the failures from inverter and electronics in the LWK survey have been aggregated into the electronics subassembly.

The three cases considered in Figures 6.17 to 6.19 are representative of a constant failure, as for the two Enercon WTs, and a steep improvement as for the Tacke WT. For all the three cases the demonstrated reliability is considerably lower than the industrial figures, indicated by the two horizontal black line. Different from gearbox and generator, the industrial range for the Electrical Control has been taken from the analysis carried out on smaller industrial converters, illustrated in Appendix A and other engineering considerations, as reported in Chapter 2. From this analysis the message that should be delivered to the wind energy power electronics industry is to improve the overall reliability of the converters by avoiding the "early failures"

Electrics subassembly proves to be more in the constant failures phase confirming the above observation and, with few exceptions, the reliability behaviour is HPP.

As for generator the only way to study failure trends is by segregating the failure data by components or failure mode. Indeed important components, such as the transformer for the electrical subassembly, would deserve such a detailed analysis. In Chapter 2 the IEEE standard for electrical equipment reliability [61] was referred to and this is based upon the hypothesis of constant failure frequency of the component or subassembly considered, either electrical or electronics. In the light of the results above the adequacy of this hypothesis is confirmed; for both the electrics and electronics the overall behaviour can be described generally with a HPP and the reliability of the subassembly can be approximated from the reliability of the various components.

Model	β	Conclusion
V27/225	0.7244	PLP (early failures)
M530	1.6480	PLP (deterioration)
TW600	0.9871	HPP
E40	0.9214	HPP
V39/500	0.8769	HPP
E66	1.0170	HPP
N52/54	0.7957	Unknown
All	1.1010	PLP (deterioration)
WSD		NOT PLP
WSDK	0.7919	PLP (early failures)

Table 6.5: The synthetic results for the electrics

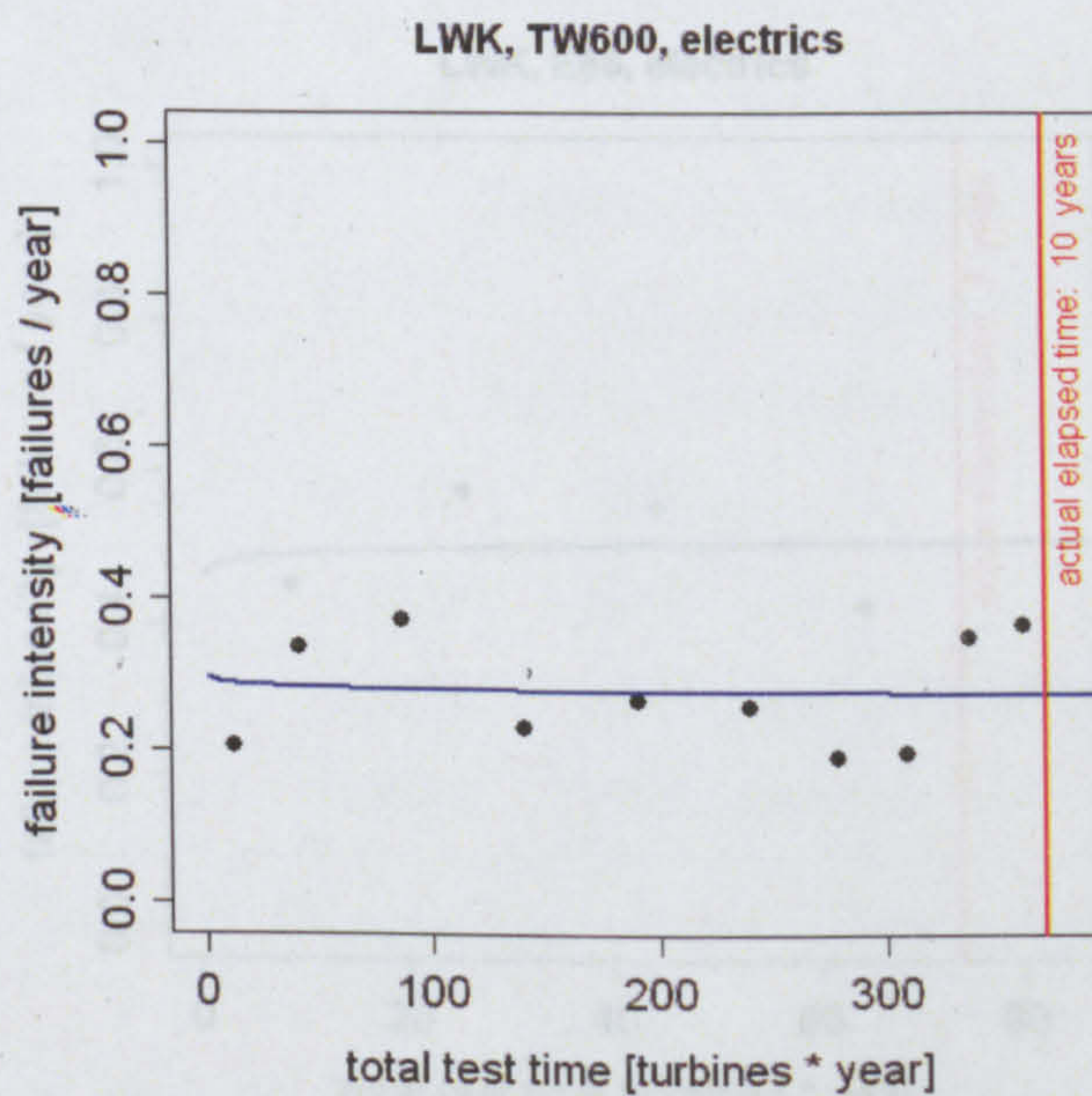


Figure 6.17: Electrics, example 1, TW600

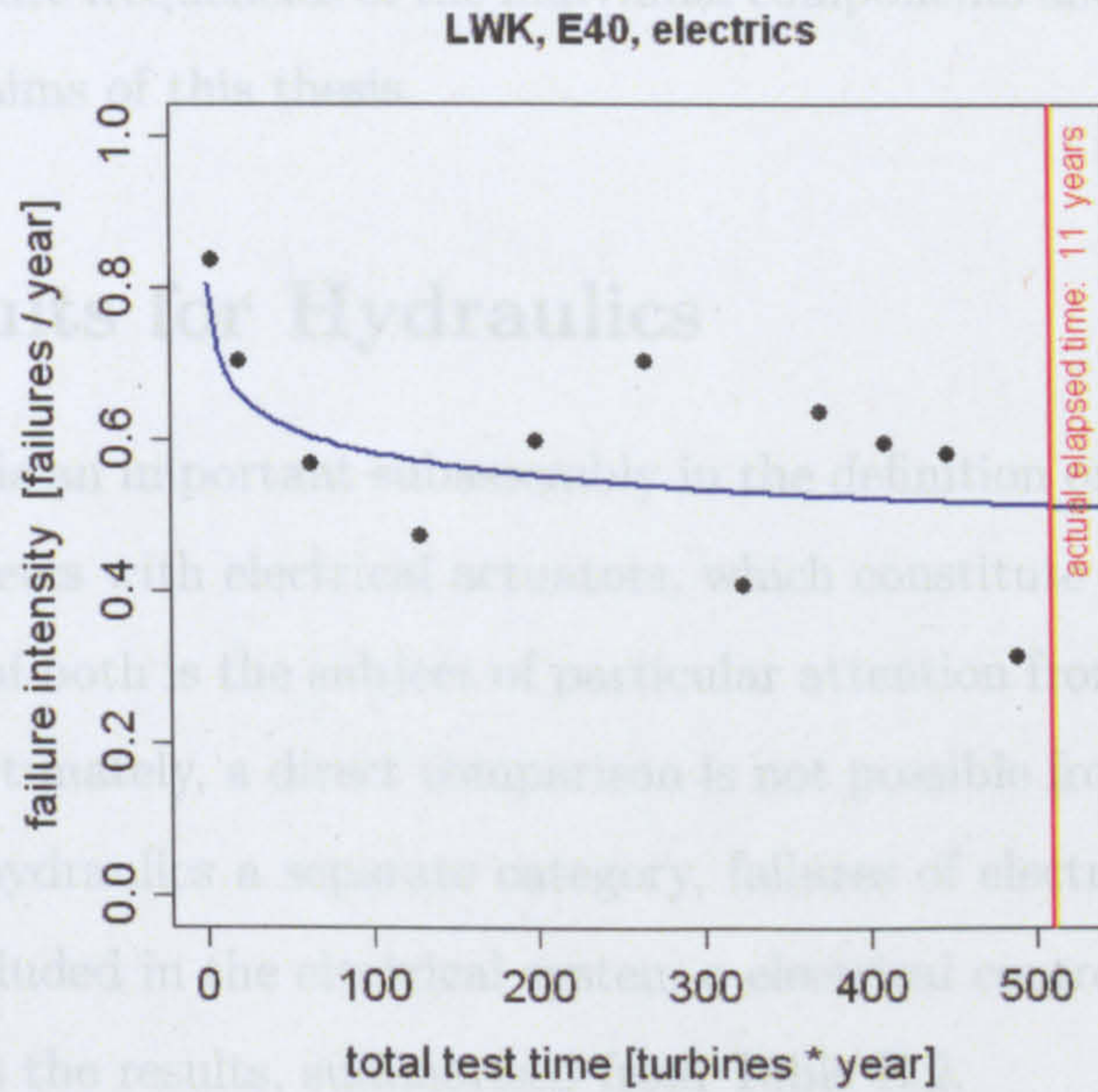


Figure 6.18: Electrics, example 2, E40

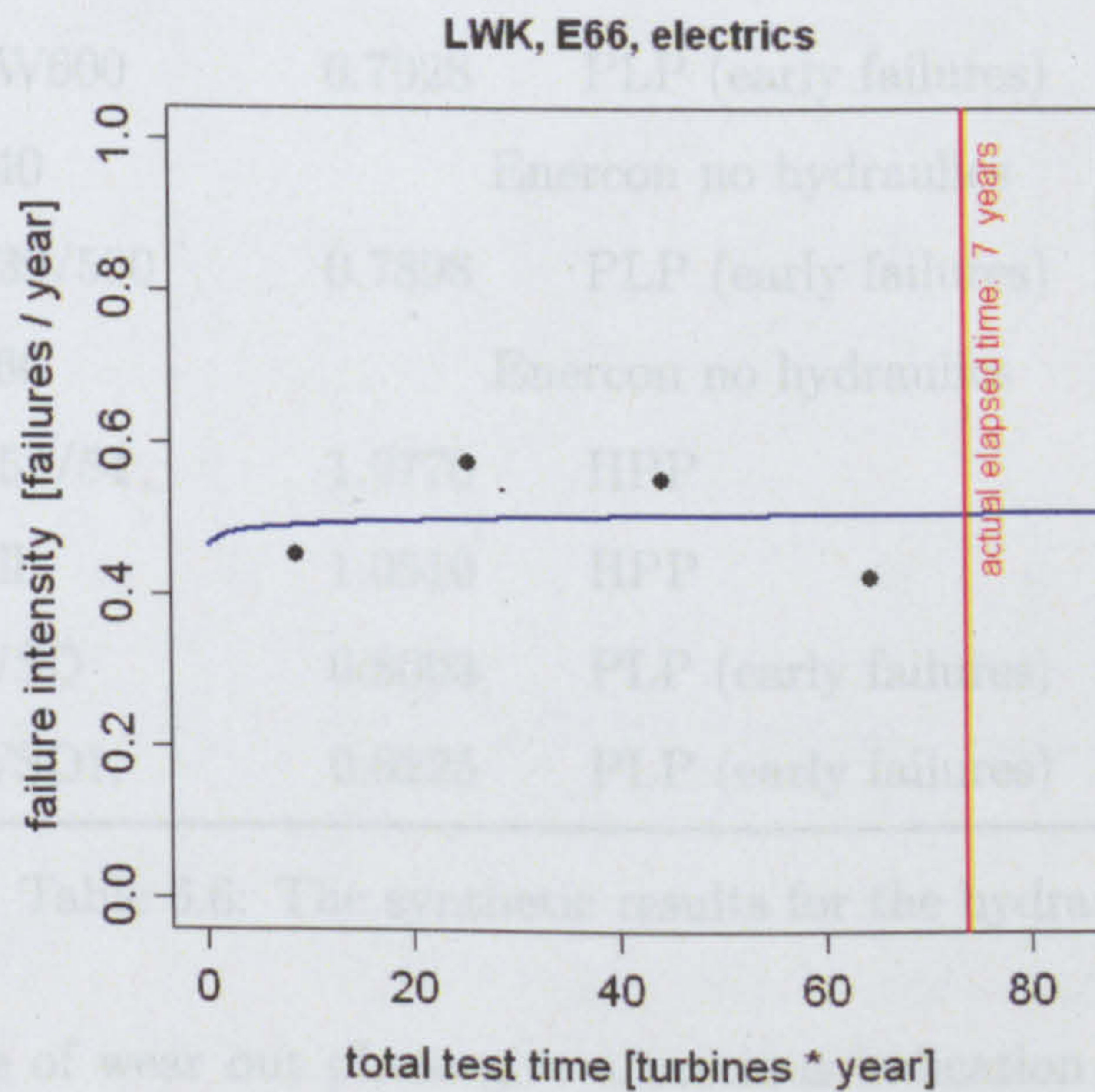


Figure 6.19: Electrics, example 3, E66

The comparison with industrial figures would require a complex investigation starting from the failure frequencies of the individual components and this analysis would be beyond the aims of this thesis.

6.6 Results for Hydraulics

The hydraulics is an important subassembly in the definition of existing turbine designs and competes with electrical actuators, which constitute a robust alternative. The reliability of both is the subject of particular attention from designer and operators but, unfortunately, a direct comparison is not possible from LWK or WS data because, with hydraulics a separate category, failures of electrical actuators, when present, are included in the electrical system or electrical control subassemblies.

Table 6.6 shows the results, summarised from Table B.2.

Model	β	Conclusion
V27/225		NOT PLP
M530		Unknown
TW600	0.7028	PLP (early failures)
E40		Enercon no hydraulics
V39/500	0.7898	PLP (early failures)
E66		Enercon no hydraulics
N52/54	1.0770	HPP
All	1.0510	HPP
WSD	0.8003	PLP (early failures)
WSDK	0.8225	PLP (early failures)

Table 6.6: The synthetic results for the hydraulics

The absence of wear out phase give a precious indication about the reliability behaviour of the hydraulics. It appears that the hydraulics behave like the electrics subassembly and the wear out phase, typical of mechanical subassembly as gearbox is not shown. Conversely for some turbine models, and the two WS populations the

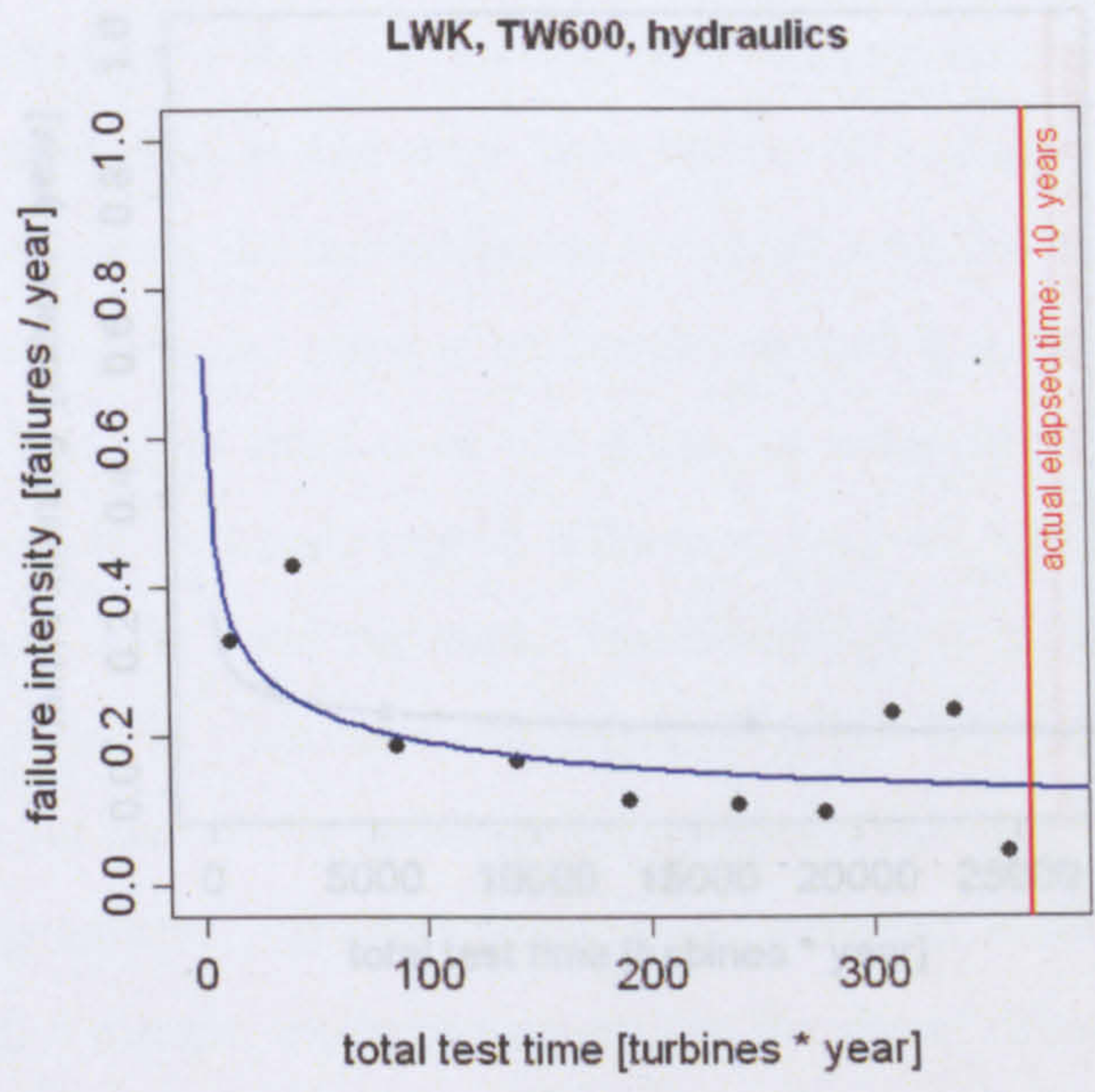


Figure 6.20: Hydraulics, example 1, TW600

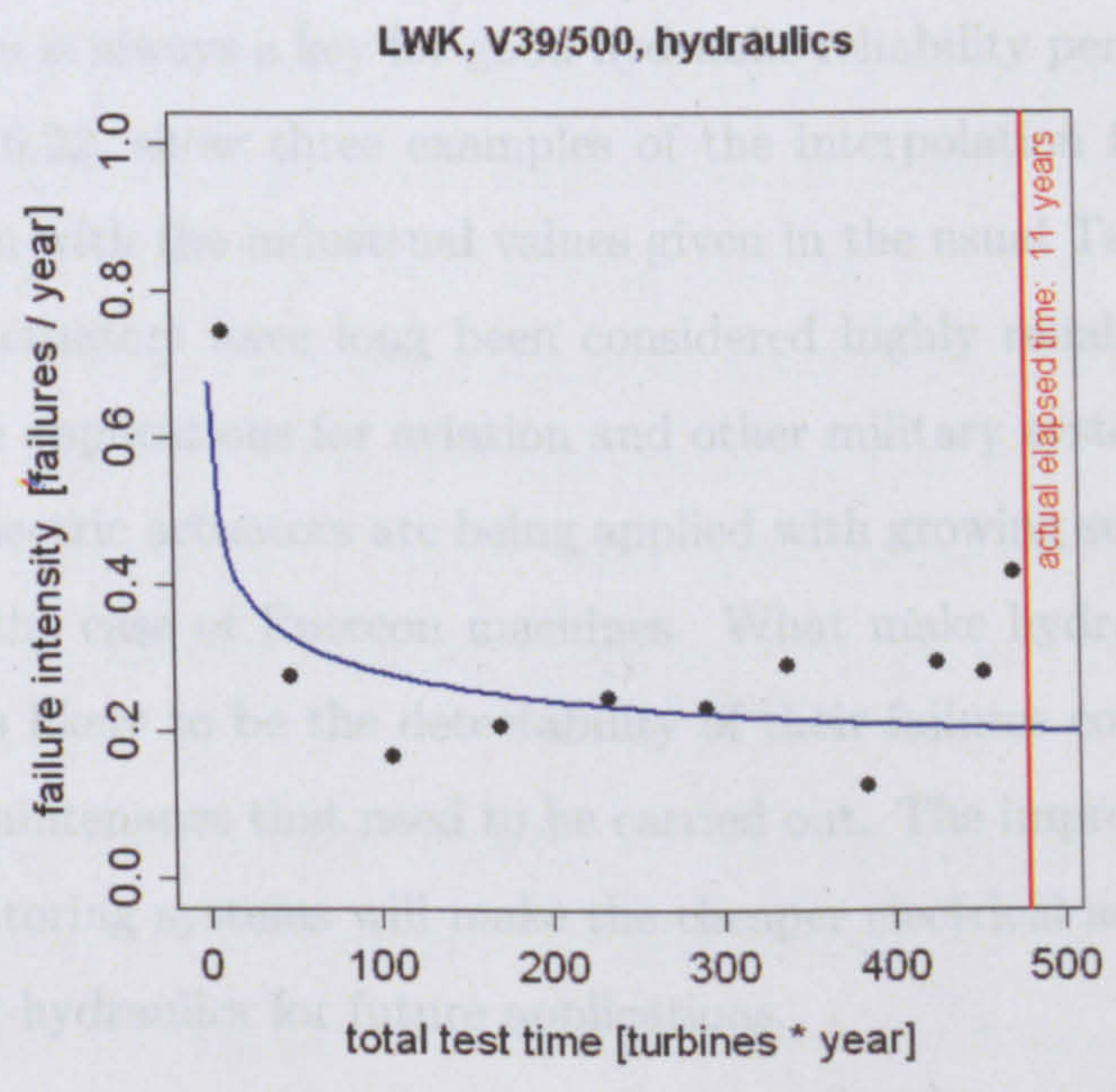


Figure 6.21: Hydraulics, example 2, V39

6.7 Conclusions

WindStats, Germany, hydraulics

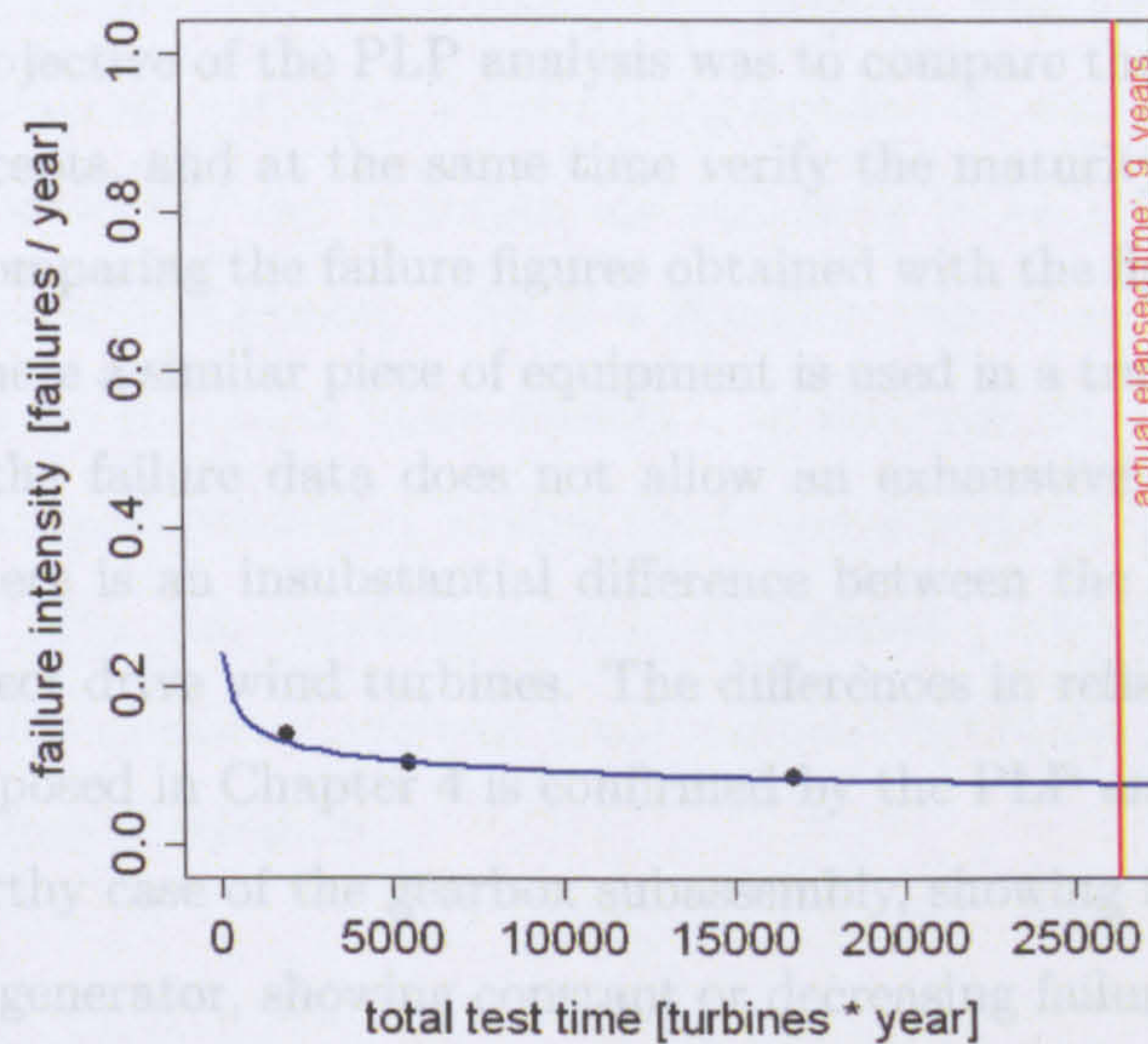


Figure 6.22: Hydraulics, example 3, All WTs

hydraulics have been subjected to a clear improvement. It is likely that in the case of hydraulics this improvement has arisen primarily from maintenance strategy, rather than by design and probably through maintaining a high oil cleanness. Maintenance of the hydraulics is always a key for good hydraulic reliability performance. Figures 6.20, 6.21 and 6.22, show three examples of the interpolation for hydraulics and comparing them with the industrial values given in the usual Table 2.6.

Hydraulic actuators have long been considered highly reliable and widely are used in delicate applications for aviation and other military systems. Nevertheless, electric actuators are being applied with growing success, also in wind energy, as for the case of Enercon machines. What make hydraulics perceived as more reliable is likely to be the detectability of their failures consequent upon the high level of maintenance that need to be carried out. The improving technology of condition monitoring systems will make the cheaper electrical actuators even more attractive than hydraulics for future applications.

6.7 Conclusions

An important objective of the PLP analysis was to compare the reliability of different turbine concepts, and at the same time verify the maturity of the wind power technology by comparing the failure figures obtained with the figures of other industrial surveys, where a similar piece of equipment is used in a traditional application. The nature of the failure data does not allow an exhaustive investigation but it appears that there is an insubstantial difference between the overall reliability of direct and indirect drive wind turbines. The differences in reliability related to the WT size and exposed in Chapter 4 is confirmed by the PLP analysis in Chapter 5.

The noteworthy case of the gearbox subassembly, showing increasing failure intensity and the generator, showing constant or decreasing failure intensity, suggests that there is still a margin for improvement for the direct drive turbine, hence, the possibility for the direct drive concept to become intrinsically more reliable in the future. The behaviour of the gearbox appears to be well defined and predictable, a situation that can be particularly useful for the prediction of availability and cost of maintenance.

The large direct drive generators, mounted on the E40 and E66 wind turbines, are of particular interest because their reliability is poor compared to other wind turbines and to industrial generator benchmarks. It is known that manufacturing problems can arise for machines built in small number, as in this case. Furthermore the utilization of a large diameter synchronous machine for wind power application has highlighted some problems with the insulation that have been progressively solved over a number of years. This is clearly shown in the very low β in Table 6.4. It is also clear that the E66 generator design is a very considerable improvement on that installed in the E40.

Some manufacturers are now replacing the hydraulic actuator with electrical actuators. Comparing the relative results it appears that this could be a wise choice. Unfortunately the electrics subassembly incorporates the failures of the entire electrical system, but the failure figures are comparable to the figures for the hydraulics subassembly alone. An increased failure frequency of the electrics subassembly of the Enercon machines suggests this. For both subassemblies the HPP suits the relia-

bility behaviour but for different reasons; the complexity of the electrics subassembly with overlapping failure modes and component failures, and, for the hydraulics subassembly, a substantial maturity of technology assisted by a high level of preventive maintenance. Failures of the hydraulics are also easy to be predicted and maintenance is effective for this reason. This is a situation that in an FMECA analysis is quantified by a quantity called “detectability”. In this case the electrics subassembly appears to be the most promising having the larger margin of improvement. In [32] this is reported after the experiences with the Naval , where for a new warship weaponry actuator electrical systems have replaced hydraulic systems, achieving a much higher degree of reliability.

Chapter 7

Simulation of Failure Events

7.1 Introduction

Applying the reliability growth model to WT failure data has allowed the author to uncover some important features of the WT failure data, as reliability trends of the WT subassemblies.

The knowledge of the mathematics, which forms the basis of this model, allows us to numerically generate failure events of a certain PLP population. If we assume that failures of such a population follow a PLP and we generate an array of data, we can check the validity and limits of the interpolation method illustrated in Chapter 5, effectively reverse engineering the results developed in previous chapter.

The need to simulate failure patterns has arisen in order to check the validity of the predictions from grouped data, for which neither reliability theory nor inferential methods are as well developed as they are for other types of collected data.

On the basis of the random data generated, a sensitivity analysis has been carried out, to study the variation of the model output to changes of the five degrees of freedom, namely; shape and scale parameter of the intensity function, number and length of the grouping periods and number of wind turbines in the population.

The simulation method can be summarised in the following basic steps:

1. Definition of the assumptions about the PLP population, including the number of WTs and the parameters of the intensity function.

2. Numerical generation of a failure data array for the population and aggregation of the data for the entire population of turbines.
3. Aggregation of the data for time intervals, of the chosen interval length, and over the entire population of WTs.
4. Interpolation of the data array with the PLP model described in Chapter 5
5. Comparison of the model results (calculated intensity function) with the original intensity function

The full cycle of production of simulated failure data, interpolation and comparison with the original values is illustrated by the flowchart of Fig. 7.1. For each of the flow chart blocks the variables involved in the simulation are shown.

Since the result of the interpolation depends on the absolute number of failures in the array of data, the analysis has been simplified by keeping the number of WTs constant. In the analysis the number of failures in the array generated has been modified by changing the scale parameter of the intensity function. However, increasing the scale parameter has an effect equivalent to increasing the number of WTs in the population and keeping the scale parameter constant.

The effect of increasing the population can be seen in section 7.3, where the method of generation of simulated values is presented. In this context only the the distribution parameters is kept constant and the number of items changed.

A major objective of the simulation was to verify the relation between the total number of failures in the grouping period and the “robustness” of the interpolation that is the ability of the model to produce consistent results. In those cases where the model did not prove robust determining how the model output changes for different grouping periods was also paramount. Indeed the investigation over the effect of the grouping period has been inspired by the most remarkable difference between the three failure data WSDK, WSD and LWK, with different grouping periods, which is the different aggregation of the data.

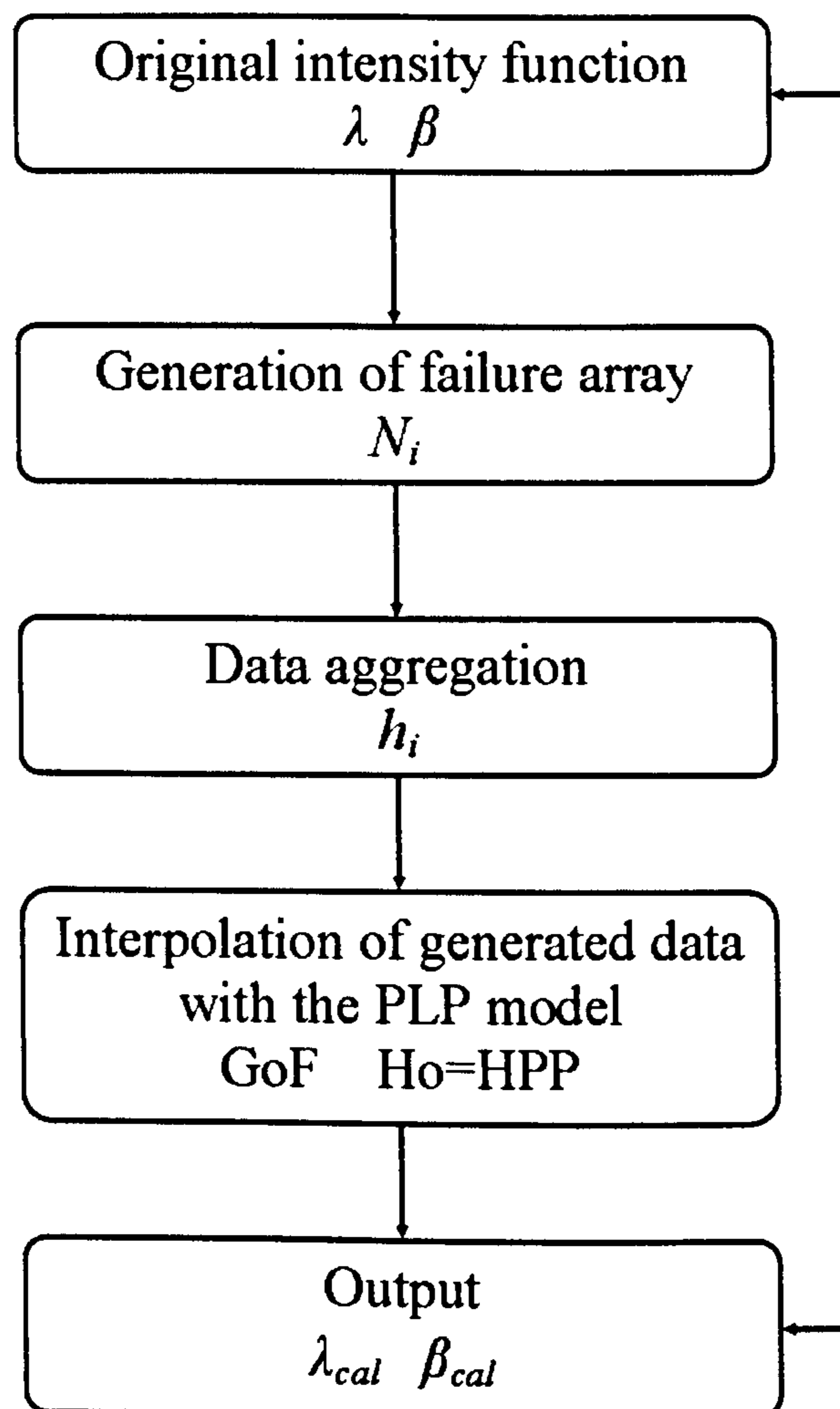


Figure 7.1: The representation of the simulation cycle

7.2 Generation of PLP random numbers

Simulation of failure data is based on the generation of a TTF (Time To Failure) starting from its distribution. Assuming that the item failures follow a PLP with intensity function given from the usual Weibull function of equation 3.19:

$$\lambda(t) = \rho \beta t^{\beta-1}$$

from the theory [42] we know that the distribution of TTF of the *first* failure $f_1(t_1)$ is:

$$f_1(t_1) = \lambda(t_1) \exp\left(-\int_0^{t_1} \lambda(u) du\right) \quad (7.1)$$

$$= \rho \beta t_1^{\beta-1} \exp\left(-\rho t_1^\beta\right) \quad (7.2)$$

A numerical method that generates random numbers from a certain distribution is the inverse *cdf* method [19]. This implies the inversion of the *cdf* and the consequent calculation of the values corresponding to a set of normal pseudo-random numbers in the range $[0, 1)$. The *cdf* is the integral of the probability density function and in this case we have:

$$\Lambda_1(t_1) = \int_{-\infty}^{+\infty} \lambda_1(t_1) = 1 - \exp\left(-\rho t_1^\beta\right) \quad (7.3)$$

Whose inversion gives:

$$t_1 = \theta \log\left(\frac{1}{1-y}\right)^{\frac{1}{\beta}} \quad (7.4)$$

where

$$\theta = \frac{1}{\lambda^{\frac{1}{\beta}}} \quad (7.5)$$

and y is the value of the random number to be obtained from the homogeneous distribution in $[0, 1)$, with any pseudo-random generator. The distribution of the TTF of the *ith* failure f_i conditioned to the occurrence of the last failure at time t_{i-1} is:

$$f_i(t|t_{i-1}) = \frac{\beta}{\theta^\beta} t^{\beta-1} \exp\left(-\int_{t_{i-1}}^{t_i} \frac{\beta}{\theta^\beta} u^{\beta-1} du\right) \quad (7.6)$$

and its integral (*cdf*) is:

$$\Lambda_1(t_i) = 1 - \exp\left(\frac{t_{i-1}^\beta - t_i^\beta}{\theta^\beta}\right) \quad (7.7)$$

then inverting:

$$t_i = \left(t_i^\beta - \theta^\beta \log(1 - y) \right)^{\frac{1}{\beta}} \quad (7.8)$$

with the same meaning for y .

Knowing the distribution of the first and all successive TTFs, again using the inverse *cdf* method, a matrix of values can be generated. The rows representing the failure number and the columns representing the number of wind turbine systems. The Table 7.1 represents an example of such a matrix, where the time to failure is expressed in years.

failure number	Wind Turbine System				
	1	2	3	4	...
...					
699	...				
700	0.9120	2.0500	0.0523	0.9530	...
701	0.9320	2.0681	0.0563	0.9830	...
702	...				
...	...				

Table 7.1: Matrix of the TTF of the simulated occurrences

The next step is to re-organize the matrix, discarding the events occurring beyond reasonable limits, for example the failures earlier than 0.005 hours and later than 10 years. It must be noted that in the case of the Weibull distribution for the intensity function, the curve of failures against *TTT* is asymptotic with *Y* axis, that is the probability of having a failure here, in the very first period, is extremely high. Consequently a large number of failures are likely to occur in the first period. At this point for every single period, whose length is decided at the beginning of the simulation and simulates the data grouping interval, all the failures occurring are counted and summed over the entire population of wind turbines, resulting in a data array similar to those shown in Figures 7.2 and 7.3 for six months and four months grouping, respectively.

The data arrays so generated can be analysed with the methods illustrated in the previous chapters of this thesis. In particular for each grouping period, the

semester	n	semester	n
1	33036	11	291
2	1953	12	229
3	1174	13	257
4	857	14	232
5	631	15	226
6	503	16	193
7	411	17	166
8	366	18	192
9	379	19	145
10	305	20	155

Table 7.2: Simulated number of failures: 200 WT, grouped by semester

quarter	n	quarter	n	quarter	n	quarter	n
1	30692	11	229	21	150	31	88
2	1992	12	263	22	139	32	77
3	1102	13	239	23	128	33	99
4	807	14	191	24	133	34	91
5	626	15	193	25	120	35	89
6	478	16	190	26	128	36	77
7	433	17	155	27	109	37	85
8	373	18	162	28	104	38	74
9	369	19	158	29	107	39	83
10	296	20	153	30	108	40	87

Table 7.3: Simulated number of failures: 200 WT, grouped by quarter

average failure rate can be worked out by applying Equation 4.1. The results of the generation of PLP simulated data are presented in the next paragraph.

7.3 Simulation Results

Figures 7.2 and 7.3 display the comparison between the intensity function chosen and the resulting average failure frequency of each grouping period of the simulated data for different population sizes, namely; 10, 50, 100, 200, 500 or 2000 WT, for both monthly and yearly aggregation of failure data and for the same intensity function. The goodness of the interpolation of the simulated data will be systematically evaluated below, but Figures 7.2 and 7.3 are shown here to give a visual impression. The original intensity function, shown in red, is better approximated for larger size populations of WTs but from the comparison of Figures 7.2 and 7.3 the beneficial effect of aggregating failures into longer grouping periods stands out. For both the figures the shape parameter is 0.7 and the scale parameter is chosen to obtain a failure intensity in line with the real data.

It has to be noted that the time scale here is in calendar time, but without conflicting with the previous section 5.10 since the number of WTs is, here constant throughout the entire period length. In this case the time axis could be scaled to TTT, by multiplying by the number of WT.

It can be noted, as a main result, that there is a very strong relationship between the number of WTs in the population and the minimum length of grouping period to give satisfactory accuracy in the determination of the underlying intensity function. Only a large population permits a short grouping period or, alternatively, a population with a high number of failures. This would be especially true if the interpolation was carried with the least square method for which the variability of data is not beneficial. The least square method in fact minimises the distance between the interpolating curve and the average failure frequency of each time cell. Once the simulated failure data record has been produced it has been interpolated with the method implemented on real data.

To test the MLE method used for the implementation of the PLP on the real data, the simulated data have been interpolated with the same algorithm used in Chapter 5. The idea was to compare the resulting interpolated intensity function with the original intensity function, verifying how the former changes to variations of parameters of the latter. The effect of different grouping period lengths, for the

December 6, 2008

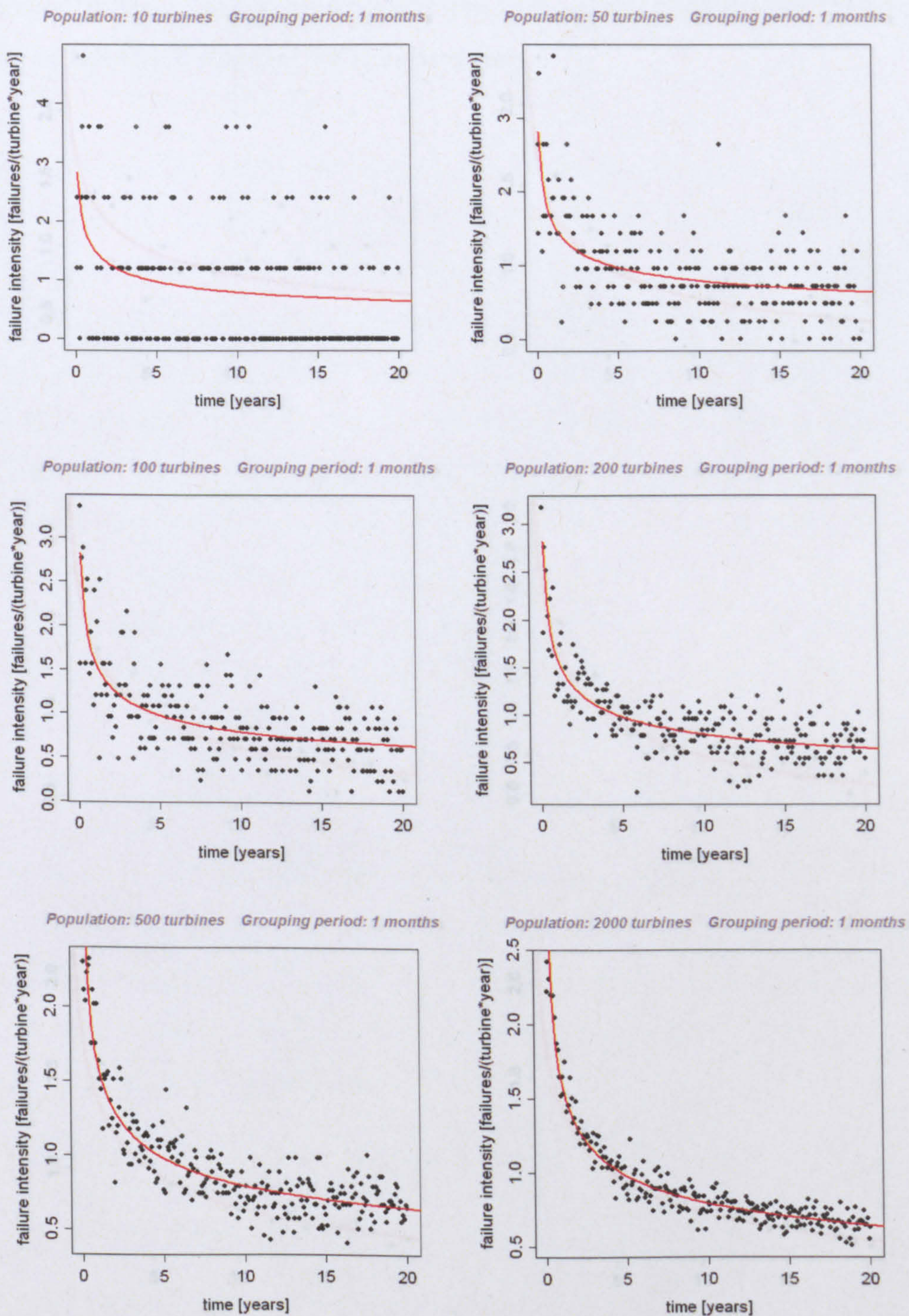


Figure 7.2: From left to right and from top to bottom: simulate failure intensity time curve for monthly grouped data for populations of 10, 50, 100, 200, 500 or 2000 WTs. The original intensity function for the population is shown in red.

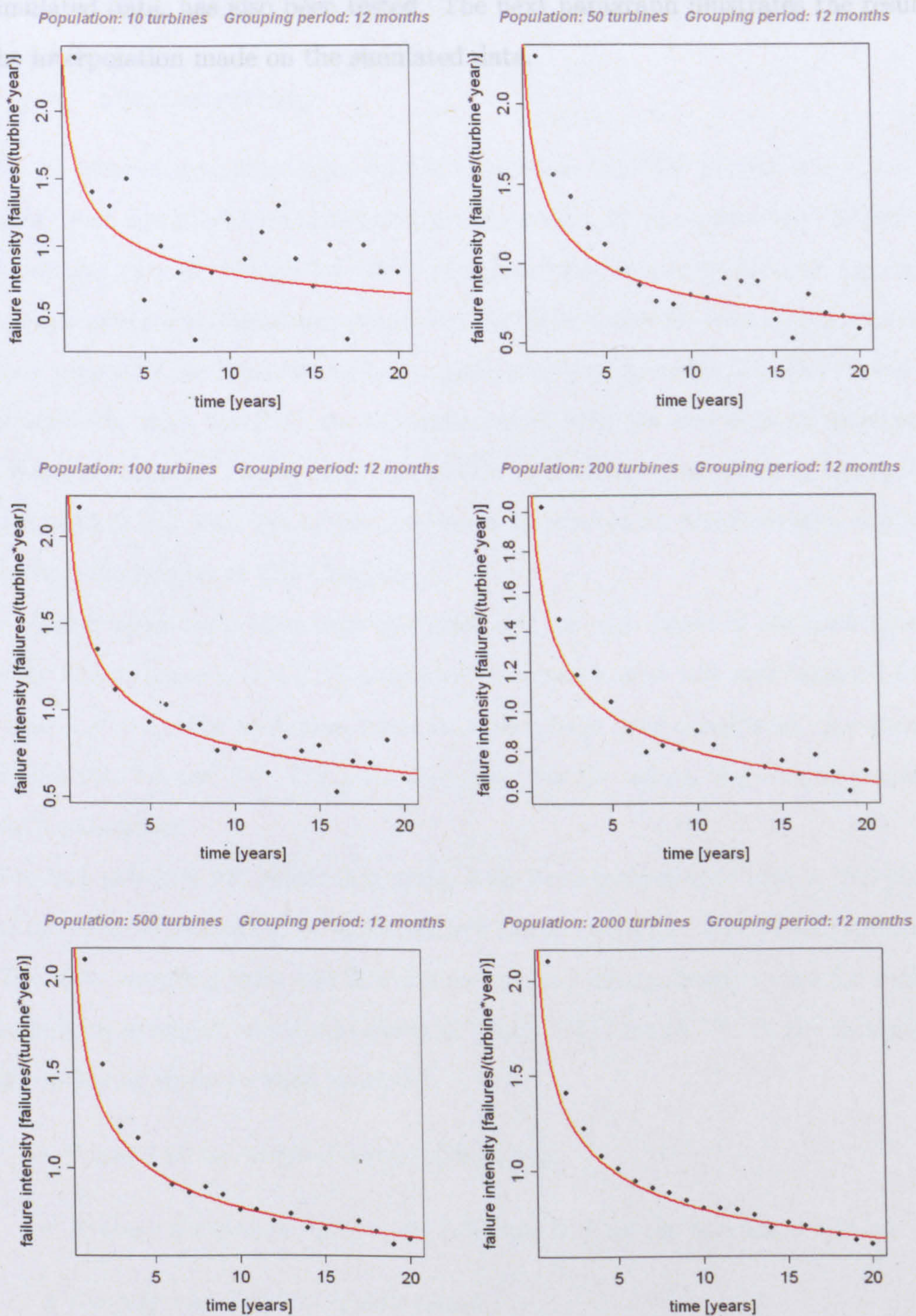


Figure 7.3: From left to right and from top to bottom: resulting failure intensity time curve of yearly grouped data for populations of 10, 50, 100, 200, 500 or 2000 WTs. The original intensity function for the population is shown in red

simulated data, has also been tested. The next paragraph illustrates the results of the interpolation made on the simulated data.

7.4 PLP Model's Sensitivity Analysis

7.4.1 Introduction

On the basis of the failure data generated as above the PLP growth model has been tested with the procedure illustrated in this section. It was important to verify how the model output changes for different values of scale parameter and aggregation interval, given a certain shape parameter of the intensity function. Thus, the failure data generated as illustrated above, from a chosen intensity function, have been interpolated with the PLP model implemented with the real data as illustrated in Chapters 5 and 6. The cycle of production of simulated failure data, interpolation and comparison with the original values is illustrated by the flowchart of Fig. 7.1 in the introduction of this Chapter.

Three main cases have been analysed, one for each phase of the bathtub curve; early failure (case 1, $\beta = 0.7$), deterioration (case 2, $\beta = 1.8$) and constant failures (case 3, $\beta = 1$). For each case, some sub-cases have been considered, as reported in Tables 7.4, 7.5 and 7.6. The sub-cases differ for the values of grouping period and scale parameter.

For each sub-case 200 simulation cycles have been generated so that a “full picture” of the possible results can be achieved, in a fashion used for Monte-Carlo simulations. The data resulting from the 200 simulation and interpolation cycles for each case have been averaged and summarised in Tables 7.4, 7.5 and 7.6. In the results tables the following data are then reported:

- β and θ of the original intensity function.
- Average number of failures in each time cell for the simulated failures.
- Average and variance of calculated β .
- Time interval of the simulated values, expressed in months.
- Occurrence of GoF acceptance expressed in percent.
- Occurrence of $H_0 = \text{HPP}$ acceptance expressed in percent.

Average and variance of β , as well as occurrence of acceptances of the two tests are calculated over the 200 values obtained for each sub-case.

The calculated average and variance of the calculated λ are not reported for the sake of brevity, as the parameter β is the only useful trend indicator. The number of WTs in the population and the length of period are the same for all the four cases were equal to 50 WT and 12 years respectively. As reported in the introduction of this chapter the the number of failures has been modulated by modifying the scale parameter. For each of the cases a picture will show an example of the interpola-

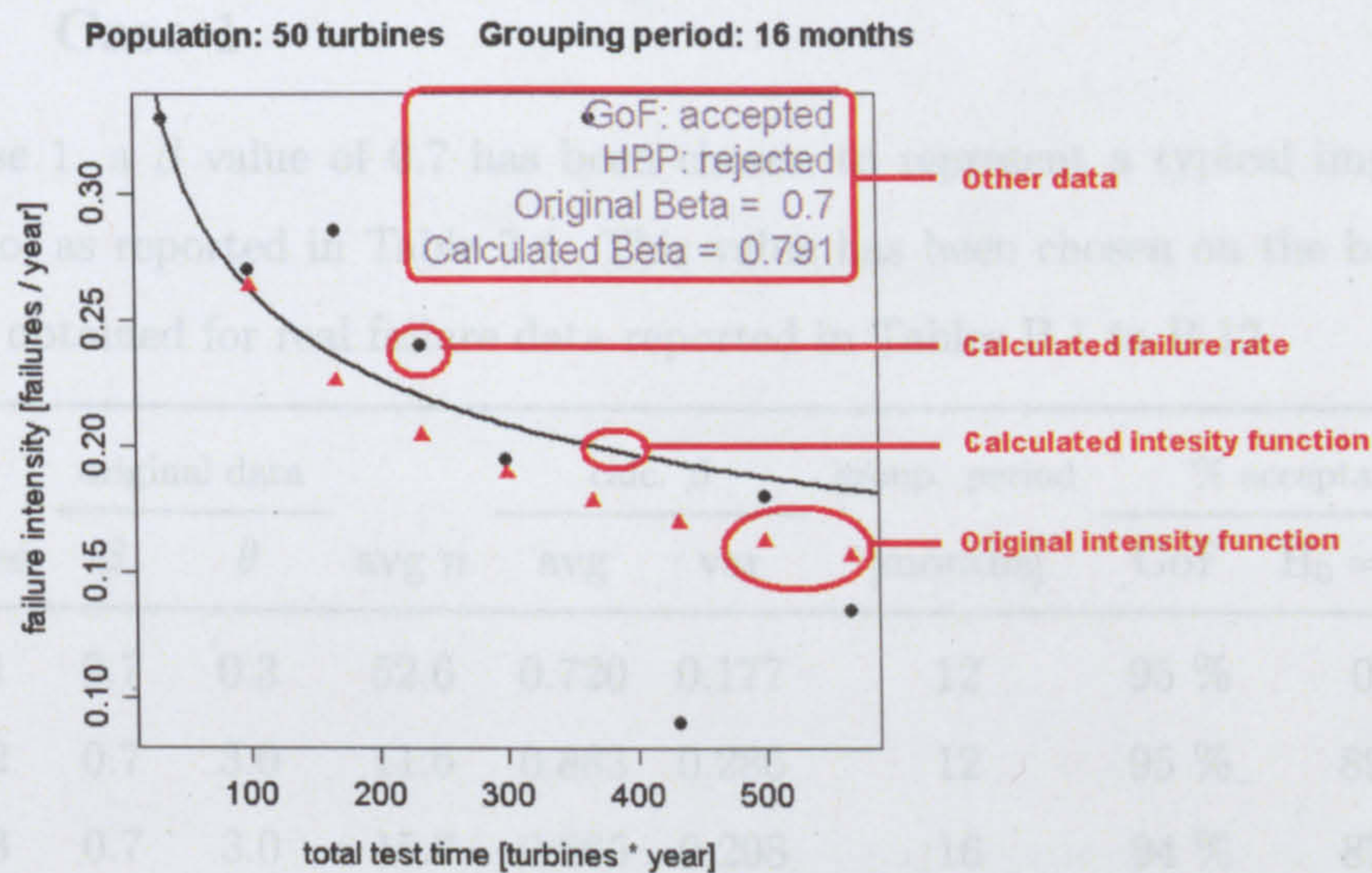


Figure 7.4: An example of the data reported on the figures below. The failure rate refers to a single WT, $[\text{failure} / \text{year}] = [\text{failure} / \text{WT} / \text{year}]$

In these examples various elements characterising the example considered are reported (see Fig. 7.4), namely:

- The original underlying intensity function (red triangles)
- The average failure frequency of each of the grouping period (black dots)
- The resulting interpolated intensity function (continuous black line)
- The GoF test result (top right corner first line)

- The original PLP intensity function shape parameter (top right corner third line)
- The calculated PLP intensity function shape parameter (top right corner fourth line)

It must be noted that in the results refer to a single WT so the units used for the intensity function [failure / year] shall be generalised and read as [failure / WT / year].

7.4.2 Case 1

For case 1, a β value of 0.7 has been chosen to represent a typical improvement scenario, as reported in Table 7.4. This value has been chosen on the basis of the results obtained for real failure data reported in Tables B.1 to B.12.

case	original data			calc. β		group. period [months]	% acceptance	
	β	θ	avg n	avg	var		GoF	$H_0 = \text{HPP}$
1.1	0.7	0.3	52.6	0.720	0.177	12	95 %	0 %
1.2	0.7	3.0	11.6	0.883	0.286	12	95 %	89 %
1.3	0.7	3.0	15.2	0.885	0.298	16	94 %	87 %
1.4	0.7	3.0	20.3	0.862	0.305	24	96 %	79 %
1.5	0.7	3.0	31.7	0.847	0.322	48	91 %	69 %
1.6	0.7	0.3	109	0.719	0.178	24	91 %	0 %

Table 7.4: Results for the first cycle of simulations, $\beta = 0.7$

Fig. 7.5 shows a typical successful interpolation of failure data (case 1.1). The underlying or original intensity function is represented by the red triangles, while the calculated one is represented by black continuous line. The black dots are the simulated average failure frequency in each time cell. The curves are plotted in terms of TTT , and the cumulative calendar time can be worked out by dividing the abscissa by the number of WT in the population, which is fixed at 50 units.

For case 1.1, the original intensity function produces an array of data similar to the LWK data; with a length of period of 12 years and yearly grouping. In this case

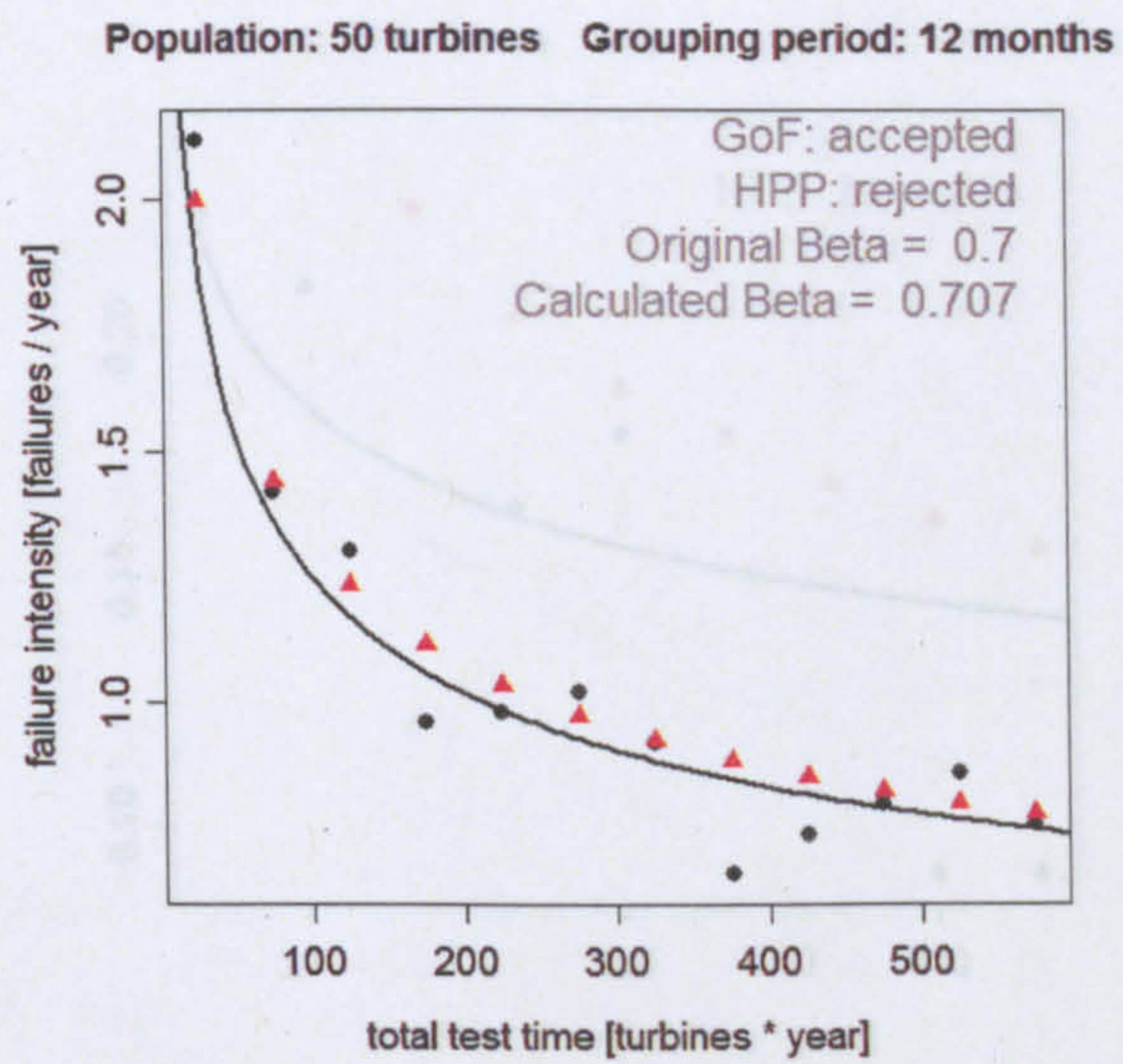


Figure 7.5: Simulation case 1.1

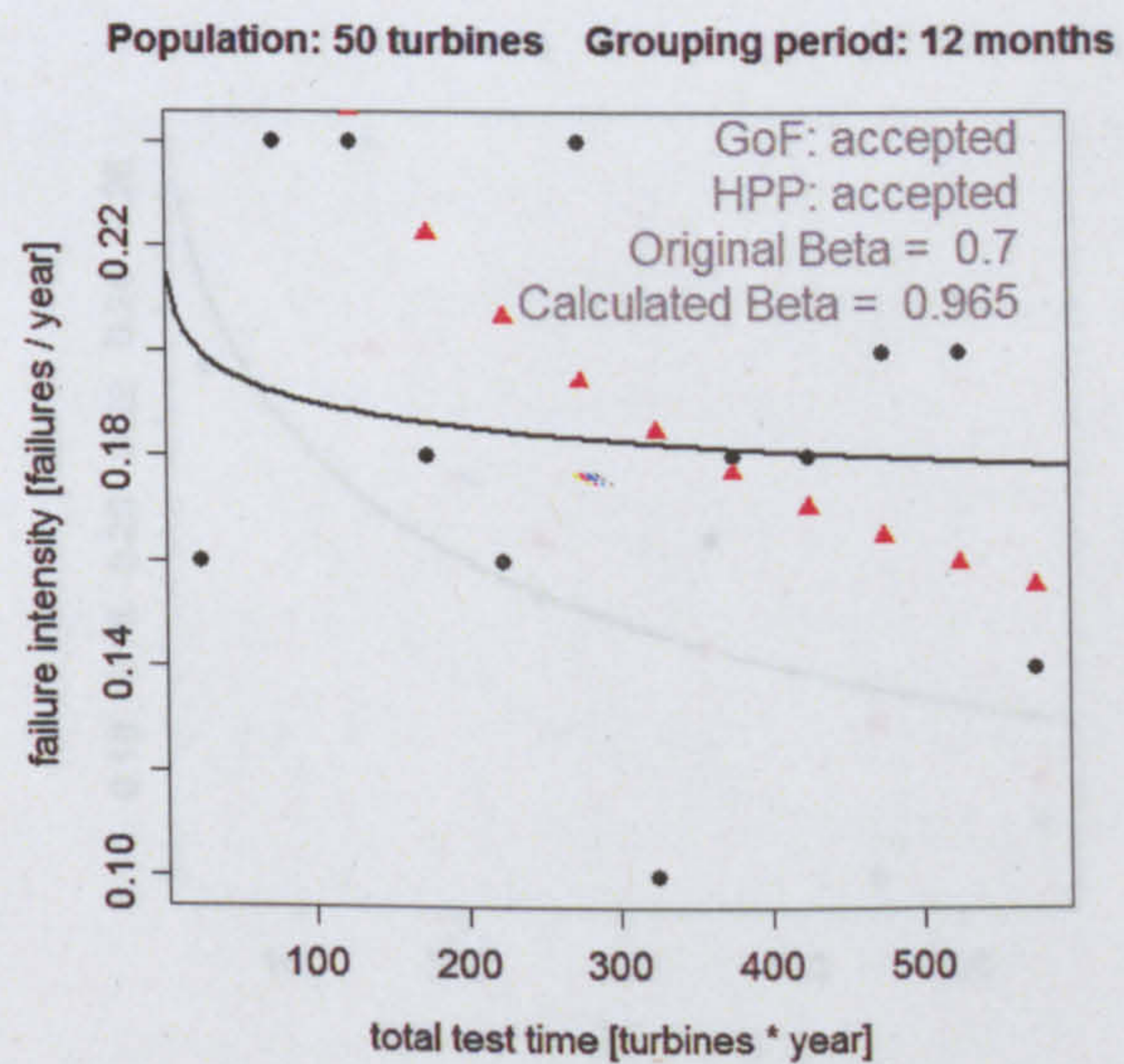


Figure 7.6: Simulation case 1.2

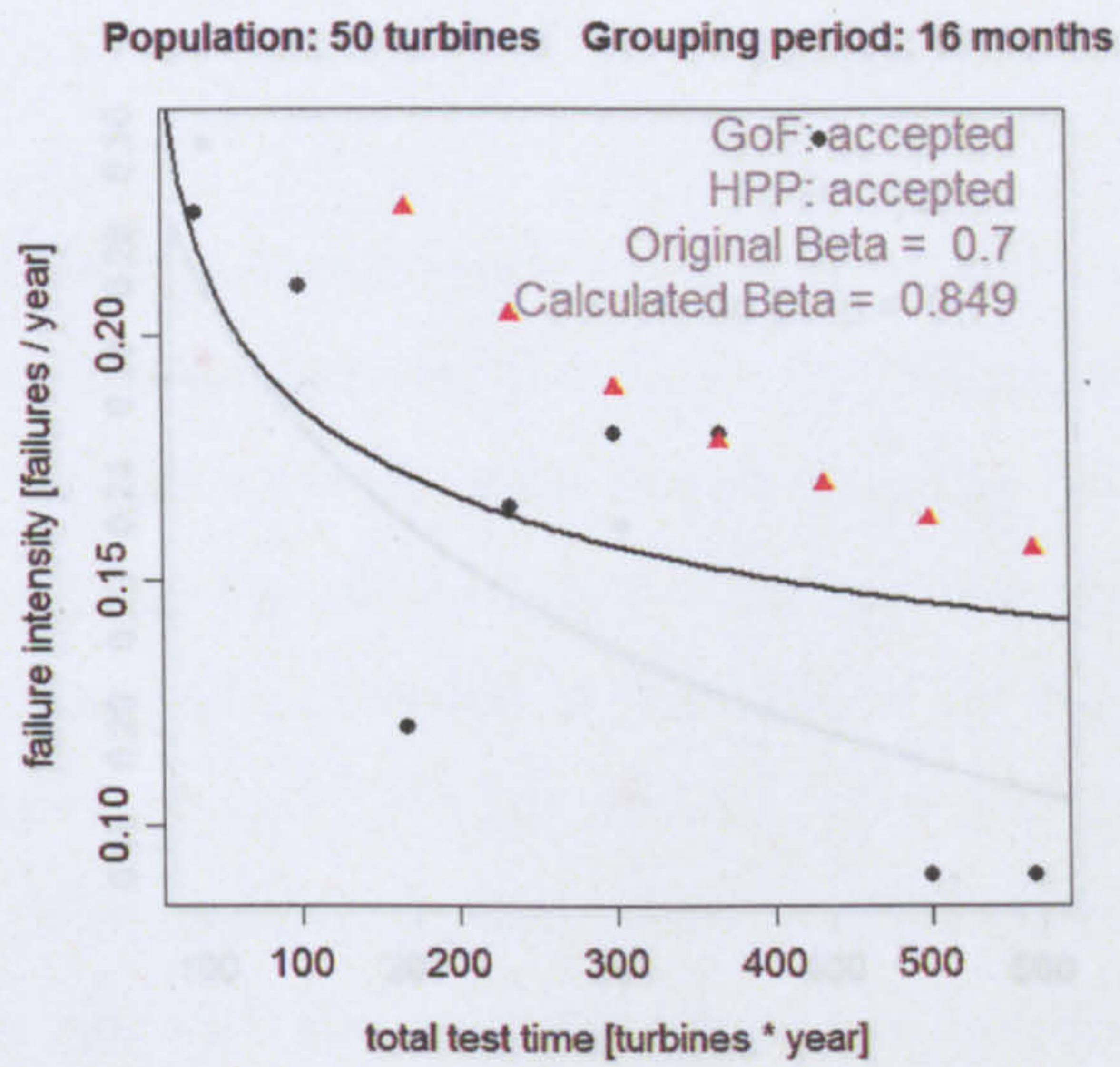


Figure 7.7: Simulation case 1.3

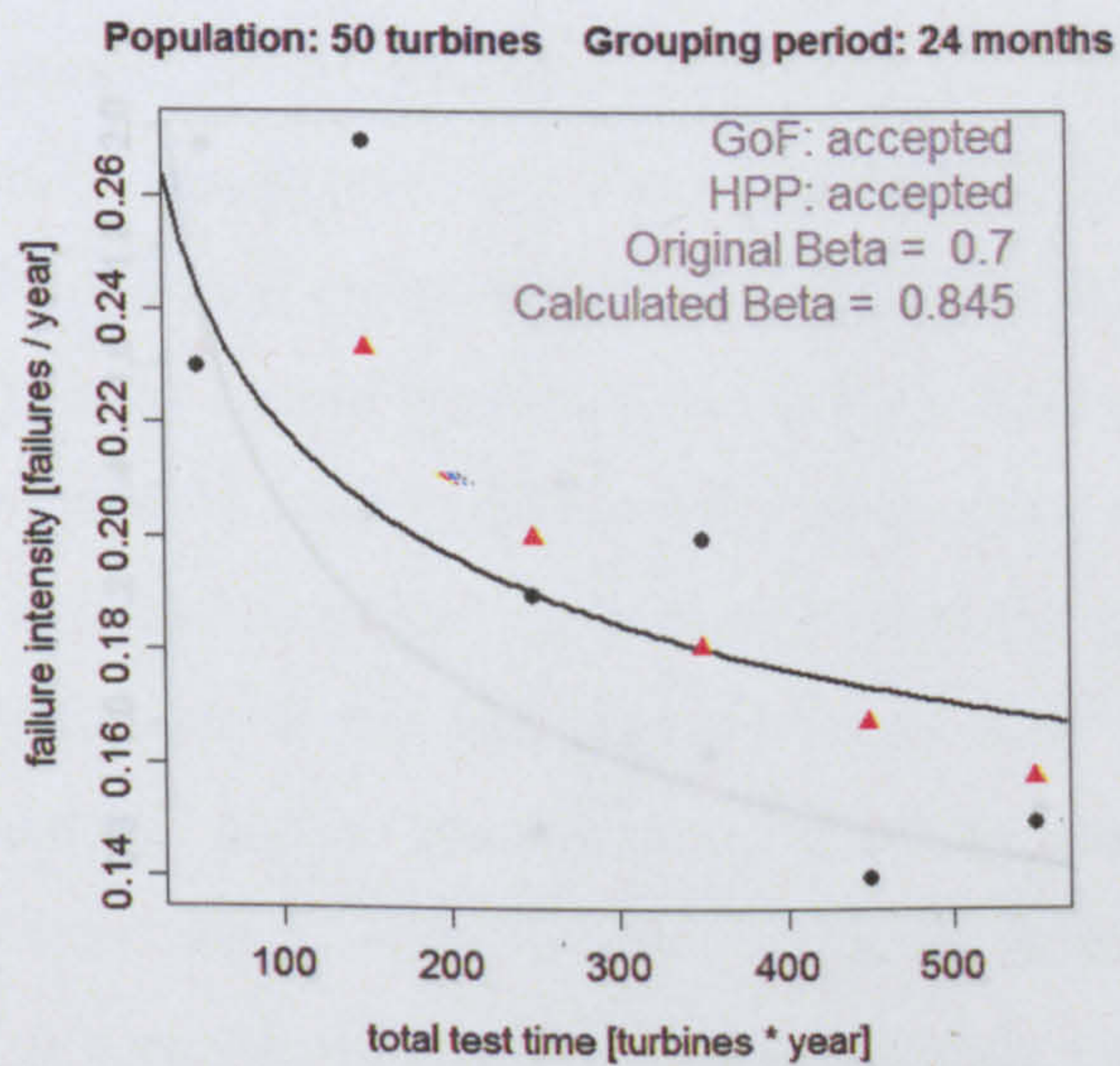


Figure 7.8: Simulation case 1.4

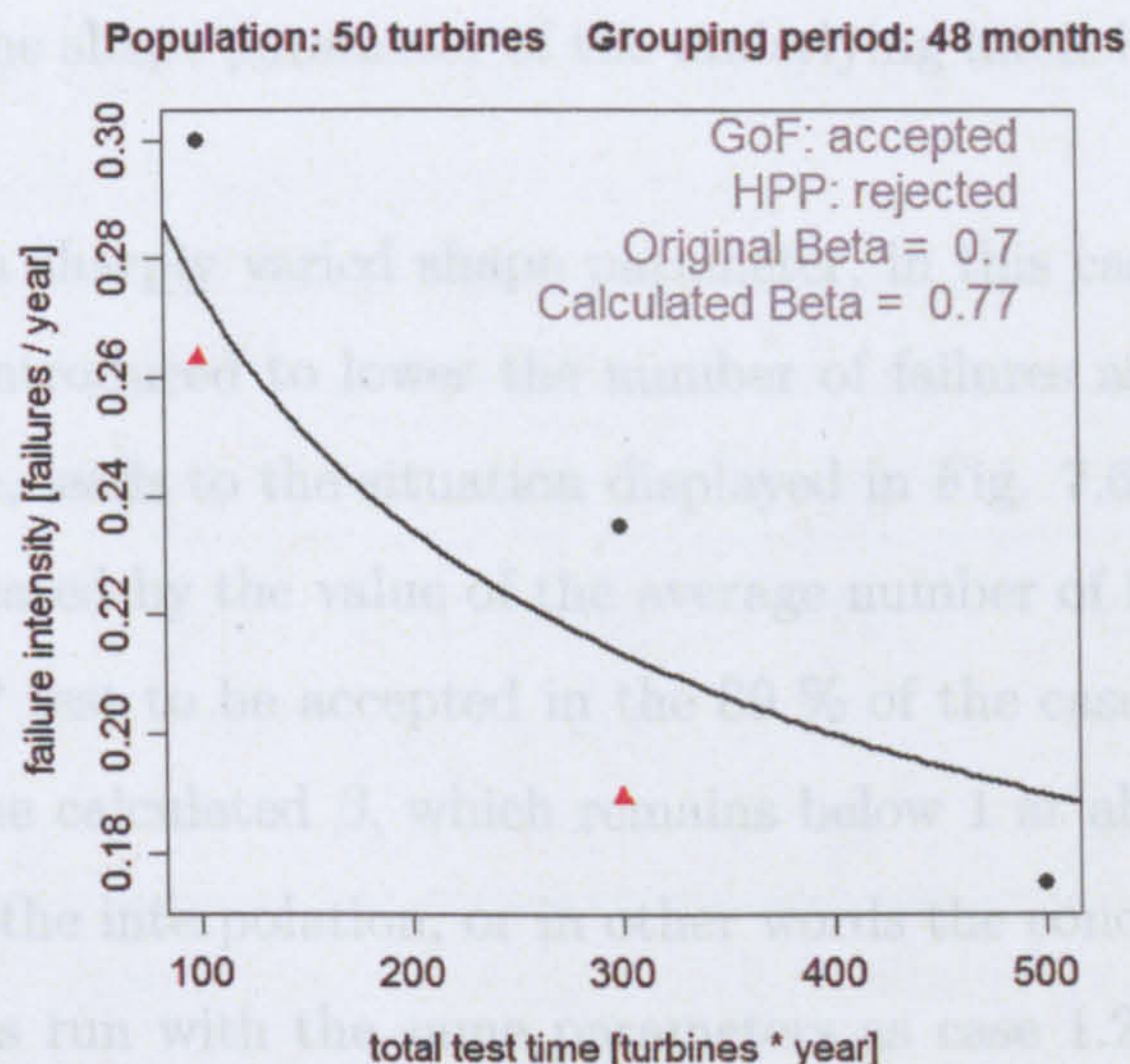


Figure 7.9: Simulation case 1.5

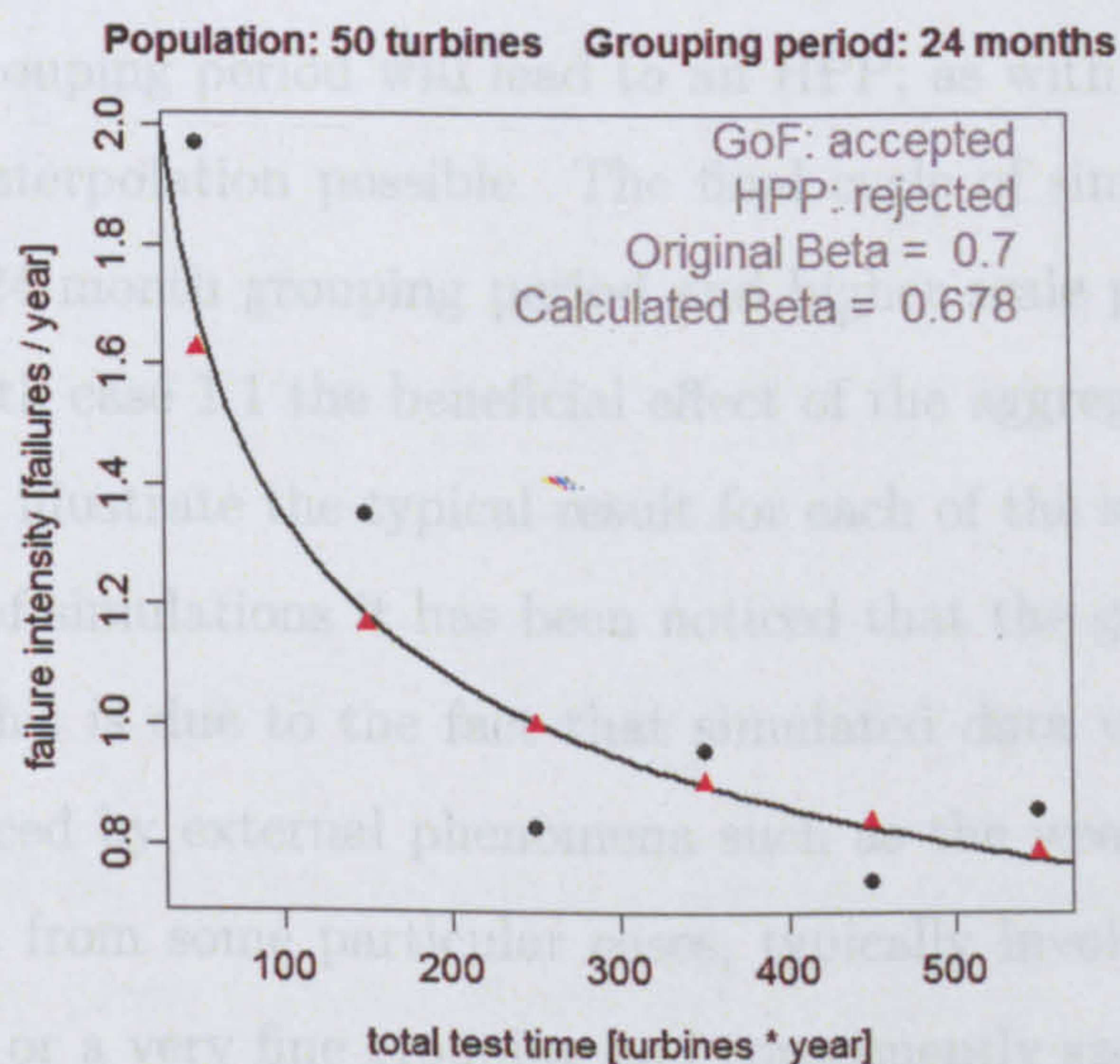


Figure 7.10: Simulation case 1.6

the two statistical tests lead, in the vast majority of the cases, to the adoption of the conclusion "PLP early failure", with the beta indicated by the interpolation, which is very similar to the shape parameter of the underlying intensity function (average 0.72).

For case 1.2 with a sharply varied shape parameter, in this case a higher θ resulting in a lower λ , introduced to lower the number of failures and consequently the interpolating curve, leads to the situation displayed in Fig. 7.6. The lower number of failures, as indicated by the value of the average number of failures of Table 7.4, results in the HPP test to be accepted in the 89 % of the cases. In this situation, the low value of the calculated β , which remains below 1 at about 0.85, leads to a non acceptance of the interpolation, or in other words the conclusion "NOT PLP". If the simulation is run with the same parameters as case 1.2, but modifying the aggregation period, now of 16, 24 and 48 months respectively, results in an improvement of the HPP hypothesis rejection, which is now accepted at a lower percentage in cases 1.3, 1.4 and 1.5, corresponding to a higher probability of accepting the "early failures" case.

The shape parameter β is close to the original value throughout these cases but its variance widens with the length of the aggregation interval. Indeed an over-reduction of the grouping period will lead to an HPP; as with one single time cell HPP is the only interpolation possible. The final cycle of simulations of case 1.6 was made with a 24 month grouping period and higher scale parameter (lower θ). Comparing this with case 1.1 the beneficial effect of the aggregation appears clear. Figures 7.5 to 7.10 illustrate the typical result for each of the sub-case considered.

For a number of simulations it has been noticed that the goodness of fit test is rarely rejected. This is due to the fact that simulated data was not subjected to the volatility induced by external phenomena such as the weather, unlike the real data. Thus, apart from some particular cases, typically involving either very few number of failures or a very fine grouping and consequently sparse data arrays, the interpolation of PLP data actually leads to a PLP result.

7.4.3 Case 2

A similar analysis has been carried out varying the value of the shape parameter of the original function, to $\beta = 1.8$, a typical situation for systems that are deteriorating, as shown in Table 7.5 and Figures 7.11 to 7.13.

case	original data		avg n	calc. β		group. period [months]	% acceptance	
	β	θ		avg	var		GoF	$H_0 = \text{HPP}$
2.1	1.8	3.5	35.3	1.50	0.265	12	27 %	0 %
2.2	1.8	7.0	13.3	1.19	0.298	12	79 %	54 %
2.3	1.8	7.0	25.2	1.21	0.305	24	78 %	49 %

Table 7.5: Results for the second cycle of simulations, $\beta = 1.8$

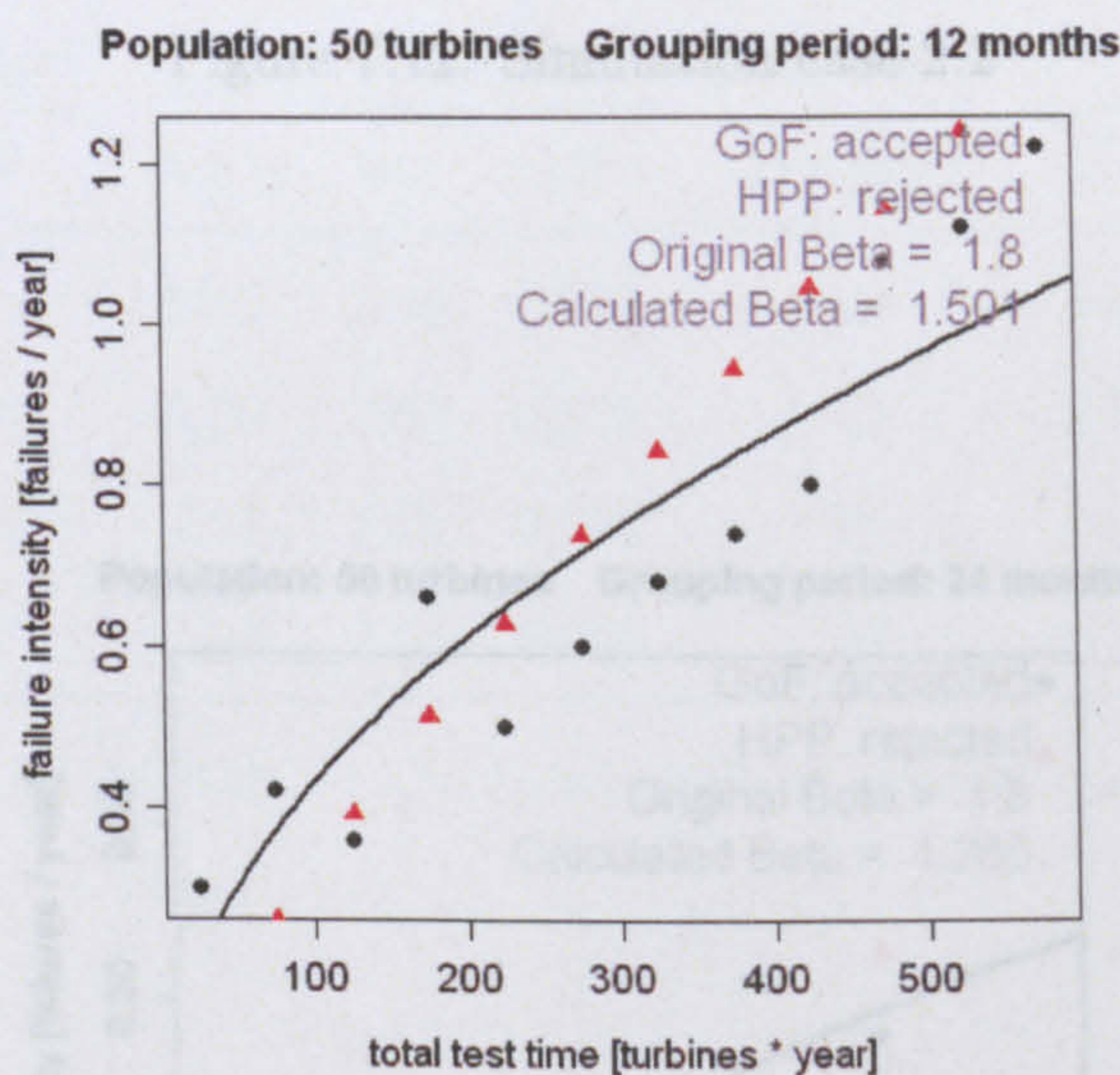


Figure 7.11: Simulation case 2.1

As for the real data the determination of the shape parameter is more difficult for the deterioration phase and is characterised by a greater volatility. The results for this case have to be considered with a larger margin of uncertainty. However the three typical cases of Figure 7.11 to 7.13 show again the beneficial effect of a larger aggregation of data. Similarly to Case 1 $\beta = 0.7$, it appears that the robustness of the model is conditioned by a minimum number of failures per grouping period of

roughly 20.

7.4.4 Case 3

Population: 50 turbines Grouping period: 12 months

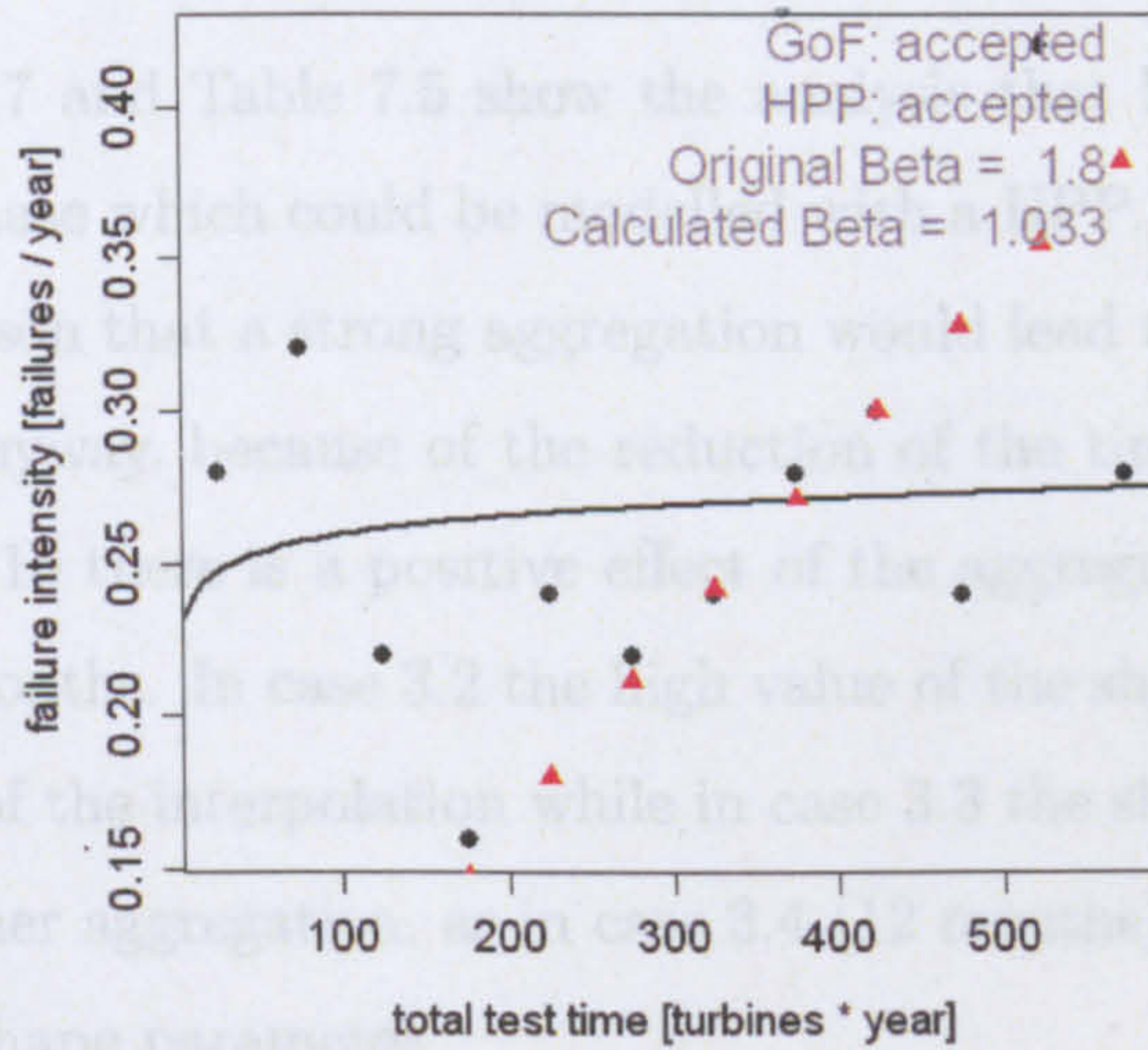


Figure 7.12: Simulation case 2.2

case	original data		interpolated data				% acceptance	
	β	θ	avg n	avg	var	[months]	GoF	H ₀ - HPP
3.1	1.0	1.0	50.7	1.00	0.214	12	94 %	94 %
3.2	1.0	10	5.00	1.02	0.378	12	97 %	95 %
3.3	1.0	10	7.11	1.01	0.385	16	91 %	92 %
3.4	1.0	30	11.2	1.01	0.405	24	97 %	96 %

Population: 50 turbines Grouping period: 24 months

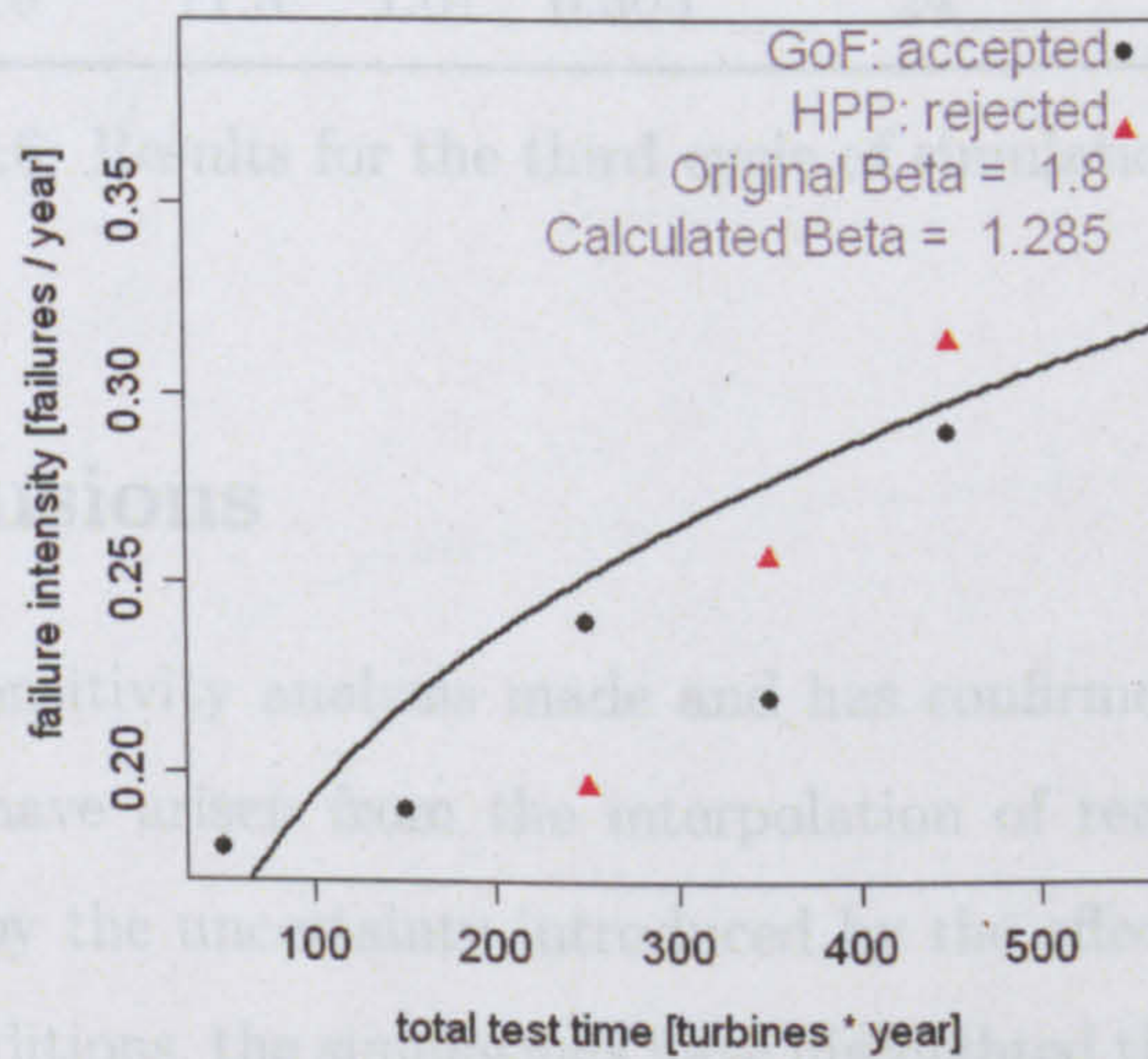


Figure 7.13: Simulation case 2.3

7.5 Conclusions

The simulation sensitivity analysis made in this paper has confirmed some features of the PLP model that have been observed in the interpolation of real data. Although real data are affected by the unmodelled effect of weather and other environmental conditions, the simulation results showed the following behaviours:

- The average number of failures per turbine per year, is important to produce a solid interpolation of the data.

roughly 20.

7.4.4 Case 3

Figures 7.14 to 7.17 and Table 7.5 show the analysis that has been made for the intrinsic failures phase which could be modelled with a HPP. The HPP case is more delicate for the reason that a strong aggregation would lead to an acceptance of the HPP hypothesis anyway, because of the reduction of the time cells. But as shown in Fig. 7.15 and 7.16 there is a positive effect of the aggregation, in this case from 12 months to 16 months. In case 3.2 the high value of the shape parameter leads to a non-acceptance of the interpolation while in case 3.3 the shape parameter is close to 1 again. A further aggregation, as in case 3.4 (12 months) leads to a larger error in the calculated shape parameter.

case	original data		avg n	calc. β		group. period [months]	% acceptance	
	β	θ		avg	var		GoF	$H_0 = \text{HPP}$
3.1	1.0	1.0	50.7	1.00	0.214	12	94 %	94 %
3.2	1.0	10	5.00	1.02	0.378	12	97 %	95 %
3.3	1.0	10	7.11	1.01	0.385	16	91 %	92 %
3.4	1.0	10	11.3	1.01	0.305	24	97 %	95 %

Table 7.6: Results for the third cycle of simulations, $\beta = 1.0$

7.5 Conclusions

The simulations sensitivity analysis made and has confirmed some features of the PLP model that have arisen from the interpolation of real data. Although real data are affected by the uncertainty introduced by the effect of weather and other environmental conditions, the simulations have highlighted the following behaviours:

- The average number of failures in each grouping period, is important to produce a solid interpolation of the data.

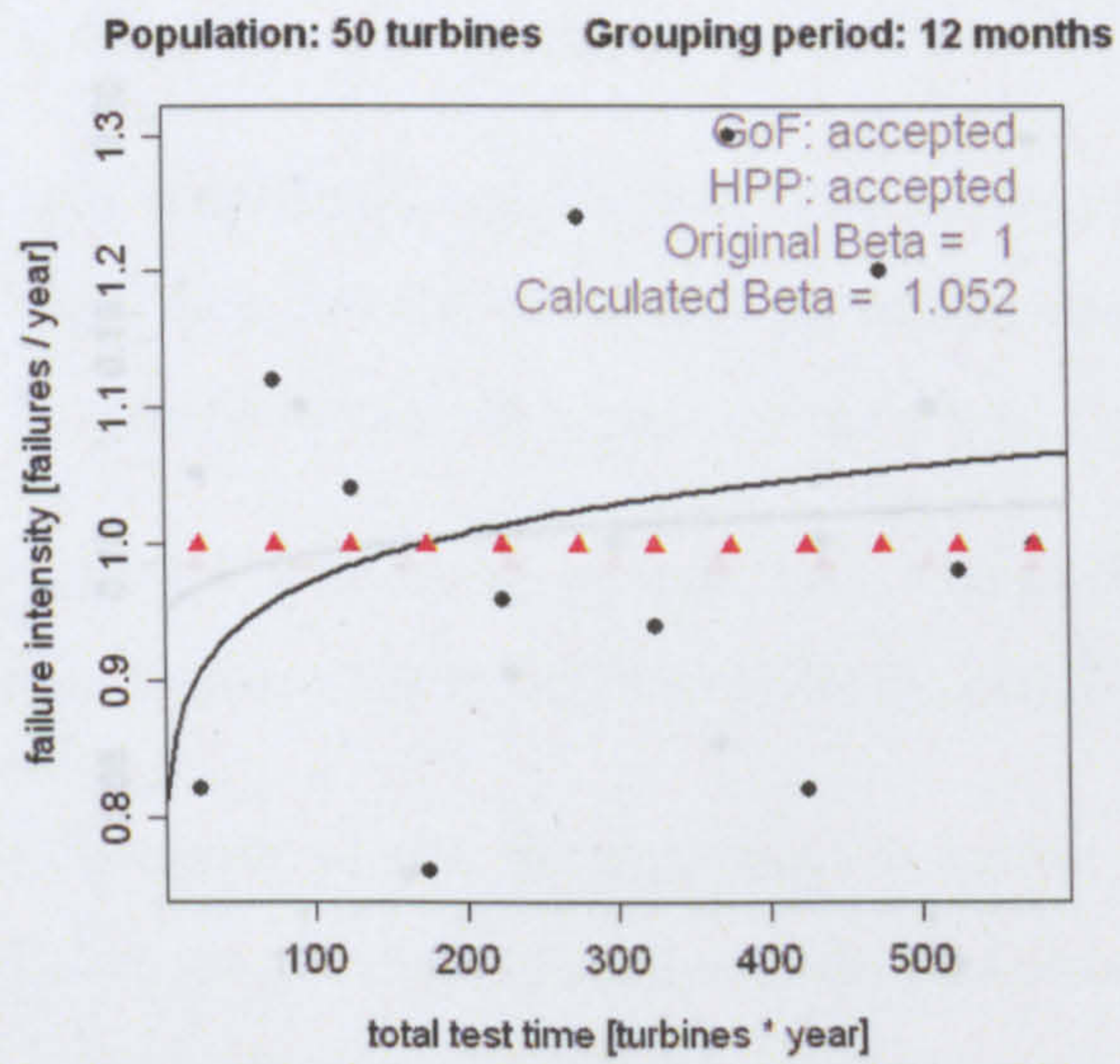


Figure 7.14: Simulation case 3.1

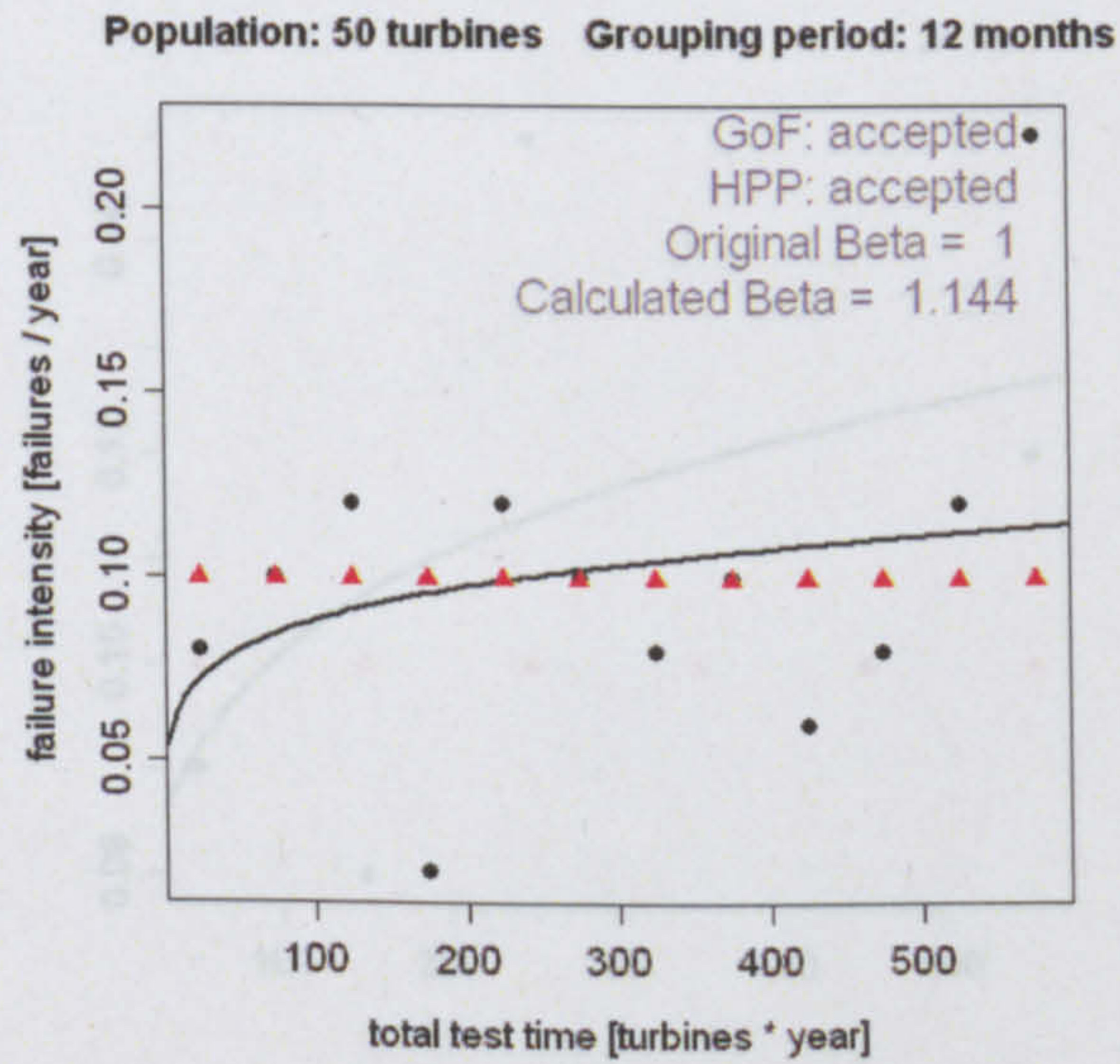


Figure 7.15: Simulation case 3.1

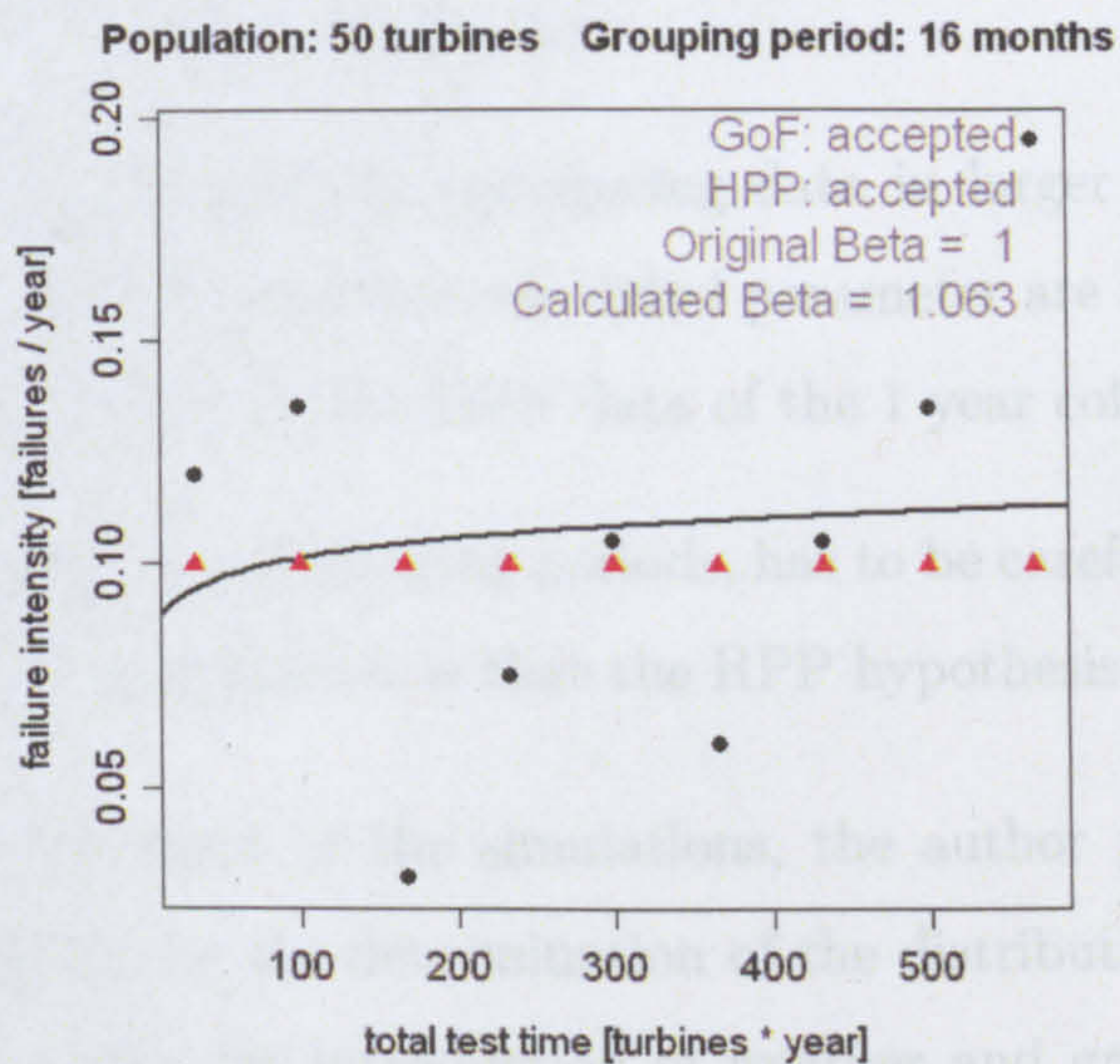


Figure 7.16: Simulation case 3.1

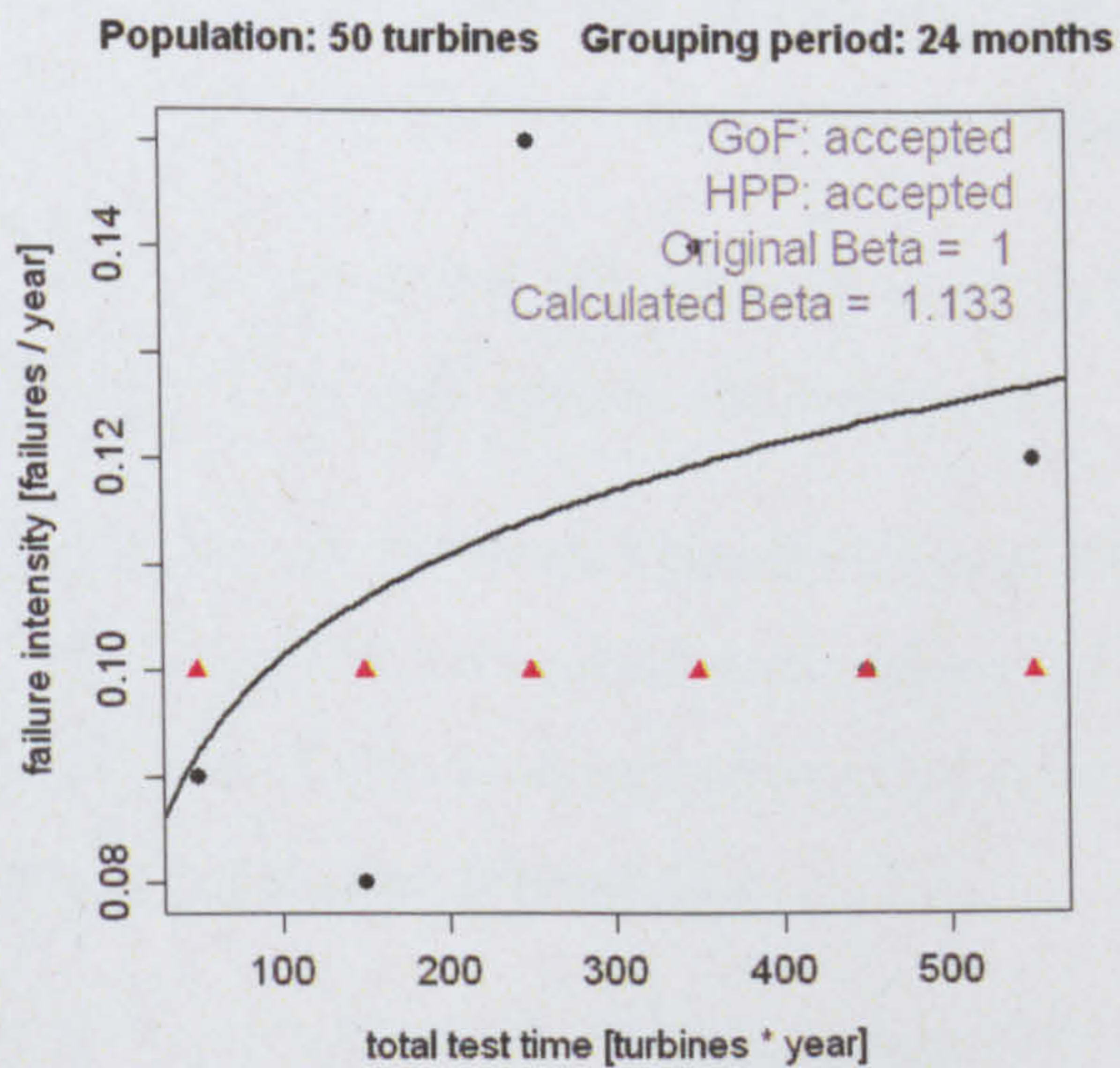


Figure 7.17: Simulation case 3.1

- Differently from the real life case, very large simulated data set are always interpolated. This is because simulated data are not affected by random environmental effects such as the weather.
- For all the cases considered, aggregating data in larger periods has generically a beneficial effect and the calculated parameter are more accurate. This emphasises the benefit in the LWK data of the 1 year collection period.
- The further reduction of grouping periods, has to be carefully considered. The results of a large aggregation is that the HPP hypothesis is always accepted.

As a future improvement of the simulations, the author proposes a complete Monte Carlo simulation for the determination of the distribution of the calculated parameters β and θ with the introduction of weather and grid effects. Once the failure frequency of the various subassemblies has been completely understood, the effect of the disturbance of weather and other environmental effects in the simulated failure data could be a further step for the prediction and understanding of the “intrinsic” reliability of the subassemblies.

Chapter 8

Conclusions

8.1 Introduction

The thesis has illustrated the analysis carried out on failure data from more than 6000 wind turbines, from three different surveys, in a period spanning over ten years. Despite some deficiencies of the data considered, the only publicly accessible data currently available, the results achieved by implementing the different analytical methods described above, are illuminating.

The research effort that has been made has proven valuable for various aspects characterising the collection and analysis of wind turbines failure data, namely:

- The identification of the perceived reliability of wind turbines given the lack of previous rigorous analysis and specific reliability data.
- The necessity of a standard, taxonomic classification of WT parts, subassemblies and failure modes, to be recognized and adopted at international level. As well as the definition of standard procedures and methods for failure data collection, storage, analysis and presentation.
- The “crystallization” of the knowledge about current WTs reliability, from the data available and the determination of the weakest subassemblies arising from the calculation of average failure frequency of large population of turbines.
- The importance of considering and analysing possible reliability trends that

can characterise the long term reliability of wind turbines to validate or discard the hypothesis of constant failures.

- The comparison between WT concepts, for the selection of the best WT architecture in view of the forthcoming mass installation offshore.
- The importance of testing WT parts, whenever economically feasible, in order to reduce the effect of infant mortality, as for the converters, see Appendix A.

The conclusions, illustrated in this final chapter, are organised, for the sake of clarity, in four main topics; data, subassemblies, WT concepts and, finally, future work, where some suggestion for further extension of models and analysis methods are provided.

8.2 WT Reliability Data

The data considered have been sufficient to highlight some WT's reliability features as reported below. The aggregation of data in larger grouped intervals, at first considered a disadvantage, has turned out to be beneficial. Larger grouping periods, in fact, overcome the noise induced by random external phenomena as grid instability or weather, which overlap the "intrinsic" reliability of the systems, due to average working conditions and/or reliability growth.

The time aggregation is linked to the population of turbines considered; thus, a yearly aggregation of failure data for a population of 50 WTs can roughly be considered sufficient and suitable for analysis using the methods considered above. For the most reliable subassemblies a further aggregation may be necessary because of the low number of failures. An acceptable failure record requires a number of failures in each grouping period in the order of 5 to 20, as simulations have revealed.

A certain periodicity, noted in the WSDK and WSD failure data, is ascribed to weather. The correlation of WT's failure data with the latter is evident and proven by a specific study, although further study, is required to formalise the correlation.

The question of the data "quality" is crucial for an accurate analysis. As a future recommendation it is suggested that to improve both collection and categorization

of data with a more rigid standardization of the terminology, adding at the same time further information about failure modes or components affected by the failure. Information about external conditions at the moment of the failure, as wind speed or grid perturbations, is also desirable.

The segregation of failure data by WT model has been shown to be valuable and allows the comparison of the different technologies, as the analysis of LWK survey has shown. WT technical specification, location and age are data that would also improve and facilitate the reliability analyst's work.

In the specific case of the three surveys considered there is consistency between the failure frequency of the various subassemblies of the two German population, WSD and LWK, while WSDK shows a higher reliability with a slightly different distribution among the subassemblies. Furthermore, while the two WS populations present a downward trend throughout the recording period, which is less clear in WSDK, LWK is slightly increasing. This is associated with the fact that the LWK population of WTs is relatively constant with an increasing average age. Conversely WSD refers to a large population of German WTs continuously being updated with the addition of new, more modern and larger WTs whose failure frequency is higher but decreasing in a more rapid way. Using the terminology adopted by the bathtub curve model, WSD WTs are in the early failure phase, WSDK WTs are in the constant failure phase and LWK WTs are approaching the wear out phase. LWK WTs population is in fact constituted, in large part, by very small wind turbines that are not considered further in the analysis.

When put in a historical context the reliability of WTs reveals the progress made in the last years. The overall WT reliability has overtaken the reliability of conventional generation technology such as diesel generation sets and approaches the reliability of CCGT. The reliability of steam generation is, however, still much higher. Nevertheless, the maintenance to which steam generation units are subjected is very high, as is revealed by higher values of the overall availability.

8.3 WT Subassemblies

Subassemblies is the name used in this thesis for the groups of WT components used for the classification of failure data. From the analysis of the overall average failure rate of the three surveys WSD, WSDK and LWK the three subassemblies with the highest failure frequency are, in descending order:

1. Electrical system.
2. Rotor or blades.
3. Electrical control (converter and electronics).

Other electromechanical subassemblies follow this group

4. Yaw system.
5. Generator.
6. Hydraulics.
7. Gearbox.

The result is striking and contrary to the perceived idea from the survey, that considers gearboxes as the least reliable subassembly. This does not alter the huge importance of the gearboxes contribution to the operating cost of WTs, given the severity of any failure occurring to the gearbox, well represented by the histogram of hours lost per failure.

Electrical system and electrical control stand out as the most problematic subassemblies. To improve the reliability of wind turbines designers will have to focus on the two electrical related subassemblies, the Electrical System and the Electrical Control.

Mechanical and electro-mechanical subassemblies, such as gearbox and generator, already show a reliability comparable with that of similar subassemblies installed in other industrial environments. Gearboxes in particular appear to be a well understood or “mature” technology, at least the gearbox mounted in small and medium

sized WTs but this may change for larger multi-megawatt WTs.

The ways to improve the electrical system of a WT can be revealed with the analysis of the failure modes. The effects of the grid, leading to non-catastrophic faults, eventually recorded as failures, constitutes an important part of the problem. Furthermore it is known that traditionally the electric industry focuses on performance testing rather than reliability testing, particularly for costly items such as transformers or switchgear.

The reliability behaviour of gearboxes, exhibited by the reliability growth analysis, is well defined; on one hand the initial reliability is acceptable, when compared to other industrial application, WT gearboxes wear out in a roughly linear progression. The last consideration originates from the values of the shape parameter of the intensity function shown in Chapter 5, whose value is consistently below 2. As a result the gearboxes can be considered a mature technology. Possible improvements to gearbox availability have to concern the O&M strategy and implementation of an adequate condition monitoring system for limiting the gearboxes degradation gradient.

The failure frequency of the direct drive synchronous generator is about twice that of more conventional indirect drive generators, which are asynchronous machines. Reasons for this can be ascribed to

- The larger diameter, leading to more problematic sealing.
- Manufacturing problems, caused by the smaller number of machines produced.
- Lack of knowledge of the specific application of large synchronous machines.

It is clear, however, that direct drive generators reliability has been subjected to an important improvement in the LWK data during the considered period, and this is particularly true for large machines, as for the case of E66 wind turbine. Since the presence of an early failure phase has been verified, it is desirable, for future machines, to avoid this early failures, uneconomic phase. This could be achieved by reliability oriented design, testing, accurate maintenance strategies and implementation of adequate condition monitoring systems will be beneficial for the

reduction of the effects of the early failures phase and generally to improve the reliability of those key machines.

Many failures in the WT are related to the drive train. These subassemblies failures can sum to more than 50% of the total failures occurring to WTs. Monitoring the power output, with a study in the domain of the frequencies, can spot failures of subassemblies strictly related to the drive train, as rotor, gearbox, pitch mechanism, shaft and generator [54].

Blades are important contributors to the failure frequency of the WT. It has been noted a certain positive correlation between blade failure frequency and the absence of pitch control. The conclusion is that aeroelastic vibrations, induced by blade flutter during stall turbulent conditions and in stall regulated machines, have a negative effect on the reliability of blades, reducing the life because of high cycle fatigue. The common idea of building stall-regulated machines, to reduce the failure rate with a simplification of the design, is not well-founded in the analysis here.

Replacing hydraulic by electrical actuators represents a good solution for reducing costs and increasing reliability. However, a careful reliability study has to be carried out on electrical systems, given the reduced predictability of failure occurring to electrical systems, when compared to their hydraulic alternative. The high failure frequency of electrical system of the WT models, where a full replacement of hydraulics has been adopted, confirms the above observation.

8.4 WT Concepts

The final considerations about the most suitable WT concepts, are drawn by synthesising the results for subassemblies and different turbines models.

The WT size is correlated to the failure frequency; the larger the size the higher the failure rate. There are three reasons that can explain this observation:

- The increased complexity of larger WTs, leading to an increased failure frequency.
- The maturity of WT technology. Larger WTs, developed in a relatively short period of time, on the basis of successful smaller machines, are subjected

to scaling problems. Scaling problems arise from the non linearity of the electromechanical loads involved.

- Larger WTs, being newer, are in the early failure phase of the bathtub curve.

The observations about size and failure frequency can be synthesised by the following approximate rule:

- Group I ($\simeq 300$ kW) 1 failure / year
- Group II ($\simeq 500$ kW) 2 failures / year
- Group III (≥ 1 MW) ≥ 3 failures / year

New WTs are in the multi-megawatt range and their improvement, because of the costs involved, constitutes an exiting and challenging field. Lessons from the past can be learned by applying the reliability growth methods illustrated.

The comparison of concepts was a major aim of this research.

Direct drive WTs are not necessarily more reliable than geared WTs. Aggregate failure frequencies of generators and converters in direct drive WTs are greater than the aggregate failure frequency of gearboxes, generators and converters in geared WTs. Therefore the price paid by direct drive WTs for the reduction of failure frequency by the elimination of a gearbox is a substantial increase in the failure frequency of electrical-related subassemblies.

However, it has been shown that the downtime of electrical-related subassemblies is lower than the downtime of gearboxes. This suggests that an all-electric, direct drive WT may ultimately have an intrinsically higher availability than an indirect drive WT.

As reported in the note above, a basic concept with no active control is not desirable, because the reduction of the failure frequency of the pitch mechanism, achieved through its elimination, results in an increased failure frequency of blades, which have a much higher MTTR.

It is proposed that offshore WTs should have their subassemblies tested more thoroughly than at present, particularly converters and generators, to eliminate

early failures. A suggestion is that WT nacelles could be tested complete, at full or varying load, at elevated temperature, to accelerate early failures during a 6 hour test so that they enter service with an improved reliability. This approach has been adopted successfully by conventional industrial generator, gearbox and converter manufacturers.

8.5 Future Work

It has been mentioned the effects that random phenomena such as weather and grid instability, have an effect on wind turbine failure data. The study of the correlation between grid or weather and failure intensity would be beneficial to many aspects such as:

- Construction of the best maintenance strategy, particularly useful for offshore installations
- Prediction of energy output, via a Monte Carlo simulation
- Verification of the intrinsic failure frequency of the various subassemblies

The last point will be achieved by filtering the data from the peaks induced by extreme weather conditions.

With the implementation of the model illustrated in Chapter 5, a way has been suggested to model wind turbines failure data starting from the assumption of the bathtub curve. The natural extension of such modelling would be a full implementation of a Monte-Carlo simulation for the prediction of energy output, and hence the economic performance of a wind farm. The model should take into account, along the turbines reliability, other parameters, namely:

- MTTR
- O&M costs
- Weather conditions
- Grid effects

- Load variations

The major difficulty of the research work presented in this thesis can be identified in the problematic access to real failure data, which are normally held by wind industry operators and are not publicly available. Although fully understanding the commercial relevance of such delicate information the author considers such a policy to be counter-productive for the wind industry, in the long run. Solving the question of the reliability of the wind turbines, despite the current crisis of traditional sources of energy, still needs some governmental support, and is crucial to overcome the remaining scepticism that accompanies wind energy, particularly by those investors that still have to be fully convinced by the economic sustainability of wind energy. It is highly desirable to increase the collaboration between manufacturers, operators and investors in order to allow the analysis of high quality data. For the coordination of this process the role of academic research, such as that presented here, would be central.

Appendix A

Weibull Analysis of Converters Failure Data

A.1 Introduction

In chapters 4 and 5 the importance of the reliability of the power converter has been illustrated. The power converter is at the heart of the electrical side of wind turbines and its impact on the reliability of the wind turbine, is similar to the impact that the gearbox has on the mechanical side of the system. The importance of a deeper understanding of the reliability of the converter is therefore clear.

For wind turbines failure the data that have been used in the previous chapters, the electronic converter does not constitute a separate subassembly and its failures are embedded in either “electrics” or “electronics” subassemblies and it is has been necessary to have recourse to alternative sources of data.

An important firm, specialised in the manufacturing of power electronic converters, has agreed to disclose actual failure data of some of the converters produced. The data have been analysed in a systematic way, and this appendix reports methods and results of such investigation. The method is based on the Weibull distribution which is described in chapter 3.

The work was subject to a confidentiality agreement, so neither the company nor the converter models can be explicitly named in this thesis. The company will be referred to as “the manufacturer” and the seven converter types will be named with

letters from A to G, ranging in size from 0.32 kW to 132 kW.

The size of the converters involved in the survey is smaller than the typical size of the converters that equip the wind turbines. Nevertheless, larger converters are often the aggregation of smaller converters connected in parallel, therefore the results may still be considered valid in relation to wind turbines.

A.2 Data Set

The converter data relate to warranty return records of failed converters, and have been in the form illustrated in the example of Table A.1. The example is for a particular converter model, “Type A”. Each row represents a different production batch, which is identified by the production period reported in the first column. The second column reports the total number of items sold for that batch. All the other columns represent the age of each batch, and, in each cell, the cumulative number of items that have failed and been returned at that age is entered. It is important to underline that the columns do not represent the calendar time, as it was for wind turbine failure data; therefore the first row is longer because the first batch is older and has been operating for a longer period, which corresponds to the length of the observation period. The triangular shape of the table is due to the same reason; the newly produced batches have been operating for a shorter period of time.

For this particular analysis time is measured in “periods”, referring to the periods of three months that characterises the collection of data, as reported in Table A.1.

The data have been successively transformed in the format shown in Table A.2, that is more suitable for the analysis. In the new format the number of failures occurred during the batch age period, or time cell, replaces the cumulative number of failures. This is sometimes referred to in the reliability literature as the “Nevada” format.

The fact that the data concern items that, once failed, progressively disappear from the original population suggests that we are dealing with a non repairable system; the implications of this have been extensively explained in chapter 3. In this case the “non repairability” is purely a feature of the data set and does not

Period	Sales	Batch Age [month]													
		03	06	09	12	15	18	21	24	27	30	33	36	39	42
2002/05-02/07	253	0	0	0	6	6	8	9	12	14	16	16	17	21	21
2002/08-02/10	488	0	0	10	11	18	23	32	38	40	42	43	45	47	
2002/11-03/01	324	0	1	1	2	4	5	8	10	12	13	15	16		
2003/02-03/04	1114	0	0	1	5	8	13	19	28	29	35	37			
2003/05-03/07	2082	2	4	5	11	27	31	44	48	58	62				
2003/08-03/10	2139	0	0	4	11	16	23	29	37	44					
2003/11-04/01	2463	1	1	6	10	19	25	36	50						
2004/02-04/04	2657	0	3	14	21	26	37	41							
2004/05-04/07	3605	0	5	13	20	38	46								
2004/08-04/10	4639	0	6	14	44	59									
2004/11-05/01	4632	1	4	20	25										
2005/02-05/04	6254	0	5	25											
2005/05-05/07	6974	1	5												
2005/08-05/10	7735	2													

Table A.1: An example of the original data failure data; converter A

Period	Sales	Batch Age [months]															
		03	06	09	12	15	18	21	24	27	30	33	36	39	42		
2002/05-02/07	253	0	0	0	6	0	2	1	3	2	2	0	1	4	0		
2002/08-02/10	488	0	0	10	1	7	5	9	6	2	2	1	2	2			
2002/11-03/01	324	0	1	0	2	2	1	3	2	2	1	2	1				
2003/02-03/04	1114	0	0	1	4	3	5	6	9	1	6	2					
2003/05-03/07	2082	2	2	1	6	16	4	13	4	10	4						
2003/08-03/10	2139	0	0	4	7	5	7	6	8	7							
2003/11-04/01	2463	1	0	5	4	9	6	11	14								
2004/02-04/04	2657	0	3	11	7	5	11	4									
2004/05-04/07	3605	0	5	8	7	18	8										
2004/08-04/10	4639	0	6	8	30	15											
2004/11-05/01	4632	1	3	16	5												
2005/02-05/04	6254	0	5	20													
2005/05-05/07	6974	1	4														
2005/08-05/10	7735	2															
Total	45352	7	29	84	78	80	49	53	46	24	15	5	4	6	0		

Table A.2: The failure data of converter A converted into the "Nevada" format

reflect the fact that the device is actually replaced rather than repaired, in one or more of its components. Nevertheless, it is common practice to replace a failed converter with a new one, and this is particularly true for the smaller converter sizes, which are typically mass produced with highly efficient manufacturing processes and therefore of low first cost.

The next paragraph is dedicated to illustrate the method that has been used to analyse the data, which is called “Weibull Analysis” and is a powerful and widely adopted reliability tool for the analysis of fleets of non repairable items. As the name suggests the Weibull Analysis is based on the Weibull distribution, see equation 4.2, in its application to the non repairable case.

A.3 Weibull Analysis

The rudiments of Weibull Analysis are described in reliability textbook such as [39,62] but in [1] the method, including the interpretation of the results and a large set of examples, is thoroughly illustrated.

The basic assumption is that the TTF of a the population under investigation is Weibull distributed.

As illustrated in chapter 3, for Weibull distributed populations the relative hazard function is a power law function and the cumulative distribution function has the form:

$$F(t) = 1 - e^{-\rho t^\beta} \quad (\text{A.1})$$

where the parameter β and ρ have the usual meaning. By definition the *cdf* of a non repairable population is

$$F(t) = \frac{N(t)}{n} \quad (\text{A.2})$$

Where n is the total number of items in the population and $N(t)$ is the expected number of failures in a time t . Substituting equation A.2 in equation A.1:

$$N(t) = \left(1 - e^{-\rho t^\beta}\right) n \quad (\text{A.3})$$

and with a simple manipulation we obtain:

$$\lg \left(\lg \left(\frac{1}{1 - \frac{N(t)}{n}} \right) \right) = \beta \ln(t) + \ln(\rho) \quad (\text{A.4})$$

The relationship of equation A.4 is linear if plotted on a special chart, of which the abscissa scale is logarithmic and the ordinate is scaled with the function represented by the left side of equation A.4. This function will be referred to as the “Weibull Plotting Function” or simply “Plotting Function” for the sake of brevity, and is, in words, the double logarithm of the cumulative hazard function. A set of Weibull distributed failures lies on a straight line, when plotted on the special chart described. It must be noted that this scale can also be expressed in terms of percentage of unreliability, which is the term $N(t)/n$ that appears in equation A.4. In all the above equations the time variable is the life of the item, that is the TTF. The method consists of representing on the chart the plotting function, calculated in each time cell, and interpolating the set of data with a straight line, which represents the Weibull distribution of the failure data. Assuming that the interpolation is satisfactory, the parameters of the distribution can be read directly from the chart;

- The slope of the line corresponds to the shape parameter β .
- The scale parameter ρ is defined by the intersection between the interpolation line and the horizontal line corresponding to 63.2% of the cumulative number of failures.

The first point can easily be verified by observing equation A.4. The second point is true independently from β ; for $t = 1/\rho$.

For $t = 1/\rho^{1/\beta}$ is

$$F(t) = 1 - e^{\rho \left(\frac{1}{\rho}\right)^{\frac{\beta}{\beta}}} = 1 - \left(\frac{1}{e}\right) = 0.632 \quad (\text{A.5})$$

Figure A.1 illustrates an example of the graphical procedure for the calculation of the two parameters.

As a goodness of fit test [1] suggests the adoption of the squared correlation coefficient (SCR) r^2 . According to [1] the linear fit is considered valid for high

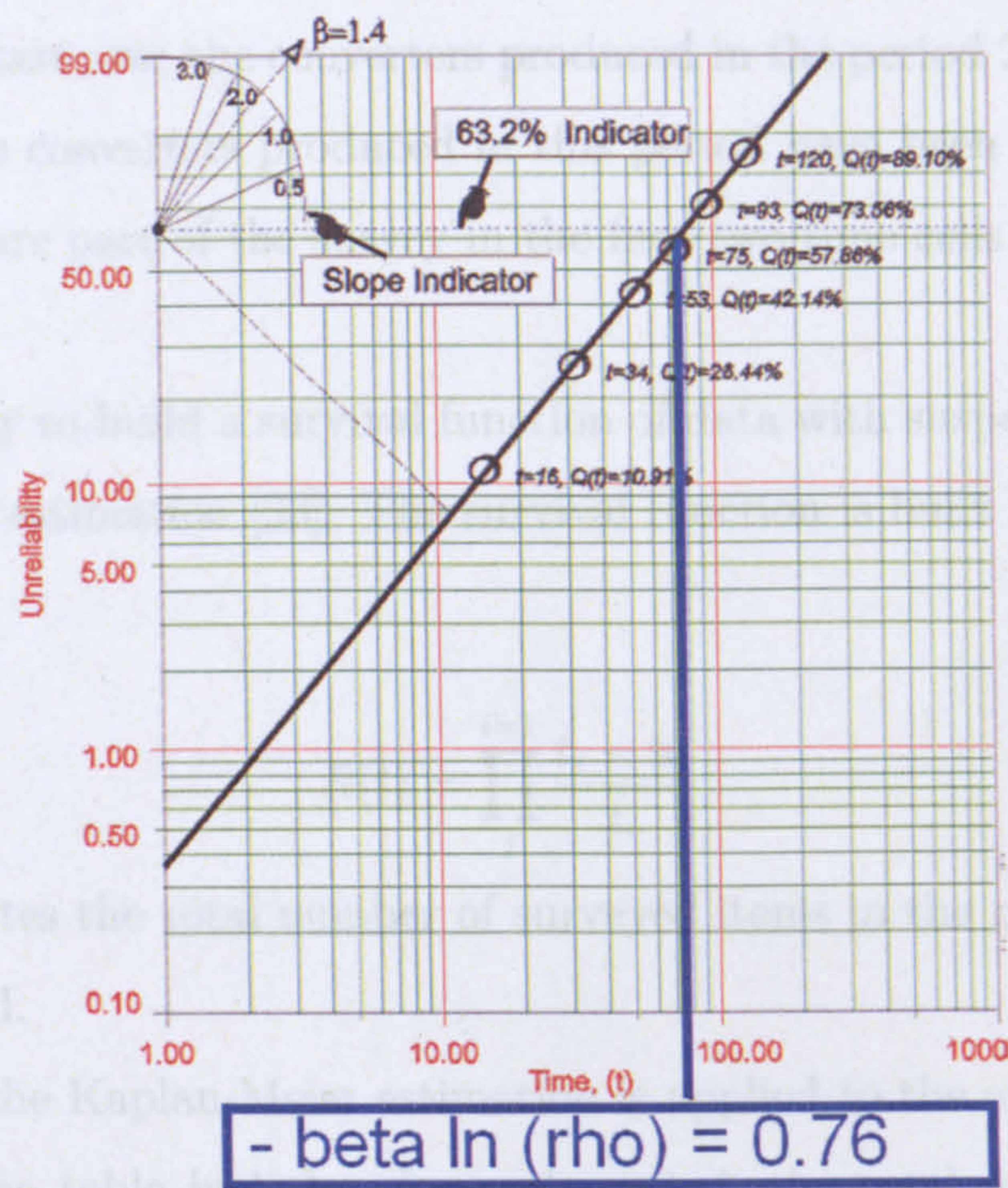


Figure A.1: The graphical calculation of shape and scale parameters

values of r^2 , typically higher than 0.9. Values smaller than 0.9 normally indicate a poor fit and the Weibull distribution can not be considered representative of the population.

The data supplied in the Nevada format needs further manipulation. The original data was aggregated by column, that is by items of the same age, as reported in the last row of Table A.2. Each cell of the resultant array contains the number of item failed at that age interval, over the entire population of objects, that is all the batches that have been produced. The data presented in this form are called “interval censored” or grouped data, with which we are already familiar.

Given the Nevada format and given the data aggregation that has been discussed above, in each time cell of the aggregated data there are three kind of items; the failed items, the surviving items, that is the items that have not failed, and the suspended or censored items. The suspended items disappear from the next time cell by virtue of the fact that the relative batch has been recently produced and the survey extends beyond the age of that production batch. For the same reason the data table has a triangular form. As an example refer to Table A.2 third cell of the

aggregated array, last row; the converters produced in the period 2005/05-05/07 are not surveyed. The converters produced in this period have been operating for two periods only and are part of the survey in the first two time cells of the aggregated period.

A practical way to build a survival function of data with suspensions is given by the Kaplan-Meier estimation [33]. The survival function is built with the following formula:

$$R(t) = \prod_I^{i=1} \frac{t_i - n_i}{t_i} \quad (\text{A.6})$$

Where t_i denotes the total number of surveyed items in the period i the and n_i are the item failed.

In Table A.3 the Kaplan-Meier estimation is applied to the example of data set of Table A.2. The table includes, for each period, the total number of items in the population, the failed items, the censored items since the previous period, the surviving items, the unreliability and the plotting function.

A.4 Actuarial Correction

Data presented in Nevada format suspensions are dominated by the suspensions, that is the items that do not fail but that are not considered in the next period. In this case the suspension is due to the age of that subset of items.

According to [1], in these cases it is suggested to apply the ‘‘Actuarial Correction’’ by subtracting in each interval half of the suspended item s_i from the total number of units starting the interval t_i . The correction is based on the assumption that the suspensions are uniformly distributed in the interval. Consequently the Kaplan-Maier survival function has to be calculated as follows

$$R(t) = \prod_I^{i=1} \frac{t_i - n_i - \frac{s_i}{2}}{t_i - \frac{s_i}{2}} \quad (\text{A.7})$$

Age Period	1	2	3	4	5	6	7	8	9	10	11	12	13	14
Total items	45359	37624	30650	24396	19764	15125	11520	8863	6400	4261	2179	1065	741	253
Failed items	7	29	84	78	80	49	53	46	24	15	5	4	6	0
Censored items	0	7728	6945	6170	4553	4559	3556	2604	2417	2115	2067	1109	320	482
Survived items	45352	37595	30566	24317	19684	15076	11467	8817	6376	4246	2174	1061	735	253
Unreliability	1.69E-04	1.02E-03	4.07E-03	7.60E-03	1.22E-02	1.59E-02	2.10E-02	2.71E-02	3.16E-02	3.63E-02	3.94E-02	4.40E-02	5.65E-02	5.65E-02
Plotting Function	-8.69	-6.89	-5.50	-4.88	-4.40	-4.14	-3.85	-3.60	-3.44	-3.30	-3.21	-3.10	-2.84	-2.84

Table A.3: Calculation of the unreliability using the Kaplan-Meier ranking method [62]

A.5 Results: First Data Set, Type A

Figure A.2 shows the Weibull plot of the data relative to the Type A converter, together with the results acquired for scale and shape parameters, and the goodness of fit test r^2 .

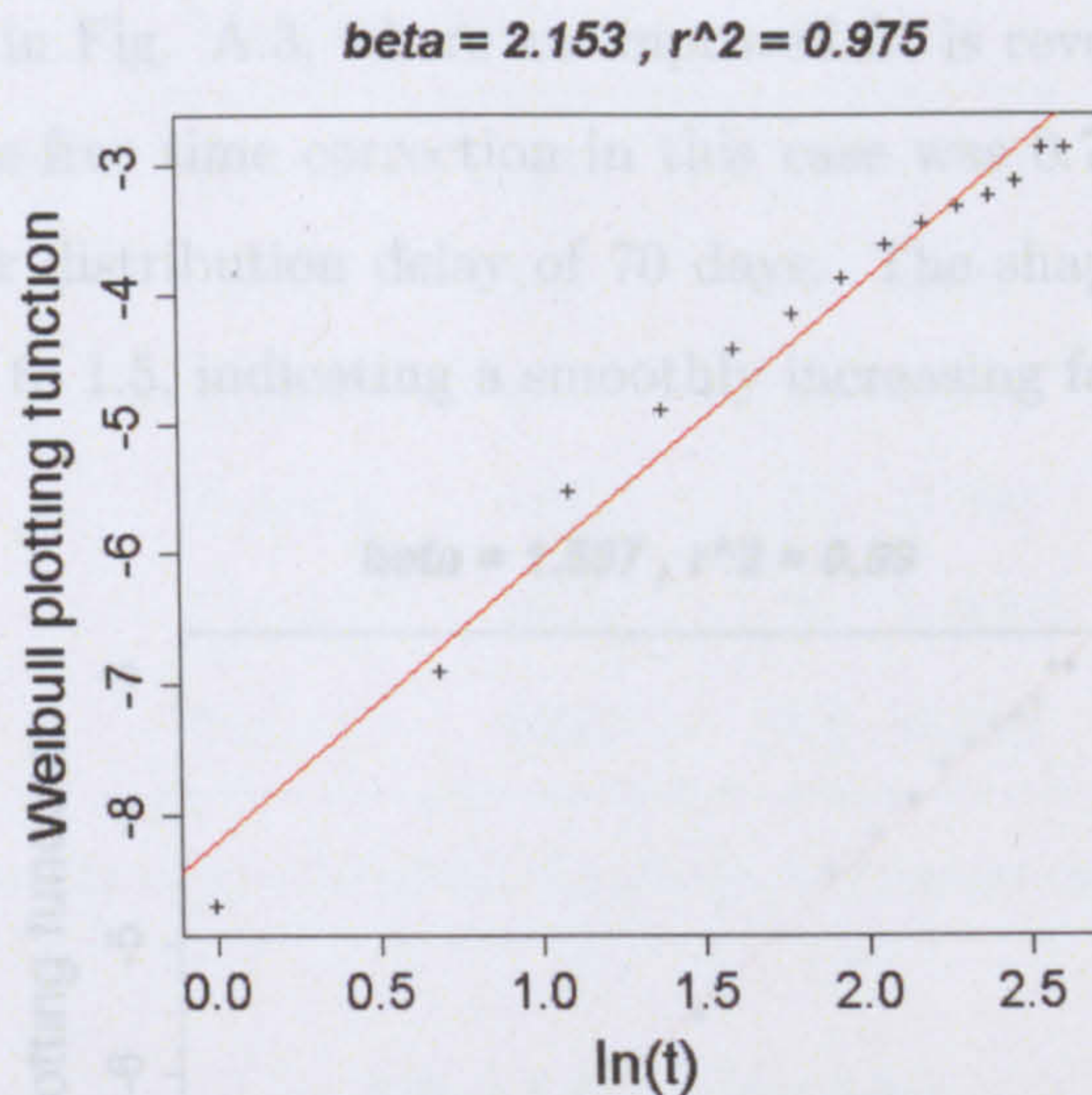


Figure A.2: Weibull Analysis result for Type A converter

The interpolation can be considered satisfactory, given the high value of r^2 , and consequently the reliability of the population being described by a Weibull distribution. Nevertheless, the evident concave shape of the plot unveils a feature of the population that can be ascribed to one of the two causes:

- That the population could be better described by a different distribution family, such as the Lognormal distribution.
- There is a failure-free time problem with the data.

The first point is a typical consequence of burn-in testing that removes from the population products prone to early failure, thus changing the shape of the hazard function of the surviving population. This is a feature of the totality of mass-produced power converters and maybe a lesson for the manufacturers of wind turbines. The second case may indicate a failure-free time that is an initial period

with no failures. The failure-free time can be due to either the physics of the failure mode or, as suggested by the manufacturer, a delay in the products introduction into service as a result of shipping and/or distribution delays, this was suggested to be about two months. The value corrected by removing from the data a period of time representing the failure-free time. The advantage of the failure-free time correction is clear in Fig. A.3, where an improved fit is revealed by an increase in the r^2 . The failure-free time correction in this case was 0.775 periods, equivalent to shipping and/or distribution delay of 70 days. The shape parameter after the correction reduces to 1.5, indicating a smoothly increasing failure rate.

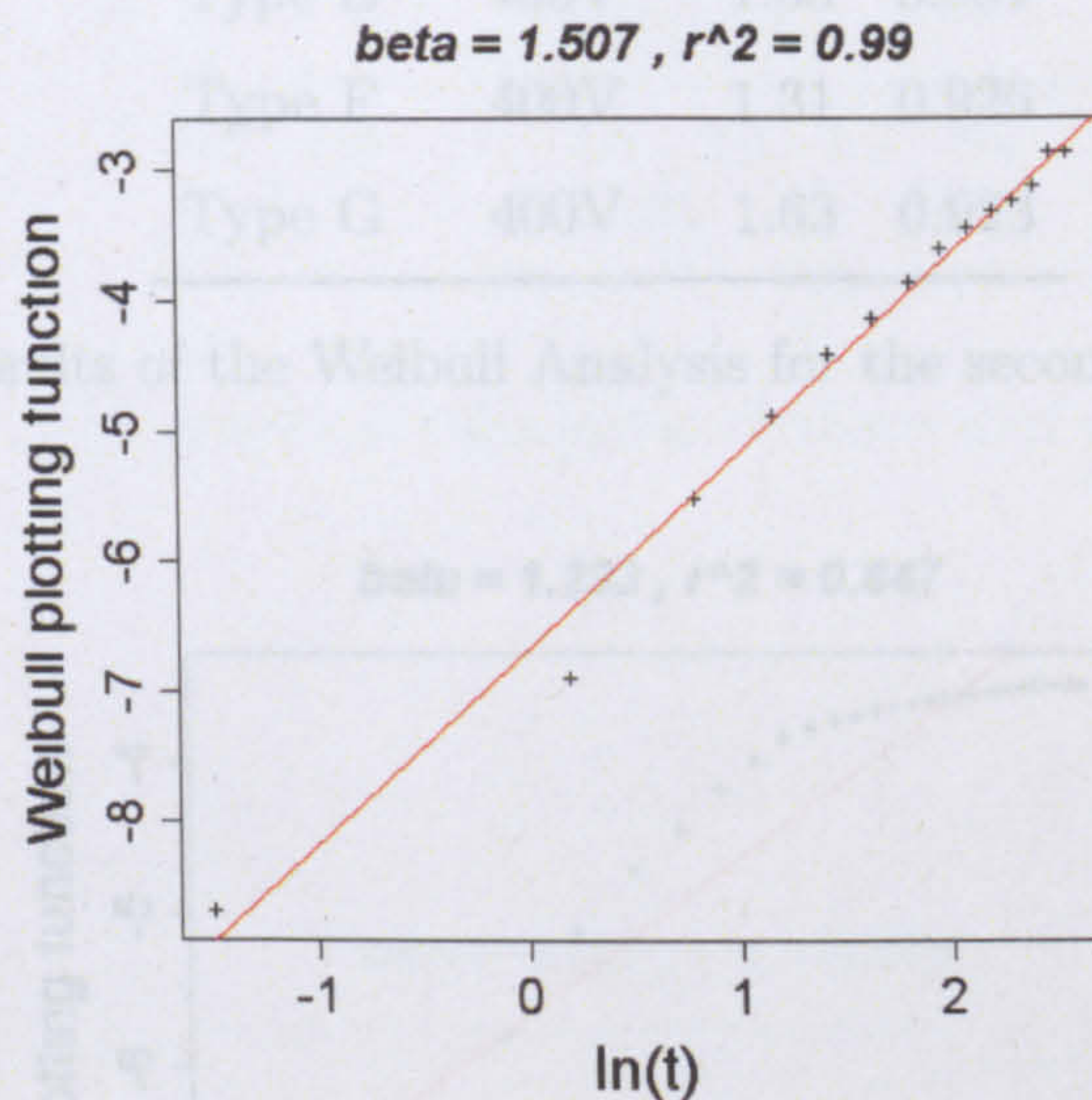


Figure A.3: Weibull Analysis result for Type A converter after removal of delivery delay period of 70 days

The results for the Type A converter can therefore be summarised as follows:

- The product is in the early wear out phase, or increasing failure rate, characterised by a shape parameter of 1.5. The investigation of the increasing failure rate needs additional information about design, manufacturing or testing procedures to which the system is subjected.
- There is a failure-free time of about 70 days, probably due to shipping and/or distribution delays, as suggested by the manufacturer.

A.6 Results: Second Data Set: Types B-H

The analysis done to the second set of data, six products of a different converter family has produced a complete set of Weibull plots, Figures A.4 to A.9 shown below. The results are summarised in Table A.4.

Model	Voltage	β	r^2
Type B	200V	1.23	0.847
Type C	200V	1.08	0.853
Type D	400V	1.30	0.818
Type E	400V	1.35	0.891
Type F	400V	1.31	0.926
Type G	400V	1.63	0.923

Table A.4: The results of the Weibull Analysis for the second set of converter data

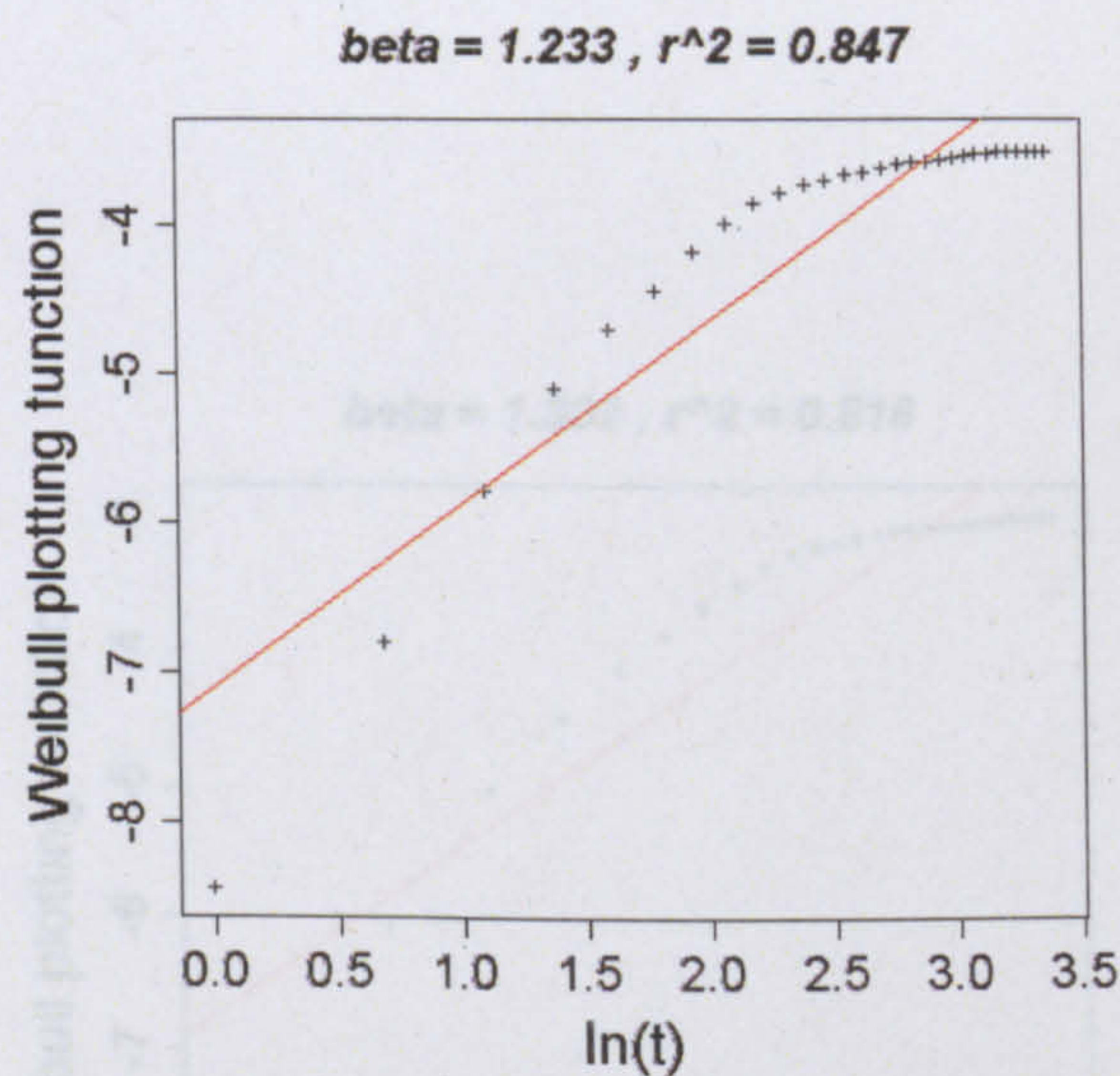


Figure A.4: The graphical calculation of shape and scale parameters

There are some observations one can make:

- All the converters of the second set exhibit a similar failure rate behaviour.
- As for the type A, the Weibull plots for the second set of data do not fit a straight line, as indicated by a low value for the statistical test r^2 , see Table

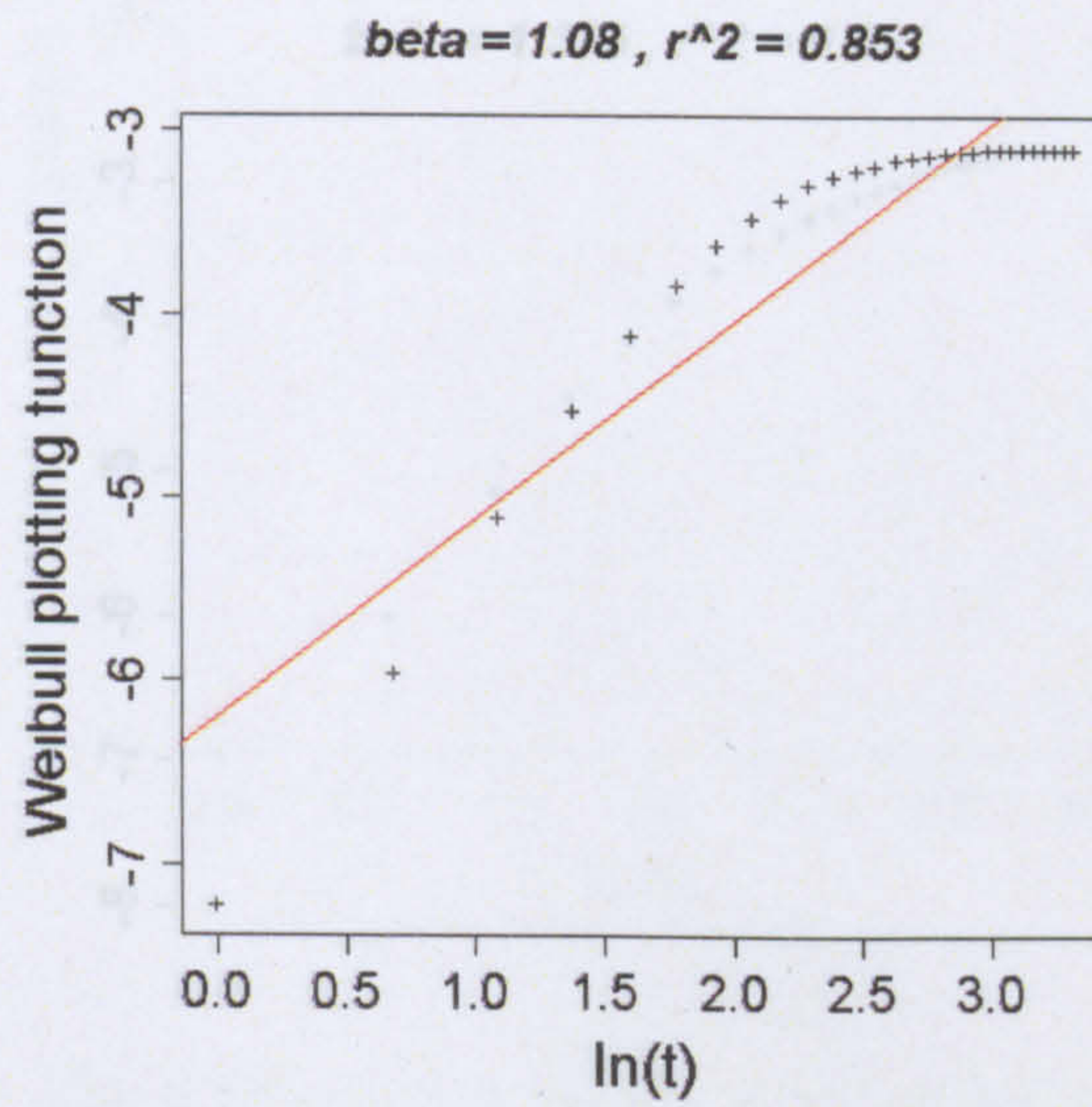


Figure A.5: The graphical calculation of shape and scale parameters

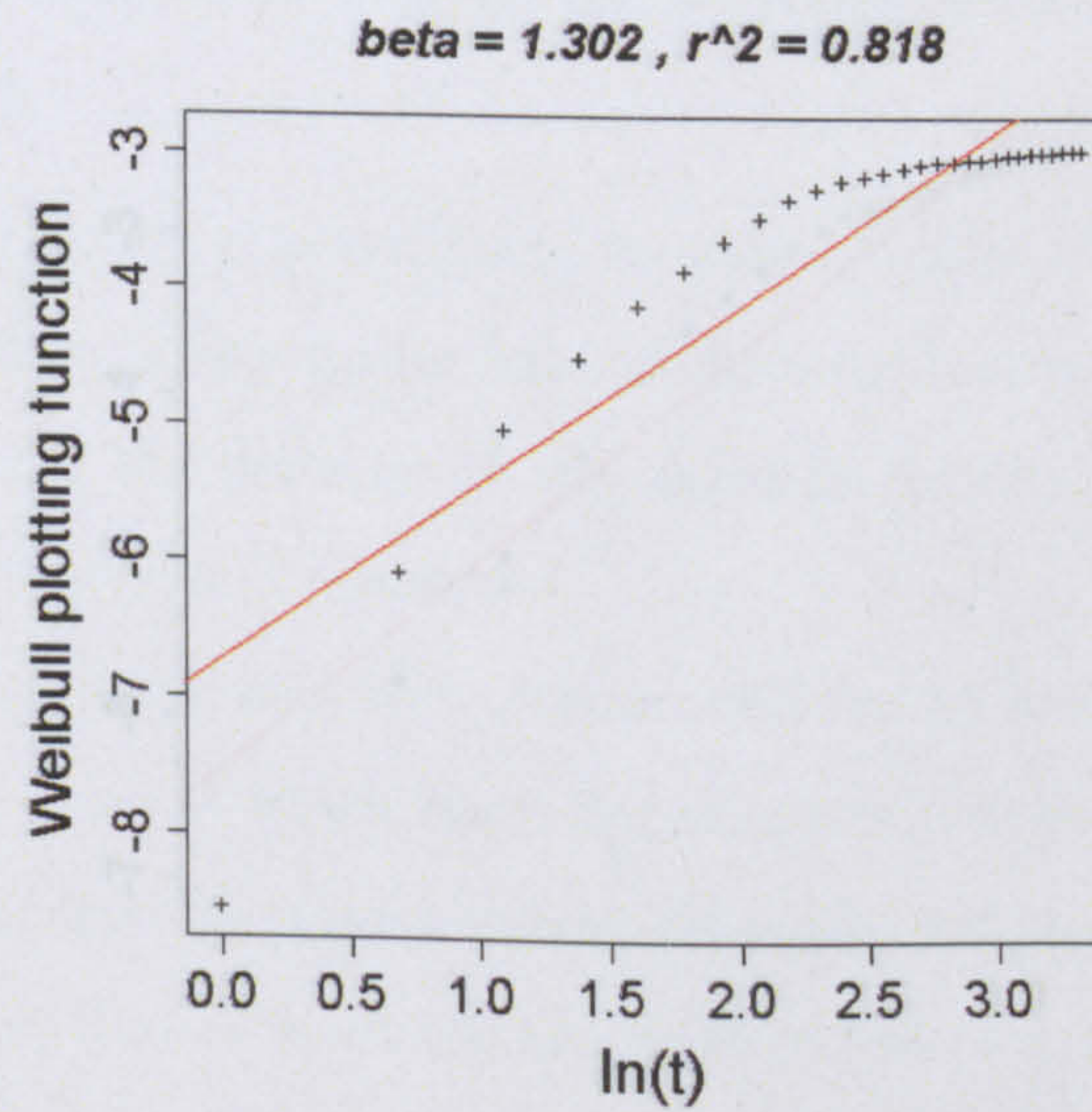


Figure A.6: The graphical calculation of shape and scale parameters

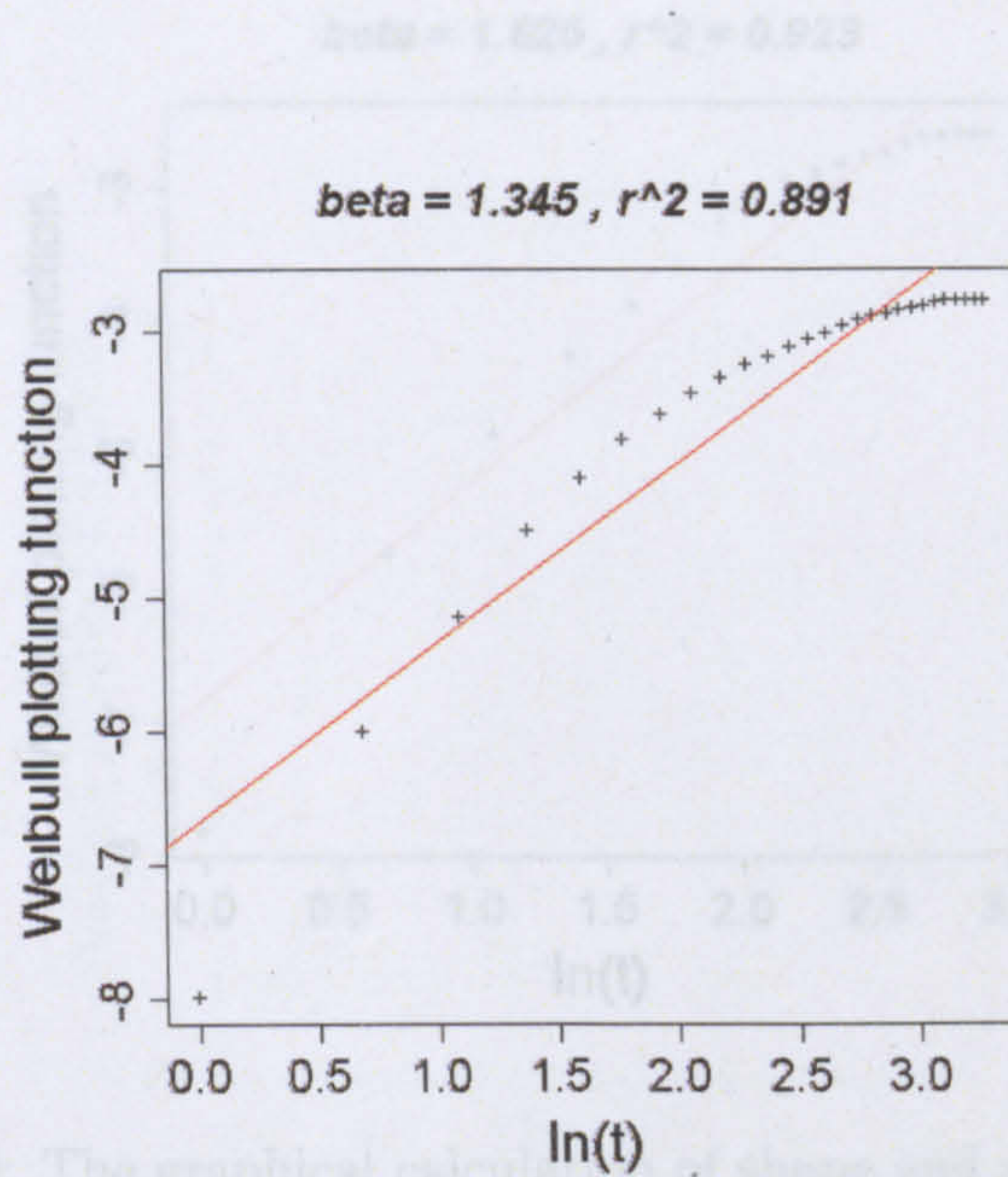


Figure A.7: The graphical calculation of shape and scale parameters

at both engineering and manufacturing levels

- The shape of the Weibull plots shown in Figures A.4 to A.9, all exhibit a substantial knee, suggesting that a major variation in design, manufacture or component quality in the product has occurred, leading to a noticeable change in failure rate.

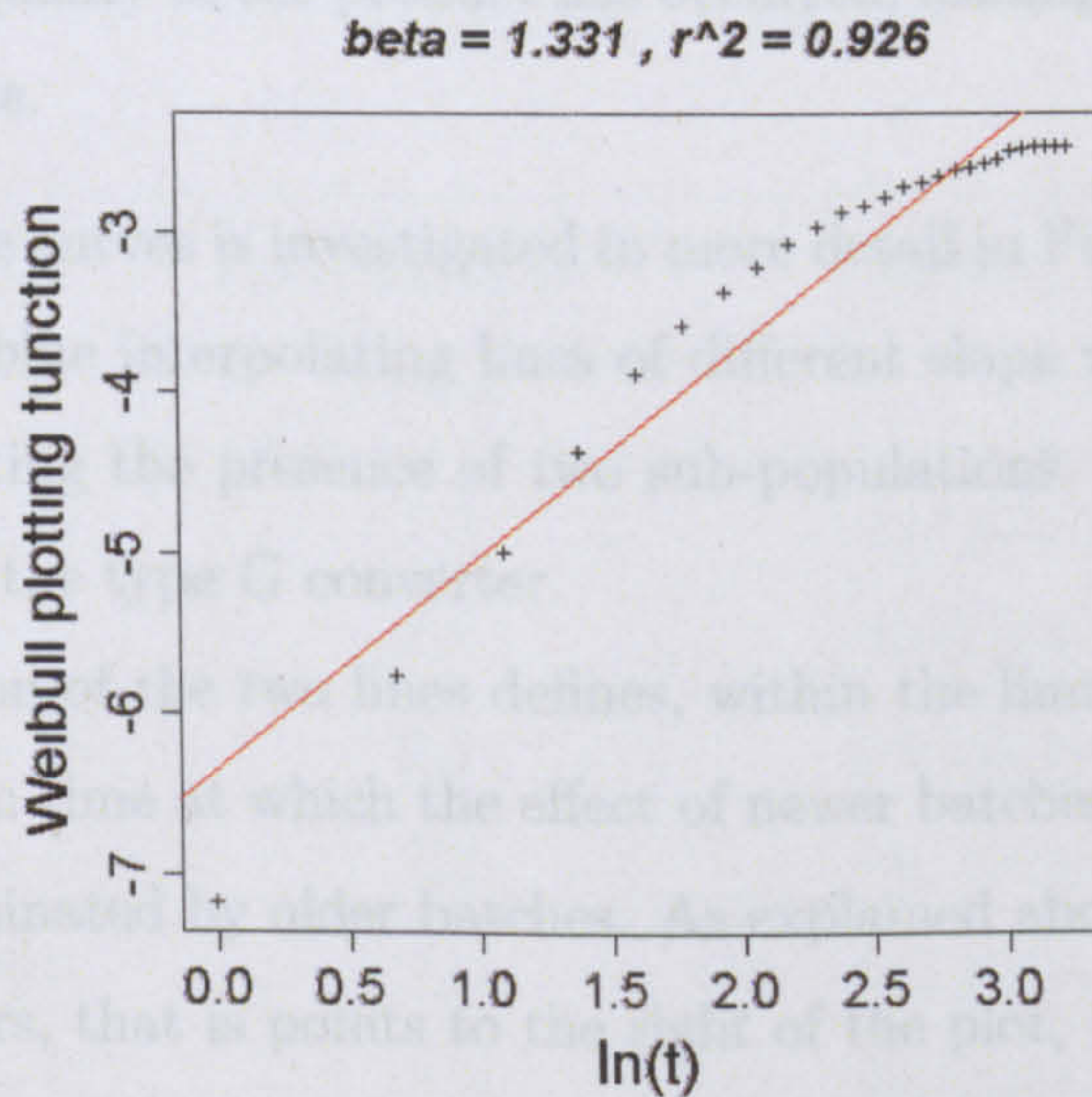


Figure A.8: The graphical calculation of shape and scale parameters

There is a high degree of consistency in the intersection point obtained from 6 different products. Products produced after the period May - Jul 2004 show a

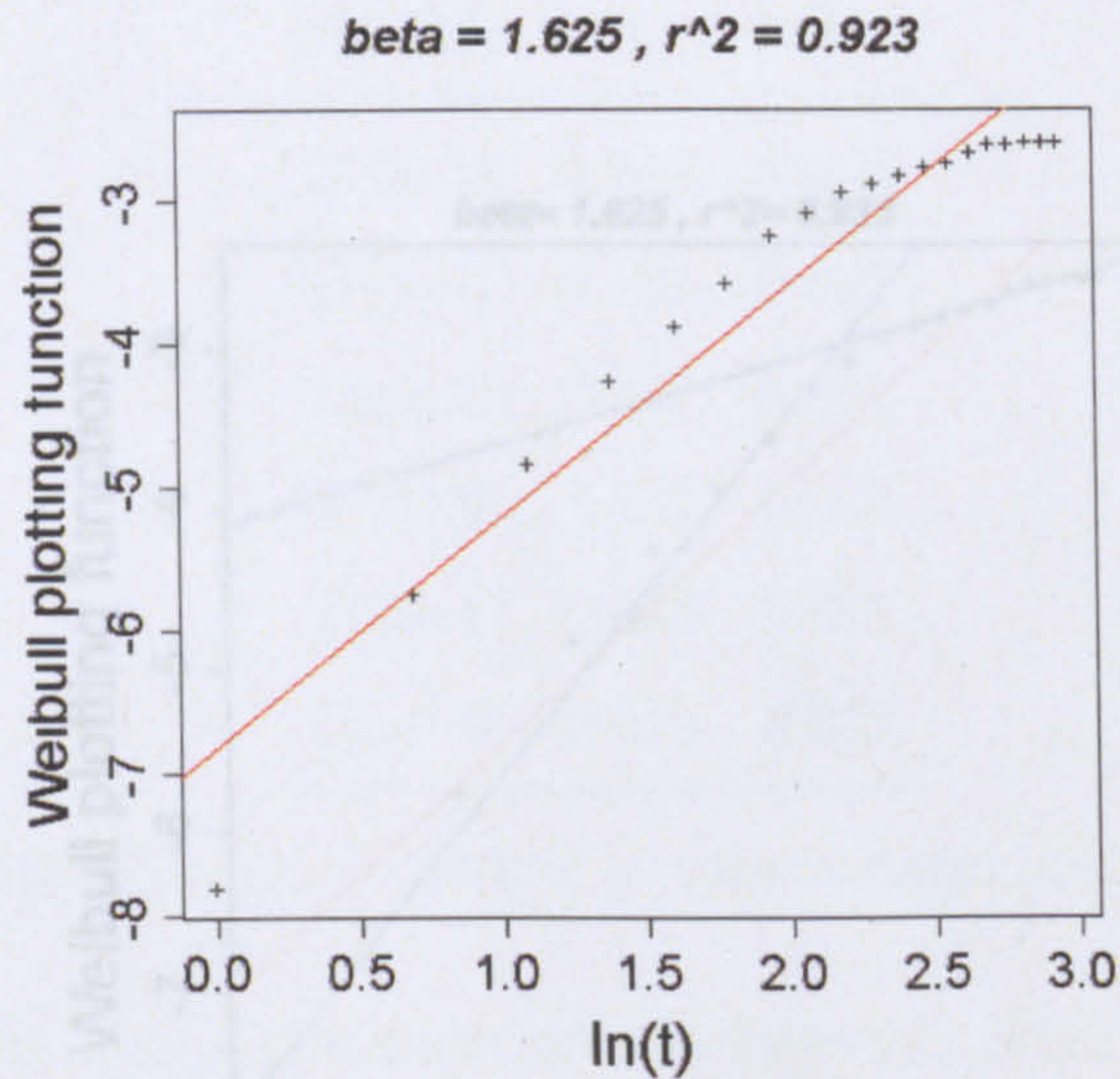


Figure A.9: The graphical calculation of shape and scale parameters

A.4. There can be many reasons for a poor fit and they should be investigated at both engineering and manufacturing levels.

- The shape of the Weibull plots shown in Figures A.4 to A.9, all exhibit a substantial knee, suggesting that a major variation in design, manufacture or component quality in the product has occurred, leading to a noticeable change in failure rate.

The knee in the curves is investigated in more detail in Figure A.10, where it can be seen that two blue interpolating lines of different slope would fit the plot more accurately, indicating the presence of two sub-populations. The example shown in Fig. A.9 refers to the type G converter.

The intersection of the two lines defines, within the limits of graphical interpolation, the point in time at which the effect of newer batches terminates and failure rate becomes dominated by older batches. As explained above, the older the population of converters, that is points to the right of the plot, the less the influence of newly produced batches. Hence, the production period that determined the change in failure rate can be worked out, with the results tabulated in Table A.5:

There is a high degree of consistency in the intersection point obtained from 6 different products. Products produced after the period May Jul 2004 show a

December 6, 2008

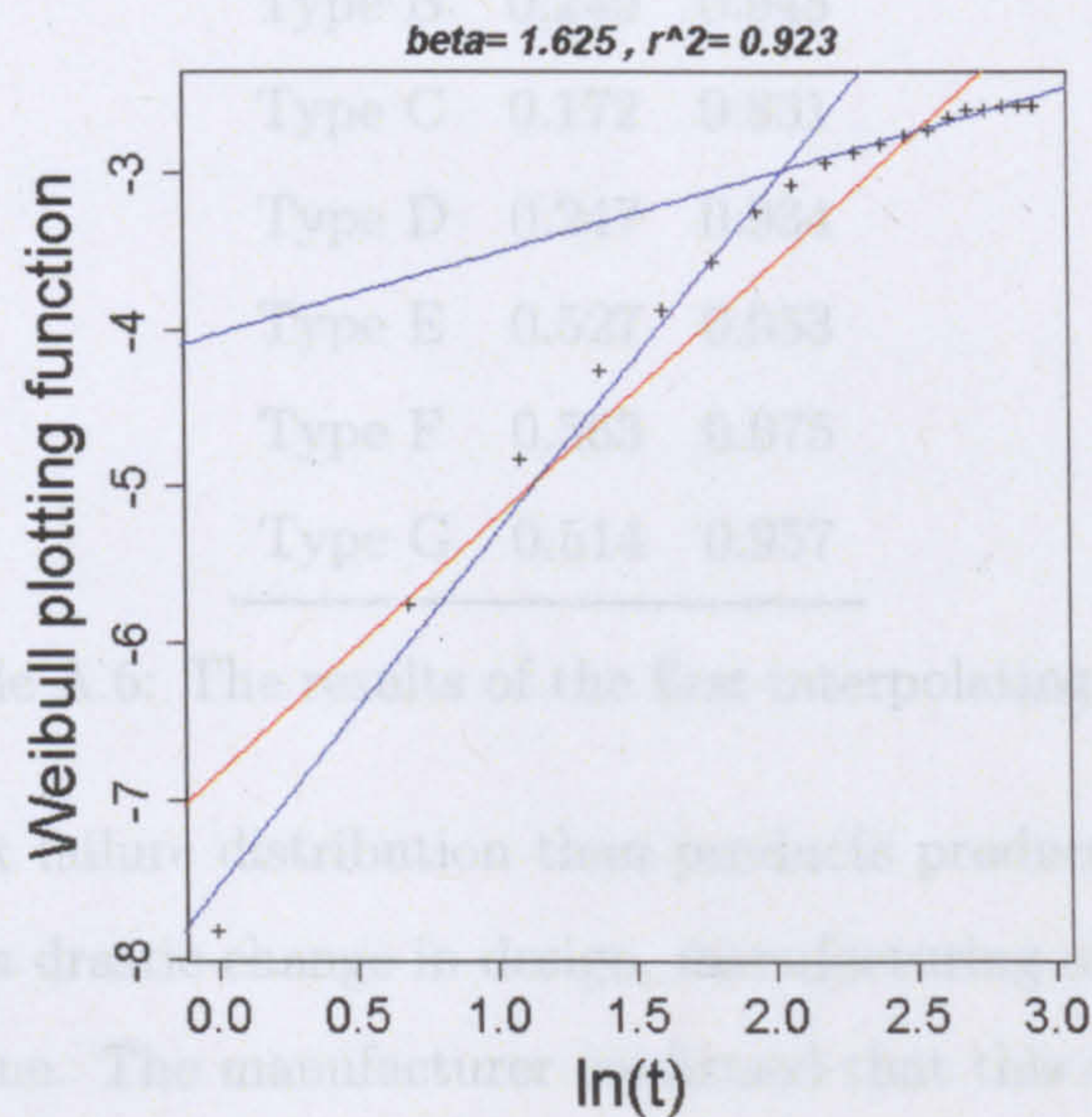


Figure A.10: Example of Bi-Weibull: two interpolating lines fit better the Weibull chart of type G converter

Having identified the batch problem, the Weibull fit has been performed on two separate sub-populations of each product.

Model	Intersection Point	Correspondent Date
Type B	2.2	05/2004-07/2004
Type C	2.2	05/2004-07/2004
Type D	2.3	02/2004-04/2004
Type E	2.2	05/2004-07/2004
Type F	2.2	05/2004-07/2004
Type G	2.3	02/2004-04/2004

Table A.5: The intersection point for each converter type

Model	β	r^2
Type B	0.249	0.945
Type C	0.172	0.831
Type D	0.247	0.934
Type E	0.527	0.953
Type F	0.563	0.975
Type G	0.514	0.957

Table A.6: The results of the first interpolating line

remarkably different failure distribution than products produced before that date. This suggests that a drastic change in design, manufacturing or component quality occurred at that time. The manufacturer confirmed that this change was due to a relocation of production to a different site, combined with a significant change to the product design at that time. The knee of transition from the first interpolating line to the second, is sharp for Type B converter, gradually becomes smoother for the other larger types, see Figures from A.4 to A.4. The radius of the knee increases as the converter size increases, indicating a trend.

Having identified the batch problem, the Weibull fit has been performed on two separate sub-populations of each product.

According to the column data aggregation method presented above, the first sub-population includes all the batches produced up to the date, the early produced ones. The second sub-population also includes the newer batches, produced after that date. In practical terms, for each converter product, the parameters of the two interpolating lines have been calculated and are summarised in Tables A.6 and A.7:

Tables A.6 and A.7 the two sub-populations show remarkably consistent values of β , independently of the converter model. The high value of the r^2 GoF coefficient in the two subpopulations confirms that the linear fit is satisfactory. It is interesting to compare the GoF coefficient before and after the double interpolation. The first sub-population shows a low β , between 0.2 and 0.5, indicating a clear infant mortality phase. A more selective test programme before shipping product would wash out that portion of the population prone to early failure. Conversely, the second sub-

Model	β	r^2
Type B	2.11	0.989
Type C	1.80	0.994
Type D	2.28	0.958
Type E	2.16	0.982
Type F	1.94	0.997
Type G	2.23	0.985

Table A.7: The results of the second interpolating line

population, shown in Table A.7 is characterised by a high value of β , between 1.8 and 2.3, indicating a gently increasing failure rate, leading to the wear-out phase. As for the Type A converter, this is clearly a case of early wear-out and is of concern because a thorough review of design, manufacturing and component quality is required. However, the nature of the data and the lack of detailed information about the failure patterns and manufacturing processes do not allow further consideration about the origin of the reliability features of the converters.

There are some important issues to be considered regarding the data quality.

- Firstly, the aggregation in periods, typical of warranty returns data, makes the analysis less precise, due to the lack of the information about real life, usage and environmental conditions. The most important missing information is the time of failure for each product, which is usually required for reliability analysis. However the absence of time to failure data can be overcome with specific mathematical tools, which have been applied and reduce accuracy but produce acceptable results.
- Secondly, reliability analysis should include information about the failure modes of each return. The effectiveness of the bare failure data analysis is increased when it is accompanied by an investigation of the physics of the failure mode. In a highly complex system, such as the converter, real failure mode classification is difficult. So it is recommended to segregate the failure data into the main converter subassemblies, for example; rectifier, inverter, dc-link, protec-

tion and controller. The identification of weak components will be improved by the reliability analysis of each subassembly dataset.

A.7 Conclusions

- For the Type A converter product the Weibull plot analysis shows a good fit, especially after the failure-free time correction. The data shows that the product is in early failure phase ($\beta = 1.5$), with a failure-free period of 70 days.
- For the Types B-G converters the Weibull plot analysis indicates a remarkable consistency between the different products analysed, which were of a variety of sizes and therefore incorporating a range of different components.
- However, for the Types B-G converters a batch problem is indicated due to a substantial change in the design, manufacture or component quality, after the production period May-July 2004
- Early batches, produced before May-July 2004, were characterized by a low β and are therefore in the infant mortality phase. The problem could be solved by more thorough testing.
- Later batches, produced after May-July 2004, are characterised by a higher β in the early part of the curve and appear to be in the early part of the wear-out phase. This is a case of early wear-out, which should be resolved by a more thorough investigation over design, manufacturing or components quality.
- More complete analysis could be done with an increased data quality, including information about failure modes, subassemblies and converter technical specifications.
- Reliability analysis has different objectives and it would be beneficial to specify reliability goals for the converter products in order to improve the analysis. For example, recording when substantial changes occur in the product would allow comparison before and after the change.

Finally, the following lessons for the reliability of wind turbines were suggested by this analysis:

1. Early burn-in testing of converters and their subassemblies are very effective in reducing early life failures.
2. The Weibull plot has shown itself to be a useful tool for analysing the trends in reliability in converter products, with the potential to be able to predict forthcoming life of the converter.
3. This kind of analysis is a very effective quality control on a product over a period of time, providing the data is recorded in a controlled way as suggested by this appendix.

Appendix B

Reliability Growth Results Tables

Whole Wind Turbine, All Subassemblies										
Survey	PLP parameters				values		tests results			
	Model	β	ρ	Initial	Final	Avg	GoF	$H_0 =$	HPP	Conclusion
				[failures year ⁻¹]						
	V27/225	0.7467	4.8780	2.420	0.790	1.060	rejected	rejected		PLP (early failures)
	M530	0.9553	1.4000	1.240	1.047	1.090	accepted	accepted		HPP
	TW600	0.9585	2.8010	2.512	2.100	2.190	accepted	accepted		HPP
LWK	E40	0.8926	4.7530	3.570	2.170	2.430	accepted	rejected		PLP (early failures)
	V39/500	0.8731	4.0960	2.910	1.630	1.870	accepted	rejected		PLP (early failures)
	E66	0.9447	3.0760	2.660	2.290	2.420	accepted	accepted		HPP
	N52/54	0.9896	2.8040	2.729	2.640	2.670	accepted	accepted		HPP
	All					1.840	rejected	rejected		NOT PLP
WS	Germany					1.540	rejected	rejected		NOT PLP
	Denmark					0.763	rejected	rejected		NOT PLP

Table B.1: The PLP model results for the whole turbine

Hydraulics										
Survey	Model	PLP parameters			values		tests results			Conclusion
		β	ρ	Initial	Final	Avg	GoF	$H_0 =$	HPP	
						[failures $year^{-1}$]				
	V27/225					0.0480	rejected			NOT PLP
	M530		not enough failures			0.0299				unknown
	TW600	0.7028	1.0770	0.4690	0.1300	0.1860	accepted	rejected		PLP (early failures)
	E40									Enercon no hydraulic actuator
LWK	V39/500	0.7898	0.9397	0.5290	0.2030	0.2570	accepted	rejected		PLP (early failures)
	E66									Enercon no hydraulic actuator
	N52/54	1.0770	0.1340	0.1640	0.2050	0.1910	accepted	accepted		HPP
	All	1.0510	0.0852	0.0972	0.1380	0.1310	accepted	accepted		HPP
WS	Germany	0.8007	0.7290	0.4240	0.0768	0.0959	accepted	rejected		PLP (early failures)
	Denmark	0.8225	0.2456	0.1520	0.0358	0.0435	accepted	rejected		PLP (early failures)

Table B.2: The PLP model results for the hydraulics

Gearbox										
Survey	Model	PLP parameters			values		tests results			Conclusion
		β	ρ	Initial	Final	Avg	GoF	$H_0 = HPP$		
	V27/225					0.0936	rejected		NOT PLP	
	M530					0.0640	rejected		NOT PLP	
	TW600	1.8350	0.0014	0.0097	0.3550	0.1940	accepted	rejected	PLP (deterioration)	
LWK	E40									
									Enercon direct drive machines	
	V39/500	1.8440	0.0009	0.0064	0.3000	0.1630	accepted	rejected	PLP (deterioration)	
	E66									
									Enercon direct drive machines	
	N52/54	1.2840	0.1401	0.2840	0.6540	0.5090	accepted	accepted	PLP (deterioration)	
	All					0.1340	rejected		NOT PLP	
WS	Germany	0.9257	0.1962	0.1620	0.0862	0.0930	accepted	rejected	PLP (early failures)	
	Denmark	1.1170	0.0078	0.0120	0.0483	0.0413	accepted	rejected	PLP (deterioration)	

Table B.3: The PLP model results for the gearbox

Survey	Generator									
	PLP parameters					values		tests results		
Model	β	ρ	Initial	Final	Avg	GoF	$H_0 = HPP$	Conclusion		
					[failures year ⁻¹]					
V27/225	0.4295	1.2740	0.2185	0.0175	0.0408	accepted	rejected	PLP (early failures)		
M530	0.6242	0.5972	0.2040	0.0480	0.0768	accepted	rejected	PLP (early failures)		
TW600	1.0860	0.1130	0.1410	0.2040	0.1880	accepted	accepted	HPP		
E40	1.0110	0.3327	0.3420	0.3590	0.3550	accepted	accepted	HPP		
V39/500					0.0772	rejected		NOT PLP		
E66	0.4666	1.3430	0.2660	0.0632	0.1350	accepted	rejected	PLP (early failures)		
N52/54		not enough failures			0.1170			unknown		
All	1.2020	0.0249	0.0413	0.1670	0.1390	accepted	rejected	PLP (deterioration)		
Germany					0.1050	rejected		NOT PLP		
Denmark	0.8422	0.2200	0.1440	0.0398	0.0473	accepted	rejected	PLP (early failures)		

Table B.4: The PLP model results for the generator

Rotor and Blades									
Survey	PLP parameters				values		tests results		
	β	ρ	Initial	Final	Avg	GoF	$H_0 =$	HPP	Conclusion
Model									
V27/225		not enough failures			0.0936				unknown
M530	1.1620	0.0493	0.0744	0.1390	0.1200	accepted	accepted	HPP	
TW600	1.8350	0.0014	0.0097	0.3550	0.1940	accepted	rejected	PLP (deterioration)	
E40	0.5748	3.5180	1.0200	0.1430	0.2480	accepted	rejected	PLP (early failures)	
V39/500	0.7471	0.8053	0.4000	0.1260	0.1690	accepted	rejected	PLP (early failures)	
E66		not enough failures			0.1490			unknown	
N52/54	0.7362	1.5490	0.7460	0.3440	0.4670	accepted	accepted	PLP (early failures)	
All	1.0420	0.0877	0.1470	0.1970	0.1900	accepted	accepted	HPP	
Germany					0.2000	rejected		NOT PLP	
Denmark					0.0439	rejected		NOT PLP	

Table B.5: The PLP model results for the rotor

Electrics										
Survey	PLP parameters				values		tests results			
	β	ρ	Initial	Final	Avg	GoF	$H_0 = \text{HPP}$	Conclusion		
Model	β	ρ	Initial	Final	Avg	GoF	$H_0 = \text{HPP}$	Conclusion		
					[failures $year^{-1}$]					
V27/225	0.7244	1.3780	0.6410	0.1890	0.2620	accepted	rejected	PLP (early failures)		
M530	1.6480	0.0049	0.0227	0.2740	0.1660	accepted	rejected	PLP (deterioration)		
TW600	0.9871	0.3016	0.2920	0.2760	0.2800	accepted	accepted	HPP		
E40	0.9214	0.9087	0.7380	0.5130	0.5560	accepted	accepted	HPP		
V39/500	0.8769	0.7360	0.5300	0.3020	0.3440	accepted	accepted	HPP		
E66	1.0170	0.4660	0.4870	0.5100	0.5010	accepted	accepted	HPP		
N52/54	0.7957	0.6984	0.4000	0.2200	0.2760	accepted	accepted	Unknown		
All	1.1010	0.1348	0.1750	0.3530	0.3200	accepted	rejected	PLP (deterioration)		
Germany					0.2940	rejected		NOT PLP		
Denmark	0.7919	0.3364	0.1910	0.0350	0.0442	accepted	rejected	PLP (early failures)		

Table B.6: The PLP model results for the electrical system

Electronics (including Converter)										
Survey	PLP parameters				values			tests results		
	Model	β	ρ	Initial	Final	Avg	GoF	$H_0 = \text{HPP}$	Conclusion	
				[failures year ⁻¹]						
	V27/225	0.6699	1.7040	0.6710	0.1560	0.2330	accepted	rejected	PLP (early failures)	
	M530	0.6884	0.9813	0.4090	0.1230	0.1790	accepted	rejected	PLP (early failures)	
	TW600	0.8673	0.3124	0.2190	0.1240	0.1420	accepted	accepted	HPP	
	E40	0.9119	0.5447	0.4310	0.2870	0.3140	accepted	accepted	HPP	
LWK	V39/500	0.8975	0.5060	0.3860	0.2410	0.2690	accepted	accepted	HPP	
	E66	1.0020	0.3094	0.3110	0.3120	0.3110	accepted	accepted	HPP	
	N52/54	0.8978	0.2534	0.1930	0.1430	0.1590	accepted	accepted	HPP	
	All	0.8710	0.7140	0.5060	0.2080	0.2390	accepted	rejected	PLP (early failures)	
WS	Germany					0.1810	rejected		NOT PLP	
	Denmark					0.1410	rejected		NOT PLP	

Table B.7: The PLP model results for the electronics

Yaw System										
Survey	Model	PLP parameters			values		tests results			Conclusion
		β	ρ	Initial	Final	Avg	GoF	$H_0 =$	HPP	
	V27/225	0.6763	0.5412	0.217	0.0519	0.0768	accepted	accepted	accepted	unknown
	M530	0.7871	0.2591	0.145	0.0638	0.0811	accepted	accepted	accepted	unknown
	TW600	0.9577	0.2176	0.1950	0.1620	0.1690	accepted	accepted	accepted	HPP
LWK	E40	0.6641	0.9206	0.3560	0.0752	0.1130	accepted	rejected	rejected	PLP (early failures)
	V39/500	1.226	0.2381	0.042	0.118	0.096	accepted	accepted	accepted	unknown
	E66		not enough failures			0.1760				unknown
	N52/54		not enough failures			0.1270				unknown
	All	1.0100	0.1061	0.1090	0.1170	0.1160	accepted	accepted	accepted	HPP
WS	Germany					0.1080	rejected			NOT PLP
	Denmark					0.0617	rejected			NOT PLP

Table B.8: The PLP model results for the yaw system

Pitch Control									
Survey	PLP parameters			values			tests results		
	β	ρ	Initial	Final	Avg	GoF	$H_0 =$	HPP	Conclusion
Model			[failures year ⁻¹]						
V27/225	1.738	0.0007812	0.00446	0.117	0.0672	accepted	accepted		unknown
M530				Micon M530 stall regulated					
TW600				Tacke TW600 active stall control					
E40	1.0273	0.2520	0.2700	0.3070	0.2980	accepted	accepted		HPP
V39/500		bad data quality			0.2660	rejected			NOT PLP
E66	0.9890	0.4960	0.4830	0.4690	0.4740	accepted	accepted		HPP
N52/54				Nordex N52/54 stall regulated					
All	1.5690	0.0006	0.0025	0.1310	0.0832	accepted	rejected		PLP (deterioration)
Germany				0.0894		rejected			NOT PLP
Denmark				0.0133		rejected			NOT PLP

Table B.9: The PLP model results for the pitch control

Air Brake									
Survey	PLP parameters			values			tests results		
	Model	β	ρ	Initial	Final	Avg	GoF	$H_0 =$ HPP	Conclusion
				[failures year ⁻¹]					
	V27/225			Vestas V27 no air brake					
	M530	0.8034	0.1872	0.1100	0.0514	0.0640	accepted	accepted	HPP
	TW600		not enough failures			0.0108			unknown
LWK	E40		not enough failures			0.0020			unknown
	V39/500			Vestas V39 no air brake					
	E66	0.8782	0.8007	0.5780	0.4160	0.4740	accepted	accepted	HPP
	N52/54		not enough failures			0.0637			unknown
	All	1.0230	0.0325	0.0346	0.0406	0.0397	accepted	accepted	HPP
WS	Germany					0.0411	rejected		NOT PLP
	Denmark	0.8278	0.0833	0.0523	0.0129	0.0156	accepted	accepted	HPP

Table B.10: The PLP model results for the air brake

Mechanical Brake									
Survey	PLP parameters			values			tests results		
	β	ρ	Initial failures	Final	Avg	GoF	$H_0 = \text{HPP}$	Conclusion	
Model			[failures year ⁻¹]						
V27/225		not enough failures	0.0120					unknown	
M530	0.4883	0.7661	0.1640	0.0229	0.0469	accepted	rejected	unknown	
TW600	0.8673	0.3124	0.2190	0.1240	0.1420	accepted	accepted	HPP	
E40		not enough failures			0.0059			unknown	
V39/500		not enough failures			0.0208			unknown	
E66		not enough failures			0.0271			unknown	
N52/54		not enough failures			0.0849			unknown	
All	1.2430	0.0069	0.0128	0.0688	0.0554	accepted	rejected	PLP (deterioration)	
Germany		not enough failures			0.0331			unknown	
Denmark	0.8063	0.1811	0.1070	0.0221	0.0262	accepted	rejected	PLP (early failures)	

Table B.11: The PLP model results for mechanical brake

Main Shaft									
Survey	PLP parameters			values			tests results		
	β	ρ	Initial	Final	Avg	GoF	$H_0 =$	HPP	Conclusion
Model			[failures $year^{-1}$]						
V27/225	not enough failures		0.0048						unknown
M530	not enough failures		0.0000						unknown
TW600	0.8673	0.3124	0.2190	0.1240	0.0242	accepted	accepted		HPP
E40	1.1910	0.0254	0.0412	0.1000	0.0840	accepted	accepted		HPP
V39/500	not enough failures		0.0897						unknown
E66	not enough failures		0.0541						unknown
N52/54	not enough failures		0.7430						unknown
All	1.3370	0.0018	0.0040	0.0416	0.0311	accepted	accepted		PLP (deterioration)
Germany	not enough failures		0.0212						unknown
Denmark	0.9716	0.0111	0.0103	0.0082	0.0085	accepted	accepted		HPP

Table B.12: The PLP model results for mechanical brake

Appendix C

A Survey Among WT Experts

Questionnaire on the Reliability of Wind Turbines

Fabio Spinato

10th November 2006

C.1 Preface

The New & Renewable Energy Group (NAREG) of the School of Engineering of Durham University (<http://www.dur.ac.uk/engineering/nareg/>), part of the EPSRC Supergen GBP 2.55M Wind Energy Technologies Consortium, has been investigating the reliability of wind turbines for the past 3 years, producing a number of publications on this subject, see Section C3.

The following questionnaire aims to evaluate the reliability of onshore wind turbines by comparing the results of a rigorous investigation carried out at Durham University with the engineering knowledge and experience of professionals, with specific expertise on design or Operation & Maintenance of wind turbines. Expert brainstorming is a recognised procedure for investigating systems reliability whenever there is lack of failure field or test data and this questionnaire is an attempt to gain informed views to allow such brainstorming to take place. This investigation is concerned primarily with the reliability of the turbines and neglects repair times and their influence on availability, although we do ask responders to give us their view of typical availability targets for onshore and offshore turbines.

The answers will be used in my PhD research work and will not be disclosed to others without your express permission.

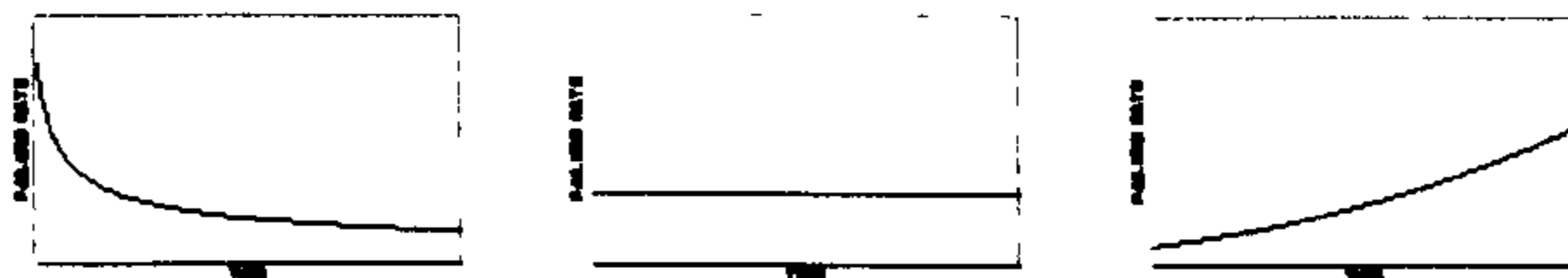
C.2 Questionnaire

1. What in your experience is the overall average availability of large (> 1 MW) onshore wind turbines?

December 6, 2008

- (a) < 90 %
 - (b) 90 - 95 %
 - (c) 95 - 97 %
 - (d) > 97 %
2. What in your experience is the overall failure rate, in failures per turbine per year, of large (> 1 MW) onshore wind turbines?
- (a) < 0.6
 - (b) 0.6 - 1
 - (c) 1 - 1.5
 - (d) > 1.5
3. What is the "useful life" in years of onshore wind turbines?
- (a) < 10
 - (b) 10 - 12
 - (c) 12 - 14
 - (d) > 14
4. Among the following wind turbine subassemblies, which in your opinion is the least reliable? Can you rank them in ascending order of reliability?
- (a) Hydraulic system
 - (b) Generator
 - (c) Transformer
 - (d) Gearbox
 - (e) Pitch control
 - (f) Blades
 - (g) Inverter
 - (h) Other (specify in the box):

5. Indicate what is the most common failure mode or root cause for the sub-assembly chosen as the least reliable above:
6. Representing the failure rate as a function of time, which of the graphs below, in your experience, would best represent the failure pattern of a wind turbine gearbox?



a)

b)

c)

7. Can you briefly justify the reasons that determine the graph chosen above? (for example in Case b): the reliability deteriorates but the maintenance is sufficient to stabilise its behaviour):

8. Repeat points 5 and 6 for the generator:

(a) Curve a) b) c)

(b) Reason (specify in the box):

9. Repeat points 5 and 6 for the blades:

(a) Curve a) b) c)

(b) Reason (specify in the box):

10. Comparing direct and indirect drive turbines, which do you consider the most reliable?
- (a) Direct drive (synchronous generator with fully rated converter)
 - (b) Indirect drive (fixed speed asynchronous generator with a gearbox and no inverter)
 - (c) Indirect drive (variable speed doubly fed induction generator with a gearbox and partially rated converter)
11. From the reliability point of view, what would you consider to be the main obstacle to the installation of the wind turbines in an offshore environment?
- (a) Harsher wind conditions
 - (b) Foundation stress
 - (c) Corrosion
 - (d) Increased dynamic loads on the drive train
 - (e) The necessity of utilising turbines of higher rating (scaling effects)
12. What availability, in your opinion, should offshore wind turbines be trying to achieve?
- (a) < 80 %
 - (b) 80 - 85 %
 - (c) 85 - 90 %
 - (d) 90 - 95 %
 - (e) > 95
13. What, in your opinion is the maximum economically acceptable failure rate, in failures per turbine per year, for offshore installed wind turbines?
- (a) < 0.5
 - (b) 0.5 - 0.75
 - (c) 0.75 - 1.0

- (d) 1.0 - 1.5
- (e) > 1.5

C.3 References

1. Tavner P J, Xiang J. Wind turbine reliability, how does it compare with other embedded generation sources. IEE RTDN Conference, London, 2005.
2. Tavner P J, Xiang J, Spinato F. Improving the reliability of wind turbine generation and its impact on overall distribution network reliability. IEE 18th International Conference on Electrical Distribution, CIRED, Turin, 2005.
3. Tavner P J, Edwards C, Brinkman A, Spinato F, Influence of Wind Speed on Wind Turbine Reliability, Wind Engineering, Volume 30, No. 1, 2006
4. Tavner P J, Xiang J, Spinato F, Reliability Analysis for Wind Turbines, Wind Energy Journal, 2006; Published online in Wiley Interscience (www.interscience.wiley.com) DOI: 10.1002/we.204.

Prepared by Fabio Spinato

10th November 2006

December 6, 2008

Bibliography

- [1] R. B. Abernethy. *The New Weibull Handbook*. R. B. Abernethy publisher, North Palm Beach, Florida, USA, 2000.
- [2] P. F. Albrecht and R. M. McCoy. Assessment of the reliability of motors in utility applications. *IEEE Transaction on Energy Conversion*, 1(3), 1986.
- [3] K. Aleklett and C.J.Campbell. The peak and decline of world oil and gas production. *Minerals and Energy*, 18:5(20), 2003.
- [4] J. D. Andrews and T. R. Moss. *Reliability and Risk Assessment*. Professional Engineering Publishing, London, 2002.
- [5] Vattenfall Danmark A/S. Capital grant scheme for offshore wind, annual report january 2006 december 2006. Technical report, DTI, 2007.
- [6] Various authors. Wind energy report deutschland. Technical report, ISET, Insitut fur Solare Energieversorgungstechnik, Kassel, Germany, 2006.
- [7] Intergovernmental Panel On Climate Change. Climate change 2007 : the scientific basis: contribution of working group i to the fourth assessment report of the intergovernmental panel on climate change 2001. Technical report, Intergovernmental Panel on Climate Change. Working Group I, New York, 2007. Cambridge University Press.
- [8] F. Coolen. *personal communication*, 2006.
- [9] F.P.A. Coolen, F. Spinato, and D. Venkat. On modelling of grouped reliability data for wind turbines. *Journal of Management Mathematics, special edition Mathematical Modelling on Reliabilitys*, Oxford Press, 2008. To be published.
- [10] L. Crow. *Reliability Growth and Repairable System Analysis Ref*. ReliaSoft Publishing, 2005.
- [11] E. de Vries. Gearbox failures and design solutions. *Renewable Energy World Wind Power*, 2006.
- [12] Department of Defense, Washington. *MIL-HDBK-189 - Reliability Growth Management*, 1981.
- [13] DTI. Energy white paper, our energy future - creating a low carbon economy. Technical report, Department of Trade and Industry, London, 2003. The Stationary Office.

- [14] DTI. Meeting the energy challenge a white paper on energy. Technical report, Department of Trade and Industry, London, 2007. The Stationary Office.
- [15] W. Eggersgl & (ed). *Wind Energie. Praxisergebnisse*, Landwirtschaftskammer Schleswig-Holstein, Rendsburg, Germany. V-XVI, 1993-2004.
- [16] W. Eggersgl & (ed). *Wind energie. Technical Report VIII, Praxisergebnisse*, Landwirtschaftskammer Schleswig-Holstein, Rendsburg, Germany, 1996.
- [17] M. K. Koch et al. *WindStats Newsletter*. William Canter ed., Knebel, Denmark. vol 9 n.3 - vol 17 n.3, 1996-2004.
- [18] R.W. Bentley et al. The peak and decline of world oil and gas production. *Energy Policy*, Volume 35(12), 2007.
- [19] E. J. Gentle. *Random Number Generation and Monte Carlo Methods*. Springer, New York, 1998.
- [20] H. Goldberg. *Extending the Limits of Reliability Theory*. John Wiley & Sons, New York, 1981.
- [21] R. Harrison, H. Hau, and H. Snel. *Large Wind Turbines, Design and Economics*. John Wiley & Sons, Chichester, West Sussex, 2000.
- [22] Matthias Heymann. Signs of hubris: The shaping of wind technology styles in germany, denmark, and the united states, 1940-1990. *Technology and Culture*, 39(4), 1998. pp. 641-670.
- [23] J.T. Houghton. Climate change 2001 : the scientific basis: contribution of working group i to the third assessment report of the intergovernmental panel on climate change 2001. Technical report, Intergovernmental Panel on Climate Change. Working Group I, New York, 2001. Cambridge University Press.
- [24] <http://commons.wikimedia.org>. *The MOD-5 wind turbine*, 2008.
- [25] <http://telosnet.com>. *The MOD-2 wind turbine*, 2008.
- [26] <http://telosnet.com>. *The two bladed wind turbine designed by Ulrich Hutter*, 2008.
- [27] <http://www.eibis.com>. *The high speed shaft of a WT gearbox*, 2008.
- [28] M. King Hubbert. Energy from fossil fuels. *Science*, 109(2823), 1949. the American Association for the Advancement of Science.
- [29] M. King Hubbert. Nuclear energy and the fossil fuel. Technical report, Shell Development Company, exploration and Production Research Division, Houston, Texas, 1956. Publication Number 95.
- [30] David A. King. Climate change science: Adapt, mitigate, or ignore? *Science*, 303, 2004.

- [31] M. Knowles. Failure modes and effects analysis for a large wind turbine. Technical report, Durham University, 2006. Final Year Project Report.
- [32] A. Kyte. Failure modes and effects analysis on indirect and direct drive large wind turbines. Technical report, Durham University, 2007. Final Year Project Report.
- [33] Kaplan E. L. and Meier P. Non parametric observation of incomplete observation. *Journal of American Statistical Association*, 53(282), 1958.
- [34] SINTEF Industrial Management. Oreda, offshore reliability data, 4th edition. Technical report, various participants, 2002.
- [35] United Nations. Kyoto protocol to the united nations framework convention on climate change. Technical report, United Nations Framework Convention on Climate Change, UNCCC, New York, 1998.
- [36] P. Nielsen. New danish wind energy index calculation. Technical report, EMD international, Aalborg, Denmark, 2004.
- [37] npower Renewables Limited. Capital grant scheme for the north hoyle offshore wind farm annual report july 2004 june 2005. Technical report, DTI, 2005.
- [38] npower Renewables Limited. Capital grant scheme for the north hoyle offshore wind farm annual report july 2005 june 2006. Technical report, DTI, 2006.
- [39] Patrick D. T. O'Connor. *Practical Reliability Engineering*. Wiley, 2002.
- [40] J.R. Petit, J. Jouzel, and et. al. Climate and atmospheric history of the past 420 000 years from the vostok ice core in antarctica. *Nature*, 399, 1999. Published in : Vital climate graphics, the impacts of climate change, UNEP and Grid Arendal, 2000.
- [41] J. Ribrant and L. M. Bertling. Survey of failures in wind power systems with focus on swedish wind power plants during 19972005. *IEEE Transaction on Energy Conversion*, 22(1), 2007.
- [42] Steven E. Rigdon and Asit P. Basu. *Statistical Methods for the reliability of Repairable Systems*. John Wiley & Sons, New York, 2000.
- [43] Sheldon M. Ross. *Introduction to probability and Statistics for Engineers and Scientist*. Academic Press, London, 2000.
- [44] A.J. Seebregts, L.W.M.M Rademakers, and B.A. van den Horn. Reliability analysys in wind turbine engineering. *Microelectronics Reliability*, 1995. Vol. 35, Nos 9-10, pp. 1285-1307.
- [45] M. R. Simmons. *Twilight in the desert*. Wiley And Sons, Hoboken, New Jersey, 2006.
- [46] F. Spinato, P. J. Tavner, and G.J.W. van Bussel. Reliability-growth analysis of wind turbines from fleet field data. In *Proceedings of Advances in Risk and Reliability Technology Symposium (AR2TS)*, Loughborough, 2007.

- [47] P. J. Tavner. *availability figure of an onshore American wind farm*, 2006. personal communication.
- [48] P. J. Tavner, C. Edwards, A. Brinkman, and F. Spinato. Influence of wind speed on wind turbine reliability. *Wind Engineering*, 30(1), 2006.
- [49] P. J. Tavner and J. P. Hasson. Predicting the design life of high integrity rotating electrical machines. In *proceedings of the the EM&D Conference*, Canterbury, 1999.
- [50] P. J. Tavner and J. P. Xiang. Wind turbine reliability, how does it compare with other embedded generation sources. In *proceedings of RTDN conference*, London., 2005.
- [51] P. J. Tavner, J. P. Xiang, and F. Spinato. Improving the reliability of wind turbine and its impact on overall distribution network reliability. In *proceedings of CIRED conference*, Turin, 2005.
- [52] P. J. Tavner, J. P. Xiang, and F. Spinato. Reliability analysis for wind turbines. *Wind Energy*, 10(1), 2007.
- [53] P. J. Tavner, G.J.W. van Bussel, and F. Spinato. Machine and converter reliabilities in wind turbines. In *Proceedings of International Conference on Power Electronics, Machine and Drives*, Dublin, 2006.
- [54] P.J. Tavner. *A review of condition monitoring of rotating electrical machines*. IET proceedings, to be published, 2008.
- [55] DOWEC team. Estimation of turbine reliability figures within the dowec project. Technical Report 10048/4, Dutch Offshore Wind Energy Converter (DOWEC), 2002.
- [56] O. V. Thorsen and M. Dalva. Failure identification and analysis for high voltage induction motors in the petrochemical industry. *IEEE Transaction on Industry Applications*, 35(4), 1999.
- [57] E.ON UK. Capital grant scheme for offshore wind, annual report january 2005 december 2005. Technical report, DTI, 2006.
- [58] E.ON UK. Capital grant scheme for offshore wind, annual report january 2006 december 2006. Technical report, DTI, 2007.
- [59] G.J.W van Bussel and Chr. Schontag. Operation and maintenance aspects of large offshore wind farms. In *proceedings of the 1997 European Wind Energy Conference*, Dublin, Ireland, 1997. pp. 272-279.
- [60] G.J.W van Bussel and M. B. Zaaijer. Dowec concept study, reliability, availability and maintenance aspects. In *Proceedings of the Marine Renewable Energy Conference (MAREC)*, Newcastle, UK, 2001.

-
- [61] Various. *The Gold Book, Design of Reliable Industrial and Commercial Power systems*. Institute of Electrical and Electronics Engineers, New York, 1998.
- [62] Various. *Handbook of Reliability Engineering*. Hoang Pham Editor, 2003.
- [63] D. Wallace and J. Houghton et. al. A guide to facts and fictions about climate change. Technical report, The Royal Society, London, 2005.
- [64] www.4energia.ee/index.php/lang/eng/article/316. *The Gedser Mill wind turbine*, 2008.
- [65] www.hdwp.cn. *Details of a yaw system*, 2008.
- [66] www.moonofalabama.org. *A large rotor being mounted on the nacelle*, 2008.
- [67] www.ncl.ac.uk. *The connection scheme of a DFIG*, 2008.
- [68] www.vestas.com/. *The Vestas 90 wind turbine*, 2008.
- [69] www.windmesse.de. *The Enercon E82 wind turbine*, 2008.
- [70] www.windsofchange.dk. *The european WEGA 1 (Tjaereborg) wind turbine*, 2008.